KINEMATIC AND DYNAMIC ASPECTS OF COORDINATED DUAL ARM MANIPULATOR IN HANDLING OPERATION

By

SAMIRAN MANDAL

DEPARTMENT OF MECHANICAL ENGINEERING

INDIAN INSTITUTE OF TECHNOLOGY KANPUR

JUNE, 1993

KINEMATIC AND DYNAMIC ASPECTS OF COORDINATED DUAL ARM MANIPULATOR IN HANDLING OPERATION

A Thesis Submitted
in Partial Fulfilment of the Requirements
for the Degree of
DOCTOR OF PHILOSOPHY

By

SAMIRAN MANDAL

to the

DEPARTMENT OF MECHANICAL ENGINEERING
INDIAN INSTITUTE OF TECHNOLOGY KANPUR

JUNE, 1993

CERTIFICATE

It is certified that the work contained in the thesis entitled "KINEMATIC AND DYNAMIC ASPECTS OF COORDINATED DUAL ARM MANIPULATOR IN HANDLING OPERATION", by SAMIRAN MANDAL, has been carried out under our supervision and that this work has not been submitted elsewhere for a degree.

Prof. Amitabha Ghosh

Prof. Himanshu Hatwal

Department of Mechanical Engineering
I.I.T. Kanpur

Date: 4.6.1993

SYNOPSIS

The dual-arm manipulators have an important role to play in the modern industrial applications. A single-arm manipulator has limitations in carrying a heavy pay-load or holding objects with odd geometrical shapes. Besides offering easier handling in such cases, the dual-arm manipulators also provide the necessary flexibility in assembly operations where the assembly task is performed by both the arms and hence the redundant degrees of freedom are available.

This thesis attempts to solve two problems of dual-arm manipulators. In the first problem, a kinematically redundant dual-arm manipulator is considered and the kinematic inverse solutions are investigated. The second problem is that of trajectory planning where the dual-arm system has torque redundancy and the results are sought for minimum time and minimum electrical energy criteria.

The first problem considers a peg-in-hole type assembly operation where the relative movement between the end-effectors of two arms is specified. Due to kinematic redundancy the inverse solution is not unique and hence the assembly can take place anywhere in the workspace. The kinematic inverse problem in this work is posed as an optimization problem. The relative path is specified by a sequence of knot points. Three optimization criteria have been used to do a comparative study. The three optimization procedures respectively lead to minimum velocity norm solution, minimum acceleration norm solution, and increased

manipulability solution. All these three schemes optimize locally on the path. The numerical results for inverse kinematics are obtained for a planar case where two arms, each with three revolute joints, are employed for a peg-in-hole assembly in a plane. The minimum acceleration norm solution is shown to result in low fluctuations in the joint velocities at the expense of somewhat larger magnitudes of velocities as compared to minimum velocity norm solutions. Maximizing manipulability leads to large joint movements needed to reconfigure the arms. Instead, increasing the manipulability gradually, as the assembly progresses, is shown to be a better strategy.

The major part of this thesis is devoted to the trajectory planning problem of a dual-arm manipulator where each arm has six degrees of freedom. The task assigned is that of carrying a rigidly grasped object along a specified path. The two arms alongwith the rigidly held object between end effectors form a closed chain. This closed chain does not have kinematic redundancy. But as all the twelve joints of the dual-arm system are considered to be active joints, there is torque redundancy in the system, i.e. the resultant force exerted on the object (which has six components) is exerted by the twelve joint torques and so the joint torque distribution is not unique. The trajectory planning problem (i.e., determination of time histories of joint torques, velocities etc. along the specified path) is therefore posed with some additional criteria, as an optimization problem. The formulation of the problem is done in the following two stages.

In the first stage, the torque redundancy is resolved according to either the criterion of minimum norm of joint torque vector or that of minimum actuator power. At this stage, assuming that the object trajectory (position, velocity and acceleration) is known, the complete nonlinear dynamics of the closed chain (two arms and the object) is written and a closed form expression is obtained for the joint torques resolved according to above two criteria.

The second stage involves determination of the time histories of joint variables. To this end, the trajectory planning problem is posed as minimum time problem, or minimum energy (electrical energy) problem or minimum time and energy problem. This optimization problem is subject to both equality and inequality constraints. The equality constraints are the torque redundancy resolution relations and the condition that the joint velocities be zero at the beginning and end of the trajectory. The inequality constraints are due to the limits on the joint torques and joint velocities.

The continuous dynamic model is then discretized to implement numerical schemes. For this,the specified object path is divided into number of knot points. The inverse of time intervals between two successive knot points,i.e. the reciprocal time intervals are taken as a set of independent variables. All the relevant equations of optimization formulation are now written in discrete form in terms of the reciprocal time intervals with the help of implicit trapezoidal (smoothing) rule of discretization. This discretization yields the velocities as linear functions of the set of reciprocal time intervals, whereas

the objective function and the torque relations are obtained as nonlinear functions.

The optimization scheme adopted is that of successive linear programming. For this purpose the nonlinear equations are linearized with respect to the set of reciprocal time intervals. An initial guess on reciprocal time intervals is made and then linear programming is applied to improve the solution iteratively till convergence is achieved. The convergence process is also studied through "warm start" where the initial guess values are guided by the trial runs.

The numerical results are presented for a dual-arm system where each arm is modelled as PUMA-560 manipulator. The rigid object has the shape of rectangular parallelopiped. The object is grasped rigidly between the two end effectors. In the first example, a vertically straight trajectory of the object, with fixed orientation along the path, is considered. With the optimization scheme outlined above, three solutions corresponding to minimum time problem, minimum energy problem and minimum time and energy problem are presented. This example is discussed in detail for the effect of changing the number of knot points on the object path and the viability of warm starting the iterative procedure by making an improved guess at the starting stage. The successive linear programming approach is shown to be particularly suitable for minimum time problems where the convergence can be made very fast. The minimum energy term slows down the convergence substantially. The travel time in the minimum time case is obviously restricted by the limits on the joints torques and joint velocities. In minimum energy case, the tendency of the

dual-arm system to move very slow, in order to consume low energy, is opposed by the gravity induced torques which tend to speed up the system. The time of travel is much longer (about two and half times) for minimum energy case as compared to that for minimum time case. The minimum time and energy case yields an intermediate set of results.

The numerical results are presented for two more examples. The second example is an extension of the first example where the object orientation is also changed along the vertical path. The resulting effect is in changing the torque and velocity distributions and a different set of joints now reach the velocity limits without any joint reaching the torque limit. The third and the last example considers a parabolic path for the object in a curvilinear trajectory. This trajectory has been selected to study a case where the velocities undergo reversal of sign. Finally some conclusions and scope of further work are presented.

ACKNOWLEDGEMENT

First of all I wish to extend my sincere gratitude to my supervisors, Prof. Amitabha Ghosh and Prof. Himanshu Hatwal for their whole hearted support towards my work and constant encouragement. I thank prof. Hatwal for the valuable time he has spent on correcting the drafts of this thesis and arranged the materials which improved the style of presentation.

Next I thank Anupam Bagchi, K.G.Shastry, Subrata Saha, Praveen Bhatia, Laxmi Prasad and Dipankar Sanyal with whom I spent the earlier years of my long stay here.

I would like to express my deep gratitude to my friends and colleagues, in particular Anirvan Dasgupta, Soumya Bhattachayya, Shyamal Chatterjee, Biswajit Basu, Sanjay Saha, Santanu Bhattacharyya, Rangan Guha, Manab Das ,Prasanta Deb, Saibal Ganguly , Subir Bhattacharyya who have given me company during my work.

I wish to thank Susmit Sen , S.R.Pandian and other staff of Robotics Centre for their help and cooperation.

Thanks are also due to Y.D.S.Aryya, Nirmal Roberts , V.S.Seal and Jagannath Mishra of Computer Centre for their timely help in my work.

My special thanks are due to Sudipta Mukhopadhyay and Ngo Sy-Loc for their special helps in preparing the sketches used in the thesis and many other works.

Lastly I thank Vivek Shukla for his patient typing and S.S.Khushwaha for making nice figures.

Samiran Mandal

DEDICATED TO MY PARENTS

CONTENTS

LIST OF FIGURES

LIST OF TABLES

LIST OF SYMBOLS

a_{li}	geometric parameter associated with the ith joint of the lth arm
c_1, c_2	torque vectors due to gravity
c^g_{li}	gear ratio of the ith joint of the lth arm
C_{tbl},C_{tb2}	cost matrices of arm 1 and arm 2 used in torque resolution
C_{tpl},C_{tp2}	cost matrices of arm 1 and arm 2 based on power consumption
$CTM_{li2}(k)$	MxM matrix of coefficients of torque at the i2th joint of the lth arm during kth interval
c^r_{li}	power supply resistance of joint i of the lth arm the centre of the object
$ctv_{li2}(k)$	Mx1 vector of coefficients of torque of the lth arm and i2th joint during kth interval
$ctc_{li2}(k)$	constant term in torque of the lth arm and the i2th joint during the kth interval
D_l	inertia matrices of the lth arm.
d_{li}	geometric parameter associated with the ith joint of the lth arm.
^wf_c	resultant generalized force at the object centre.
^wf_l	interactive force by the object on the l th end effector.
^wg	acceleration due to gravity.
H(k)	kth reciprocal time interval.

h_1, h_2	joint vector torque due to centrifugal and Coriolis acceleration
${}^{w}I_c$	inertia matrix of the object in the world coordinate
${}^{c}I_c$	inertia matrix of the object in the object frame
J_{1c}, J_{2c}	transmission matrices
J_l	manipulator jacobian matrix of the lth arm
J_{rel}	relative Jacobian matrix
M	number of time intervals
mc	manipulability coefficent vector
mp	manipulability
Δmp	change of manipulability between two sucessive knot points
n_l	degrees of freedom of lth arm
p_{rel}	translation vector of T_{rel}
${}^{w}p_{l\,n_l}$	translation vector of ${}^{w}T_{ln_l}$
${}^{w}p_c$	position vector of the object mass center with respect to world coordinate frame
${}^{w}p_{l6}$	postion vector of the lth end effector with respect to world coordinate frame
Δp_{relp}	incremental change of p_{rel}
q_{aug}	augmented joint vector at a knot point
q_{augp}	augmented joint vector at the previous knot point
Δq_{augp}	incremental change of q_{augp}

q_l	joint position vector of the lth arm
$\dot{q}_l$	join velocity vector of the lth arm
$\dot{q}_{1imin}$, $\dot{q}_{2imin}$	lower velocity limit of i th joints of arm 1 and arm 2
$\dot{q}_{1imax}$, $\dot{q}_{2imax}$	upper velocity limit of ith joints of arm 1 and arm 2
$q_{lp}(k)$	p th joint postion of the lth arm at the k th knot point
$\Delta q_{lp}(k-1)$	p th joint displacement of lth arm during the (k-1) th interval
${}^{w}R_c$	the rotation matrix of ${}^{w}T_c$
R_{rel}	rotation matrix of T_{rel}
${}^{w}r_{li}$	postion vector of the mass centre of the link i of the lth arm
${}^{w}r_l$	moment arm of the interactive forces acting between the object and the arms
${}^{w}S_{r1}$	skew symmetric matrix of ${}^{w}r_1$
${}^{w}S_{r2}$	skew symmetric matrix of ${}^{w}r_2$
${}^{w}T_{l0}$	Transformation matrix of the base frame of lth arm with respect to world coordinate frame
${}^{l0}T_{li}$	Transformation matrix of the ith frame with respect to base frame
${}^{l0}T_{l6}$	Transformation matrix of the end effector frame of lth arm with respect to its base frame
${}^{w}T_{l6}$	Transformation matrix of end effector frame of lth arm with respect to world coordinate frame

$^{w}T_{c}$	Transformation matrix of object frame with respect to world frame
T_{rel}	the transformation matrix of arm 2 with respect to arm 1
tr_{rel}	relative task vector
$\Delta t(k-1)$	time interval between the (k-1) th and the kth knot points
$^{w}T_{1\ n1}$, $^{w}T_{2\ n2}$	transformation matrix of the end effector frame with respect to world coordinate frames of arm 1 and arm 2 with n1 and n2 degrees of freedom
$^{w}v_{c}$	linear velocity vector of the object with respect to world coordinate frame
Z_{te}	hybrid object function for trajectory planning
Z_{um}	objective function with minimum acceleration and increased manipulability weightage criteria
α_{li}	geometric parameter associated with lth arm and ith joint.
β_1, β_2	weightages of minimum time and minimum energy criteria in Z_{te}
β_m	weightage of manipulability
β_u	weightage of minimum acceleration
γ_1, γ_2	weightages of two performance criteria of minimum torque and minimum power for torque resolution
ϕ_1, ϕ_2, ϕ_3	Euler angles
$\Delta\Phi_{relp}$	incremental change of Φ_{relp}
$\phi_{r1}, \phi_{r2}, \phi_{r3}$	relative Euler angles.

τ_{1max}, τ_{2max}	upper joint torque limits of arm 1 and arm 2
τ_{1min}, τ_{2min}	lower joint torque limits of arm 1 and arm 2
τ_l	joint torque vector of the l th arm
$\bar{\tau}_l$	joint torque vector needed to move the arms in unconstrained manner
${}^{w}\Omega_c$	angluar velocity vector of object with respect to world coordinate frame

CHAPTER 1

INTRODUCTION

1.1. Introduction

The robotic systems have been employed in industrial applications for a long time. There are now variety of types of robotic systems with their applications being spread to much wider areas. One important class is that of multi-arm robotic systems which encompasses cooperating manipulators, mechanical hands and walking robots.

The design and development of robotic systems has been greatly influenced by the structure and working behaviour of humans and other living organisms. For example, the walking robot design is guided by the walking traits of quadrupeds, hexapods etc. Likewise the dexterous mechanical hands are along the lines of human fingers. Thus it is natural that like the two human hands there should be two-arm (or even multi-arm) cooperating manipulators. The main feature common to all these robotic systems is that of coordinated motion but the discussions in this thesis are restricted to cooperating manipulators with two arms, which will be refereed to as dual-arm systems.

The coordinated motion of dual-arm systems has been broadly classified into two categories as tightly coordinated motion and loosely coordinated motion. The tightly coordinated motion corresponds to cases where the two arms perform a common

operation, e.g. two hands handling a common object or two arms together performing an assembly operation. The loosely coordinated motion implies that the two arms share a common workspace but perform independent tasks like while one arm loads the other arm unloads.

The tightly coordinated dual-arm manipulators are particularly needed when the object being handled is either too heavy or too long for a single arm manipulator. The open chain structure of a single arm itself makes it unsuitable for high payload duty operations. The objects which have large dimension(s) are difficult to hold in a balanced way with a single arm and again the dual-arm manipulator is useful. Besides this, many assembly operations also will be easier with dual-arm manipulators so that assembly is carried out by the two arms configured in the most appropriate positions in the workspace (for example, the configurations which are away from singularities). Moreover, the two arms can also be used in independent operations in a loosely coordinated motion thereby having a larger workspace and faster operations.

The arms can be made similar if identical features are required in both arms like load sharing, control etc. Alternately, the two arms can be made complementary to each other like human arms. For example, one arm may have higher payload capacity but slower motion and lower precision while the other arm is light, fast and precise such that the first arm takes care of a heavier part and the other arm carries out the compensatory precise motion

required for assembly.

In many applications, a single arm manipulator is provided redundancy in order to have more maneuverability to avoid singularities, and to have different choices in task distribution. The multi degrees-of-freedom system is essentially broken into subsystems of smaller degrees of freedom to result in multi-arm manipulators. The basic problem of these multi-arm systems is in producing coordinated motion of the subsystems. This coordination is needed both at the kinematic level and at the force level.

If the number of task variables is less than the total degrees of freedom of the dual-arm system then there is kinematic redundancy. The kinematic inverse solution is then not unique and some additional criteria of distributing the task have to be imposed to solve the problem. This offers various choices like having the solution that produces minimum norm of joint velocities, or yields best manipulable arm configurations etc. In addition, a paramount problem is collision avoidance. Kinematic redundancy again can be used to configure the arms in a collision free state.

The dual-arm manipulators usually have torque redundancy (while it may not have kinematic redundancy, for example two six degrees-of-freedom arms forming a closed chain through a common rigidly held object), i.e. the number of actuated joints is more than what is required to produce the motion. Therefore, the coordinated motion requires proper force distribution among the

actuated joints and/or the held object. The inverse dynamics problem of determining the actuator forces/torques is generally posed as a constrained force optimization problem. The force constraint equations are in the form of equality constraints as dynamic equations of the systems, inequality constraints on the torque limits of actuators, and inequality constraints arising due to interactions with the held object which is not rigidly grasped as in case of multi-fingered hands.

There are two approaches to the trajectory planning of dual-arm manipulators. In the first approach the path planning is done without considering dynamics and then a path tracker (based on PID scheme, computed torque scheme etc.) is employed to control the systems. The second approach considers the manipulator dynamics and trajectory planning problem is reposed as an optimization problem to take care of redundancy in actuation. The optimum trajectory is usually based upon the minimum time and minimum energy criteria, the path may or may not be specified and trajectory planning yields the time histories of joint variables like position, velocity and torque.

This work attempts to address two problems of dual-arm manipulators. The first one is that of resolving the kinematic redundancy and the second problem is of trajectory planning with a dynamic model of the system.

1.2 Literature Survey

This review of literature is focused mainly upon the

topics related to redundant manipulators and two arm manipulators. The topics are discussed below under three major headings, namely i) kinematics, ii) dynamics and iii) trajectory planning.

1.2.1. *Kinematics*

The kinematic studies can be broadly classified into two categories as i) kinematics of nonredundant arms, and ii) kinematics of redundant arms. A dual-arm manipulator may be kinematically nonredundant if it forms a closed chain when an object is rigidly held between two arms, and the closed chain thus formed has six degrees of freedom in the general case of space motion of the object. This study will address only the works related to kinematically redundant arms.

Lee [1989] presented a comprehensive survey on inverse kinematic solution of redundant arms. The solutions of the under-defined set of kinematic equations have traditionally been obtained by imposing additional constraints based upon some performance criteria. He classified these approaches into four major categories as follows: 1) The Jacobian pseudo-inverse solution as the minimum norm solution [Yoshikawa,1984]. 2) The modified Jacobian pseudo-inverse solution in which the Jacobian null space solution is added to the Jacobian pseudo-inverse solution to maximize a performance index indicating manipulability, collision, joint stop avoidance, etc. [Whitney, 1972]. 3) The extended Jacobian solution in which extra constraints obtained from the condition of optimal joint

configurations are added to the forward kinematics to yield the extended Jacobian [Baillieul, 1985]; in case only one degree of freedom of redundancy exists, the extended Jacobian provides an explicit solution. 4) The optimization of the lagrangian formed by a certain performance index and by forward kinematics as constraints [Chang,1986]. Kazerounian and Wang [1988] considered global optimization of joint velocities and concluded that globally optimum solutions are described as the minimum acceleration norm solution. Chevallerean and Khalil [1988] extended the pseudo-inverse kinematic procedures for redundant arms to take care of several criteria, including that of increasing the manipulability.

Lee [1989] and Chiacchio et al. [1991a] extended the concept of manipulability ellipsoids for single arm to the case of dual-arm and multi-arm manipulators, respectively. Lee [1989] defined task-oriented dual-arm manipulability as the measure of geometrical similarity between the desired manipulability ellipsoid and the dual-arm manipulability ellipsoid and this task-oriented dual-arm manipulability measure approximately represented the volume of intersection between two individual manipulability ellipsoids. This was used then to optimize the dual-arm joint configurations. Chiacchio et al. [1991a] adopted a global kinetostatic formulation of the closed chain created by multiple tightly cooperating arms to define external and internal force manipulability ellipsoids. The corresponding absolute and relative velocity manipulability ellipsoids were derived on the

basis of duality principle. These were utilized to determine optimal postures for redundant multi-arm system.

Ahmad and Luo [1989] dealt with the problem of coordinating a positioning table and a seven axis manipulator. The cartesian motions of the manipulator were selected from a cartesian coordinate nonlinear optimization process to maximize the manipulator maneuverability and avoid manipulator singularities and track motion limits. This process was claimed to be advantageous over pseudo-inverse techniques from the point of view of inaccuracies and computational loads. Suh and Shin [1989] considered the case of coordinated motion of dual-arm carrying a solid object held at two ends. When the object was held rigidly there was no kinematic redundancy. In this work while one arm (leader) was moving, the second arm (follower) was changing grasp position along the object surface while supporting and thereby added one more degree of freedom to the system and consequently gave more maneuvering capability.

1.2.2. *Dynamics*

The dynamics of manipulators is generally discussed in two groups. In the first, the dynamic models and the associated forward and inverse dynamics issues are studied. The second group addresses the control aspects of dynamic models of manipulators. Since the present work focuses only on the inverse dynamics of dual-arm manipulator, the relevant literature is reviewed first, and a brief review of control aspects then follows.

A closed chain mechanism may not be kinematically redundant e.g., a dual-arm manipulator rigidly holding an object in space, where each arm has six degrees of freedom. But if all the manipulator joints are active then torque redundancy does exist. The following discussions are limited to the works related to the dynamics of manipulators having redundancy in actuation.

Hayati [1986] concentrated on the dynamic model of a closed chain (dual-arm with rigidly held object between arms) through Lagrange formulation, while taking care of the interaction forces between the object and the end effector. The task space was decomposed into a position control subspace and a force control subspace; each subspace being controlled independently. Freeman [1987] obtained the dynamic model through principle of virtual work and an inner product operator. Koivo and Unseren [1990] studied the coupling effects between the manipulators due to common rigid load and their impact on the modelling of the closed chain. Huang [1992] presented a unified formulation for constrained robot systems, including dual-arm manipulator holding an object. Thus all the possible systems were of closed chain type. The equations of motion and constraint equation (of algebraic type) were combined to form a "singular system of differential equations" and shown to be an appropriate model to describe the system.

Pennock and Ryuh [1987] considered only six joints as active joints (where torques are to be applied) and rest of the

joints were taken as passive joints. Luh and Zheng [1987] used holonomic constraints to establish the coordinated relationship between the two arms, one called as leader and other as follower. Thus for a desired trajectory they obtained the complete kinematic relations including accelerations and then used Lagrange formulation to get the joint torques of each arm. Zheng and Luh [1988] used a similar approach to consider the dynamics of two arms involved in assembly. Unseren and Koivo [1989,1991] proposed a concept of pseudo velocity and pseudo acceleration to build the reduced order model for a closed chain dynamics. Then a decoupled control was discussed based upon the reduced order model and the generalized contact forces. Walker et al. [1991] concentrated an internal loading of the object in a multi-arm configuration. They introduced "nonsqueezing" pseudo-inverse consistent with the kinematic constraints, and developed motion and squeezing effects. Chiacchio et al. [1991b] developed a systematic method to perform dynamic analysis in the task space for a system composed of multiple arms holding a rigid object. They introduced the term dynamic manipulability ellipsoid to obtain quantitative indices of the system capability, in each configuration, of performing object accelerations along given task space directions. The ellipsoid was derived on the basis of the mapping of object accelerations on to joint driving torques via the proper kineto-static and dynamic equations of the system. Li et al. [1991] performed the dynamic workspace analysis of multi-arm robots (closed chain model) to find the maximum force that the robots can jointly generate at

each point within the common workspace. The problem was posed as an optimization problem with constraints on torque limits of joints and the maximum internal force that the object (in contact with arms) can withstand.

A common approach to resolve the torque redundancy has been generally through posing an optimization problem. Orin and Oh [1981] analysed the dynamics of legged vehicles, or equivalently multiple arm manipulator system forming a closed kinematic chain with a rigid body object. The input torques were determined by taking care of the redundancy in torques through an optimization problem which minimizes the power consumption and optimizes the load sharing between several chains. The works along these lines differ mainly in selecting the optimal performance criteria and in the method of solution. Nakamura et al. [1987] minimized internal forces, later Nakamura [1988] minimized the strain energy of the object; many researchers used the power or electrical energy as the minimization criteria as by Orin and Oh [1981], Carignan and Akin [1988, 1989], Zheng and Luh[1989] etc. An optimal torque distribution by using a quadratic cost function of torques was obtained by Zheng [1989], Carignan and Akin [1988, 1989] and Djurovic et al. [1990]. Zheng and Luh [1988] proposed to reduce the computational complexity by minimizing the forces on the object at the expense of energy consumption. Carignan and Akin [1988] had also added the force minimization and thus broken the problem into two suboptimal problems. Nahon and Angeles [1992a], on the other hand, proposed that minimization of power losses in

the motors is an useful criterion.

The optimization algorithms used in the literature include linear programming [Orin and Oh, 1981], nonlinear programming [Nakamura et al.1987], compact dual linear programming [Cheng and Orin, 1989], quadratic programming [Nahon and Angeles, 1992b] and linear optimal control theory [Tarn et.al 1987]. The debate as to which method is better is inconclusive. Cheng and Orin [1989] proposed that Compact-Dual LP method is computationally efficient while optimizing the contact forces between arms and the object. It was pointed out by Nahon and Angles [1992b] that quadratic programming is better for handling the situations where minimization of internal forces also appears. Instead of an end effector, which can grasp rigidly, they considered fingers to hold an object and this had inequality constraints appearing on the constraint forces.

Tarn et al. [1987] modelled the two-arm closed chain such that the contact of the end effector with the object was assumed to be a revolute joint. The dynamic equations were linearalized and decoupled using differential geometric system theory. Then linear optimal control theory was used to determine control law for torques.

Various control schemes for multi-arm manipulators have been proposed by researchers. Even-though the present work does not deal with this aspect, a brief summary of these works is in order for completeness. Ishida [1977] studied the force control of coordinating arms where instead of using position control the

motor torques at each joint were evaluated. Uchiyama and Dauchez [1988] proposed hybrid position/force controller for coordination of two arms and later Uchiyama and Yamashita [1991] presented experimental results of hybrid control for robust holding of a common object by two arms; these schemes did not consider the dynamic problem. Laroussi et al. [1988] studied the dynamic model of a planar two arm robot and used linear state feedback for control of the system. Seraji [1988], Hu and Goldenberg [1989], and Walker et al. [1989] discussed adaptive control schemes for coordinated motion and force control, Tao and Luh [1991] and Koga et al. [1992] discussed model-reference adaptive controllers for similar considerations. Kazerooni [1988] and Tao et al. [1990] presented compliance control of two arms carrying an object where the force control of one arm at the contact point was of main interest. Schneider and Cannon [1992] discussed the implementation of impedance control. Nonlinear feedback techniques which linearize and decouple the nonlinear dynamic equations were studied by Yun [1989] and Yun and Kumar [1991].

The dynamics and control of multi-arm manipulators have many similar features with those of multifingered hands, e.g. Cole et al. [1992], Montana [1992] and with walking machines, e.g. Shih and Gruver [1992], Kajita et al. [1992] etc.

1.2.3 *Trajectory planning*

The works in trajectory planning area can be broadly classified into two main categories. The first category addresses

the problem of finding a safe path of the manipulator(s) in the work space and is called obstacle avoidance problem. In the second category, trajectory planning is concerned with finding the time histories of joint variables on a safe path which either may have been specified or is to be planned in an obstacle free environment. These time histories (joint position, joint torque etc.) are typically determined through some criteria like minimum time criterion. In this subsection, first a brief review of obstacle avoidance problems is presented and then the works related to finding time histories of joint variables are reviewed.

The classical problem of collision avoidance, both in navigation and manipulation, has been a topic of interest to many researchers. The methods based on characterizing free space have been dealt by Schwartz and Sharir [1983a, 1983b ,1983c], Udapa [1977],Lozano-Perez [1981,1983], Lazano-Perez and Wesley [1979], Brooks [1983,1985], Wenger and Chedmail[1991] and Faverjon [1984]. Khatib [1986] proposed a method of path planning using a potential field concept which was extended by Volpe and Khosla [1990], Hwang and Ahuja [1992], Barraquand et al. [1992], Kim and Khosla [1992]. Gilbert and Jhonson [1985] presented a trajectory planning scheme minimizing a cost function in the presence of obstacles. Besides this, path planning with incomplete information about the environment has also been dealt by Lumelsky, for example in Cheung and Lumelsky [1990].

In the area of collision free motion planning for a multi-robot system, Freund and Hoyer [1985, 1986, 1988] formulated

the problem as a "find path" problem. Erdmann and Lozano-Perez [1987] explored the motion planning problem for multiple moving objects by using configuration space-time technique to handle timevarying constraints imposed on a moving object. Fortune et al. [1986] described an algorithm for finding collision free trajectories for two planar arms by characterizing the combinatorial structure of the configuration space of the two arms. Tournassoud [1986] described a technique for coordinating multiple moving object including manipulators by defining separating planes at each moment and ensuring that the object stays on the opposite sides of them. O'Donnell and Lozano-Perez [1989] posed the trajectory planning problem as scheduling problem in which space was the shared resource and the method decoupled the path specification step from the trajectory specification step. The collisions were avoided by using time without changing the path. Chien and Xue [1992] investigated the problem of planning a collision free path for a dual planar arm carrying a small object. The arms and the object formed a five link closed chain which had to move in a space full of unknown obstacles. Shin and Bien [1989] planned collision free trajectory of two arms along designated path. They introduced the concept of virtual obstacle to consider possible collision between manipulators and adopted virtual coordination space to select a collision free coordination curve. Along this curve they planned the minimum time trajectory satisfying all the dynamic constraints. Lee and Lee [1987] and Lee [1986] modeled the robots as spheres and restricted

each robot to move along a straight path. They approximated the collision regions with rectangles and showed that delaying one robot at its initial position can achieve a smaller travel time than other collision avoidance strategies. Shin and Zheng [1992] have extended the idea of Lee and Lee [1987] with accurate geometric models of robot and allowing arbitrary paths and showed that delaying one robot at its initial position can achieve minimum travel time among all collision avoidance strategies if collision region is connected. Bien and Lee [1992] solved the problem on the similar line. They started by planning time optimal trajectory of each robot independently satisfying the dynamic constraints and then transformed the collision region (defined in the coordination space) into time-versus-traveled length space with the preplanned velocity profile of one robot. In this transformed collision region, a minimal delay in the starting time of the other robot is determined to avoid collision. Jouaneh et al. [1990] considered the problem trajectory planing between a robot and a positioning table. They have posed the trajectory planing problem as minimum time and minimum energy trajectory planing problem and solved by one variable dynamic programing approach. They studied this on a three degrees of freedom robot and a two axes linear positioning table.

Trajectory planning problems in an obstacle free space with dynamic model of a single arm manipulator were studied by several researchers. Kahn and Roth [1971] studied minimum time trajectory planning problem for manipulator travelling between two

end points in which the path was not specified. The constraints imposed were the maximum forces/torques available. Luh and Lin [1981] and Luh and Walker [1977] considered cartesian velocities and accelerations as constraints instead of forces/torques which required experimental identification of cartesian velocity and acceleration bounds. Kim and Shin [1985] developed the method for minimum time path planning in joint space. The path was given in joint space by corner points. They specified absolute tolerance in the path deviation at each corner point and derived joint acceleration bounds from the arm dynamics to utilize the robot capabilities. Vukobratovic and Kircanski [1982] applied dynamic programming for solving optimal trajectory planning problem over a specified path, the forces and torques were bounded and the travel time was also given. Bobrow et al.[1985] devised a specific technique to solve minimum-time trajectory planning problem for a manipulator following a prescribed path and took the bounds on the torque function of the joint angle and angular velocities. Shin and McKay [1986] applied dynamic programming to optimal trajectory generation. They represented the path by a unique scalar parameter and rewrote the dynamic equations in terms of this parameter and its time derivative. The resulting constraints and costs were also represented by these two parameters, and the dynamic programming method applied to grid spanned by them. The technique was limited to path which could be parameterized. Singh and Leu [1987] also solved optimum path planning problem by dynamic programming but instead of parameterized path they

approximated the given path by discrete points in the joint space. Pfeiffer and Johanni [1987] solved the minimum time problem with constant torque limits by constructing switching curves. Hollerbach [1984] identified a time scaling property for the dynamics of a manipulator executing a planned trajectory. The constant time scaling was utilized to ensure dynamically feasible manipulator speeds along a prescribed trajectory.Tan and Potts [1988] proposed a minimum time trajectory planner by discrete approach in contrast to other models which use continuous time model. It included joint velocity, joint torque, and joint jerk constraints and posed the minimum time trajectory planning problem as a nonlinear optimization problem, solved by the "method of approximate programming". Tan and Potts [1989] later modified their trajectory planner by planning the position of the knots such that the time intervals between two consecutive knot points were same. The trajectory planning problem thus was a single nonlinear programming problem applied to a six degrees of freedom manipulator for minimum time and minimum energy case. The trajectory tracking problem for a single arm manipulator was dealt by Johansson [1990] as a quadratic optimal control problem and Chen et al. [1992] also considered the time-optimal control law for tracking problems. Koivo and Arnautovic [1991] discussed the dynamic optimal control for redundant manipulators where they minimized the tracking error along the path together with maximum energy. Gupta and Luh [1991] also used optimal control theory for closed loop control of redundant manipulators where the redundancy

was resolved at the joint acceleration level and then the tracking error and the control was minimized along the path.

Not much work has been reported in the trajectory planning problems of dual-arm manipulators forming a closed chain through a grasped object. Lim and Chyung [1988] dealt with the problem of trajectory planning of a dual-arm manipulator carrying an object as a nonlinear optimization problem but studied only the kinematic aspects. Benhabib and Tabarah [1989] also studied the trajectory planning for point-to point motion of dual-arm manipulators considering only the kinematic aspects in the trajectory planning. They used cubic polynomials for all joint trajectories as means of obtaining continuous joint velocities and accelerations throughout the motion. The main objective of the optimization was to minimize the number of intermediate joint configurations with the primary constaint on joint trajectories such that the task space errors were within specified tolerance values. Moon and Ahmad [1991] considered a similar problem but had considered the constraints on joint torques. The method used was time scaling of the trajectory. They assumed that the velocity profile was given without considering dynamics and checked if the trajectory violated the joint torque limits. In case of torque limit violation they modified the trajectory by time scaling. This approach did not allow optimization of the trajectory according to minimum time or minimum energy criteria.

1.3 Objective and scope of the present work

This work attempts to solve two problems of dual-arm manipulators. The first problem considers an assembly operation by two arms where the arms have kinamatic redundancy and in this problem only the kinamatic inverse solution is aimed at. The assembly operation is considered to be that of peg-in-hole insertion type. The relative movement between the end effectors of two arms is to be specified for the assembly operation. The aim is to show the advantage of assembly with kinematically redundant dual-arm robot where the same assembly operation is performed at different locations in the workspace depending upon the requirements. Traditionally ,the solution is sought by posing an optimization problem. The present work considers three optimization criteria to resolve the kinamatic redundancy. These are used to obtain the minimum velocity norm solution ,minimum acceleration norm solution and increased manipulability solution. Maximization of manipulability criterion leads to a nonlinear optimization (e.g. Lee [1989]) and, therefore, in the present work only the increase in manipulability is sought. Though this process does not yield the maximum manipulabilty at intermediate configurations, but is expected to ensure better manipulable postures (away from the singularity configuration) through a much simpler quadratic optimization problem while keeping the joint movements small.

The second problem attempts to plan the trajectory of a dual-arm manipulator where the two arms form a closed chain through a rigidly grasped object and the path, through which the

object is to be carried, is specified. Each arm has six degrees of freedom and thus the closed chain has no kinematic redundancy but does have torque redundancy as all the manipulator joints are considered to be active. Therefore, this trajectory planning problem involves two main aspects, (i) that of resolving the torque redundancy, and (ii) that of finding optimum time histories of joint variables (position, torque etc.). Though many researchers have investigated the torque redundancy in multi-arm systems (see Section 1.2.2), the trajectory planning through optimum time histories of joint variables has been mainly confined to single arm manipulators (see Section 1.2.3) where if redundancy exists then the redundancy is in actuation as well as in kinematics and so the redundancy can be resolved in the kinematic level (e.g. acceleration). Thereafter the optimal control formulation can be used to solve the minimum time problem. Since the dual-arm system considered in this part of the present work does not have kinematic redundancy , the attempt is to first resolve the torque redundancy and then use this to formulate the optimization problems to solve minimum time and minimum energy problems. A discrete formulation is used to solve the optimization problem which includes all the joint constraints.

1.4 Overview of thesis

This thesis is divided into five chapters. The first problem, addressed to the inverse kinematics of redundant dual-arm manipulator in assembly operation is dealt in Chapter 2. The

formulation of kinematic equations of redundant dual-arm, method of solution and results are discussed in this Chapter. Chapter 3 contains the formulation part of the second problem addressed to the trajectory planning problem of a dual-arm grasping a rigidly held object. This formulation mainly contains the derivation of dynamic equations of dual-arm and resolution of torque redundancy. The discrete models, for solving the problem numerically, are also developed in Chapter 3. Two PUMA-560 arms are used for simulation of the trajectory planning problem and the computed results are presented and discussed in Chapter 4. Finally Chapter 5 reports the concluding remarks and the scope for future work.

CHAPTER 2

INVERSE KINEMATICS OF REDUNDANT DUAL-ARM MANIPULATOR

2.1 Introduction

This chapter discusses the inverse kinematic solutions for a redundant dual-arm manipulator. Redundancy of the dual-arm means that the number of task coordinates is less than the number of joints of the dual-arm and hence the inverse solution is not unique. The problem is stated in Sec. 2.2. The position kinematics and the velocity relationships are discussed in Sec. 2.3 and Sec. 2.4, respectively. The inverse kinematic solution is obtained in Sec. 2.5 by posing the inverse problem as an optimization problem, with three different objective functions corresponding to minimum velocity norm condition , minimum acceleration norm condition and increased manipulability condition. The solution process outlined in Sec. 2.5 considers a general dual-arm manipulator. The results are presented in Sec. 2.6 for a planar dual-arm system and the inverse kinematic solutions obtained through different objective functions are compared.

2.2 Statement of the Problem

A kinematically redundant dual-arm manipulator is considered for peg-in-hole insertion type assembly where each arm takes a mating component. This assembly requires that the relative motion between the peg and the hole should be controlled; the absolute motion of one of the mating parts, say the peg could be anywhere in the workspace.

2.3 Description of the System and Position Kinematics

Figure 2.1 shows two arms to be used in the assembly operation. A cartesian coordinate frame (X_w, Y_w, Z_w) is taken as the reference frame (or world coordinate frame) for task description. The subscript l (l = 1,2) will be used to denote the arm number, i.e. for arm 1 l=1 and for arm 2 l=2. Thus degrees of freedom of lth arm is n_l, i.e. for arm 1 and arm 2 the degrees of freedom are n_1 and n_2, respectively. For lth arm a right-handed coordinate system (X_{l0}, Y_{l0}, Z_{l0}) at the supporting base is established. The translational and rotational relationships between adjacent links are described by Denavit and Hartenberg matrix [Fu et al.,1987]. On each link at its joint axis a cartesian frame is fixed. The coordinate frame (X_{li}, Y_{li}, Z_{li}) corresponds to joint i+1 and is fixed to link i of the lth arm. The $Z_{l\ i-1}$ axis is aligned with the axis of motion (rotary or sliding) of the ith joint of the lth arm. The origin of the ith coordinate system is established at the intersection of Z_{li} and $Z_{l\ i-1}$ axes or at the intersection of the common normal between the Z_{li} and $Z_{l\ i-1}$ axes and the Z_{li} axis. The X_{li} axis is established along the common normal between the $Z_{l\ i-1}$ and Z_{li} axes. The Y_{li} axis is assigned such that X_{li}, Y_{li} and Z_{li} form a right-handed coordinate system. The last coordinate frame of the lth arm is ($X_{l\ n_l}$, $Y_{l\ n_l}$, $Z_{l\ n_l}$). This frame is placed at the centre of hand and is parallel to ($X_{l\ n_l-1}$, $Y_{l\ n_l-1}$, $Z_{l\ n_l-1}$).

The Denavit and Hartenberg representation of a rigid link depends on four geometric parameters associated with each

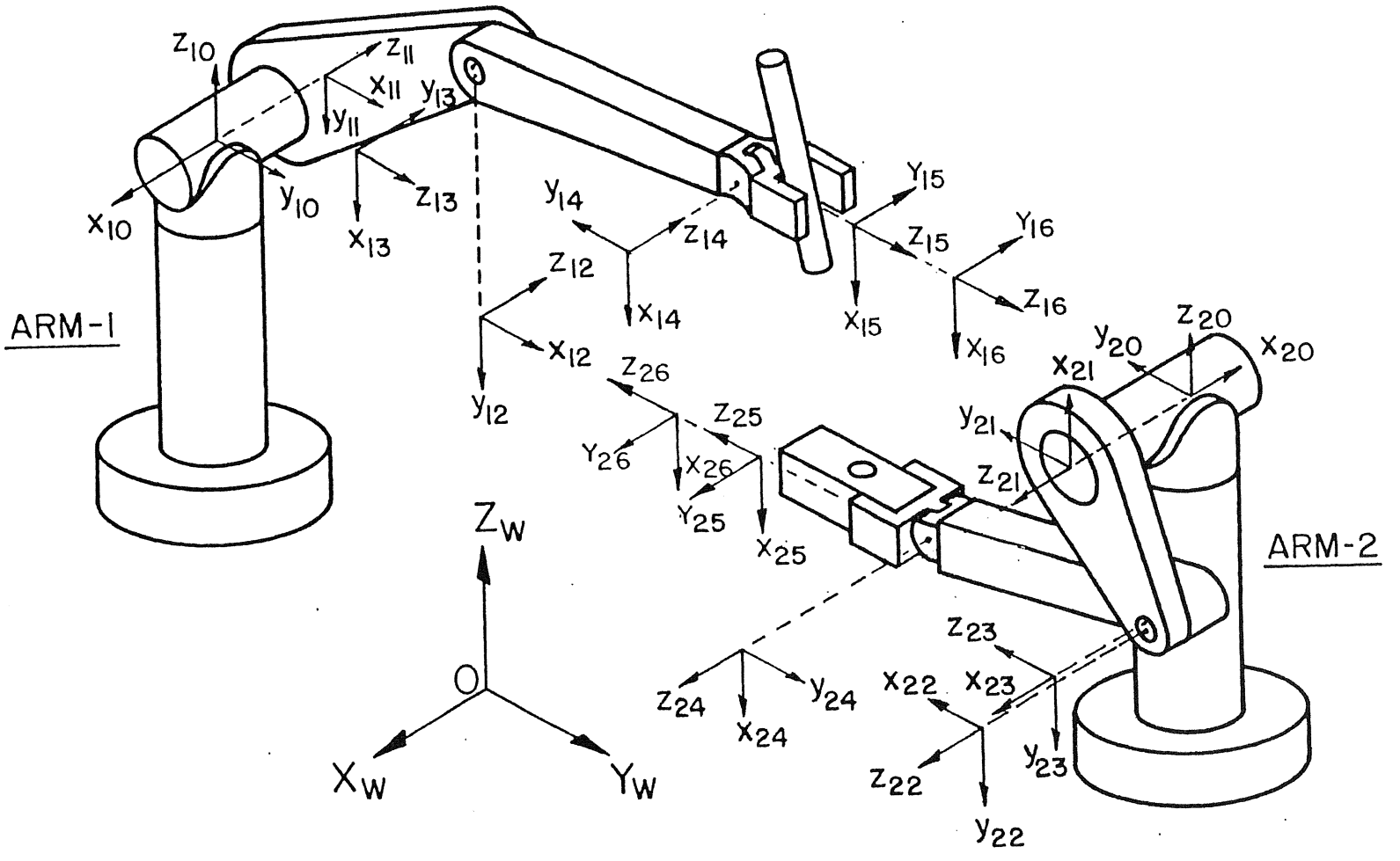

Fig. 2.1 General dual-arm manipulator for assembly

link. These parameters are θ,d,a and α. The angle θ_{1i} is the joint angle between the $X_{1\ i-1}$ axis and the X_{1i} axis about the $Z_{1\ i-1}$ axis using right hand rule. The distance from the origin of the i-1 th coordinate frame to the intersection of the $Z_{1\ i-1}$ axis and the X_{1i} axis along the $Z_{1\ i-1}$ axis is denoted by d_{1i}. The offset distance from the intersection of the $Z_{1\ i-1}$ axis with the $X_{1\ i-1}$ axis to the origin of the ith frame along the X_{1i} axis or the shortest distance between the $Z_{1\ i-1}$ axis and the Z_{1i} axis is expressed by the parameter a_{1i}. The angle α_{1i} is the offset angle from the $Z_{1\ i-1}$ axis to the Z_{1i} arms about the X_{1i} axis using the right hand rule. For a rotary joint i, the parameters d_{1i}, a_{1i}, and α_{1i} remain constant and θ_{1i} is the joint variable that changes when link i moves with respect to link i-1. For a prismatic joint θ_{1i}, a_{1i}, and α_{1i} are joint parameters while d_{1i} is the joint variable.

The position and orientation of the ith link with respect to the i-1 th link of the same arm is expressed by the following Denavit and Hartenberg matrix [Fu et al.,1987]:

$$
{}^{i-1}A_{1i} = \begin{bmatrix}
\cos\theta_{1i} & -\cos\alpha_{1i}\sin\theta_{1i} & \sin\alpha_{1i}\sin\theta_{1i} & a_{1i}\cos\theta_{1i} \\
\sin\theta_{1i} & \cos\alpha_{1i}\cos\theta_{1i} & -\sin\alpha_{1i}\cos\theta_{1i} & a_{1i}\sin\theta_{1i} \\
0 & \sin\alpha_{1i} & \cos\alpha_{1i} & d_{1i} \\
0 & 0 & 0 & 1
\end{bmatrix}
$$

(2.3-1)

The description of the coordinate frame attached to the ith link of the 1th arm with respect to its base frame is expressed by a matrix ${}^{10}T_{1i}$ as

$$^{10}T_{1i} = {}^{0}A_{11}{}^{1}A_{12}\,{}^{2}A_{13}\cdots{}^{i-1}A_{1i} = \prod_{j=1}^{i} {}^{j-1}A_{1j} \quad \text{for } i = 1,2\ldots n_1$$

$$= \begin{bmatrix} {}^{10}R_{1i} & {}^{10}p_{1i} \\ 0 & 1 \end{bmatrix} = \begin{bmatrix} {}^{10}n_{1i} & {}^{10}s_{1i} & {}^{10}a_{1i} & {}^{10}p_{1i} \\ 0 & 0 & 0 & 1 \end{bmatrix} \qquad (2.3\text{-}2)$$

where the 3x3 rotation matrix $^{10}R_{1i}$ gives the orientation of the ith coordinate frame with respect to the base coordinate frame of the 1th arm. The 3x1 vector $^{10}p_{1i}$ is the position vector of the origin of the ith coordinate system with respect to the base coordinate frame of the 1th arm. The vectors $^{10}n_{1i}$, $^{10}s_{1i}$ and $^{10}a_{1i}$ are the unit direction cosine vectors. These vectors in case of end effectors frame are called normal vector, sliding vector and approach vector, respectively (shown in Fig. 2.2). The end effector frame of the 1th arm with respect to the world coordinate frame is given by

$$^{w}T_{1\,n_1} = {}^{w}T_{10}\,{}^{0}T_{1\,n_1} \qquad (2.3\text{-}3)$$

where $^{w}T_{10}$ is the transformation matrix of the base frame of the 1th arm with respect to the world coordinate frame.

For the 1th arm the joint vector is represented by an n_1 dimensional vector q_1 and thus the joint vector of the 1th arm is

$$q_1 = \left[q_{11},\ q_{12}\cdots q_{1\,n_1}\right]^{T} \qquad 1 = 1,2 \qquad (2.3\text{-}4)$$

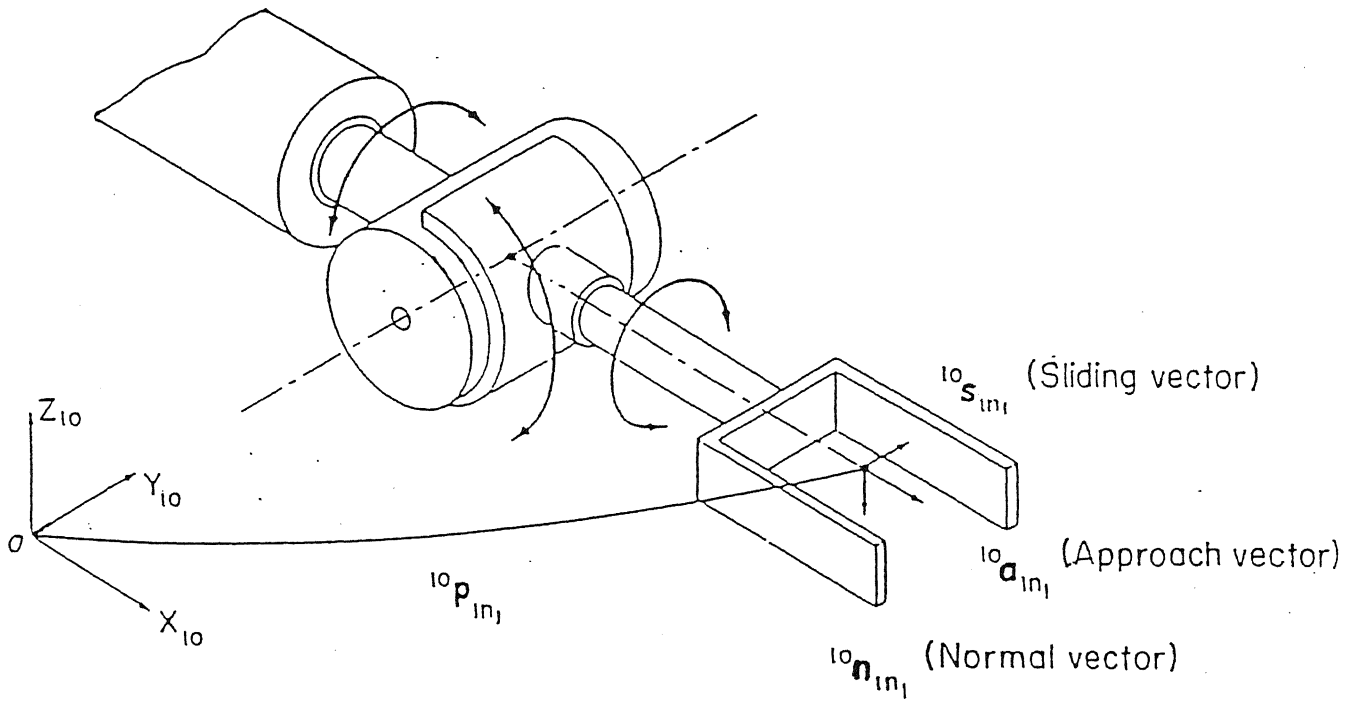

Fig. 2.2 Normal ,sliding and approach vectors of arm 1

where q_{li} denotes the ith joint angle position of the lth arm.

An assembly task with two arms is described by the relative motion of the end effector frame of arm 2 with respect to the end effector frame of arml. The transformation metrix of arm 2 with respect to arml, denoted by T_{rel}, is obtained from

$$ {}^{w}T_{1\ n_1}\ T_{rel} = {}^{w}T_{2\ n_2} $$

$$ \text{or,}\quad T_{rel} = {}^{w}T_{1\ n_1}^{-1}\ {}^{w}T_{2\ n_2} . \qquad (2.3\text{-}5) $$

The matrix T_{rel} is written in the partitioned matrix form as

$$ T_{rel} = \begin{bmatrix} R_{rel} & p_{rel} \\ 0 & 1 \end{bmatrix} \qquad (2.3\text{-}6) $$

where R_{rel} and p_{rel} denote the rotational and translational components, respectively. The rotational matrix R_{rel} is expressed as a function of Euler angles ϕ_{r1}, ϕ_{r2} and ϕ_{r3} in the form as given by (A.1) of Appendix A. This Euler angle vector Φ_{rel}(= $[\phi_{r1}, \phi_{r2}, \phi_{r3}]^T$) represents the orientation of the second end effector with respect to the first end effector. Now ${}^{w}T_{1\ n_1}$ and ${}^{w}T_{2\ n_2}$ are also written in the partitioned form as

$$ {}^{w}T_{1\ n_1} = \begin{bmatrix} {}^{w}R_{1\ n_1} & {}^{w}p_{1\ n_1} \\ 0 & 1 \end{bmatrix} \qquad (2.3\text{-}7) $$

$$ {}^{w}T_{2\ n_2} = \begin{bmatrix} {}^{w}R_{2\ n_2} & {}^{w}p_{2\ n_2} \\ 0 & 1 \end{bmatrix} \qquad (2.3\text{-}8) $$

Thus (2.3-5) yields

$$R_{rel} = {}^{w}R_{1\ n_1}^{T}\ {}^{w}R_{2\ n_2} \qquad (2.3\text{-}9)$$

and $$p_{rel} = {}^{w}R_{1\ n_1}^{T}\left[{}^{w}p_{2\ n_2} - {}^{w}p_{1\ n_1}\right] \qquad (2.3\text{-}10)$$

The right hand side of (2.3-9) is expressed in terms of its direction cosines as

$${}^{w}R_{1\ n_1}^{T}\ {}^{w}R_{2\ n_2} = \begin{bmatrix} n_{rx} & s_{rx} & a_{rx} \\ n_{ry} & s_{ry} & a_{ry} \\ n_{rz} & s_{rz} & a_{rz} \end{bmatrix} \qquad (2.3\text{-}11)$$

2.4 Velocity Relations

The end effector velocity of the 1th arm is described by the six dimensional vector $\left[{}^{w}\dot{p}_{1}{}^{T}_{\ n_1},\ {}^{w}\Omega_{1}{}^{T}\right]^{T}$ which is related to $\dot{q}_1$ by

$$\begin{bmatrix} {}^{w}\dot{p}_{1\ n_1} \\ {}^{w}\Omega_{1} \end{bmatrix} = J_1(q_1)\ \dot{q}_1 \qquad (2.4\text{-}1)$$

where $J_l(q_l)$ is the 6 x n_l manipulator Jacobian matrix relating the end effector velocity and the joint velocity and is discussed in Appendix B, and ${}^{w}\Omega_l$ is the angular velocity of the end effector of the lth arm given as

$$ {}^{w}\Omega_l = \left[{}^{w}\omega_{lx} , {}^{w}\omega_{ly}, {}^{w}\omega_{lz} \right]^T \qquad (2.4\text{-}2) $$

Referring to (B.7) of Appendix B the ith column of $J_l(q_l)$ is determined for the rotational joints by the following relation:

$$ J_{li}(q_l) = \begin{bmatrix} {}^{w}a_{l\ i-1} \times ({}^{w}p_{l\ n_l} - {}^{w}p_{l\ i-1}) \\ {}^{w}a_{l\ i-1} \end{bmatrix} \qquad (2.4\text{-}3) $$

where ${}^{w}R_{l0}$ is the rotational part of ${}^{w}T_{l0}$. The relative angular velocity vector is expressed as

$$ \Omega_{rel} = \left[\omega_{rx} , \omega_{ry}, \omega_{rz} \right]^T \qquad (2.4\text{-}4) $$

where the three components are along the x,y and z axes of the end effector frame of arm 1. This relative angular velocity vector is related to the angular velocity vectors of the two end effectors in the following way.

As $\mathbf{R}_{rel}$ is orthogonal

$$ \mathbf{R}_{rel}\ \mathbf{R}_{rel}^{T} = \mathbf{1} \qquad (2.4\text{-}5) $$

where **1** is 3x3 identity matrix. Differentiating both sides of

(2.4-5) with respect to time t, one gets

$$\frac{d}{dt}\left[R_{rel}\ R_{rel}^{T}\right] = 0 \qquad (2.4\text{-}6)$$

where 0 is the 3x3 null matrix. Now using (A.10) of Appendix A in (2.4-6) one can write [Fu et al.,1987]

$$R_{rel}\ \frac{d}{dt}\left(R_{rel}^{T}\right) = -\frac{d}{dt}\left(R_{rel}\right)R^{T}{}_{rel} = \begin{bmatrix} 0 & \omega_{rz} & -\omega_{ry} \\ -\omega_{rz} & 0 & \omega_{rx} \\ \omega_{ry} & -\omega_{rx} & 0 \end{bmatrix} \qquad (2.4\text{-}7)$$

Using (2.3-9), the quantity $R_{rel}\ \frac{d}{dt}\ (R_{rel}^{T})$ is expanded as

$$R_{rel}\ \frac{d}{dt}\left(R_{rel}^{T}\right) = \left[{}^{w}R_{1}^{T}\ {}_{n_1}\ {}^{w}R_{2}\ {}_{n_2}\right]\ \frac{d}{dt}\ \left[{}^{w}R_{1}^{T}\ {}_{n_1}\ {}^{w}R_{2}\ {}_{n_2}\right]^{T}$$

$$= {}^{w}R_{1}^{T}\ {}_{n_1}\ {}^{w}R_{2}\ {}_{n_2}\ \frac{d}{dt}\left({}^{w}R_{2}^{T}\ {}_{n_2}\right)\ {}^{w}R_{1}\ {}_{n_1} + {}^{w}R_{1}^{T}\ {}_{n_1}\ {}^{w}R_{2}\ {}_{n_2}\ {}^{w}R_{2}^{T}\ {}_{n_2}$$

$$\frac{d}{dt}\left({}^{w}R_{1}\ {}_{n_1}\right) = {}^{w}R_{1}^{T}\ {}_{n_1}\left[{}^{w}R_{2}\ {}_{n_2}\ \frac{d}{dt}\left({}^{w}R_{2}^{T}\ {}_{n_2}\right)\right]\ {}^{w}R_{1}\ {}_{n_1}$$

$$+\ {}^{w}R_{1}^{T}\ {}_{n_1}\ \frac{d}{dt}\left({}^{w}R_{1}\ {}_{n_1}\right) = {}^{w}R_{1}^{T}\ {}_{n_1}\left[\ {}^{w}R_{2}\ {}_{n_2}\ \frac{d}{dt}\left({}^{w}R_{2}^{T}\ {}_{n_2}\right)\right]\ {}^{w}R_{1}\ {}_{n_1}$$

$$+\ {}^{w}R_{1}^{T}\ {}_{n_1}\left[\ {}^{w}R_{1}\ {}_{n_1}\ \frac{d}{dt}\left({}^{w}R^{T}{}_{1}\ {}_{n_1}\right)\right]^{T}\ {}^{w}R_{1}\ {}_{n_1}.$$

(2.4-8)

For each arm, a relation similar to (2.4-7) is used to relate ${}^{w}\Omega_{1}$ of (2.4-2) with the rotation matrix ${}^{w}R_{1\ n_1}$. This yields

$$ {}^{w}R_{1\ n_1}\frac{d}{dt}\left({}^{w}R_{1\ n_1}^{T}\right)=-\frac{d}{dt}\left({}^{w}R_{1\ n_1}\right){}^{w}R_{1\ n_1}^{T}=\begin{bmatrix} 0 & {}^{w}\omega_{1z} & -{}^{w}\omega_{1y} \\ -{}^{w}\omega_{1z} & 0 & {}^{w}\omega_{1x} \\ {}^{w}\omega_{1y} & -{}^{w}\omega_{1x} & 0 \end{bmatrix} \qquad (2.4\text{-}9) $$

and

$$ {}^{w}R_{2\ n_2}\frac{d}{dt}\left({}^{w}R_{2\ n_2}^{T}\right)=-\frac{d}{dt}\left({}^{w}R_{2\ n_2}^{T}\right){}^{w}R_{2\ n_2}^{T}=\begin{bmatrix} 0 & {}^{w}\omega_{2z} & -{}^{w}\omega_{2y} \\ -{}^{w}\omega_{2z} & 0 & {}^{w}\omega_{2x} \\ {}^{w}\omega_{2y} & -{}^{w}\omega_{2x} & 0 \end{bmatrix} \qquad (2.4\text{-}10) $$

Now combine (2.4-7) through (2.4-10) to get

$$ \begin{bmatrix} 0 & \omega_{rz} & -\omega_{ry} \\ -\omega_{rz} & 0 & \omega_{rx} \\ -\omega_{ry} & -\omega_{rx} & 0 \end{bmatrix}={}^{w}R_{1\ n_1}^{T}\begin{bmatrix} 0 & {}^{w}\omega_{2z}-{}^{w}\omega_{1z} & -{}^{w}\omega_{2y}+{}^{w}\omega_{1y} \\ -{}^{w}\omega_{2z}+{}^{w}\omega_{1z} & 0 & {}^{w}\omega_{2x}-{}^{w}\omega_{1x} \\ {}^{w}\omega_{2y}-{}^{w}\omega_{1y} & -{}^{w}\omega_{2x}+{}^{w}\omega_{1x} & 0 \end{bmatrix}{}^{w}R_{1\ n_1} \qquad (2.4\text{-}11) $$

The rotation matrix ${}^{w}R_{l\ n_l}$ is the rotation part of ${}^{w}T_{l\ n_l}$ (2.3-3) and is written in terms of direction cosines as

$$ {}^{w}R_{l\ n_l} = \begin{bmatrix} n_{lx} & s_{lx} & a_{lx} \\ n_{ly} & s_{ly} & a_{ly} \\ n_{lz} & s_{lz} & a_{lz} \end{bmatrix} . \qquad (2.4\text{-}12) $$

Using (2.4-12) in (2.4-11) and comparing the elements of both sides of (2.4-11) one gets

$$ \Omega_{rel} = \begin{bmatrix} \omega_{rx} \\ \omega_{ry} \\ \omega_{rz} \end{bmatrix} = R_{tr} \left[{}^{w}\Omega_2 - {}^{w}\Omega_1 \right] \qquad (2.4\text{-}13) $$

where

$$ R_{tr} = \begin{bmatrix} s_{ly}a_{lz}-s_{lz}a_{ly} & -s_{lx}a_{lz}+s_{lz}a_{lx} & s_{lx}a_{ly}-s_{ly}a_{lx} \\ a_{ly}n_{lz}-a_{lz}n_{ly} & -a_{lx}n_{lz}+a_{lz}n_{lx} & a_{lx}n_{ly}-a_{ly}n_{lx} \\ n_{ly}s_{lz}-n_{lz}s_{ly} & -n_{lx}s_{lz}+n_{lz}s_{lx} & n_{lx}s_{ly}-n_{ly}s_{lx} \end{bmatrix} $$

$$ = \left[\mathbf{s}_l \times \mathbf{a}_l \quad \mathbf{a}_l \times \mathbf{n}_l \quad \mathbf{n}_l \times \mathbf{s}_l \right]^T = \left[\mathbf{n}_l \ \mathbf{s}_l \ \mathbf{a}_l \right]^T $$

or $R_{tr} = {}^{w}R_{1}^{T}\, n_1$. (2.4-14)

The relative linear velocity of the second end effector with respect to the first end effector is determined by differentiating (2.3-10) with respect to time to get

$$\dot{p}_{rel} = \frac{d}{dt}\left[{}^{w}R_1^T\, n_1\left[{}^{w}p_{2\, n_2} - {}^{w}p_{1\, n_1}\right]\right] = \frac{d}{dt}\left({}^{w}R_1^T\, n_1\right)\left[{}^{w}p_{2\, n_2} - {}^{w}p_{1\, n_1}\right]$$

$$+ {}^{w}R_1^T\, n_1\left[{}^{w}\dot{p}_{2\, n_2} - {}^{w}\dot{p}_{1\, n_1}\right] = {}^{w}R_1^T\, n_1\left[{}^{w}R_{1\, n_1}\frac{d}{dt}\left({}^{w}R_1^T\, n_1\right)\right]$$

$$\left[{}^{w}p_{2\, n_2} - {}^{w}p_{1\, n_1}\right] + {}^{w}R_1^T\, n_1\left[{}^{w}\dot{p}_{2\, n_2} - {}^{w}\dot{p}_{1\, n_1}\right] . \quad (2.4\text{-}15)$$

In order to expand the above equation, the vector ${}^{w}p_{1\, n_1}$ and ${}^{w}p_{2\, n_2}$ are written in terms of its elements as

$${}^{w}p_{1\, n_1} = \begin{bmatrix} p_{1x} \\ p_{1y} \\ p_{1z} \end{bmatrix} \quad (2.4\text{-}16)$$

$${}^{w}p_{2\, n_2} = \begin{bmatrix} p_{2x} \\ p_{2y} \\ p_{2z} \end{bmatrix} \quad (2.4\text{-}17)$$

Substitution of (2.4-9), (2.4-16) and (2.4-17) in (2.4-15) yields

$$\dot{p}_{rel} = {}^{w}R_{l\ n_l}^{T}\ S_p\ {}^{w}\Omega_l + {}^{w}R_{l\ n_l}^{T}\left[{}^{w}\dot{p}_{2\ n_2} - {}^{w}\dot{p}_{l\ n_l}\right] \qquad (2.4\text{-}18)$$

where S_p is a skew-symmetric matrix given by

$$S_p = \begin{bmatrix} 0 & -(p_{2z}-p_{1z}) & (p_{2y}-p_{1y}) \\ (p_{2z}-p_{1z}) & 0 & -(p_{2x}-p_{1x}) \\ -(p_{2y}-p_{1y}) & (p_{2x}-p_{1x}) & 0 \end{bmatrix}$$

and the linear velocity of the end effector of the lth arm is denoted by ${}^{w}\dot{p}_{l\ n_l}$. Now the relative angular velocity vector from (2.4-13) and the relative linear velocity vector from (2.4-18) are combined as

$$\begin{bmatrix} \dot{p}_{rel} \\ \Omega_{rel} \end{bmatrix} = \begin{bmatrix} -{}^{w}R_{l\ n_l}^{T} & {}^{w}R_{l\ n_l}^{T}\ S_p \\ 0_{3\times3} & -{}^{w}R_{l\ n_l}^{T} \end{bmatrix} \begin{bmatrix} {}^{w}\dot{p}_{l\ n_l} \\ {}^{w}\Omega_l \end{bmatrix} + \begin{bmatrix} {}^{w}R_{l\ n_l}^{T} & 0_{3\times3} \\ 0_{3\times3} & {}^{w}R_{l\ n_l}^{T} \end{bmatrix} \begin{bmatrix} {}^{w}\dot{p}_{2\ n_2} \\ {}^{w}\Omega_2 \end{bmatrix} \qquad (2.4\text{-}19)$$

Where $0_{3\times3}$ is a 3x3 null matrix. The end effector velocity vectors, namely $\left[{}^{w}\dot{p}_{l\ n_l}^{T}, {}^{w}\Omega_{l}^{T}\right]_{l=1,2}^{T}$ are related to the joint velocity vectors of the respective arm through (2.4-1). Therefore, the relative velocities can now be related to the joint velocities of both arms as

$$\begin{bmatrix} \dot{p}_{rel} \\ \Omega_{rel} \end{bmatrix} = J_{rel}\ \dot{q}_{aug} \qquad (2.4\text{-}20)$$

where the augmented joint velocity vector $\dot{q}_{aug}$ is

$$\dot{q}_{aug} = \left[\dot{q}_{11}, \dot{q}_{12}\ldots\dot{q}_{1\ n_1}, \dot{q}_{21},\ldots\dot{q}_{2\ n_2}\right]^{T}, \qquad (2.4\text{-}21)$$

J_{rel} will be called relative Jacobian matrix and is given by

$$J_{rel} = [J_{rel1} \quad J_{rel2}] \qquad (2.4\text{-}22)$$

where

$$J_{rel1} = \begin{bmatrix} -{}^{w}R_{1\ n_1}^{T} & {}^{w}R_{1\ n_1}^{T}\ S_p \\ 0_{3\times3} & -{}^{w}R_{1\ n_1}^{T} \end{bmatrix} J_1 \qquad (2.4\text{-}23)$$

and

$$J_{rel2} = \begin{bmatrix} {}^{w}R_1^T\, n_1 & 0_{3\times3} \\ 0_{3\times3} & {}^{w}R_1^T\, n_1 \end{bmatrix} J_2 \quad . \qquad (2.4\text{-}24)$$

As the prescribed rotation matrix R_{rel} in (2.3-6) is in terms of Euler angles ($\Phi_{rel} = [\phi_{r1},\ \phi_{r2},\ \phi_{r3}]^T$), the relative angular velocity vector Ω_{rel} in (2.4-20) is also expressed in terms of the rate of change of Euler angles as detailed in Appendix A. Thus (A.11) of Appendix A together with (2.4-20) leads to

$$\begin{bmatrix} \dot{p}_{rel} \\ \dot{\Phi}_{rel} \end{bmatrix} = J_r\, \dot{q}_{aug} \qquad (2.4\text{-}25)$$

where

$$J_r = J_{er}\ J_{rel} \quad , \qquad (2.4\text{-}26)$$

$$J_{er} = \begin{bmatrix} 1_{3\times3} & 0_{3\times3} \\ 0_{3\times3} & R_{er}^T \end{bmatrix} \quad , \qquad (2.4\text{-}27)$$

and the rotational matrix R_{er} is

$$R_{er} = \begin{bmatrix} 0 & \cos\phi_{r1} & \sin\phi_{r1}\sin\phi_{r2} \\ 0 & \sin\phi_{r2} & -\cos\phi_{r1}\sin\phi_{r2} \\ 1 & 0 & \cos\phi_{r2} \end{bmatrix} . \qquad (2.4\text{-}28)$$

2.5 Solution Procedure

In this work an assembly operation by a dual-arm manipulator is described by the relative path of the second end effector with respect to the first end effector. For kinematic computation, this relative path is defined by a sequence of knot points, i.e. at these knot points the six independent quantities p_{rel} and Φ_{rel} are defined. Next the transformation matrices T_{rel} are computed at these knot points using (2.3-6) and (A.1) of Appendix A. T_{rel} can also be expressed as a function of the joint vector q_{aug} through (2.3-1) to (2.3-5) and (2.4-21). As q_{aug} has $n_1+n_2(>6)$ elements, the number of unknowns is more than the number of equations and hence the system of equations has no unique solution, i.e. the inverse position kinematic solution is not unique and the system has redundancy of order n_1+n_2-6.

The kinematic redundancies prohibit a straightforward inverse solution. Therefore, this work follows the solution through incremental kinematics by imposing additional constraints on the kinematic behaviour. The following three kinematic criteria have been considered in this work:

Case I. The norm of the joint velocity vector $\dot{q}_{aug}$ at each knot point should be minimum,

Case II. The norm of the joint acceleration vector $\ddot{q}_{aug}$ at each

knot point should be minimum,

Case III. The manipulability at each knot point should be made large.

The conditions for these three cases are now discussed sequantially. Since the following procedures aim to solve for the joint velocities and joint accelerations only locally (i.e., the complete end effector paths are not used to derive instantaneous kinematic relationships), the velocity and acceleration terms are replaced by the equivalent incremental terms with the assumption that distance between the successive knot points is covered in unit time step.

Case I: The minimum norm of joint velocity vector, i.e. $\dot{q}_{aug}^T \dot{q}_{aug}$ is to be minimized (so that with lower joint velocity the required task space velocity can be achieved), where the joint space velocity vector is related to the task space velocity vector by (2.4-25). This problem is posed as

$$\text{minimize } \dot{q}_{aug}^T \dot{q}_{aug} \qquad (2.5\text{-}1)$$

$$\text{subject to } \begin{bmatrix} \dot{p}_{rel} \\ \dot{\Phi}_{rel} \end{bmatrix} = J_r \dot{q}_{aug} \quad . \qquad (2.5\text{-}2)$$

The above minimization problem is written in incremental form as

$$\text{minimize } \Delta q_{aug}^T \Delta q_{aug} \qquad (2.5\text{-}3)$$

$$\text{subject to} \begin{bmatrix} \Delta p_{rel} \\ \Delta \Phi_{rel} \end{bmatrix} = J_r \, \Delta q_{aug} \qquad (2.5\text{-}4)$$

where Δq_{aug}, Δp_{rel} and $\Delta \Phi_{rel}$ are incremental changes of q_{aug}, p_{rel} and Φ_{rel} respectively between the "current" knot point and the "next" knot point.

Case II: The norm of joint acceleration, i.e. $\ddot{q}_{aug}^T \ddot{q}_{aug}$ is minimized because this may indirectly reduce the joint torques and velocity fluctuations. This minimization problem should satisfy the constraint equation relating the joint space acceleration and the task space acceleration. The acceleration constraint equation is obtained by differentiating (2.5-2). Thus the problem is posed as

$$\text{minimize} \quad \ddot{q}_{aug}^T \ddot{q}_{aug} \qquad (2.5\text{-}5)$$

$$\text{subject to} \begin{bmatrix} \ddot{p}_{rel} \\ \ddot{\Phi}_{rel} \end{bmatrix} = J_r \, \ddot{q}_{aug} + \dot{J}_r \dot{q}_{aug} \qquad (2.5\text{-}6)$$

The expresions in (2.5-5) and (2.5-6) are written in incremental form as

$$\text{minimize} \quad \left[\Delta q_{aug} - \Delta q_{augp}\right]^T \left[\Delta q_{aug} - \Delta q_{augp}\right] \qquad (2.5\text{-}7)$$

$$\text{subject to} \begin{bmatrix} \Delta p_{rel} - \Delta p_{relp} \\ \Delta \Phi_{rel} - \Delta \Phi_{relp} \end{bmatrix} = J_r \left[\Delta q_{aug} - \Delta q_{augp}\right] + \Delta J_r \Delta q_{aug} \qquad (2.5\text{-}8)$$

where Δp_{relp}, $\Delta \Phi_{relp}$, and Δq_{augp} are incremental changes of p_{rel}, Φ_{rel} and q_{aug} between the previous knot point and the "current" knot point, and ΔJ_r is approximated as the change in J_r at the current knot point and the previous knot point.

Case III: The manipulability is mainly used to avoid the dual-arm postures with kinematic singularity. The measure of manipul- ability is determined from the manipulability ellipsoid. The manipulability ellipsoid is described by the following equation [Yoshikawa, 1984; Lee, 1989; Chiacchio et al.,1991a];

$$\begin{bmatrix} \Delta p_{rel} \\ \Delta \Phi_{rel} \end{bmatrix}^T [J_r J_r^T]^{-1} \begin{bmatrix} \Delta p_{rel} \\ \Delta \Phi_{rel} \end{bmatrix} = 1 \quad . \qquad (2.5\text{-}9)$$

From (2.5-9), the manipulability of the redundant dual arm is defined as

$$mp = \sqrt{\det[J_r J_r^T]} \quad . \qquad (2.5\text{-}10)$$

It is noted here that for a given p_{rel} and Φ_{rel}, there are infinitely possible postures due to kinematic redundancy. One approach could be to search for those postures for which the manipulability is maximum at each knot point. This gain in manipulability is obviously at the expense of large joint movements. Therefore, instead of maximizing the manipulablity alone, the criterion in this case is to have a larger value of the manipulability while maintaining that the changes in joint angles between successive knot points should not be unduly large. This is

achieved by changing Δq_{aug} between successive knot points along the maximum change in manipulability, where Δq_{aug} is also restricted by adding a penality on the joint displacements (as will be seen later in (2.5-12)). The change in manipulability can be described as a linear function of the change of joint vector as

$$\Delta(mp) = \sum_{i=1}^{n_1+n_2} \frac{\partial(mp)}{\partial q_{aug}}(i)\ \Delta q_{aug}(i) = \sum_{i=1}^{n_1+n_2} mc(i)\ \Delta q_{aug}(i)$$

$$\text{or, } \Delta(mp) = \mathbf{mc}^T \Delta q_{aug} \qquad (2.5\text{-}11)$$

where $mc(i) = \frac{\partial(mp)}{\partial q_{aug}}(i)$. Thus $\mathbf{mc}$ is the vector having n_1+n_2 elements, and $\Delta(mp)$ is to be maximized while restricting Δq_{aug} through (2.5-3) and subject to the constraint (2.5-4). Now intead of dealing separately with the above three performance criteria, a single minimization problem is posed from which all the three cases are derived. The objective function (2.5-7) and the constraint (2.5-8) reduce to those for minimum velocity norm, i.e. (2.5-3) and (2.5-4), respectively, for $\Delta q_{augp} = 0$, $\Delta p_{relp} = \Delta\Phi_{relp} = 0$ and $\Delta J_r = 0$. Therefore, the minimum acceleration criterion and the increased manipulability criterion are combined to get the following minimization problem.

$$\text{minimize } Z_{um} = \beta_u \left[\Delta q_{aug} - \Delta q_{augp}\right]^T \left[\Delta q_{aug} - \Delta q_{augp}\right] - \beta_m\ \mathbf{mc}^T \Delta q_{aug} \qquad (2.5\text{-}12)$$

$$\text{subject to } \begin{bmatrix} \Delta p_{rel} - \Delta p_{relp} \\ \Delta \Phi_{rel} - \Delta \Phi_{relp} \end{bmatrix} = \Delta J_r \Delta q_{aug} + J_r \left[\Delta q_{aug} - \Delta q_{augp} \right] \tag{2.5-13}$$

where, β_u and β_m are the weightages assigned to minimum joint acceleration and increased manipulability criteria, respectively. Since the manipulability is to be increased, its sign is inverted in the minimization problem. For convenience of writting, a task vector tr_{rel} is introduced as

$$tr_{rel} = \begin{bmatrix} p_{rel} \\ \Phi_{rel} \end{bmatrix} . \tag{2.5-14}$$

Thus the constraint (2.5-13) is rewritten as

$$\Delta tr_{rel} - \Delta tr_{relp} - \Delta J_r \, \Delta q_{aug} - J_r \left[\Delta q_{aug} - \Delta q_{augp} \right] = 0 \tag{2.5-15}$$

$$\text{where, } \Delta tr_{relp} = \begin{bmatrix} \Delta p_{relp} \\ \Delta \Phi_{relp} \end{bmatrix} \tag{2.5-16}$$

$$\text{and } \Delta tr_{rel} = \begin{bmatrix} \Delta p_{rel} \\ \Delta \Phi_{rel} \end{bmatrix} \tag{2.5-17}$$

For the minimization of the above problem the lagrangian is formed as

$$L = \beta_u \left[\Delta q_{aug} - \Delta q_{augp} \right]^T \left[\Delta q_{aug} - \Delta q_{augp} \right] - \beta_m \, mc^T \Delta q_{aug}$$

$$-\lambda^T \left[\Delta tr_{rel} - \Delta tr_{relp} - \Delta J_r \, \Delta q_{aug} - J_r \left[\Delta q_{aug} - \Delta q_{augp}\right]\right] = 0 \qquad (2.5\text{-}18)$$

where λ is the undetermined multiplier vector. To determine the optimum values of Δq_{aug} the following canditions should be satisfied.

$$\frac{\partial L}{\partial(\Delta q_{aug})} = 0 \qquad (2.5\text{-}19)$$

$$\frac{\partial L}{\partial \lambda} = 0 \qquad (2.5\text{-}20)$$

Equations (2.5-18) and (2.5-19) yield

$$2\beta_u \left[\Delta q_{aug} - \Delta q_{augp}\right] - \beta_m \, mc + \Delta J_r^T \lambda + J_r^T \lambda = 0$$

$$\text{or,} \quad \left[J_r^T + \Delta J_r{}^T\right]\lambda = \beta_m \, mc - 2\beta_u \left[\Delta q_{aug} - \Delta q_{augp}\right] . \qquad (2.5\text{-}21)$$

Multiply both sides of (2.5-21) by $J_r + \Delta J_r$ and use (2.5-15) to obtain

$$\left[J_r + \Delta J_r\right]\left[J_r^T + \Delta J_r{}^T\right]\lambda = \beta_m \left[J_r + \Delta J_r\right] mc$$

$$- 2\beta_u \left[J_r + \Delta J_r\right]\left[\Delta q_{aug} - \Delta q_{augp}\right]$$

$$= \beta_m \left[J_r + \Delta J_r\right] mc - 2\beta_u \left[\Delta tr_{rel} - \Delta tr_{relp} - \Delta J_r \, \Delta q_{augp}\right]$$

$$\text{or, } \lambda = \left[[J_r + \Delta J_r][J_r + \Delta J_r]^T\right]^{-1} \left[\beta_m \left[J_r + \Delta J_r\right] mc - 2\beta_u \left[\Delta tr_{rel} - \Delta tr_{relp} - \Delta J_r \Delta q_{augp}\right]\right] \qquad (2.5\text{-}22)$$

Combine (2.5-22) and (2.5-21) to get

$$\left[J_r + \Delta J_r\right]^T \left[[J_r + \Delta J_r][J_r + \Delta J_r]^T\right]^{-1} \left[\beta_m \left[J_r + \Delta J_r\right] mc - 2\beta_u \left[\Delta tr_{rel} - \Delta tr_{relp} - \Delta J_r \Delta q_{augp}\right]\right]$$

$$= \beta_m mc - 2\beta_u \left[\Delta q_{aug} - \Delta q_{augp}\right] \qquad (2.5\text{-}23)$$

Introducing J_{ri} as

$$J_{ri} = \left[J_r + \Delta J_r\right]^T \left[[J_r + \Delta J_r][J_r + \Delta J_r]^T\right]^{-1} , \qquad (2.5\text{-}24)$$

the relation (2.5-23) is rewritten as

$$J_{ri} \left[\beta_m \left[J_r + \Delta J_r\right] mc - 2\beta_u \left[\Delta tr_{rel} - \Delta tr_{relp} - \Delta J_r \Delta q_{augp}\right]\right]$$

$$= \beta_m mc - 2\beta_u \left[\Delta q_{aug} - \Delta q_{augp}\right]$$

$$\text{or, } \Delta q_{aug} = \left[1 - J_{ri}\Delta J_r\right] \Delta q_{augp} + \frac{\beta_m}{2\beta_u} \left[1 - J_{ri}\left[J_{ri}\Delta J_r\right]\right] mc$$

$$+ J_{ri} \left[\Delta tr_{rel} - \Delta tr_{relp}\right] \qquad (2.5\text{-}25)$$

where 1 is an unit matrix of order $n_1 + n_2$. From (2.5-25) the value of Δq_{aug} for all the individual cases may be determined as follows:

Case I : Minimum velocity norm is obtained by putting

$$\Delta q_{augp} = 0 \ , \quad \Delta tr_{relp} = 0 \ , \quad \Delta J_r = 0 \ , \ \beta_m = 0, \text{ and } \beta_u \neq 0.$$

Then (2.5-24) and (2.5-25) reduce to

$$J_{ri} = J_r^T \left[J_r J_r^T\right]^{-1} \qquad (2.5\text{-}26)$$

and

$$\Delta q_{aug} = J_{ri} \Delta tr_{rel} \qquad (2.5\text{-}27)$$

where the right hand sides are determined from (2.4-26) and (2.5-17).

Case-II : Minimum acceleration norm solutions requires $\beta_m = 0$ and $\beta_u \neq 0$. Therefore, J_{ri} is calculated from (2.5-24) and the solution (2.5-25) yields

$$\Delta q_{aug} = \left[1 - J_{ri} \Delta J_r\right] \Delta q_{augp} + J_{ri} \left[\Delta tr_{rel} - \Delta tr_{relp}\right] \ . \qquad (2.5\text{-}28)$$

Case-III : Increased manipulability solution is obtained by using

$$\Delta q_{augp} = 0 \ , \ \Delta tr_{relp} = 0 \ , \text{ and } \ \Delta J_r = 0.$$

Use of these conditions in (2.5-25) implies that

$$J_{ri} = J_r \left[J_r J_r^T\right]^{-1} \ , \qquad (2.5\text{-}29)$$

and

$$\Delta q_{aug} = \frac{\beta_m}{2\beta_u}\left[1 - J_{ri}J_r\right] mc + J_{ri}\,\Delta tr_{rel} \quad . \qquad (2.5\text{-}30)$$

2.6 Results and Discussion

This section presents the results for the inverse kinematics problem encountered in a peg-in-hole type assembly operation with a redundant planar dual-arm manipulator shown in Fig.2.3. All the manipulator joints are of revolute type. The associated transformation matrices and the Jacobian matrices for this dual-arm manipulator are detailed is Appendix C.

Both the arms are indentical with the following dimensions (see Fig.2.3):

$a_{11} = a_{21} = 50$ cm, $a_{12} = a_{22} = a_{13} = a_{23}$ 25 cm, $b_s = 125$ cm.

The assembly operation is specified by the relative path between the two end effectors (i.e., between the peg and the hole) which is inputed as T_{rel} (see (2.3-5)), where R_{rel} is computed from the specified orientations through Euler angles = Φ_{rel}. The results are presented for the following values of Φ_{rel} and p_{rel}:

The orientation remains constant and is given by $\Phi_{rel} = \begin{bmatrix} \pi & \text{rad.} \\ 0 & \text{rad.} \\ 0 & \text{rad.} \end{bmatrix}$.

(2.6-1)

At the initial stage of assembly, $p_{reli} = \begin{bmatrix} 70 & \text{cm.} \\ 0 & \text{cm.} \\ 0 & \text{cm.} \end{bmatrix}$. (2.6-2)

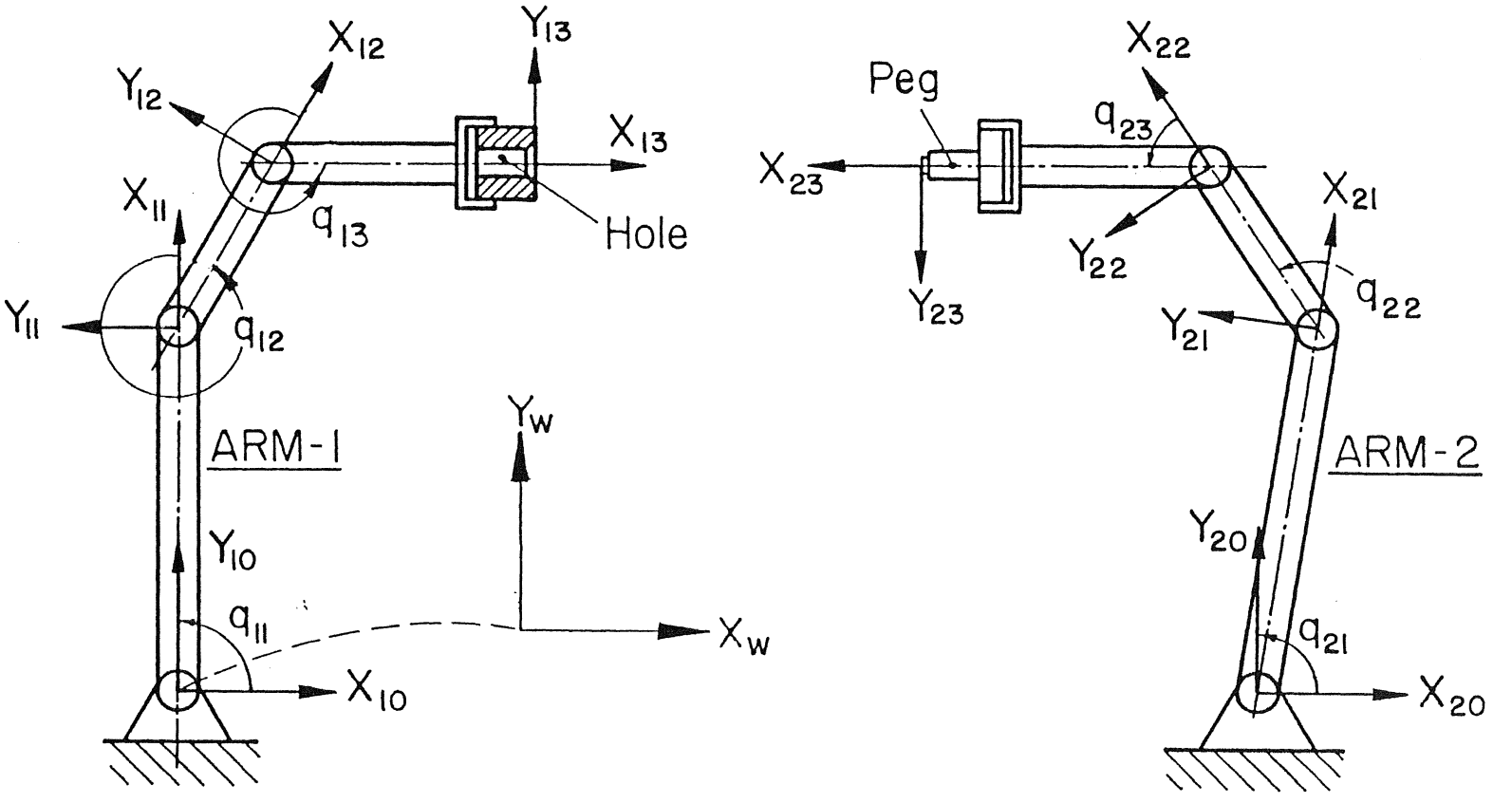

Fig. 2.3 Planar dual-arm manipulator for assembly

At the final stage of assembly, $p_{relf} = \begin{bmatrix} 10 \text{ cm.} \\ 0 \text{ cm.} \\ 0 \text{ cm.} \end{bmatrix}$. (2.6-3)

Thus the two end effectors move towards each other covering a distance of 60 cm along the straight relative path. This relative path is approximated by a sequence of equally spaced 21 knot points. The starting point is designated as the zeroeth knot point and so the final point on the path becomes the twentieth knot point. Thus p_{rel} gets reduced by $[3 \quad 0 \quad 0]^T$ between two subsequent knot points and Φ_{rel} remains constant at the value given by (2.6-1). Thus at the kth knot point (k=0,1,2,...,19), (2.5-17) implies that

$$\Delta tr_{rel} = [-3, \ 0,0,0,0,0]^T \ , \qquad (2.6-4)$$

and (2.5-16) implies that for the kth knot point (k=1,2...,19)

$$\Delta tr_{relp} = [0,0,0,0,0,0]^T \ . \qquad (2.6-5)$$

The inverse solutions (2.5-27), (2.5-28) and (2.5-30) also require the evaluation of J_{ri}, ΔJ_r and Δq_{augp} at each knot point. J_{ri} is evaluated with the help of (2.4-3), (2.4-22) to (2.4-24), (2.4-26) to (2.4-28), and (2.5-26). ΔJ_r and Δq_{augp} are needed in (2.5-28) and are evaluated from

$$\Delta J_r(k) = J_r(k) - J_r(k-1)$$

$$\Delta q_{augp}(k) = q_{aug}(k) - q_{aug}(k-1) , \qquad k = 1,2 \quad ,19 \tag{2.6-6}$$

The initial configuration of the dual-arm for the above mentioned assembly problem has been taken as

q_{11}= 20.38 deg. , q_{12}= 111.08 deg. , q_{13}= -122.1 deg.,

q_{21}= 43.15 deg. , q_{22}= 77.56 deg. , q_{23}= 68.66 deg.

The inverse kinematic solutions are presented for the following four cases :

Case 1 : Minimum velocity norm solution from (2.5-27).

Case 2 : Minimum acceleration norm solution from (2.5-28) with $\Delta tr_{rel} = \Delta tr_{relp}$ as the knot points are equispaced.

Case 3 : Increased manipulability solution from (2.5-30) with β_m/β_u= 5 at each knot point along the relative path.

Case 4 : Increased manipulability solution from (2.5-30) where the factor β_m/β_u increases in the steps of 0.25 at each knot point starting with the value zeroeth knot point.

Figures 2.4 to 2.6 show the obtained positions for joints of arm 1 for the four cases mentioned above and Figs. 2.7 to 2.9 show the results for arm 2 . The slope of the position curves for all the joints corresponding to case 2 is seen to be nearly constant as the joint accelerations are being minimized. Also from the beginning to the end of assembly ,the maximum displacements in the joints are for case 3. This is again expected since increasing manipulability requires movements in the joints which do not contribute to the end effector movements. These large joint movements are avoided in case 4 by gradually increasing the

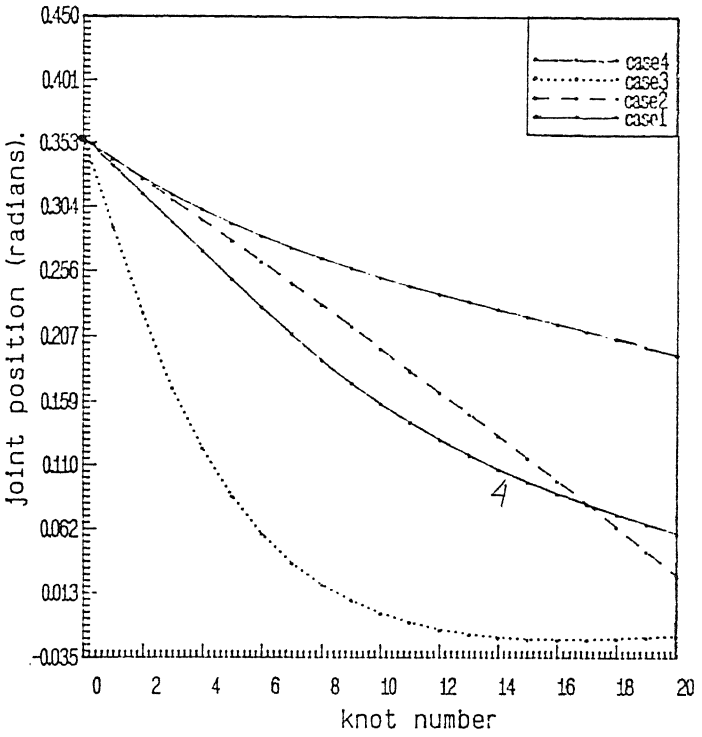

Fig. 2.4 Positions of joint 1 for arm 1 based on four performance criteria

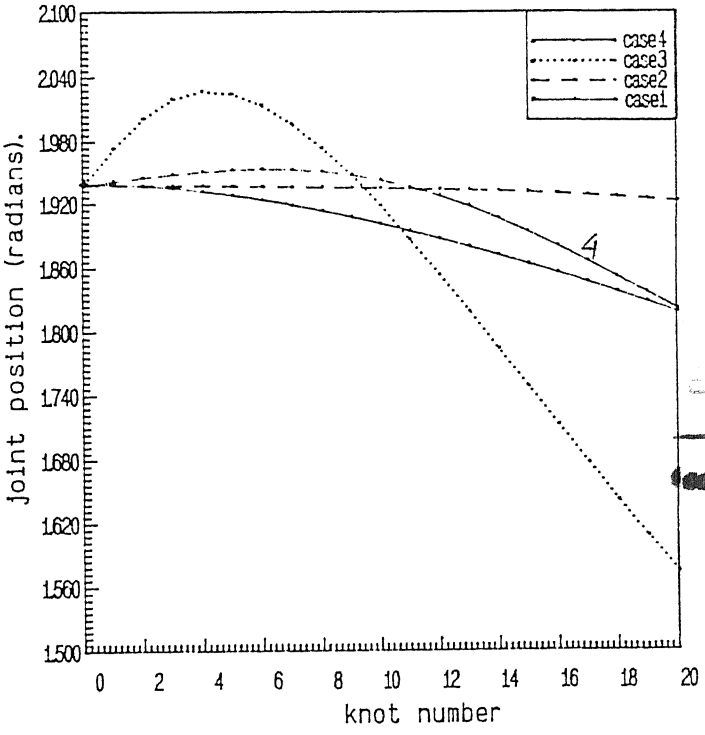

Fig. 2.5 Positions of joint 2 for arm 1 based on four performance criteria

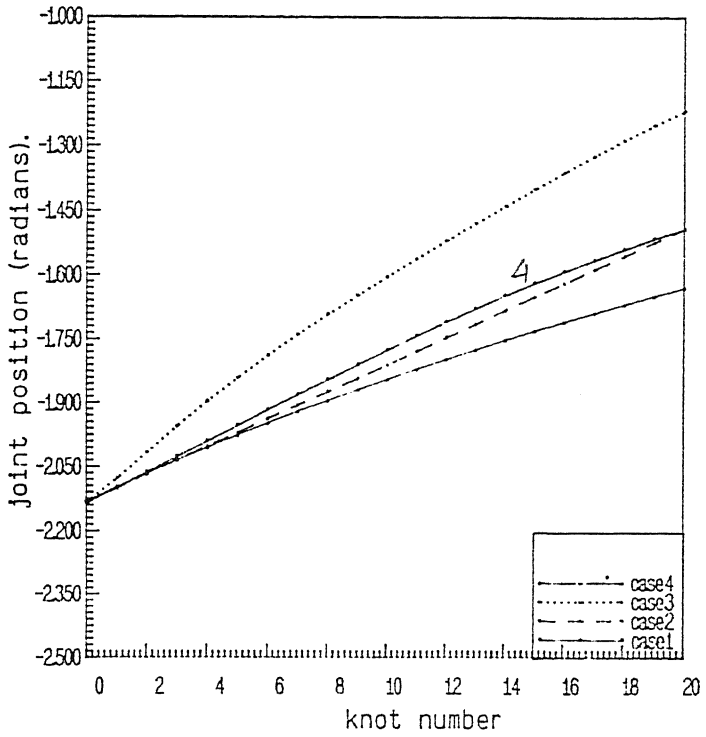

Fig. 2.6 Positions of joint 3 for arm 1 based on four performance criteria

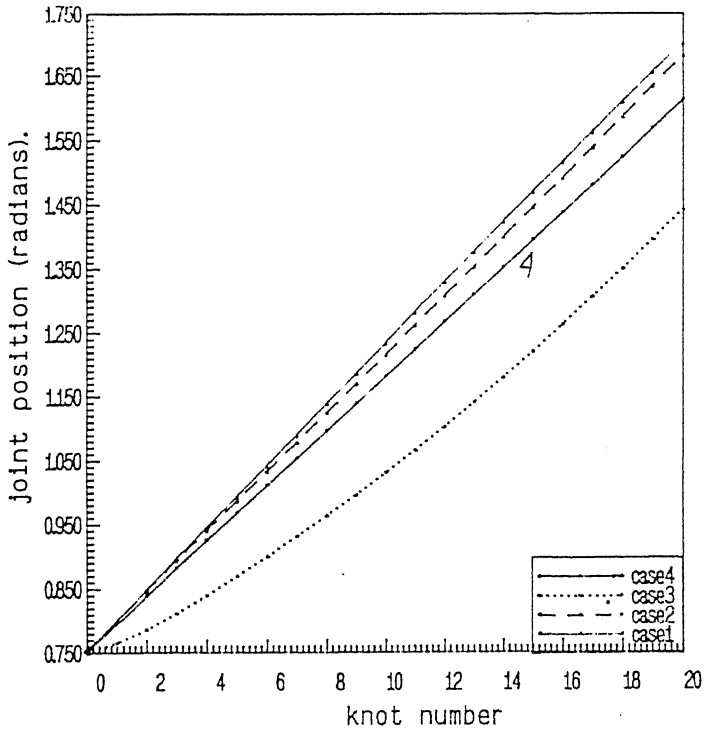

Fig. 2.7 Positions of joint 1 for arm 2 based on four performance criteria

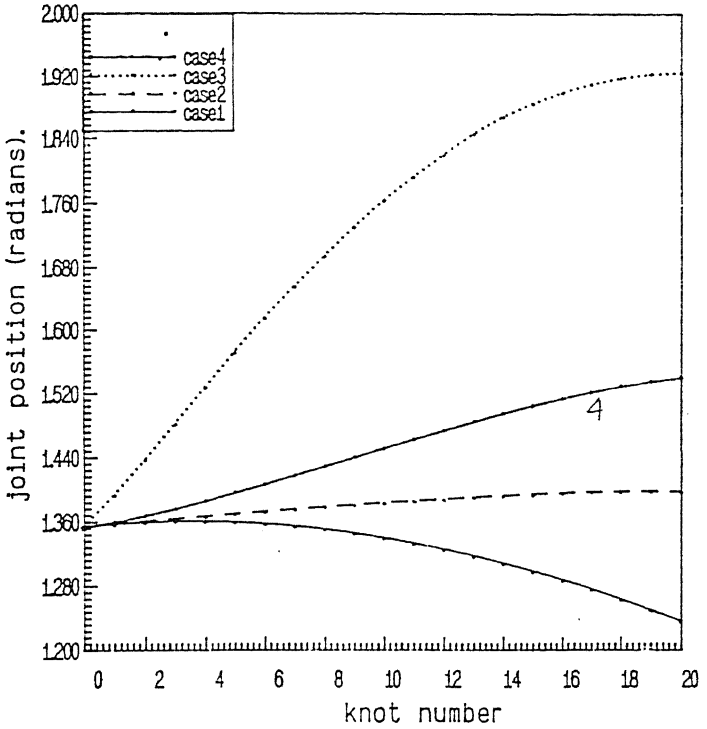

Fig. 2.8 Positions of joint 2 for arm 2 based on four performance criteria

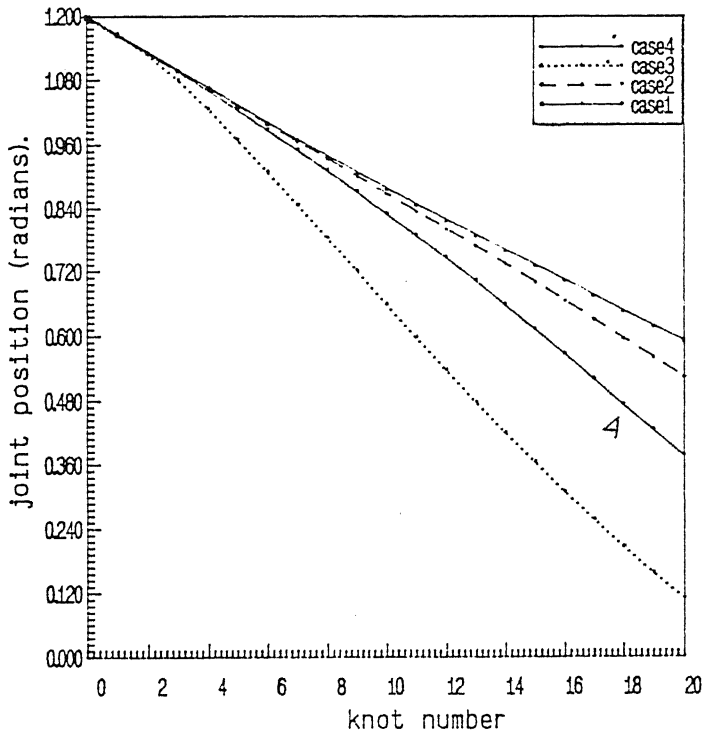

Fig. 2.9 Positions of joint 3 for arm 2 based on four performance criteria

weightage for increased manipulability.

Figures 2.10 to 2.15 show the joint increments (Δq_{augli} ; l=1,2 ; i=1,2,3) for various joints of the dual arm. It is again evident that case 2 requires minimum variations in the joint increments. Maximum variations in the joint increments is for case 3, and this variation is reduced by using the criterion for case 4. Figure 2.16 presents the norm of Δq_{aug}, which confirms that case 1 yields the minimum norm of Δq_{aug} while case 2 results in minimum variation in $|\Delta q_{aug}|$. This is even more clear in Fig.2.17 which shows the norm of $|\Delta q_{aug} - \Delta q_{augp}|$ and evidently the minimum acceleration assembly operation is achieved for case 2.

The manipulability , as defined by (2.5-10), is plotted in Fig.2.18 for all four cases. The maximum manipulability is obtained for case 3 but at the expense of large joint velocities and accelerations as seen in Figs. 2.16 and 2.17. A better compromise is obtained for case 4 which does result in increased manipulability while avoiding undue large joint rates.

Finally Figs 2.19 to 2.22 show the dual-arm configurations through various stages of the assembly for the four cases. In each figure the starting and ending configurations are marked by S and E , respectively. These figures do not reveal any new information but are more illustrative to confirm the observations made earlier.

Similar exercises were carried out for various starting configurations with similar results, though the difference in the results for the four cases was not so pronounced for some starting configurations, following two main observations were common : (i)

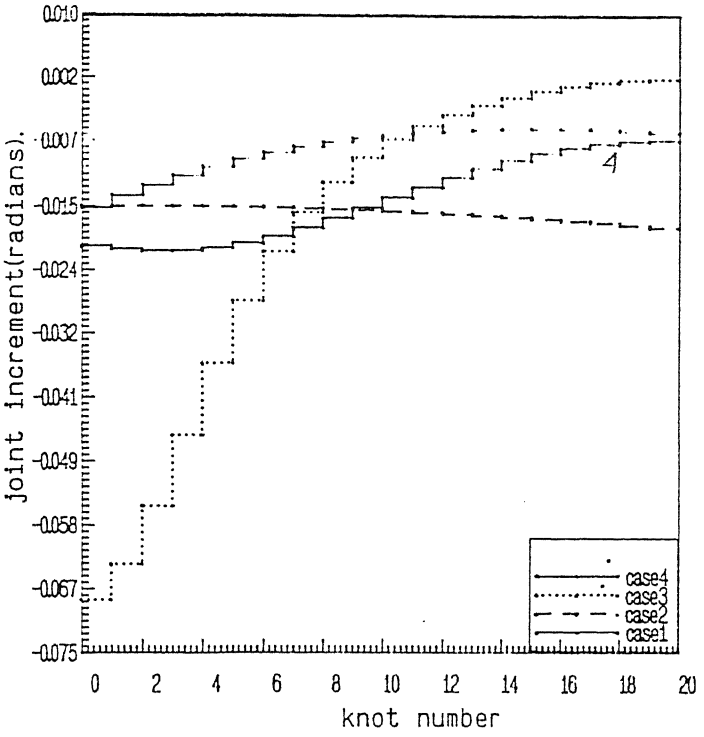

Fig. 2.10 Increments of joint 1 for arm 1 based on four performance criteria

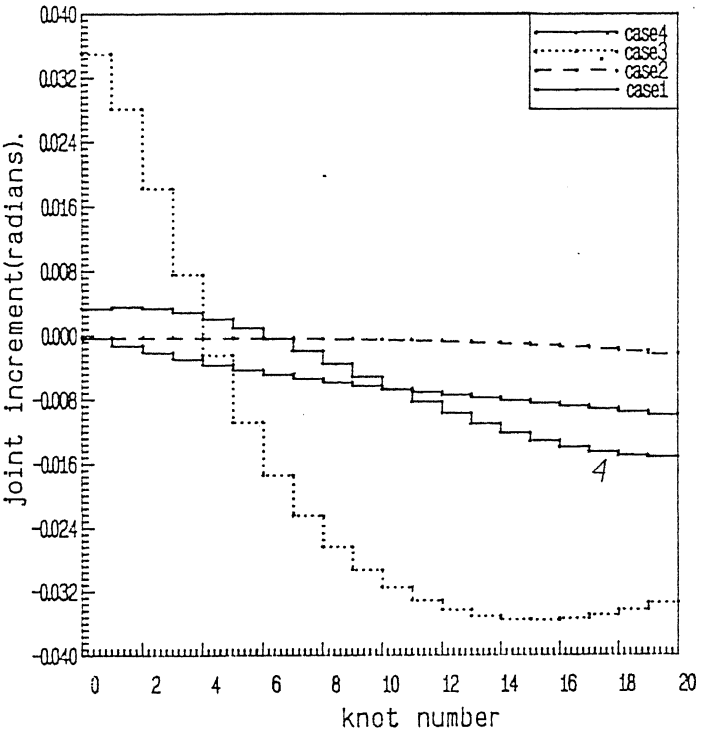

Fig. 2.11 Increments of joint 2 for arm 1 based on four performance criteria

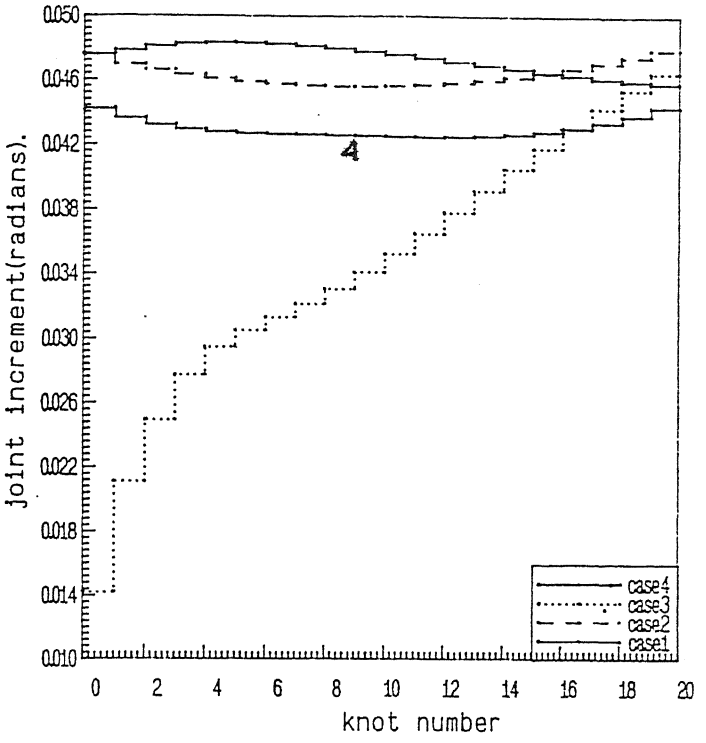

Fig. 2.13 Increments of joint 1 for arm 2 based on four performance criteria

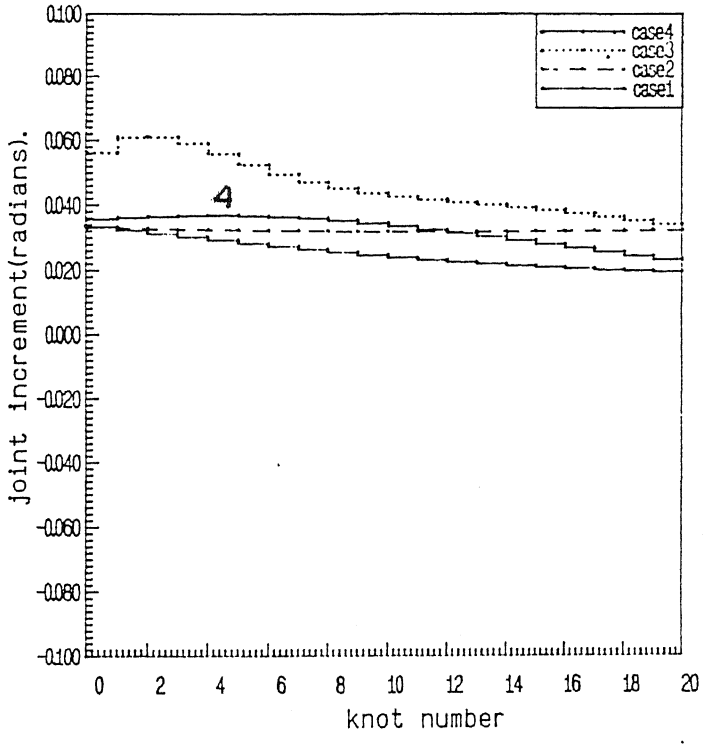

Fig. 2.12 Increments of joint 3 for arm 1 based on four performance criteria

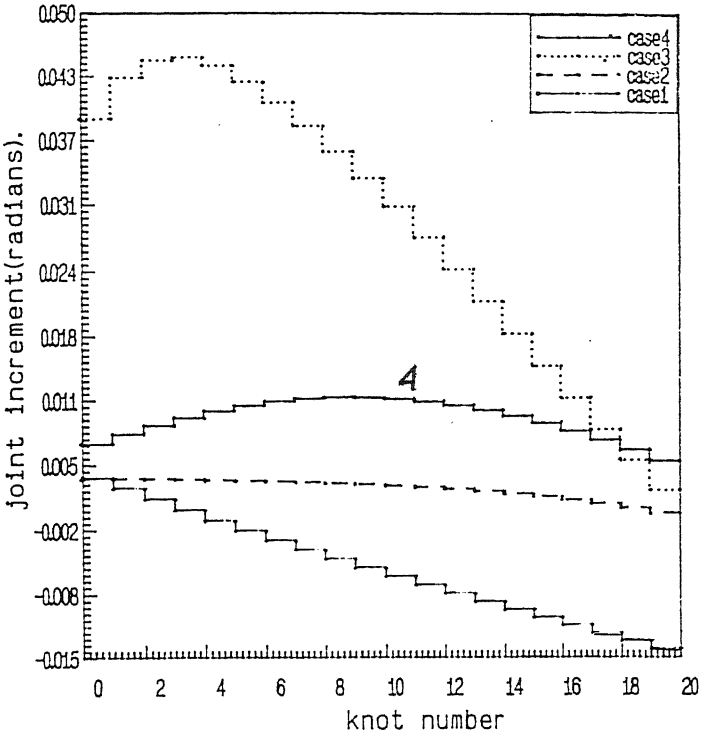

Fig. 2.14 Increments of joint 2 for arm 2 based on four performance criteria

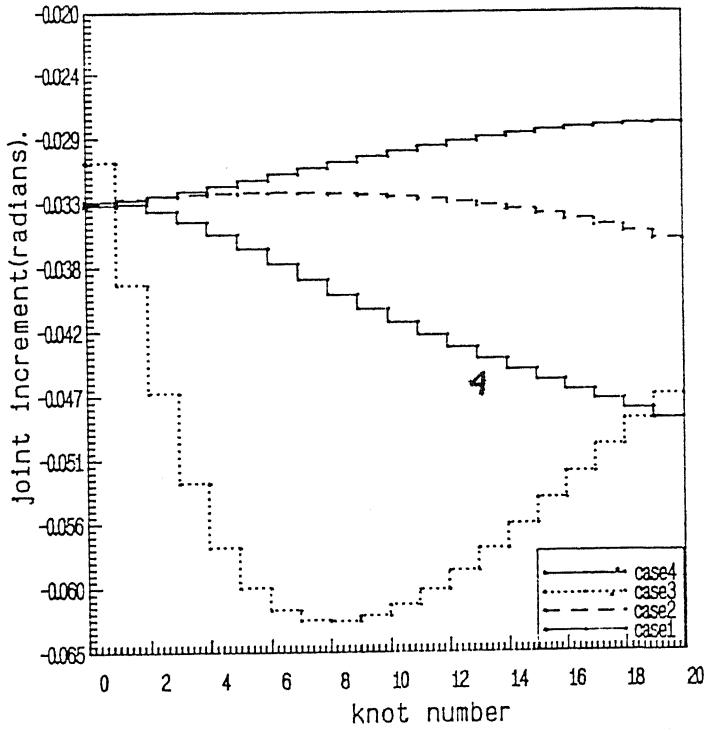

Fig. 2.15 Increments of joint 3 for arm 2 based on four performance criteria

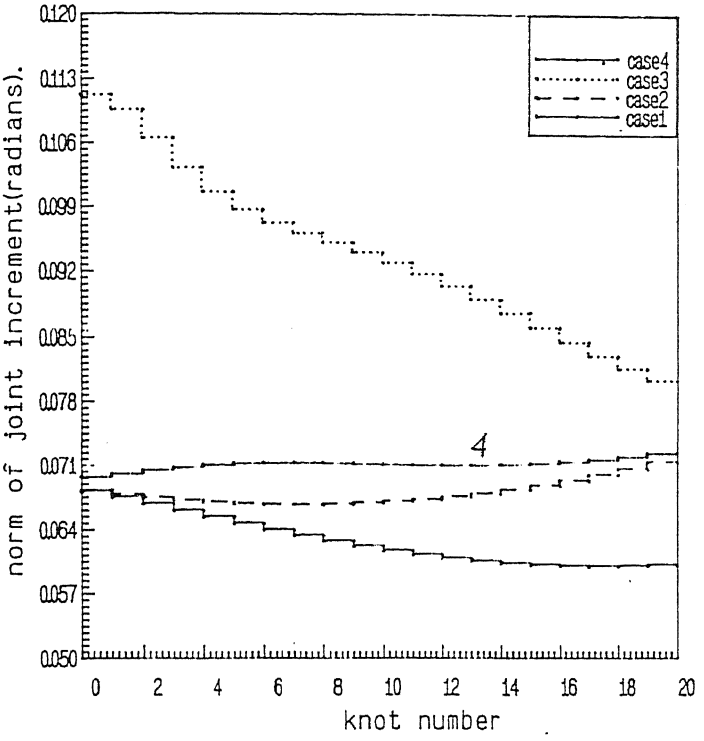

Fig. 2.16 Norms of joint increments versus knot number based on four performance criteria

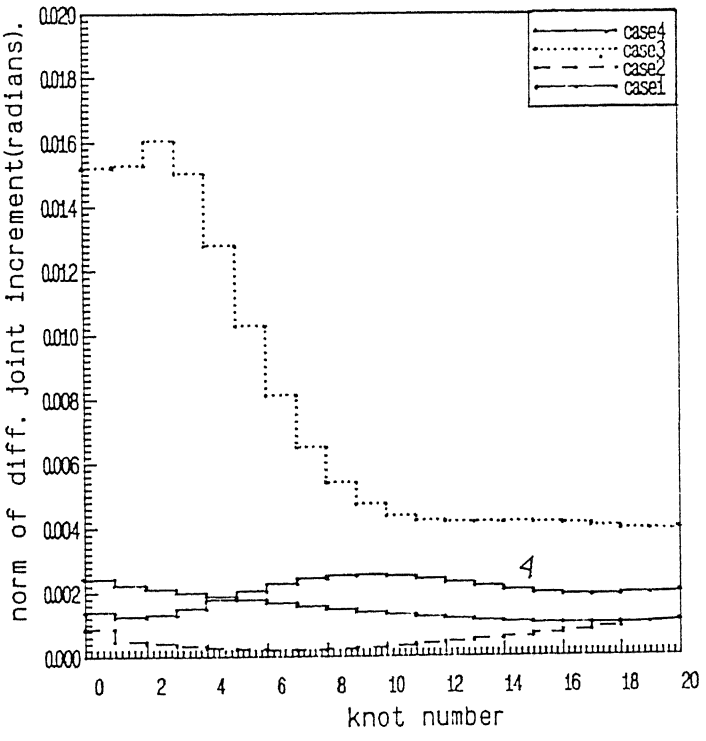

Fig. 2.17 Norms of difference of joint increments versus knot number based on four performance criteria

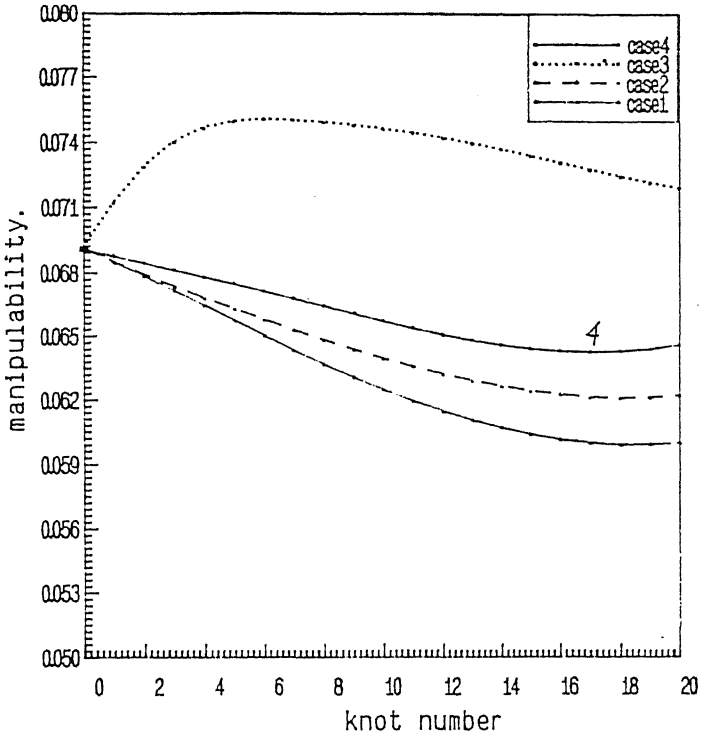

Fig. 2.18 Manipulability of dual-arm manipulator based on four performance criteria

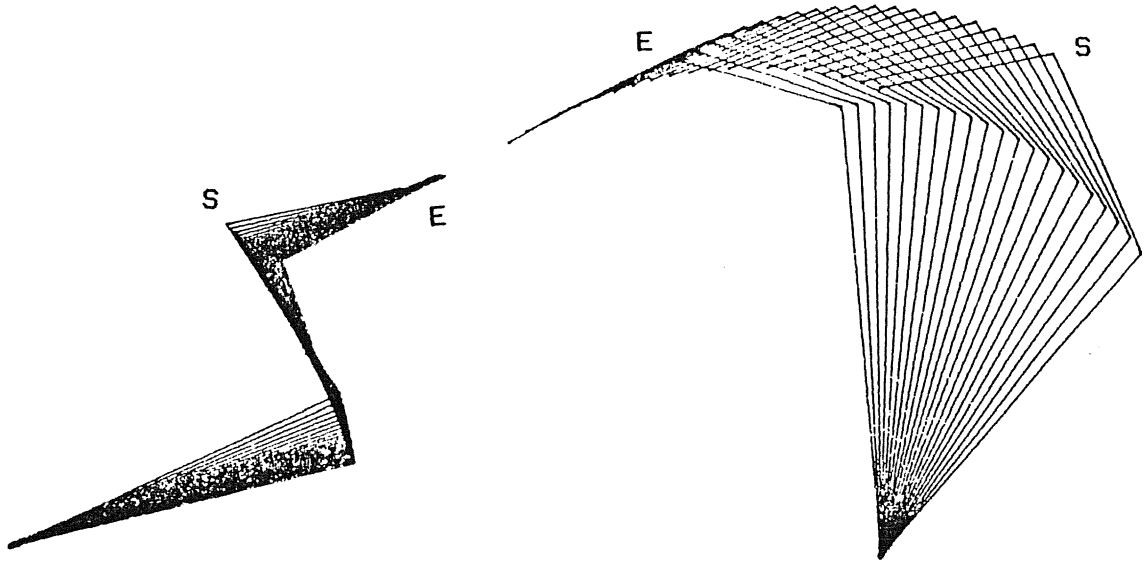

Fig. 2.19 Dual-arm manipulator configurations during assembly operation according to performance criterion 1.

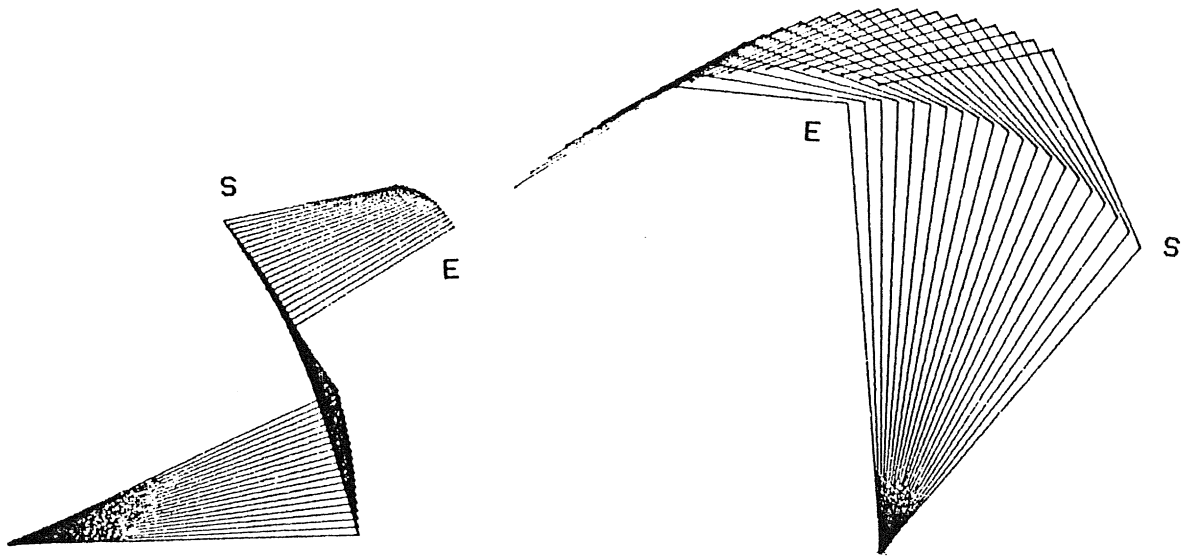

Fig. 2.20 Dual-arm manipulator configurations during assembly operation according to performance criterion 2.

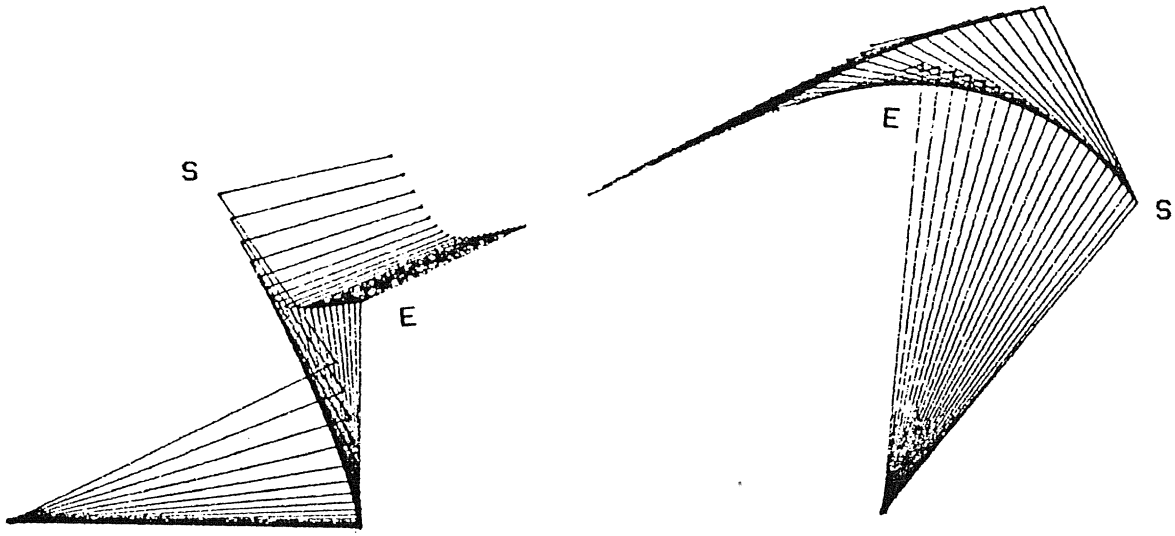

Fig. 2.21 Dual-arm manipulator configurations during assembly operation according to performance criterion 3.

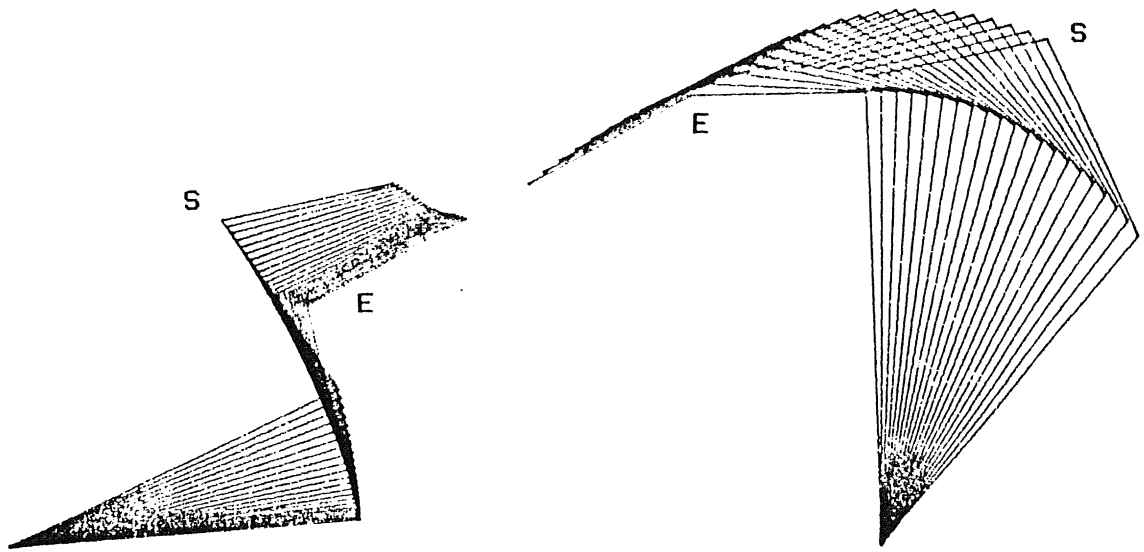

Fig. 2.22 Dual-arm manipulator configurations during assembly operation according to performance criterion 4.

The minimum acceleration norm solution results in somewhat larger joint velocities (as compared to the results from the minimum velocity norm solution) but the fluctuations in the velocities are reduced greatly. (ii) If it is desired to include a criterion which increases manipulability (so as to avoid the singularity configurations) then it is better to take the arms to a more manipulable configuration in a gradual manner as the assembly progresses. An alternate approach could have been to reconfigure the arms at the starting configuration itself so as to have a large (or maximum) manipulability; but this requires very large joint movements. Therefore,unless the arms are already in singular configuration , the criterion discussed in case 4 helps to perform the assembly without large joint motions while gradually taking the arms to always a more manipulable configuration.

CHAPTER 3

CONTINUOUS AND DISCRETE DYNAMIC MODELS OF A DUAL-ARM MANIPULATOR CARRYING AN OBJECT

3.1 Introduction

In many industrial applications, robots have to handle objects which are beyond the capacity of a single arm manipulator. The difficulty in handling by a single arm may be due to odd geometrical shape, large dimensions or heavy weight of the object. A dual-arm (or even multi-arm) manipulator may then be conveniently employed for such operations. If the end effectors of the dual-arm rigidly grasp an object then the two arms together with the object form a closed chain. This chapter considers one such system where an object, while held rigidly by the two arms, is to be carried along a specified path. For this problem, the trajectory planning is formulated in this chapter and the solution is presented later in Chapter 4.

The statement of the problem is discussed in Sec. 3.2. For the selected dual-arm manipulator and the object, position, velocity and static force relationships are presented in Sections 3.3, 3.4 and 3.5, respectively. The equations of motion for the closed-chain system are derived in Sec. 3.6. The redundancy in actuation is discussed in Sec. 3.7 and this redundancy is resolved according to minimum effort criterion and minimum electrical energy criterion. The problem of trajectory planning is posed in Sec 3.8 as a minimum time problem and minimum time plus minimum

energy problem. The numerical method, employed to solve the trajectory planning problem uses, the discretized set of equations. To this end, a discretization scheme is discussed in Sec. 3.9 and all the necessary equations are restated in discretized form in the same section. Finally, all the relevant discrete functions and equations are linearized in Sec. 3.10.

3.2 Statement of the Problem

The problem considers two serial link manipulators and an object is grasped between their end effectors. Each arm individually is an open chain mechanism consisting of 6 links. The arms grasp the object rigidly so there is no relative motion between the end effectors of the arms. Thus the arms together with the object form a closed chain mechanism which has 6 degrees of freedom. While carrying the object, all joints of both arms are considered to be active joints in the sense that each joint torque is to be determined independently. Thus the resultant force exerted on the object (which has 6 components) is generated by the 12 generalized joint forces of the arms and so the generalized joint force distribution is not unique.

The problem undertaken considers the movement of an object from one point of the workspace to another point along a specified path with specified orientation. In other words, the geometry of the path is specified and the time histories of the object and manipulator along the path is to be determined. The torque limits of the joint actuators, the ranges of movement and the velocity limits of the joints are the system constraints. The

above problem is formulated in two steps. First the torque redundancy is resolved according to minimum norm of the joint torque vector and minimum actuator energy. Then, while satisfying all kinematic and dynamic constraints, the trajectory planning problem(i.e. determining the time histories of the joint velocities, joint torques ,etc.) is posed in two ways-1) minimum time problem, and 2) minimum time plus minimum actuator energy problem. It will be noted later that consideration of only minimum actuator energy leads to trivial results.

3.3 Description of the System and Position Kinematics

A fixed cartesian coordinate frame (or world frame) (X_w, y_w, Z_w) shown in Fig. 3.1 is taken as the reference frame for the task description. The subscript l is used to identify the two arms, where l = 1 for arm 1 and l=2 for arm 2. A cartesian coordinate frame (X_{li}, Y_{li}, Z_{li}) (l=1,2 ; i=0,1,2,...6) is fixed to each link according to steps described in Sec.2.3. Following the same notations, ${}^{w}T_{l0}$ (l=1,2) then describes the base frame of lth arm with respect to the world frame, ${}^{l0}T_{l6}$ describes the end effector frame of lth arm with respect to that arm's base frame. Therefore, the end effector frames are defined with respect to the world frame through the transformation matrix ${}^{w}T_{l6}$ where

$$ {}^{w}T_{l6} = {}^{w}T_{l0}\,{}^{l0}T_{l6} \quad . \qquad (3.3\text{-}1) $$

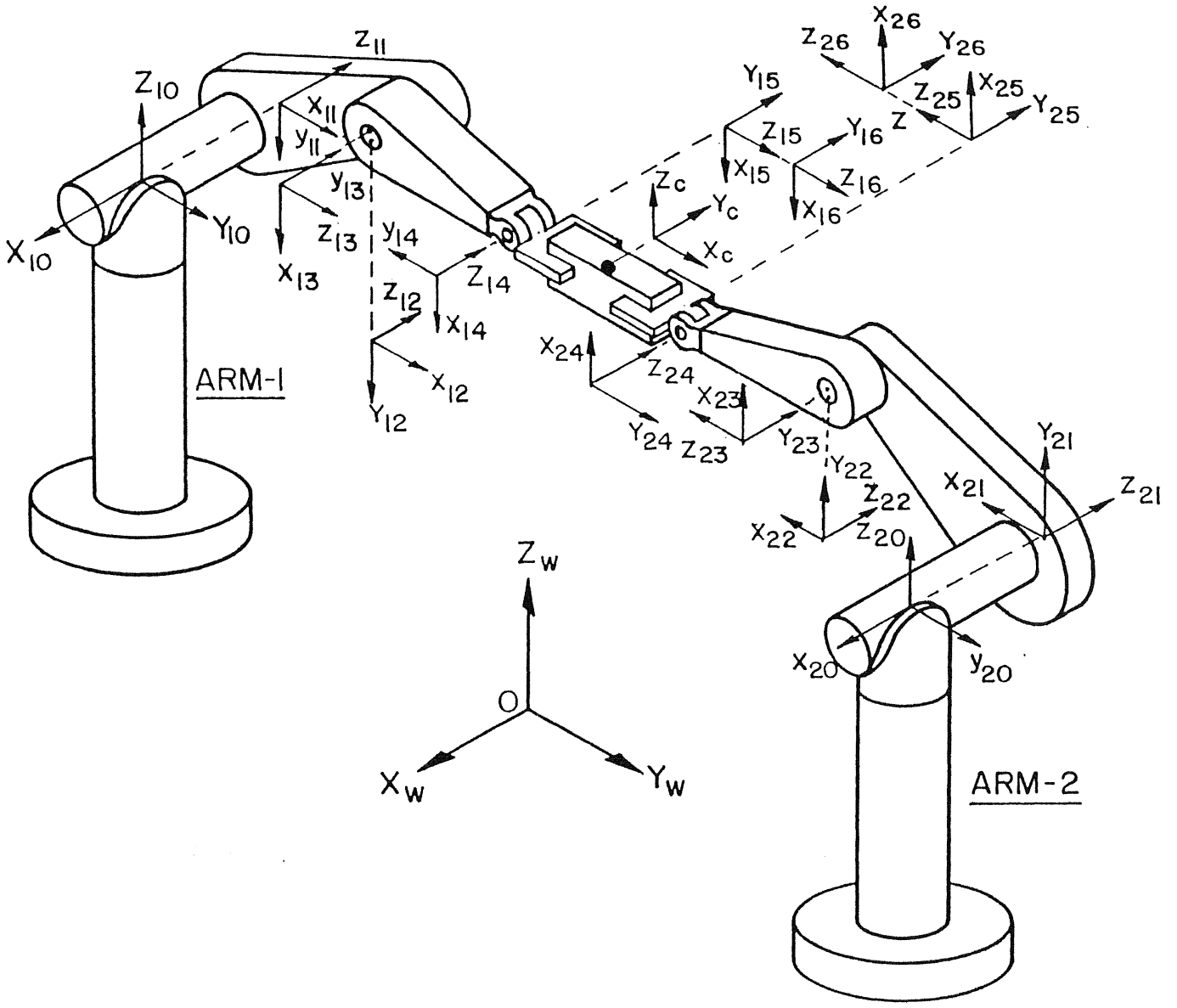

Fig. 3.1 System configuration and coordinate system assignment for a dual-arm manipulator carrying an object

To describe the position and orientation of the object, a coordinate frame (X_c, Y_c, Z_c) attached to the object as shown in Fig. 3.1 (henceforth, the subscript c will be used to refer to the object). The origin of (X_c, Y_c, Z_c) is at the mass centre Q_c of the object. The transformation matrix of the object frame with respect to the world frame is written as

$$ {}^{w}T_{c} = \begin{bmatrix} {}^{w}R_{c} & {}^{w}p_{c} \\ 0 & 1 \end{bmatrix} \qquad (3.3\text{-}2) $$

where ${}^{w}p_{c}$ is the position vector of the object mass centre with respect to the world frame. ${}^{w}R_{c}$ is the rotation matrix in terms of Euler angles ϕ_1, ϕ_2, ϕ_3 as defined in (A.1) of Appendix A.

Now if ${}^{6}T_{1c}$ describes the transformation of the object frame with respect to the end effector frame of the 1th arm then

$$ {}^{10}T_{16} = {}^{w}T_{10}^{-1} \; {}^{w}T_{c} \; {}^{6}T_{1c}^{-1} \; . \qquad (3.3\text{-}3) $$

For the problems considered, all the three transformations on the right hand side of (3.3-3) are assumed to be known and thus ${}^{10}T_{16}$ (and ${}^{w}T_{16}$ from (3.3-1)) are also determined.

The joint position vector of the 1th arm is denoted by

$$ q_1 = [q_{11}, q_{12} \ldots\ldots\ldots q_{16}]^{T} \; . \qquad (3.3\text{-}4) $$

The inverse position kinematics can now be applied to obtain the joint position vector (the details isdiscussed in Appendix E).

3.4 Velocity Relations

The velocity of the object is described by the linear velocity vector ${}^{w}\mathbf{v}_c$ and the angular velocity vector ${}^{w}\Omega_c$, whose components in the world frame are written as

$$ {}^{w}\mathbf{v}_c = \left[{}^{w}v_{cx},\ {}^{w}v_{cy},\ {}^{w}v_{cz} \right]^T \qquad (3.4\text{-}1) $$

and

$$ {}^{w}\Omega_c = \left[{}^{w}\omega_{cx},\ {}^{w}\omega_{cy},\ {}^{w}\omega_{cz} \right]^T \qquad (3.4\text{-}2) $$

The linear velocity vector is the time dertivative of the position vector ${}^{w}\mathbf{p}_c$ in (3.3-2) i.e,

$$ {}^{w}\mathbf{v}_c = \frac{d}{dt}\left[{}^{w}\mathbf{p}_c \right] \quad . \qquad (3.4\text{-}3) $$

The angular velocity vector ${}^{w}\Omega_c$ can be expressed in terms of Eular angles ϕ_1, ϕ_2, ϕ_3 and their time derivatives $\dot{\phi}_1$, $\dot{\phi}_2$, $\dot{\phi}_3$ by the following relation [Fu et al. 1987]:

$$ \begin{bmatrix} {}^{w}\omega_{cx} \\ {}^{w}\omega_{cy} \\ {}^{w}\omega_{cz} \end{bmatrix} = \begin{bmatrix} 0 & \cos\phi_1 & \sin\phi_1 \sin\phi_2 \\ 0 & \sin\phi_1 & -\cos\phi_1 \sin\phi_2 \\ 1 & 0 & \cos\phi_2 \end{bmatrix} \begin{bmatrix} \dot{\phi}_1 \\ \dot{\phi}_2 \\ \dot{\phi}_3 \end{bmatrix} \quad . $$

(3.4-4)

The derivation of the above relation is given in (A.11) of Appendix A. The end effector velocity of the 1th arm is denoted in a similar way by the six dimensional vector $[\,{}^{w}\mathbf{v}_1^T,\ {}^{w}\Omega_1^T\,]^T$. It is to be noted that ${}^{w}\Omega_c = {}^{w}\Omega_1 = {}^{w}\Omega_2$ since the object is rigidly held

between the end effectors. The end effector velocity vector is related to the joint velocity vector through the manipulator jacobian as

$$\begin{bmatrix} {}^{w}v_1 \\ {}^{w}\Omega_1 \end{bmatrix} = J_1(q_1)\,\dot{q}_1 \qquad (3.4\text{-}5)$$

where $\dot{q}_1 = [\dot{q}_{11}, \dot{q}_{12}, \ldots\ldots \dot{q}_{16}]^T$ is a six dimensional vector. $J_1(q_1)$ is called the manipulator Jacobian matrix which is in this case a 6x6 matrix. For rotary joints the ith column of the J_1 referring to (B.7) of Appendix B is given by

$$J_{1i}(q_1) = \begin{bmatrix} {}^{w}a_{1\ i-1} \times [\,{}^{w}p_{16} - {}^{w}p_{1\ i-1}] \\ {}^{w}a_{1\ i-1} \end{bmatrix} \qquad (3.4\text{-}6)$$

3.5 Static Forces

The two arms interact with each other through the object held between the end effectors. The interactive force (see Fig.3.2) exerted by the object on the end effector of 1th arm is expressed in the form of a generalized vector as

$${}^{w}f_1 = [{}^{w}f_{11}, {}^{w}f_{12} \ldots\ldots {}^{w}f_{16}]^T \qquad (3.5\text{-}1)$$

where the first three components constitute force vector and the last three components form the moment vector. Therefore, ${}^{w}f_1$ will also be written as

$$ {}^{w}f_{1} = \left[{}^{w}f_{1f}^{T} \cdot {}^{w}f_{1n}^{T} \right]^{T} \qquad (3.5\text{-}2) $$

where f_{1f} denotes the force vector and f_{1n} denotes the moment vector.This implies that the force exerted by the end-effector on the objectis $-{}^{w}f_{1}$.

Due to the generalized force ${}^{w}f_{1}$ (1=1,2), there is a net force and moment vector at the centre of the object. Let ${}^{w}f_{cf}$ and ${}^{w}f_{cn}$ represent the resultant force and moment vectors, respectively, at the object centre. Then the following relations hold (See Fig. 3.1 and Fig. 3.2)

$$ {}^{w}f_{cf} = -({}^{w}f_{1f} + {}^{w}f_{2f}) \qquad (3.5\text{-}3) $$

$$ \text{and } {}^{w}f_{cn} = {}^{w}r_{1} \times {}^{w}f_{1f} + {}^{w}r_{2} \times {}^{w}f_{2f} - {}^{w}f_{1n} - {}^{w}f_{2n} \qquad (3.5\text{-}4) $$

with the moment arms ${}^{w}r_{1}$ and ${}^{w}r_{2}$ written as (Fig.3.1)

$$ {}^{w}r_{1} = {}^{w}p_{c} - {}^{w}p_{16} $$
$$ \text{and } {}^{w}r_{2} = {}^{w}p_{c} - {}^{w}p_{26} \qquad (3.5\text{-}5) $$

where, ${}^{w}p_{c}$ and ${}^{w}p_{16}$ are the position vectors obtained from known transformations ${}^{w}T_{c}$and ${}^{w}T_{16}$ of (3.3-3) and (3.3-1).

Equation (3.5-4) is in terms of vector cross products, whereas later the dynamical equations will be written in matrix form. Therefore, all the cross product terms are written in the following form:

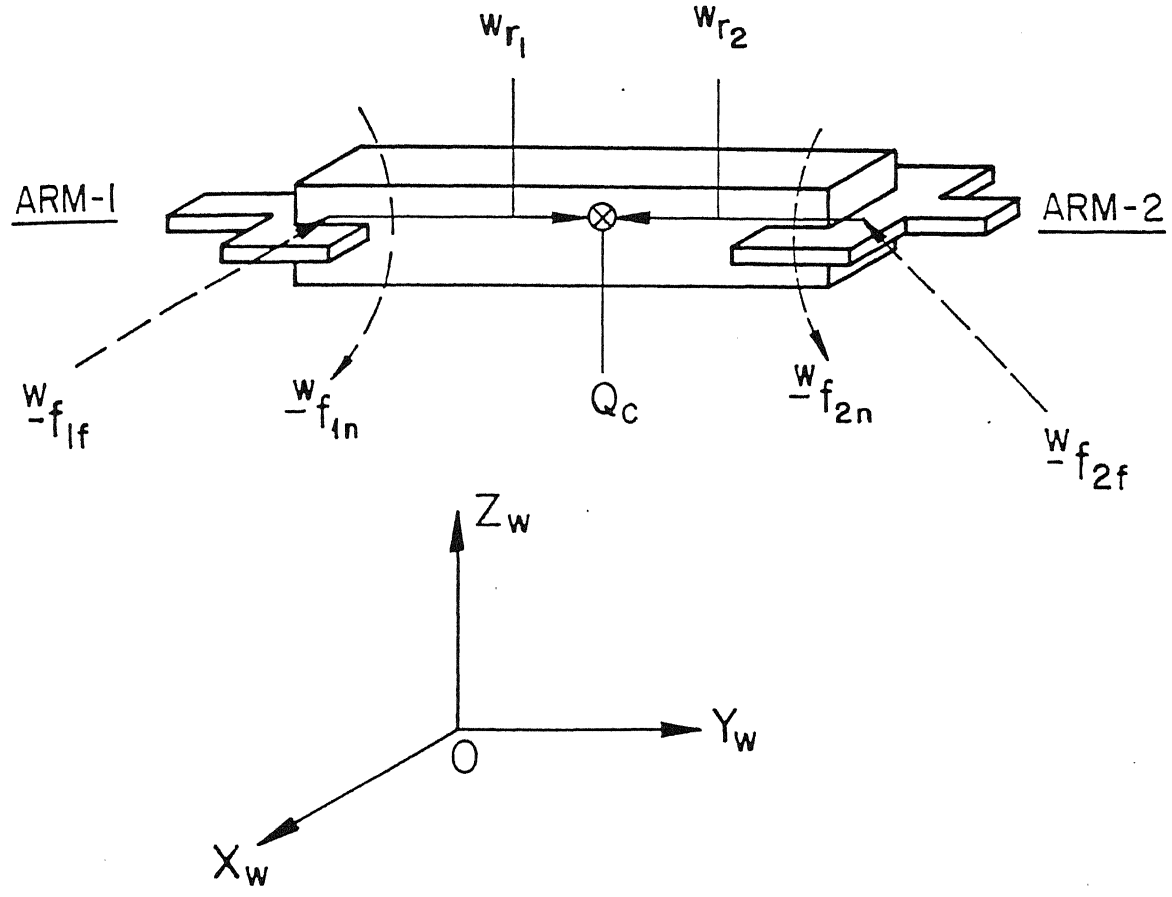

Fig. 3.2 Freebody diagram of the object carried by dual-arm manipulator

if $\mathbf{a} = \mathbf{b} \times \mathbf{c}$

then
$$\begin{bmatrix} a_x \\ a_y \\ a_z \end{bmatrix} = \begin{bmatrix} 0 & -b_z & b_y \\ b_z & 0 & -b_x \\ -b_y & b_x & 0 \end{bmatrix} \begin{bmatrix} c_x \\ c_y \\ c_z \end{bmatrix} . \qquad (3.5\text{-}6)$$

Thus
$$^{w}r_1 \times {}^{w}f_{1f} = -{}^{w}S_{r1} \, {}^{w}f_{1f} \qquad (3.5\text{-}7)$$

and
$$^{w}r_2 \times {}^{w}f_{2f} = -{}^{w}S_{r2} \, {}^{w}f_{2f} \qquad (3.5\text{-}8)$$

where
$$^{w}S_{r1} = \begin{bmatrix} 0 & {}^{w}r_{1z} & -{}^{w}r_{1y} \\ -{}^{w}r_{1z} & 0 & {}^{w}r_{1x} \\ {}^{w}r_{1y} & -{}^{w}r_{1x} & 0 \end{bmatrix} \qquad (3.5\text{-}9)$$

and
$$^{w}S_{r2} = \begin{bmatrix} 0 & {}^{w}r_{2z} & -{}^{w}r_{2y} \\ -{}^{w}r_{2z} & 0 & {}^{w}r_{2x} \\ {}^{w}r_{2y} & -{}^{w}r_{2x} & 0 \end{bmatrix} \qquad (3.5\text{-}10)$$

Now (3.5-3) and (3.5-4) are written in combined form as

$$^{w}f_c = \begin{bmatrix} {}^{w}f_{cf} \\ {}^{w}f_{cn} \end{bmatrix} = - \begin{bmatrix} 1 & 0 \\ {}^{w}S_{r1} & 1 \end{bmatrix} \begin{bmatrix} {}^{w}f_{1f} \\ {}^{w}f_{1n} \end{bmatrix} - \begin{bmatrix} 1 & 0 \\ {}^{w}S_{r2} & 1 \end{bmatrix} \begin{bmatrix} {}^{w}f_{2f} \\ {}^{w}f_{2n} \end{bmatrix} \qquad (3.5\text{-}11)$$

where $\mathbf{1}$ is a 3x3 identitly matrix, $\mathbf{0}$ is a 3x3 null matrix, and S matrices are given by (3.5-9) and (3.5-10). In a compact notation form, (3.5-11) is written as

$$^{w}f_c = - J_{1c}^{T} \, {}^{w}f_1 - J_{2c}^{T} \, {}^{w}f_2 . \qquad (3.5\text{-}12)$$

J_{1c} and J_{2c} are termed as the transmission matrices and these matrices relate the forces $-{}^{w}f_1$ and $-{}^{w}f_2$ (exerted by the end effectors on the object) to the resultant generalized force ${}^{w}f_c$ at the object centre.Finally for the static case, the end effector forces for the 1th arm are related to the respective joint torques , $\hat{\tau}_1$ as

$$\hat{\tau}_1 = J_1^T \, {}^{w}f_1 \quad . \qquad (3.5\text{-}13)$$

3.6 Dynamic Equations of Arms and Object

The general equations of motion of any manipulator can be conveniently written through the Lagrange-Euler formulation. The direct application of the lagrangian formulation, together with the Denavit-Hartenberg link coordinate representation, results in a convenient and compact algorithmic description of the manipulator equations of motion. To this end , first the expressions for kinetic energy and potential energy are to be written.

The kinetic energy of the 1th arm is expressed as [Tourassis and Neuman ,1985]

$$KE_1 = \frac{1}{2} \sum_{i=1}^{6} \sum_{j=1}^{6} \dot{q}_{1i} \, d_{1ij} \, \dot{q}_{1j} = \frac{1}{2} \dot{q}_1^T D_1 \dot{q}_1$$

(3.6-1)

where, d_{1ij}'s are the inertia coefficients given in Appendix D.

The d_{lij} terms form the inertia matrix D_l which is symmetric and positive definite. The potential energy of the lth arm is given by

$$PE_l = - \sum_{i=1}^{6} m_i \, {}^{w}g^{T} \, {}^{w}r_{li} \qquad (3.6\text{-}2)$$

where, ${}^{w}g$ is the 3 x 1 vector representing the acceleration due to gravity with reference to the world coordinate frame (with the choice of world frame as shown in Fig. 4.1, ${}^{w}g = [0 \;\; 0 \;\; -9.81]^{T}$), ${}^{w}r_{li}$ is the position vector of the mass centre of link i of the lth arm, the position vector being expressed in the world coordinate frame. Now the Lagrange-Euler equations of motion are

$$\frac{d}{dt}\left[\frac{\partial L_l}{\partial \dot{q}_{lp}}\right] - \frac{\partial L_l}{\partial q_{lp}} = \bar{\tau}_{lp} \; ; \; l = 1,2 \; ; \; p = 1,2....6 \qquad (3.6\text{-}3)$$

where, the lagrangian L_l for the lth arm is

$$L_l = KE_l - PE_l \qquad (3.6\text{-}4)$$

and $\bar{\tau}_{lp}$ is the generalized force at the p th joint of the lth arm. This $\bar{\tau}_{lp}$ is written as

$$\bar{\tau}_{lp} = \tau_{lp} + \sum_{i=1}^{6} J_{lip} \, {}^{w}f_{li} \qquad (3.6\text{-}5)$$

where, the force exerted on the end effector, i.e. ${}^{w}f_{1i}$ has been resolved on joints according to (3.5-13). Substitution of (3.6-1) and (3.6-2) in (3.6-4) and the resulting equation in (3.6-3) yields

$$\frac{d}{dt}\left[\sum_{i=1}^{6} d_{1ip}\ \dot{q}_{1i}\right] - \frac{\partial}{\partial q_{1p}}\left[\frac{1}{2}\sum_{i=1}^{6}\sum_{j=1}^{6} \dot{q}_{1i}\ d_{1ij}\ \dot{q}_{1j}\right]$$

$$+ \frac{\partial PE_1}{\partial q_{1p}} = \tau_{1p} + \sum_{i=1}^{6} J_{1ip}\ {}^{w}f_{1i} \quad ; \begin{matrix} 1 = 1,2 \\ p = 1,2..6 \end{matrix} \qquad (3.6\text{-}6)$$

The dynamical equation (3.6-6) is used in this form itself while employing Finite Difference procedures (as will be explained later in Sec. 3.9). But for the sake of using easier forms of equations in this section, (3.6-6) is symbolically expressed in the standard form as

$$\tau_1 + J_1^{T}\ {}^{w}f_1 = D_1(q_1)\ddot{q}_1 + h_1(q_1,\dot{q}_1) + c_1(q_1) \qquad (3.6\text{-}7)$$

where, D_1 is the inertia matrix, h_1 is the vector involving centrifugal and Coriolis acceleration and c_1 is the position dependent vector. The expressions for these quantities are not needed for the discussion.

The arms interact with the object through the contact forces ${}^{w}f_1$ and ${}^{w}f_2$ as defined in (3.5-1). The object velocities are expressed by ${}^{w}v_c$ and ${}^{w}\Omega_c$ in (3.4-1) and (3.4-2). Thus

Newton-Euler equation for the object are

$$\frac{d}{dt}(m_c\ {}^{w}v_c) - m_c\ {}^{w}g = {}^{w}f_{cf} \qquad (3.6\text{-}8)$$

and $$\frac{d}{dt}({}^{w}I_c\ {}^{w}\Omega_c) = {}^{w}f_{cn} \qquad (3.6\text{-}9)$$

where ${}^{w}f_{cf}$ and ${}^{w}f_{cn}$ are given by (3.5-3) and (3.5-4), respectively. ${}^{w}I_c$ is a 3x3 inertia matrix and is obtained from the relation

$${}^{w}I_c = {}^{w}R_c\ {}^{c}I_c\ {}^{w}R_c^{T} \qquad (3.6\text{-}10)$$

where, ${}^{c}I_c$ is the object inertia matrix in the object frame and is, thus, invariant, ${}^{w}R_c$ is the rotation matrix part of ${}^{w}T_c$ (a known transformation in (3.3-4)).

Using (3.5-11) and (3.5-12), the equations of motion of the object, i.e. (3.6-8) and (3.6-9) are rewritten as

$$\begin{bmatrix} \frac{d}{dt}(m_c\ {}^{w}v_c) - m_c\ {}^{w}g \\ \frac{d}{dt}({}^{w}I_c\ {}^{w}\Omega_c) \end{bmatrix} = -J_{1c}^{T}\ {}^{w}f_1 - J_{2c}^{T}\ {}^{w}f_2 . \qquad (3.6\text{-}11)$$

The dynamics of the closed chain of two arms alongwith the object is completely described by the relations (3.6-7) and (3.6-11). As the interactive forces ${}^{w}f_1$ and ${}^{w}f_2$ between the arms and object are internal forces they can be eliminated to get a set of dynamic equations which relate the motions of object and arms

with the generalized joint forces. If J_1 and J_2 are nonsingular then from (3.6-7) the generalized contact forces ${}^{w}f_1$ and ${}^{w}f_2$ can be written as [Unseren, 1991]

$$ {}^{w}f_1 = J_1^{-T} \left[D_1(q_1)\,\ddot{q}_1 + h_1(q_1, \dot{q}_1) + c_1(q_1) - \tau_1 \right] \tag{3.6-12} $$

and $$ {}^{w}f_2 = J_2^{-T} \left[D_2(q_2)\,\ddot{q}_2 + h_2(q_2, \dot{q}_2) + c_2(q_2) - \tau_2 \right]. \tag{3.6-13} $$

Substituting these expressions for ${}^{w}f_1$ and ${}^{w}f_2$ into (3.6-11) one gets

$$ \begin{bmatrix} \frac{d}{dt}(m_c\,{}^{w}v_c) - m_c\,{}^{w}g \\ \frac{d}{dt}({}^{w}I_c\,{}^{w}\Omega_c) \end{bmatrix} + J_{1c}^{T} J_1^{-T} \left[D_1(q_1)\,\ddot{q}_1 + h_1(q_1, \dot{q}_1) + c_1(q_1) \right] + J_{2c}^{T} J_2^{-T} \left[D_2(q_2)\,\ddot{q}_2 + h_2(q_2, \dot{q}_2) + c_2(q_2) \right] = J_{1c}^{T} J_1^{-T} \tau_1 + J_{2c}^{T} J_2^{-T} \tau_2 . \tag{3.6-14} $$

The relation (3.6-14) is rewritten as

$$ J_{1c}^{T} J_1^{-T} \tau_1 + J_{2c}^{T} J_2^{-T} \tau_2 - \xi = 0 \tag{3.6-15} $$

where, $$ \xi = \xi_1 + \xi_2 + \xi_3 \tag{3.6-16} $$

with

$$ \xi_1 = J_{1c}^{T} J_1^{-T} \bar{\tau}_1 , \tag{3.6-17} $$

$$ \xi_2 = J_{2c}^{T} J_2^{-T} \bar{\tau}_2 , \tag{3.6-18} $$

$$\bar{\tau}_1 = D_1(q_1)\ddot{q}_1 + h_1(q_1,\dot{q}_1) + c_1(q_1) \quad , \qquad (3.6\text{-}19)$$

$$\bar{\tau}_2 = D_2(q_2)\ddot{q}_2 + h_2(q_2,\dot{q}_2) + c_2(q_2) \qquad (3.6\text{-}20)$$

and $$\xi_3 = \begin{bmatrix} \frac{d}{dt}(m_c {}^w v_c) - m_c^w {}^w g \\ \frac{d}{dt}({}^w I_c {}^w \Omega_c) \end{bmatrix} \quad . \qquad (3.6\text{-}21)$$

It can be noted that $\bar{\tau}_1$ and $\bar{\tau}_2$ are the joint torque vectors needed to move the arms as if the end effectors are unconstrained, and ξ_3 is the generalized force at the object centre needed to move an unconstrained object.

At this stage, if it is assumed that the trajectory (i.e. the path, velocity and acceleration) is completely known then ξ in (3.6-16) can be completely determined. Then (3.6-15) results in 6 equations in terms of 12 unknowns, namely six components each of τ_1 and τ_2. The following section discusses this redundancy in actuator torques and outlines two methods of resolving the torque redundancy.

3.7 Resolution of Redundancy in Actuation

The methods to resolve the torque redundancy are based upon optimizing some performance criteria . Here two performance criteria are discussed.The first performance criterion is to have the "minimum effort" by the actuators. This is achieved by

minimizing the sum of the weighted norms of the generalized joint forces. Thus, an objective function Z_1, to be minimized (subject to constraint (3.6-15)), is written as

$$Z_1 = \tau_1^T C_{tb1} \tau_1 + \tau_2^T C_{tb2} \tau_2 \qquad (3.7\text{-}1)$$

where C_{tb1} and C_{tb2} are 6x6 diagonal cost matrices and subscript 1 and 2 correspond to arm 1 and arm 2, respectively. One way of defining the diagonal elements of the cost matrices C_{tb1} and C_{tb2} is to take the reciprocal of the squares of respective joint torque limits. The significance of defining the cost matrices in this fashion is that the joint forces will be distributed such that the joint with higher load capacity shares higher load than the joint with lower load capacity i.e. the heavy joints will have low weightage and the lighter joints should get higher weightage. Thus the matrices C_{tb1} and C_{tb2} (based upon bounds on torques) are written as

$$C_{tb1} = \text{diag}\left[\frac{1}{\tau^2_{11max}}, \frac{1}{\tau^2_{12max}}, \frac{1}{\tau^2_{13max}}, \frac{1}{\tau^2_{14max}}, \frac{1}{\tau^2_{15max}}, \frac{1}{\tau^2_{16max}} \right]$$

$$C_{tb2} = \text{diag}\left[\frac{1}{\tau^2_{21max}}, \frac{1}{\tau^2_{22max}}, \frac{1}{\tau^2_{23max}}, \frac{1}{\tau^2_{24max}}, \frac{1}{\tau^2_{25max}}, \frac{1}{\tau^2_{26max}} \right] \qquad (3.7\text{-}2)$$

where diag means C_{tb1} is a diagonal matrix having the diagonal elements $\frac{1}{\tau^2_{11max}}$, $\frac{1}{\tau^2_{12max}}$ etc.

The second performance criterion is based upon minimum electrical energy consumption. As energy is the time integral of the power, the minimization of energy consumption means power should be minimized over the trajectory. In case of electrical motors the power depends upon three main parameters, namely c^r the power supply resistance, c^g, the gear ratio between the motor and the joint, and c^m , the motor constant. If the motor torque is τ then the power is given by [Tan and potts ,1989]

$$\text{Power} = \tau^2 \; c^r \; (c^g/c^m)^2 \; .$$

Now the objective function to be minimized (subject to constraint (3.6-15)) is written as

$$Z_2 = \tau_1^T \; C_{tp1} \; \tau_1 + \tau_2^T \; C_{tp2} \; \tau_2 \qquad (3.7\text{-}3)$$

where C_{tp1} and C_{tp2} are the cost metrices (based upon power consumption) for arm1 and arm 2, respectively. The cost matrices are written as

$$C_{tp1} = \text{diag} \left[C_{tp11}, \; C_{tp12}, \; C_{tp13}, \ldots\ldots C_{tp16} \right]$$

$$C_{tp2} = \text{diag} \left[C_{tp21}, \; C_{tp22}, \; C_{tp23}, \ldots\ldots C_{tp26} \right] \qquad (3.7\text{-}4)$$

where,

$$C_{tp1i} = c_{1i}^{r} \left[c_{1i}^{g} / c_{1i}^{m} \right]^2$$

and (3.7-5)

$$C_{tp2i} = c_{2i}^{r} \left[c_{2i}^{g} / c_{2i}^{m} \right]^2$$

with c_{1i}^{r} and c_{2i}^{r} as the power supply resistances of joint i of arm 1 and arm 2, respectively. Similarly c_{1i}^{g} and c_{2i}^{g} are the gear ratios of the ith joint of arm1 and arm2. Lastly c_{1i}^{m} and c_{2i}^{m} are the motor constants for the ith joint of arm1 and arm2. The above two performance criteria may be combined to form a composite objective function Z as

$$Z = \gamma_1 Z_1 + \gamma_2 Z_2 \qquad (3.7\text{-}6)$$

where γ_1, γ_2 are weightages on the two performance criteria. Using (3.7-1) and (3.7-3) in (3.7-6) the objective function Z becomes

$$Z = \tau_1^T C_{z1} \tau_1 + \tau_2^T C_{z2} \tau_2 \qquad (3.7\text{-}7)$$

where

$$C_{z1} = \gamma_1 C_{tb1} + \gamma_2 C_{tp1}$$

and $$C_{z2} = \gamma_1 C_{tb2} + \gamma_2 C_{tp2} \quad . \qquad (3.7\text{-}8)$$

In the redundancy resolution of generalized joint forces the objective function Z of (3.7-7) is to be minimized subject to satisfying the dynamic equations (3.6-15). To find out the optimum values of τ_1 and τ_2, the lagrangian L is formed as

$$L = Z + \lambda^T \left(J_{1c}^T J_1^{-T} \tau_1 + J_{2c}^T J_2^{-T} \tau_2 - \xi \right) \qquad (3.7\text{-}9)$$

where λ is the 6 dimensional vector containing the Lagrange multipliers. To get the optimum values of τ_1 and τ_2 the lagrangian should satisfy the following conditions:

$$\frac{\partial L}{\partial \tau_1} = 0 \qquad (3.7\text{-}10)$$

$$\frac{\partial L}{\partial \tau_2} = 0 \qquad (3.7\text{-}11)$$

$$\frac{\partial L}{\partial \lambda} = 0 \qquad (3.7\text{-}12)$$

Combining (3.7-7), (3.7-9) and (3.7-10), one gets the optimum joint torque vector ,τ_1^* (for arm1) from

$$(C_{z1} + C_{z1}^T)\, \tau_1^* + J_1^{-1} J_{1c} \lambda = 0$$

$$\text{or, } \tau_1^* = - [C_{z1} + C_{z1}^T]^{-1} J_1^{-1} J_{1c} \lambda \quad . \qquad (3.7\text{-}13)$$

Similarly from (3.7-7), (3.7-9) and (3.7-11), the optimum joint torque vector τ_2^* is obtained as

$$\tau_2^* = - [C_{z2} + C_{z2}^T]^{-1} J_2^{-1} J_{2c} \lambda \; . \qquad (3.7\text{-}14)$$

The relations in (3.7-13),and (3.7-14) still contain the unknown multipliers λ. To eliminate λ, (3.7-12) is used as

$$J_{1c}^T J_1^{-T} \tau_1^* + J_{2c}^T J_2^{-T} \tau_2^* - \xi = 0 \quad . \qquad (3.7\text{-}15)$$

Substitute τ_1^* and τ_2^* from (3.7-13) and (3.7-14) in (3.7-15) to get

$$- J_{1c}^T J_1^{-T} \left[C_{z1} + C_{z1}^T \right]^{-1} J_1^{-1} J_{1c} \lambda - J_{2c}^T J_2^{-T} \left[C_{z2} + C_{z2}^T \right]^{-1}$$

$$J_2^{-1} J_{2c} \lambda - \xi = 0$$

$$\text{or,} \quad \lambda = -\left[J_{1c}^T J_1^{-T} \left[C_{z1} + C_{z1}^T \right]^{-1} J_1^{-1} J_{1c} + J_{2c}^T J_2^{-T} \left[C_{z2} + C_{z2}^T \right]^{-1} \right.$$

$$\left. J_2^{-1} J_{2c} \right]^{-1} \xi \quad . \qquad (3.7\text{-}16)$$

Finally τ_1^* and τ_2^* are obtained by substituting λ from (3.7-16) in (3.7-13) and (3.7-14). Thus

$$\tau_1^* = C_{1red} \xi \qquad (3.7\text{-}17)$$

$$\tau_2^* = C_{2red} \xi \qquad (3.7\text{-}18)$$

where

$$C_{1red} = \left[C_{z1} + C_{z1}^T \right]^{-1} J_1^{-1} J_{1c} \left[J_{1c}^T J_1^{-T} \left[C_{z1} + C_{z1}^T \right]^{-1} J_1^{-1} J_{1c} \right.$$

$$\left. + J_{2c}^T J_2^{-T} \left[C_{z2} + C_{z2}^T \right]^{-1} J_2^{-1} J_{2c} \right]^{-1} \qquad (3.7\text{-}19)$$

and

$$C_{2red} = \left[C_{z2} + C_{z2}^T \right]^{-1} J_2^{-1} J_{2c} \left[J_{1c}^T J_1^{-T} \left[C_{z1} + C_{z1}^T \right]^{-1} J_1^{-1} J_{1c} \right.$$

$$+ J_{2c}^{T} J_{2}^{-T} \left[C_{z2} + C_{z2}^{T} \right]^{-1} J_{2}^{-1} J_{2c} \Big]^{-1} \quad . \qquad (3.7\text{-}20)$$

C_{1red} and C_{2red} are the matrices to resolve the joint torque redundancy and these matrices depend upon the motor parameters (which are constants) and the joint positions (which vary along the path).

As mentioned at the end of section 3.6 ,ξ at this stage, is assumed to be known and hence τ_1^* and τ_2^* can be obtained from (3.7-17) and (3.7-18). But the problem specifies only the path, and the time histories (i.e. velocities and accelerations) are to be determined. This part of the trajectory planning is addressed in the following section.

3.8 Trajectory Planning

The trajectory planning aspect involves determination of time histories of the joints in carrying the object through the specified path. One obvious consideration is that the task be finished in minimum time. Another consideration undertaken is that the overall energy used by the arms in performing the task should be minimum. To this end two objective functions are formulated as follows:

Case I: Minimum Time Problem: The objective function for the minimum time can be expressed as

$$Z_t = \int_{0}^{t_f} dt \qquad (3.8\text{-}1)$$

where t_f is the final time to reach the end of the path.

According to this criterion the total time of travel is most important so the system will try to be always at the maximum limits of actuator forces and actuator velocities whichever is reached first.

Case II: Minimum Energy Problem:one might consider a minimization criterion based upon the electrical energy consumption. In that case, from relation (3.7-3), the total energy consumption can be written as

$$z_e = \int_0^{tf} (\tau_1^{*T} C_{tp1} \tau_1^* + \tau_2^{*T} C_{tp2} \tau_2^*) \, dt \qquad (3.8\text{-}2)$$

where τ_1^* and τ_2^* are given by (3.7-17) and (3.7-18) and the cost matrices C_{tp1} and C_{tp2} are explained in (3.7-4) and (3.7-5). It may be noted here that minimizing the energy consumption alone over the trajectory does not yield practical and interesting results since the system behaviour is to move at very low velocities over a long time span and thus consume low power.

Case III. Minimum Energy plus Minimium Time problem: For this (3.8-1) and (3.8-2) are weighted and combined to form the hybrid objective function Z_{te} as

$$Z_{te} = \beta_1 \int_0^{tf} dt + \beta_2 \int_0^{tf} (\tau_1^{*T} C_{tp1} \tau_1^* + \tau_2^{*T} C_{tp2} \tau_2^*) \, dt \qquad (3.8\text{-}3)$$

where β_1 and β_2 are weightages of minimum time and minimum energy criteria. The trajectory planning problem is now stated as follows:

Minimize (3.8-1) for case-I and minimize (3.8-3) for case-II subject to the following constraints:

i) The torques τ_1^* and τ_2^* satisfy the torque redundancy resolution (3.7-17) and (3.7-18).

ii) While in motion, the actuators of the arms should not cross their velocity limits. These constraints are given by

$$\dot{q}_{1imin} \leq \dot{q}_{1i}(t) \leq \dot{q}_{1imax}$$

$$\dot{q}_{2imin} \leq \dot{q}_{2i}(t) \leq \dot{q}_{2imax} \quad ; \quad i=1,\ldots 6 \; ; \; 0 < t < t_f \qquad (3.8\text{-}4)$$

iii) Initially the object is at rest and at the end of the trajectory it should come to rest . Hence the joint velocities of the arms should be zero at the begining and end of the trajectory.These constraints are given by

$$\dot{q}_{1i}(0) = \dot{q}_{2i}(0) = 0$$

$$\dot{q}_{1i}(t_f) = \dot{q}_{2i}(t_f) = 0 \quad ; \quad i = 1, \ldots 6 \qquad (3.8\text{-}5)$$

iv) Every joint actuator has some joint force saturation limit. The trajectory planning should be such that no joint saturates during motion. The joint force constraints are given as

$$\tau_{1imin} \leq \tau_{1i}^*(t) \leq \tau_{1imax}$$
$$\tau_{2imin} \leq \tau_{2i}^*(t) \leq \tau_{2imax} \quad ; \quad i = 1,\ldots 6 \; ; \; 0 \leq t \leq t_f \qquad (3.8\text{-}6)$$

3.9 Discrete Time Formulations

The dynamic equations of the arms developed in the earlier sections are highly coupled and nonlinear. The closed form solutions of the dynamic equations are not possible. Hence some numerical method is to be employed to solve these equations. In the subsequent sections the numerical method used for solving the dynamic equations is discussed and these schemes follow the work in Tan and Potts [1989].

3.9.1 Discretization Schemes

The dynamic equations of the arms and object are differential equations which involve position, velocity and acceleration terms of the joints and object .The Finite Difference Method is a numerical method where positions, velocities and accelerations are represented by discrete time functions. Thus the differential equations are converted to algebraic equations which are called difference equations. The process of generating discrete time functions from continuous time functions is called "discretization" which was developed from the principles of numerical integration [Rice 1983]. The most popular discretization schemes for dynamic physical system modeling are the forward and backward Euler (or rectangular) algorithms and the trapezoidal (or Tustin) rule [Palm, 1983; Franklin, 1980]. The explicit forward and implicit backward Euler algorithms are easy to apply. The implicit trapezoidal rule is more accurate than the Euler algorithms. The trapezoidal rule is also called smoothing formula [Rice, 1983]. This formula has two following fundamental

properties:

1) In the limit (as the step-size goes to zero), the trapezoidal rule approaches the definition of the dervative [Franklin 1980].

2) the trapezoidal rule produces (at each sampling constant) a cubic spline function from which the position can be determined at any point within the sampling period [Jain 1979].

In the present work the discretization scheme uses the trapezoidal (smoothing) formula to approximate the differential relations.

3.9.2 Discretization of Dynamic Models of Arms and Object

The problem under consideration specifies the position and orientation of the object along a path for doing a task. The path is described by a succession of points in the workspace with proper orientation of the object. The specified path is divided into M intervals by choosing M+1 knot points along the path. By inverse kinematics the joint positions of the arms corresponding to each knot point are determined. The position, velocity and forces are functions of time in continuous dynamic model. These functions at different knot points are distinguished by their knot point numbers. Thus ,the position for the lth arm and the pth joint at the kth knot point is designated by $q_{lp}(k)$ where $k=0,\ldots,M$; $l = 1,2$; and $p=1,\ldots,6$. Similarly $\dot{q}_{lp}(k)$ is the joint velocity of the pth joint of the lth arm and at the kth knot. If $t(k)$, $k=0,\ldots,M$, denotes the time when the object is at the kth

knot point of the path, then the time required for the arms and object to move from the kth knot point to (k+1) th knot point is $\Delta t(k) = t(k+1) - t(k)$, for k=0, ...,M-1, and the corresponding reciprocal time interval is defined as

$$H(k+1) = \frac{1}{\Delta t(k)} = \frac{1}{t(k+1) - t(k)} \quad \text{for } k=0,\ldots,M-1 \ . \tag{3.9-1}$$

If $q_{lp}(k)$, $q_{lp}(k-1)$,$\dot{q}_{lp}(k-1)$ and $\Delta t(k-1)$ are known then $\dot{q}_{lp}(k)$ (velocity of pth joint of lth arm) can be determined by using the following trapezoidal smoothing formula:

$$q_{lp}(k) - q_{lp}(k-1) = \frac{1}{2} \Delta t(k-1) \, (\dot{q}_{lp}(k) + \dot{q}_{lp}(k-1)) \tag{3.9-2}$$

Replacing $\Delta t(k-1)$ by $H(k)$ the relation (3.9.2) is rearranged to get the recursive relation for joint velocity $\dot{q}_{lp}(k)$ as

$$\dot{q}_{lp}(k) = - \dot{q}_{lp}(k-1) + 2H(k)(q_{lp}(k) - q_{lp}(k-1))$$

$$\text{for } k=1,2,\ldots M \tag{3.9-3}$$

$$\text{or, } \dot{q}_{lp}(k) = (-1)^k \dot{q}_{lp}(0) + 2(-1)^k \sum_{i=1}^{k} (-1)^i \Delta q_{lp}(i-1)H(i)$$

$$; \ k = 1,\ldots,\ M \tag{3.9-4}$$

$$\text{where } \Delta q_{lp}(k-1) = q_{lp}(k) - q_{lp}(k-1) \quad . \tag{3.9-5}$$

For compact notations needed later ,(3.9-4) is rewritten as

$$\dot{q}_{lp}(k) = cv_{lp}(k,0) + \sum_{i=1}^{M} cv_{lp}(k,i)\, H(i) \qquad (3.9\text{-}6)$$

$$; \; l=1,2 \quad p=1,2,\ldots 6 \quad k=1,2,..M$$

where,

$$cv_{lp}(k,0) = (-1)^k \dot{q}_{lp}(0) \quad , \qquad (3.9\text{-}7)$$

$$cv_{lp}(k,i) = 2\,(-1)^{k+i}\, \Delta q_{lp}(i-1) \quad \text{for} \quad i=1,\ldots,k \qquad (3.9\text{-}8)$$

and $cv_{lp}(k,i) = 0 \qquad \text{for } i=(k+1).....M$.

3.9.3 Discrete Dynamic Equations for the Arms

For discretization of the equations of motions, the Lagrange- Euler equation (3.6-6) is used. The first term of (3.6-6), which is the time rate of change of the momentum, is discretized as

$$\frac{d}{dt}\left[\sum_{i=1}^{6} d_{lip}\, \dot{q}_{li}\right] \simeq$$

$$\frac{1}{\Delta t(k-1)} \sum_{i=1}^{6} \left[d_{lip}(k)\, \dot{q}_{li}(k) - d_{lip}(k-1)\, \dot{q}_{li}(k-1) \right] ;$$

$$k=1,\ldots,M \; ; \; l=1,2 \; . \qquad (3.9\text{-}9)$$

In (3.9-9) $d_{lip}(k)$ and $d_{lip}(k-1)$ are discrete inertia coefficients at the kth and (k-1) th knot points. The continuous variable $\dot{q}_{li}(t)$ is replaced by its discrete form $\dot{q}_{li}(k-1)$ and $\dot{q}_{li}(k)$ at the (k-1) th and k th knot points. The second term of (3.6-6), which includes the coriolis and centrifugal effcts and is in the form of partial derivative with respect to the pth joint variable, is discretized as

$$-\frac{\partial}{\partial q_{lp}}\left[\frac{1}{2}\sum_{i=1}^{6}\sum_{j=1}^{6}\dot{q}_{li}\; d_{lij}\; \dot{q}_{lj}\right] \simeq$$

$$-\frac{1}{q_{lp}(k)-q_{lp}(k-1)}\left\{\frac{1}{2}\sum_{i=1}^{6}\sum_{j=1}^{6}\left[d_{lij}(p;k)-d_{lij}(p;k-1)\right]\right.$$

$$\left.\frac{1}{2}\left[\dot{q}_{li}(k-1)\,\dot{q}_{lj}(k)+\dot{q}_{li}(k)\,\dot{q}_{lj}(k-1)\right]\right\} \; ; \; k=1,..M \qquad (3.9\text{-}10)$$

where the quantities $d_{lij}(p;k)$ and $d_{lij}(p;k-1)$ are hybrid discrete inertia coefficients [Tan and Potts, 1989], and are defined as

$$d_{lij}(p;k) = d_{lij}\left[q_{l1}(k-1),\ldots,q_{l\,p-1}(k-1),\; q_{lp}(k),\right.$$

$$\left.q_{lp+1}(k),\ldots,q_{l6}(k)\right] \qquad (3.9\text{-}11)$$

$$\text{and } d_{1ij}(p;k-1) = d_{1ij}\left[q_{11}(k-1), \ldots\ldots, q_{1\,p-1}(k-1), q_{1p}(k-1), q_{1\,p+1}(k), \ldots\ldots\ldots, q_{16}(k)\right] . \qquad (3.9\text{-}12)$$

The discrete time functions in (3.9-11) and (3.9-12) are hybrid because in (3.9-12) p coordinates and in (3.9-11) p-1 coordinates are evaluated at the beginning of the kth sampling period and the remaining 6-p (or (6-p+1)) coordinates are evaluated at the end of the sampling period. The third term of (3.6-6) is the effect of gravitational force on joint p of the 1th arm, and is a function of the joint coordinates. This term is discretized as

$$\frac{\partial PE_1}{\partial q_{1p}} = \frac{PE_1(p;k) - PE_1(p;k-1)}{q_{1p}(k) - q_{1p}(k-1)} \; ; \; k = 1,2....M . \qquad (3.9\text{-}13)$$

In (3.9-13) the terms $PE_1(p;k)$ and $PE_1(p;k-1)$ are hybrid discrete functions similar to the ones in (3.9-10). Thus the discrete terms $PE_1(p;k)$ and $PE_1(p;k-1)$ are defined as

$$PE_1(p;k) = PE_1\left[q_{11}(k-1), \ldots\ldots, q_{1\,p-1}(k-1), q_{1p}(k), q_{1\,p+1}(k), \ldots\ldots\ldots, q_{16}(k)\right] \qquad (3.9\text{-}14)$$

$$\text{and } PE_1(p;k-1) = PE_1\left[q_{11}(k-1), \ldots\ldots, q_{1p-1}(k-1), q_{1p}(k-1), q_{1\,p+1}(k), \ldots\ldots\ldots, q_{16}(k)\right] . \qquad (3.9\text{-}15)$$

The first term on the right hand side of (3.6-6) is the geeralized joint force at joint p. This torque is discretized as a variable which is piecewise constant over the k th time interval. Thus the continuous variable $\tau_{lp}(t)$ is discretized as

$$\tau_{lp}(t) \simeq \tau_{lp}(k) \quad \text{for } t(k-1) \leq t < t(k) \; k = 1,2...M \; . \qquad (3.9\text{-}16)$$

The second term on the right side of (3.6-6) is due to interactive forces with the object. This term is a function of joint coordinates. Therefore, the discrete form is

$$\sum_{i=1}^{6} J_{lip}{}^{w}f_{li} \simeq \sum_{i=1}^{6} J_{lip}(k)\,{}^{w}f_{li}(k) \qquad (3.9\text{-}17)$$

where $J_{lip}(k)$ is the element of the pth row and ith column of the transposed Jacobian matrix of the lth arm at the kth knot point. ${}^{w}f_{li}(k)$ denotes the value of the intractive force at the kth knot point and is assumed to be piecewise constant like the joint torque τ_l.

Now the complete form of the discrete dynamic model of the lth arm is written by combining (3.9-9), (3.9-10), (3.9-13), (3.9-16) and (3.9-17) as

$$H(k)\sum_{i=1}^{6}\left[d_{lip}(k)\,\dot{q}_{li}(k) - d_{lip}(k-1)\dot{q}_{li}(k-1)\right]$$

$$-\frac{1}{\Delta q_{lp}(k-1)}\left\{\frac{1}{2}\sum_{i=1}^{6}\sum_{j=1}^{6}\left[d_{lip}(p;k) - d_{lip}(p;k-1)\right]\right.$$

$$\left.\frac{1}{2}\left[\dot{q}_{li}(k-1)\,\dot{q}_{lj}(k) + \dot{q}_{li}(k)\dot{q}_{lj}(k-1)\right]\right\} + \frac{PE_l(p;k) - PE_l(p;k-1)}{\Delta\, q_{lp}(k-1)}$$

$$= \tau_{lp}(k) + \sum_{i=1}^{6} J_{lip}{}^{w}f_{li}(k) \quad \text{for } k = 1,2\ldots M \;;\; l = 1,2 \;;$$

$$p = 1,2\ldots.6 \qquad (3.9\text{-}18)$$

where $H(k)$ and $q_{lp}(k-1)$ are as given by (3.9-1) and (3.9-5), respectively. The above equation is written in a compact form as

$$\sum_{il=1}^{M}\sum_{jl=il}^{M} Ctmo_{lp}(k,il,jl)\; H(il)H(jl) + \sum_{il=1}^{M} ctvo_{lp}(k,il)H(il)$$

$$+ ctco_{lp}(k)$$

$$= \tau_{lp}(k) + \sum_{i=1}^{6} J_{lip}(k)^{w}f_{li}(k) \;;\; l=1,2 \;;\; p=1,2..6 \;;\; k=1,2..M,$$

$$(3.9\text{-}19)$$

where, the expressions for $\dot{q}_{lp}(k)$ have been substituted from (3.9-8) to yield the coefficaents in (3.9-19) as

$$Ctmo_{lp}(k,il,jl) = \varepsilon \sum_{i=1}^{6}\left(d_{lip}(k)\; cv_{li}(k;il) - d_{lip}(k-1)cv_{li}(k-1,il)\right.$$

$$- \frac{1}{\Delta q_{lp}(k-1)} \left\{ \frac{1}{2} \sum_{i=1}^{6} \sum_{j=1}^{6} \left[d_{lip}(p;k) - d_{lip}(p;k-1) \right] \right.$$

$$\frac{1}{2} \left[cv_{li}(k-1,il)\, cv_{lj}(k;jl) + cv_{li}(k-1,jl)\, cv_{lj}(k,il) \right.$$

$$\left. \left. + cv_{li}(k,il)\, cv_{lj}(k-1,jl) + cv_{li}(k,jl)\, cv_{lj}(k-1,il) \right] \right\}$$

$$\text{for } il < k \text{ and } jl \leq k;$$

$$\text{and } \varepsilon = \begin{cases} 1 & \text{for } jl = k \\ 0 & \text{for } jl \neq k. \end{cases}$$

$$\text{and } Ctmo_{lp}(k,il,jl) = 0 \text{ for } il > k \text{ or } jl > k \qquad (3.9\text{-}20)$$

$$ctvo_{lp}(k,il) = \varepsilon \sum_{i=1}^{6} \left(d_{lip}(k)\, cv_{li}(k;0) - d_{lip}(k-1) cv_{li}(k-1,0) \right)$$

$$- \frac{1}{\Delta q_{lp}(k-1)} \left\{ \frac{1}{2} \sum_{i=1}^{6} \sum_{j=1}^{6} \left[d_{lip}(p;k) - d_{lip}(p;k-1) \right] \right.$$

$$\frac{1}{2} \left[cv_{li}(k-1,0) cv_{lj}(k;il) + cv_{lj}(k,0)\, cv_{li}(k-1,il) \right.$$

$$\left. \left. + cv_{li}(k,0)\, cv_{lj}(k-1,il) + cv_{lj}(k-1,0)\, cv_{lj}(k,il) \right] \right\}$$

$$\text{for } il \leq k$$

$$\text{and} \quad \varepsilon = \begin{cases} 1 & \text{for } i_1 = k \\ 0 & \text{for } i_1 \neq k. \end{cases}$$

$$\text{and } ctvo_{1p}(k,il) = 0 \quad \text{if } il > k \qquad (3.9\text{-}21)$$

$$ctco_{1p}(k) - \frac{1}{\Delta q_{1p}(k-1)} \left\{ \frac{1}{2} \sum_{i=1}^{6} \sum_{j=1}^{6} \left[d_{1ip}(p;k) - d_{1ip}(p;k-1) \right] \right.$$

$$\left. \frac{1}{2} \left[cv_{1i}(k-1,0)\, cv_{1j}(k,0) + cv_{1i}(k,0)\, cv_{1j}(k-1,0) \right] \right\}$$

$$+ \frac{PE_1(p;k) - PE_1(p;k-1)}{\Delta q_{1p}(k-1)} \quad . \qquad (3.9\text{-}22)$$

In the above equation, $Ctmo_{1p}(k,il,jl)$ is the coefficient of the quadratic term $H(il)H(jl)$, $ctvo_{1p}(k,il)$ is the coefficient of the linear term $H(il)$, and $ctco_{1p}(k)$ represents the constant terms in H's.

3.9.4. Discrete Dynamic Equations for the Object

The position of the object at the kth knotpoint is given by the vector ${}^{w}\mathbf{p}_c(k)$, where ${}^{w}\mathbf{p}_c$ is as defined in (3.3-2). The orientation of the object at the kth knot point is given by the Euler angle vector $[\phi_1(k), \phi_2(k), \phi_3(k)]^T$ (see (3.3-2) and (A.1) of Appendix A). Now using the trapezoidal smoothing formula the linear and angular velocity vectors may be related to the respective linear and angular displacements vectors as

$$ {}^{w}p_c(k) - {}^{w}p_c(k-1) = \frac{1}{2}\,\Delta t(k-1)\left[{}^{w}\dot{p}_c(k) + {}^{w}\dot{p}_c(k-1)\right] \qquad (3.9\text{-}23) $$

$$ \text{and } \Phi_1(k) - \Phi_1(k-1) = \frac{1}{2}\,\Delta t(k-1)\left[\dot{\Phi}_1(k) + \dot{\Phi}_1(k-1)\right] . \qquad (3.9\text{-}24) $$

The relations (3.9-23) and (3.9-24) are expressed in terms of the reciprocal time interval $H(k) = 1/\Delta t(k-1)$ to get the linear and angular velocity vectors at the k th knot point as

$$ {}^{w}\dot{p}_c(k) = - {}^{w}\dot{p}_c(k-1) + 2H(k)\,\Delta {}^{w}\dot{p}_c(k-1) \qquad (3.9\text{-}25) $$

$$ \text{and} \quad \dot{\Phi}(k) = - \dot{\Phi}(k-1) + 2H(k) + \Delta\Phi(k-1) \qquad (3.9\text{-}26) $$

where

$$ \Delta {}^{w}P_c(k-1) = {}^{w}P_c(k) - {}^{w}P_c(k-1) \qquad (3.9\text{-}27) $$

$$ \text{and} \quad \Delta\Phi(k-1) = \Phi(k) - \Phi(k-1) . \qquad (3.9\text{-}28) $$

The linear velocity vector of the object with respect to the world coordinate frame is

$$ {}^{w}v_c(k) = {}^{w}\dot{P}_c(k) . \qquad (3.9\text{-}29) $$

By repeated use of (3.9-25) over k time intervals one gets

$$ {}^{w}v_c(k) = {}^{w}\dot{p}_c(k) = \sum_{i=1}^{k} (-1)^{i+k}\, 2\Delta {}^{w}p_c(i-1)\, H(i) + (-1)^{k}\, {}^{w}v_c(0) $$

$$; \; k = 1,2.....M . \qquad (3.9\text{-}30) $$

The equation (3.9-30) is rewritten in the form

$$w_{v_c}(k) = cv_c\ (k,0) + \sum_{i=1}^{M} cv_c\ (k,i)\ H(i) \qquad (3.9\text{-}31)$$

where,

$$cv_{cx}\ (k,0) = (-1)^k\ w_{v_{cx}}(0)\ ,$$

$$cv_{cx}\ (k,i) = (-1)^{i+k}\ 2\Delta^{w}p_{cx}\ (i-1) \quad \text{for } i \leq k$$

$$= 0 \quad \text{for } i > k\ ,$$

$$cv_{cy}\ (k,0) = (-1)^k\ w_{v_{cy}}(0)\ ,$$

$$cv_{cy}\ (k,i) = (-1)^{i+k}\ 2\Delta^{w}p_{cy}\ (i-1) \quad \text{for } i \leq k$$

$$= 0 \quad \text{for } i > k\ ,$$

$$cv_{cz}\ (k,0) = (-1)^k\ w_{v_{cz}}(0)$$

and $$cv_{cz}\ (k,i) = (-1)^{i+k}\ 2\Delta^{w}p_{cz}\ (i-1) \quad \text{for } i \leq k$$

$$= 0 \quad \text{for } i > k\ .$$

(3.9 - 32)

Similarly (3.9-26) can be recursively applied to obtain

$$\dot{\Phi}(k) = \begin{bmatrix} \dot{\phi}_1(k) \\ \dot{\phi}_2(k) \\ \dot{\phi}_3(k) \end{bmatrix} = \begin{bmatrix} ce_{c1}(k,0) + \sum_{i=1}^{M} ce_{c1}(k,i)\, H(i) \\ ce_{c2}(k,0) + \sum_{i=1}^{M} ce_{c2}(k,i)\, H(i) \\ ce_{c3}(k,0) + \sum_{i=1}^{M} ce_{c3}(k,i)\, H(i) \end{bmatrix}$$

$$= ce_c(k,0) + \sum_{i=1}^{M} ce_c(k,i)\, H(i) \qquad (3.9\text{-}33)$$

where

$$ce_{c1}(k,0) = (-1)^k \dot{\phi}_1(0) \ ,$$

$$ce_{c1}(k,i) = (-1)^{i+k}\, 2\Delta\phi_1\, (i-1),$$

$$ce_{c2}(k,0) = (-1)^k \dot{\phi}_2(0) \ ,$$

$$ce_{c2}(k,i) = (-1)^{i+k}\, 2\Delta\phi_2\, (i-1),$$

$$ce_{c3}(k,0) = (-1)^k \dot{\phi}_3(0)$$

and $$ce_{c3}(k,i) = (-1)^{i+k} 2\Delta\phi_3 (i-1) \ .$$

(3.9-34)

The components of the object angular velocity in the world frame

$\left[{}^{w}\omega_{cx}, {}^{w}\omega_{cy}, {}^{w}\omega_{xz}\right]^T$ and the rate of change of Euler angles $\left[\dot{\phi}_1, \dot{\phi}_2, \dot{\phi}_3\right]^T$ are related by (3.4-4). Therefore, if the instanteneous angular velocity vector is expressed in terms of the reciprocal time intervals by

$$ {}^{w}\Omega_c(k) = \begin{bmatrix} {}^{w}\omega_{cx}(k) \\ {}^{w}\omega_{cy}(k) \\ {}^{w}\omega_{cz}(k) \end{bmatrix} = \begin{bmatrix} cn_{cx}(k) + \sum_{i=1}^{M} cn_{cx}(k,i)\, H(i) \\ cn_{cy}(k) + \sum_{i=1}^{M} cn_{cy}(k,i)\, H(i) \\ cn_{cz}(k) + \sum_{i=1}^{M} cn_{cz}(k,i)\, H(i) \end{bmatrix} \qquad (3.9\text{-}35) $$

then from (3.4-4) and (3.9-33) the coefficients in (3.9-35) are obtained as

$$ cn_{cx}(k) = ce_{c2}(k,0)\cos\phi_1(k) + ce_{c3}(k,0)\sin\phi_1(k)\sin\phi_2(k), $$

$$ cn_{cx}(k,i) = ce_{c2}(k,i)\cos\phi_1(k) + ce_{c3}(k,i)\sin\phi_1(k)\sin\phi_2(k), $$

$$ cn_{cy}(k) = ce_{c2}(k,0)\sin\phi_1(k) - ce_{c3}(k,0)\cos\phi_1(k)\sin\phi_2(k), $$

$$ cn_{cy}(k,i) = ce_{c2}(k,i)\sin\phi_1(k) - ce_{c3}(k,i)\cos\phi_1(k)\sin\phi_2(k), $$

$$ cn_{cz}(k) = ce_{c1}(k,0) + ce_{c3}(k,0)\cos\phi_2(k) $$

and $$ cn_{cz}(k,i) = ce_{c1}(k,i) + ce_{c3}(k,i)\cos\phi_2(k) . \qquad (3.9\text{-}36) $$

Now the left hand side of (3.6-11) is to be discretized. The rate

of change of linear momentum is written as

$$\frac{d}{dt}\left(m_c \, {}^{w}\mathbf{v}_c \right) = m_c \, {}^{w}\dot{\mathbf{v}}_c \qquad (3.9\text{-}37)$$

where ${}^{w}\dot{\mathbf{v}}_c$ is the linear acceleration of the object and is expressed in the discretized form as

$$\begin{aligned} {}^{w}\dot{\mathbf{v}}_c(k) &= \left[{}^{w}\mathbf{v}_c(k) - {}^{w}\mathbf{v}_c(k-1) \right] H(k) \\ &= \mathbf{cl}_c(k,0)\, H(k) + \sum_{i=1}^{M} \mathbf{cl}_c(k,i)\, H(i)\, H(k) \end{aligned} \qquad (3.9\text{-}38)$$

where

$$\mathbf{cl}_c(k,0) = \mathbf{cv}_c(k,0) - \mathbf{cv}_c(k-1,0)$$

and $$\begin{aligned} \mathbf{cl}_c(k,i) &= \mathbf{cv}_c(k,i) - \mathbf{cv}_c(k-1,i) \quad \text{if } i \le k \\ &= 0 \quad \text{if } i > k \; . \end{aligned} \qquad (3.9\text{-}39)$$

The discretization of the rate of change of angular momentum is done in the following manner.

$$\frac{d}{dt}\left[{}^{w}\mathbf{I}_c \, {}^{w}\Omega_c \right] = H(k) \left[{}^{w}\mathbf{I}_c(k) \, {}^{w}\Omega_c(k) - {}^{w}\mathbf{I}_c(k-1) \, {}^{w}\Omega_c(k-1) \right]$$

$$; \; k = 1,2,\ldots M \qquad (3.9\text{-}41)$$

where, $H(k) = \dfrac{1}{\Delta t(k-1)}$,

$^{w}I_{c}(k) = {}^{w}R_{c}(k)\ {}^{c}I_{c}\ {}^{w}R_{c}(k)^{T}$ from (3.6-10) .

$^{w}R_{c}(k)$ is the rotation part of $^{w}T_{c}$ in (3.3-2) at the kth knot point, and $^{w}\Omega_{c}(k)$ is obtained from (3.9-35).

At this stage, the left hand side of (3.6-11) is also put in the form of (3.9-19) so that quadratic and linear terms in H's and the constant terms are collected.

To this end, first (3.9-37) is expanded with the help of (3.9-39) and (3.9-32) to get

$$m_{c}\ {}^{w}\dot{v}_{c}(k) - m_{c}\ {}^{w}g =$$

$$\begin{bmatrix} crc_{1}(k) + \sum_{il=1}^{M} crv_{1}(k,il)\ H(il) + \sum_{il=1}^{M}\sum_{jl=1}^{M} crm_{1}(k,il,jl)H(il)H(jl) \\ crc_{2}(k) + \sum_{il=1}^{M} crv_{2}(k,il)\ H(il) + \sum_{il=1}^{M}\sum_{jl=1}^{M} crm_{2}(k,il,jl)H(il)H(jl) \\ crc_{3}(k) + \sum_{il=1}^{M} crv_{3}(k,il)\ H(il) + \sum_{il=1}^{M}\sum_{jl=1}^{M} crm_{3}(k,il,jl)H(il)H(jl) \end{bmatrix}$$

(3.9-41)

where,

$$crc_{1}(k) = -\ m_{c}\ {}^{w}g_{x} \ ,$$

$$crv_{1}(k,il) = m_{c}(cv_{cx}(k,0) - cv_{cx}(k-1,0)) \qquad \text{if } il = k$$

$$= 0 \qquad \text{if } il \neq k,$$

$$crm_1(k,il,jl) = m_c(cv_{cx}(k,il) - cv_{cx}(k-1,il)) \quad \text{if } jl = k$$
$$= 0 \quad \text{if } jl \neq k,$$

$$crc_2(k) = -m_c {}^{w}g_y ,$$
$$crv_2(k,il) = m_c(cv_{cy}(k,0) - cv_{cy}(k-1,0)) \quad \text{if } il = k$$
$$= 0 \quad \text{if } il \neq k,$$

$$crm_2(k,il,jl) = m_c(cv_{cy}(k,il) - cv_{cy}(k-1,il)) \quad \text{if } jl = k$$
$$= 0 \quad \text{if } jl \neq k,$$

$$crc_3(k) = -m_c {}^{w}g_z ,$$
$$crv_3(k,il) = m_c(cv_{cz}(k,0) - cv_{cz}(k-1,0)) \quad \text{if } il = k$$
$$= 0 \quad \text{if } il \neq k ,$$

and $$crm_3(k,il,jl) = m_c(cv_{cz}(k,il) - cv_{cz}(k-1,il)) \quad \text{if } jl = k$$
$$= 0 \quad \text{if } jl \neq k.$$

(3.9-42)

Next the rate of change of angular momentum (3.9-40) is expanded with the help of (3.9-35) to yield

$$\frac{d}{dt}\left[{}^{w}I_c\,{}^{w}\Omega_c\right] = H(k)\left[{}^{w}I_c(k)\,(cn_c(k) + \sum_{i=1}^{M} cn_c(k,i)\,H(i))\right.$$

$$\left. - {}^{w}I_c(k-1)\,(cn_c(k-1) + \sum_{i=1}^{M} cn_c(k-1,i)\,H(i))\right]$$

or, $$\frac{d}{dt}\left[{}^{w}I_c\,{}^{w}\Omega_c\right] =$$

$$\begin{bmatrix} crc_4(k) + \sum_{il=1}^{M} crv_4(k,il)\,H(il) + \sum_{il=1}^{M}\sum_{jl=1}^{M} crm_4(k,il,jl)H(il)H(jl) \\ crc_5(k) + \sum_{il=1}^{M} crv_5(k,il)\,H(il) + \sum_{il=1}^{M}\sum_{jl=1}^{M} crm_5(k,il,jl)H(il)H(jl) \\ crc_6(k) + \sum_{il=1}^{M} crv_6(k,il)\,H(il) + \sum_{il=1}^{M}\sum_{jl=1}^{M} crm_6(k,il,jl)H(il)H(jl) \end{bmatrix}$$

(3.9-43)

where

$$crc_4(k) = crc_5(k) = crc_6(k) = 0,$$

$$\begin{aligned} crv_4(k,il) &= {}^{w}I_{cxx}(k)\, cn_{cx}(k) + {}^{w}I_{cxy}(k)\, cn_{cy}(k) \\ &\quad + {}^{w}I_{cxz}(k)\, cn_{cz}(k) - {}^{w}I_{cxx}(k-1)\, cn_{cx}(k-1) \\ &\quad - {}^{w}I_{cxy}(k-1)\, cn_{cy}(k-1) - {}^{w}I_{cxz}(k-1)\, cn_{cz}(k-1) \\ &\qquad\qquad\qquad\qquad\qquad\qquad \text{if } il = k \\ &= 0 \qquad\qquad\qquad\qquad\qquad\qquad \text{if } il \neq k\ , \end{aligned}$$

$$\begin{aligned} crm_4(k,il,jl) &= {}^{w}I_{cxx}(k)\, cn_{cx}(k,il) + {}^{w}I_{cxy}(k)\, cn_{cy}(k,il) \\ &\quad + {}^{w}I_{cxz}(k)\, cn_{cz}(k,il) - {}^{w}I_{cxx}(k-1)\, cn_{cx}(k-1,il) \\ &\quad - {}^{w}I_{cxy}(k-1)\, cn_{cy}(k-1,il) - {}^{w}I_{cxz}(k-1)\, cn_{cz}(k-1,il) \\ &\qquad\qquad\qquad\qquad\qquad\qquad \text{if } jl = k, \\ &= 0 \qquad\qquad\qquad\qquad\qquad\qquad \text{if } jl \neq k, \end{aligned}$$

$$\begin{aligned} crv_5(k,il) &= {}^{w}I_{cyx}(k)\, cn_{cx}(k) + {}^{w}I_{cyy}(k)\, cn_{cy}(k) \\ &\quad + {}^{w}I_{cyz}(k)\, cn_{cz}(k) - {}^{w}I_{cyx}(k-1)\, cn_{cx}(k-1) \\ &\quad - {}^{w}I_{cyy}(k-1)\, cn_{cy}(k-1) - {}^{w}I_{cyz}(k-1)\, cn_{cz}(k-1) \end{aligned}$$

$$= \quad \emptyset \qquad \text{if } il \neq k \ ,$$

$$crm_5(k,il,jl) = {}^{w}I_{cyx}(k)\ cn_{cx}(k,il) + {}^{w}I_{cyy}(k)\ cn_{cy}(k,il) + {}^{w}I_{cyz}(k)\ cn_{cz}(k,il) - {}^{w}I_{cyx}(k-1)\ cn_{cx}(k-1,il) - {}^{w}I_{cyy}(k-1)\ cn_{cy}(k-1,il) - {}^{w}I_{cyz}(k-1)\ cn_{cz}(k-1,il) \qquad \text{if } jl = k$$

$$= \emptyset \qquad \text{if } jl \neq k,$$

$$crv_6(k,il) = {}^{w}I_{czx}(k)\ cn_{cx}(k) + {}^{w}I_{czy}(k)\ cn_{cy}(k) + {}^{w}I_{czz}(k)\ cn_{cz}(k) - {}^{w}I_{czx}(k-1)\ cn_{cx}(k-1) - {}^{w}I_{czy}(k-1)\ cn_{cy}(k-1) - {}^{w}I_{czz}(k-1)\ cn_{cz}(k-1) \qquad \text{if } il = k$$

$$= \emptyset \qquad \text{if } il \neq k,$$

$$crm_6(k,il,jl) = {}^{w}I_{czx}(k)\ cn_{cx}(k,il) + {}^{w}I_{czy}(k)\ cn_{cy}(k,il) + {}^{w}I_{czz}(k)\ cn_{cz}(k,il) - {}^{w}I_{czx}(k-1)\ cn_{cx}(k-1,il) - {}^{w}I_{czy}(k-1)\ cn_{cy}(k-1,il) - {}^{w}I_{czz}(k-1)\ cn_{cz}(k-1,il) \qquad \text{if } jl = k$$

$$= \emptyset \qquad \text{if } jl \neq k.$$

(3.9-44)

${}^{w}I_{cxx}(k)$ etc are the elements of the inertia matrix ${}^{w}I_{c}(k)$ given by

$$ {}^{w}I_{c}(k) = \begin{bmatrix} {}^{w}I_{cxx}(k) & {}^{w}I_{cxy}(k) & {}^{w}I_{cxz}(k) \\ {}^{w}I_{cyx}(k) & {}^{w}I_{cyy}(k) & {}^{w}I_{cyz}(k) \\ I_{czx}(k) & I_{czy}(k) & I_{czz}(k) \end{bmatrix} \qquad (3.9\text{-}45) $$

and $cn_{cx}(k)$ etc.are the elements of $\mathbf{cn}_c$ from (3.9-36). Now instead of writing the complete object dynamics (3.6-11) in discrete form, the combined arms plus object dynamics is considered, which is given by (3.6-15). As mentioned in Sec. 3.7, the torque redundancy arising in (3.6-15) is resolved according to (3.7-17) and (3.7-18).

3.9.5 Discrete form of Torque Redundancy Resolution

The optimum torque distribution among the arm actuators is directly written from (3.7-17) and (3.7-18) as

$$ \tau_l^{*}(k) = \mathbf{C}_{l\ red}(k)\,\xi(k) \qquad ;\quad l = 1,2 \qquad (3.9\text{-}46) $$

where, $\xi(k) = \xi_1(k) + \xi_2(k) + \xi_3(k)$ from (3.6-16) to (3.6-19). (3.9-47)

The explicit discrete relations for ξ's, which are six dimensional vectors, are written in terms of the components of ξ's. First considering $\xi_1(k)$ and $\xi_2(k)$, their components are expressed as

$$ \xi_l(k) = \left[\xi_l(k,1),\ \xi_l(k,2),\ \ldots\ldots\ldots \xi_l(k,6)\right]^{T} ; \quad l=1,2. \qquad (3.9\text{-}48) $$

That is, the components of $\xi_1(k)$ (1=1,2) are $\xi_1(k,i2)$, for i2= 1,2..6. Now from (3.6-17) and (3.6-18) and the left hand side of (3.9-19), the components of $\xi_1(k)$ and $\xi_2(k)$ become

$$\xi_1(k,i2) = \sum_{i1=1}^{M} \sum_{j1=1}^{M} ctmr_{1\ i2}(k,i1,j1)\ H(i1)H(j1)$$

$$+ \sum_{i1=1}^{M} ctvr_{1\ i2}(k,i1)\ H(i1) + ctcr_{1\ i2}(k)$$

$$1 = 1,2\ ;\quad i2 = 1,2...6 \qquad (3.9\text{-}49)$$

where

$$ctmr_{1\ i2}(k,i1,j1) = \sum_{j2=1}^{6} J_{g1}(k,i2,j2)\ ctmo_{1\ j2}(k,i1,j1),$$

$$ctvr_{1\ i2}(k,i1) = \sum_{j2=1}^{6} J_{g1}(k,i2,j2)\ ctvo_{1\ j2}(k,i2),$$

$$ctcr_{1\ i2}(k) = \sum_{j2=1}^{6} J_{g1}(k,i2,j2)\ ctco_{1\ j2}(k).$$

(3.9-50)

$ctm0_{1\ j2}(k,i1,j1)$, $ctv0_{1\ j2}(k,i1)$ and $ctc0_{1\ j2}(k)$ are given in (3.9-20) and (3.9-22). $J_{g1}(k,i2,j2)$ denotes the element in the i2 th row and j2 th column of

$$J_{g1}(k) = J_{1c}^{T}(k)\ J_{1}^{-T}(k)\ . \qquad (3.9\text{-}51)$$

In a similar fashion, the six components of $\xi_3(k)$ in (3.9-47) are

written with help from (3.9-41) and (3.9-43) to obtain

$$\xi_3(k,i2) = \sum_{i1=1}^{M} \sum_{j1=1}^{M} crm_{i2}(k,i1,j1)\, H(i1)H(j1)$$

$$+ \sum_{i1=1}^{M} crv_{i2}(k,i1)\, H(i1) + crc_{i2}(k)$$

$$i2 = 1,2...6 \ . \qquad (3.9\text{-}52)$$

Thus $\xi(k)$ in (3.9-47) is determined by adding $\xi_1(k)$ and $\xi_2(k)$ from (3.9-49) and $\xi_3(k)$ from (3.9-52) and hence the optimum torque $\tau_1^*(k)$ is determined from (3.9-46) in the following form:

$$\tau_1^*(k,i2) = \sum_{i1=1}^{M} \sum_{j1=1}^{M} ctm_{1\ i2}(k,i1,j1)\, H(i1)H(j1)$$

$$+ \sum_{i1=1}^{M} ctv_{1\ i2}(k,i1)\, H(i1) + ctc_{1\ i2}(k);$$

$$1 = 1,2 \ ; \quad i2 = 1,2...6 \qquad (3.9\text{-}53)$$

where

$$CTM_{1\ i2}(k,i1,j1) = \sum_{j2=1}^{6} C_{1\ red}(k,i2,j2) \left\{ ctmr_{1\ j2}(k,i1,j1) \right.$$

$$\left. + ctmr_{2\ j2}(k,i1,j1) + crm_{j2}(k,i1,j1) \right\},$$

$$ctv_{1\ i2}(k,i1) = \sum_{j2=1}^{6} C_{1\ red}(k,i2,j2) \left\{ ctvr_{1\ j2}(k,i1) \right.$$

$$+ ctvr_{2\ j2}(k,i1) + crv_{j2}(k,i1) \Big\} ,$$

$$ctc_{1\ i2}(k) = \sum_{j2=1}^{6} C_{1\ red}(k,i2,j2) \Big\{ ctcr_{1\ j2}(k) + ctcr_{2\ j2}(k) + crc_{j2}(k) \Big\} \quad . \qquad (3.9\text{-}54)$$

$C_{1\ red}(k,i2,j2)$ is the element in the i2 th row and j2 th column of $C_{1\ red}(k)$ from (3.7-19) and (3.7-20) and $Ctmr_{1j2}(k,i1,j1)$, $Ctvr_{1j2}(k,i1)$ etc are from (3.9-50), (3.9-42) and (3.9-44). Finally (3.9-53) is represented as

$$\tau_1^*(k,i2) = \mathbf{h}^T \mathbf{CTM}_{1\ i2}(k)\ \mathbf{h} + \mathbf{h}^T \mathbf{ctv}_{1\ i2}(k) + ctc_{1\ i2}(k)$$

$$1 = 1,2 \ ;\ i2=1,2,..6 \ ;k = 1,..M \qquad (3.9\text{-}55)$$

where $\mathbf{h}$ is an Mx1 vector such that its ith element, H(i), denotes the reciprocal time internal between the (i-1)th and ith knot points, $\mathbf{CTM}_{1\ i2}(k)$ is an MxM matrix of coefficients of quadratic terms in H such that the element corresponding to the ith row and jth column of this matrix is $CTM_{1\ i2}(k,i,j)$ with the condition that $CTM_{1\ i2}(k,i,j) = 0$ if $i>k$ or $j>k$, $ctv_{1\ i2}(k)$ is an Mx1 vector of coefficents of linear terms in H with a condition on its i th element that $ctv_{1\ i2}(k,i) = 0$ if $i > k$, and $ctc_{1\ i2}(k)$ represents the constant term.

3.9.6 Discretized Trajectory Planning

The trajectory planning problem which is developed in Sec. 3.8 may be converted to a discrete form by discretizing the objective function and different constraints. Thus the problem is restated as

minimize Z_{te}, where

$$Z_{te} = \beta_1 \sum_{i=1}^{M} \frac{1}{H(i)} + \beta_2 \sum_{i=1}^{M} \left[\tau_1^{*T}(i) C_{tp1} \tau_1^{*T}(i) + \tau_2^{*T}(i) C_{tp2} \tau_2^{*T}(i)\right] H(i) \qquad (3.9\text{-}56)$$

subject to satisfying

i) the joint torque dynamics of (3.9-55),

ii) the constraints on joint velocity limits

$$\dot{q}_{1imin} \leq \dot{q}_{1i}(k) \leq \dot{q}_{1imax}$$
$$\dot{q}_{2imin} \leq \dot{q}_{2i}(k) \leq \dot{q}_{2imax} \quad \text{for } k = 1\ldots,M \quad i = 1\ldots.6 \qquad (3.9\text{-}57)$$

iii) That at the begining and end of the trajectory energy joint should be at rest.

$$\dot{q}_{1i}(0) = \dot{q}_{2i}(0) = 0$$

$$\dot{q}_{1i}(M) = \dot{q}_{2i}(M) = 0 \qquad i = 1,\ldots.6 \qquad (3.9\text{-}58)$$

and iv) the constraints on joint torque limits

$$\tau_{1imin} \leq \tau_{1i}^{*}(k) \leq \tau_{1imax}$$
$$\tau_{2imin} \leq \tau_{2i}^{*}(k) \leq \tau_{2imax} \quad \text{for } k = 1\ldots,M \; ; \; i = 1\ldots.6. \qquad (3.9\text{-}59)$$

3.10 Linearization of Discrete Model

The trajectory planning problem posed as above essentially attempts to find those values of H(k), k= 1,2,..M, for which the function Z_{te} in (3.9-56) is minimum. The discrete dynamic models of arms and object developed in the earlier sections are nonlinear functions of the reciprocal time interval vector **h**. Thus the trajectory planning problem is an optimization problem which is nonlinear. In the next chapter the problem is solved by successive linear programming method, which requires all the functions and equations to be linearized about some nominal trajectory to get linear functions and equations. The objective function for the (j+1) th iteration is linearized about $\mathbf{h}^j$ i.e. the **h** vector at the jth iteration. This is expressed as

$$Z_{te}(\mathbf{h}^{j+1}) = Z_{te}(\mathbf{h}^j + \delta\mathbf{h})$$

$$= Z_{te}(\mathbf{h}^j) + \sum_{k=1}^{M} \frac{\partial Z_{te}(\mathbf{h}^j)}{\partial H^j(k)} \delta H^j(k) \qquad (3.10\text{-}1)$$

where

$$\delta H^j(k) = H^{j+1}(k) - H^j(k) \qquad (3.10\text{-}2)$$

and $$\frac{\partial Z_{te}}{\partial H^j(k)} = -\frac{\beta_1}{(H^j(k))^2} + \sum_{i1=1}^{M} 2\beta_2 \left[\tau_1^{*j^T} C_{tp1} \frac{\partial \tau_1^{*j}(i1)}{\partial H^j(i)} \right.$$

$$+ \tau_2^{*j^T}(i1)\, C_{tp2}\, \frac{\partial \tau_2^{*j}(i1)}{\partial H^j(i)} \Bigg] \frac{1}{(H^j(k))^2} \qquad (3.10\text{-}3)$$

where from (3.9-53)

$$\frac{\partial \tau_1^{*j}(i1,i2)}{\partial H^j(k)} = \sum_{j1=1}^{M} \Big[CTM_{1\ i2}(i1,k,j1)H(j1)$$

$$+ CTM_{1\ i2}(i1,j1,i)H(j1) + ctv_{1\ i2}(i1,k) \Big] \qquad \text{for} \quad 1 = 1,2. \qquad (3.10\text{-}4)$$

The relation (3.10-4) is also used to write the constraints on the torque limits as

$$\tau_{1\ min} \le \tau_1^{*j}(k) + \sum_{i=1}^{M} \frac{\partial \tau_1^{*j}(k)}{\partial H^j(i)} \delta H^j(i) \le \tau_{1max}; \quad 1 = 1,2.$$

$$k = 1,2..M \qquad (3.10\text{-}5)$$

Similarly, the joint velocity vector at the (j+1) th iteration is linearized about the j th iteration and the velocity constraints are written as

$$\dot{q}_{1\ min} \le \dot{q}_1^j(k) + \sum_{i=1}^{M} \frac{\partial \dot{q}_1^j(k)}{\partial H^j(i)} \delta H^j(i) \le \dot{q}_{1max}$$

$$1 = 1,2 \ ; k = 1,2..M-1$$

and from (3.9-58)

$$\dot{q}_1^j(M) + \sum_{i=1}^{M} \frac{\partial \dot{q}_1^j(M)}{\partial H^j(i)} \delta H^j(i) = 0 \qquad (3.10\text{-}6)$$

where, from (3.9-4)

$$\frac{\partial \dot{q}_{1i2}^j(i1)}{\partial H^j(i)} = cv_{1\ i2}(i1,i) \quad . \qquad (3.10\text{-}7)$$

CHAPTER 4

COMPUTER SIMULATION RESULTS AND DISCUSSIONS

4.1 Introduction

This chapter presents and discusses the results for three problems of trajectory planning. The system, i.e., the two arms and the object, remains same for all the problems and the problems differ mainly in specifying the base separation of two arms and the object trajectory. For problem 1, the object trajectory is a straight line path with its orientation remaining unchanged throughout the path. Problem 2 is an extension of the problem 1 where the object orientation is also changed along the vertical path. Lastly problem 3 considers a parabolic path for the object with orientation remaining unchanged . This trajectory has been selected to study a case where the velocities undergo reversal of sign.

4.2 Problem 1: Solution Procedure, Results and Discussions

The first problem considers an object being lifted vertically up by the two arms. The object is initially at rest and is again brought to rest at the end of vertical trajectory. Each trajectory planning problem is solved in two major stages. In the first stage all the kinematic and dynamic parameters are inputed

or evaluated. These quantities depend on the path geometry, geometric and inertial parameters of the object and arms. The next stage is to solve the minimization problem through successive linear programming. This stage is iterative and the quantities determined are functions of time. The steps (denoted by S1.1, S1.2 etc.) of these two solution stages are described below in sections 4.2.1 and 4.2.2, respectively.

4.2.1 Kinematic and Dynamic Parameters

S1.1: Input parameters of the arms: Each arm is considered to be PUMA-560 manipulator (Fig.4.1), whose kinematic and dynamic parameters are listed in Appendix F. These include the link parameters (length, twist etc.), inertial parameters of the links, joint velocity limits, joint torque limits, gear ratios, and motor constants.

S1.2: Input parameters of the object. The object is considered to be rectangular parallelopiped (Fig.4.2) with the specifications given in Table 4.1.

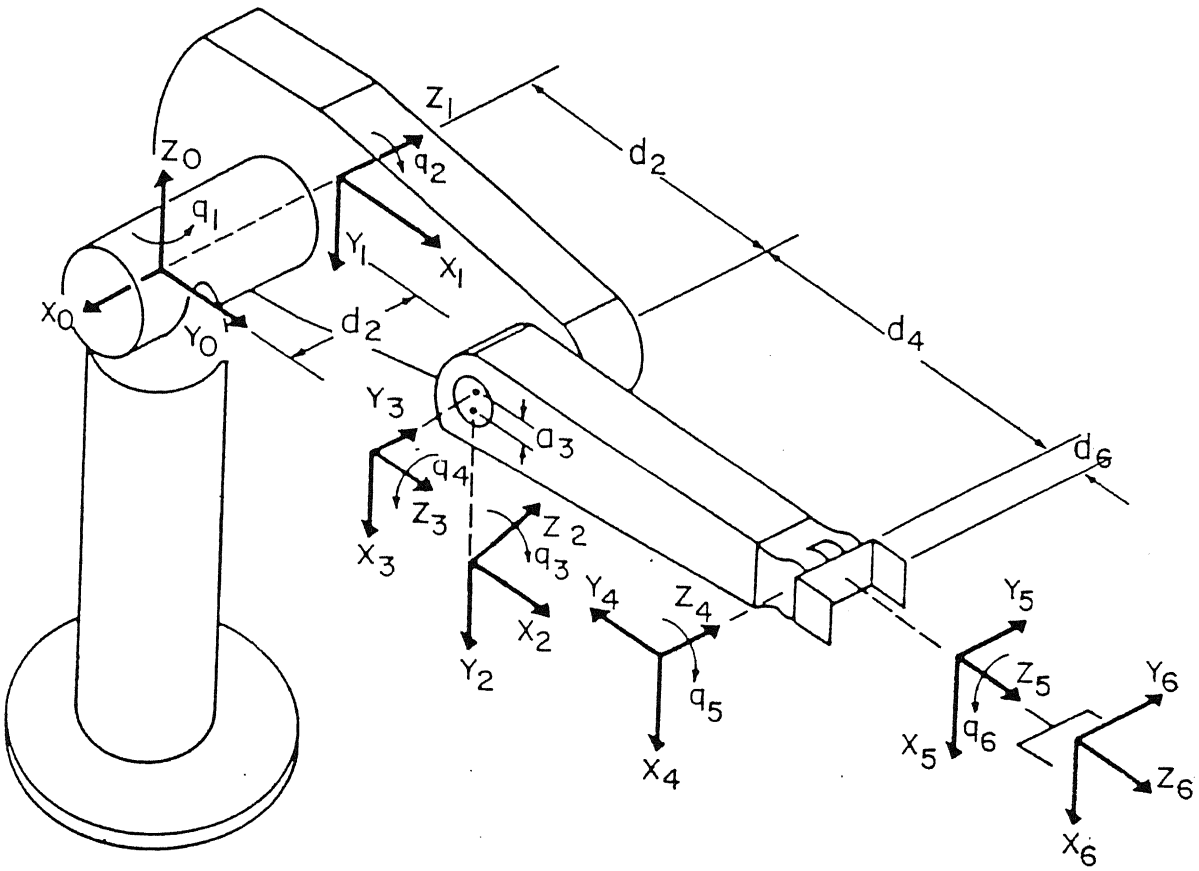

Fig. 4.1 Establishing link coordinate system for a PUMA robot

Table 4.1 Specification of the object

Parameter	Value
Length (L)	0.4 meter
Breath (b)	0.25 meter
Width (w)	0.01 meter
Mass	4.953 kg
I_{xx}	0.06587 kgm^2
I_{yy}	0.09182 kgm^2
I_{zz}	0.0258 kgm^2

S1.3: Input transformation matrices. Following transformation matrices are inputed i) Define arm base frames with respect to world frame (see (3.3-1)) by

$$ {}^{w}T_{10} = \begin{bmatrix} 1.0 & 0.0 & 0.0 & 0.0 \\ 0.0 & 1.0 & 0.0 & 0.0 \\ 0.0 & 0.0 & 1.0 & 0.0 \\ 0.0 & 0.0 & 0.0 & 1.0 \end{bmatrix} \qquad (4.2\text{-}1) $$

and

$$ {}^{w}T_{20} = \begin{bmatrix} -1.0 & 0.0 & 0.0 & 1.2 \\ 0.0 & -1.0 & 0.0 & 0.0 \\ 0.0 & 0.0 & 1.0 & 0.0 \\ 0.0 & 0.0 & 0.0 & 1.0 \end{bmatrix} \qquad (4.2\text{-}2) $$

ii) Define object frames with respect to end effector frames (see (3.3-3)) by

$$ {}^{6}T_{1c} = \begin{bmatrix} 1.0 & 0.0 & 1.0 & 0.0 \\ 0.0 & 1.0 & 0.0 & 0.0 \\ 0.0 & 0.0 & 1.0 & -0.2 \\ 0.0 & 0.0 & 0.0 & 1.0 \end{bmatrix} \qquad (4.2\text{-}3) $$

and

$$ {}^{6}T_{2c} = \begin{bmatrix} -1.0 & 0.0 & 0.0 & 0.0 \\ 0.0 & 1.0 & 0.0 & 0.0 \\ 0.0 & 0.0 & -1.0 & 0.2 \\ 0.0 & 0.0 & 0.0 & 1.0 \end{bmatrix} \qquad (4.2\text{-}4) $$

S1.4: Input the object path and compute ${}^{w}T_{c}$. Discrete positions of the object along the path are described by the transformations ${}^{w}T_{c}(k)$ at the kth knot point. These transformations are calculated from the specified object position, ${}^{w}p_{c}(k)$, and rotations $\Phi(k)$ with the help of (3.3-2) and (A.1) of Appendix A. For the first problem undertaken, the object path is specified by

$$ {}^{w}P_{c}\ (0) = \begin{bmatrix} 0.6 & \text{meter} \\ 0.0 & \text{meter} \\ 0.6 & \text{meter} \end{bmatrix} $$

$$ {}^{w}P_{c}\ (1) = \begin{bmatrix} 0.6 & \text{meter} \\ 0.0 & \text{meter} \\ 0.6015 & \text{meter} \end{bmatrix} $$

$$ {}^{w}P_{c}\ (k) = \begin{bmatrix} 0.6 & \text{meter} \\ 0.0 & \text{meter} \\ 0.6 + .005\ (k-1) & \text{meter} \end{bmatrix} ; \quad k = 2, \ldots 25 $$

$$ {}^{w}P_{c}\ (26) = \begin{bmatrix} 0.6 & \text{meter} \\ 0.0 & \text{meter} \\ 0.7235 & \text{meter} \end{bmatrix} $$

$$ {}^{w}P_{c}\ (27) = \begin{bmatrix} 0.6 & \text{meter} \\ 0.0 & \text{meter} \\ 0.725 & \text{meter} \end{bmatrix} \qquad (4.2\text{-}5) $$

$$ \Phi(k) = \begin{bmatrix} 90 & \text{degrees} \\ 90 & \text{degrees} \\ 0 & \text{degrees} \end{bmatrix} \quad \text{for} \quad k = 0,1,.....27 $$

$$ q_1(0) = q_2(0) = \begin{bmatrix} -154.30 & \text{degrees} \\ -78.50 & \text{degrees} \\ 15.26 & \text{degrees} \\ 133.09 & \text{degrees} \\ 36.44 & \text{degrees} \\ 130.70 & \text{degrees} \end{bmatrix} \qquad (4.2\text{-}6) $$

The above description of ${}^{w}p_{c}(k)$ and $\Phi(k)$ implies that the object is being vertically lifted without changing its orientation. The total path length is 0.125 m and this path is divided into 28 knot points, i.e. M = 27. Except for the first three and last three knot points, all other knot points are equispaced. Beginning and end points are more closely spaced to allow for maximum torque utilization.

S1.5: Compute the transformation matrices of the end effectors. The know transformation are ${}^{w}T_{10}$, ${}^{w}T_{20}$, ${}^{w}T_{c}(k)$, ${}^{6}T_{1c}$ and ${}^{6}T_{2c}$. The end effector transformation matrices are then calculated at each point from (3.3-3).

S1.6: Solve the inverse postion kinematics from Appendix E to obtain the joint postions vectors for two arms. Thus at each knot point, $q_1(k)$ and $q_2(k)$ are known.

S1.7: At each knot point, compute the A matrices for both arms from (2.3-1). These are needed to evaluate Jacobian matrices and inertia coefficients.

S1.8: At each knot point, compute the Jacobian matrices $J_1(k)$ and $J_2(k)$ from (3.4-6), and transmission matrices J_{1c} and J_{2c} from (3.5-11).

S1.9: At each knot point, compute object velocity coefficients and constants from (3.9-32), (3.9-34) and (3.9-36), and constants and coefficients of joint velocities from (3.9-7) and (3.9-8).

S1.10:At each knot point, compute pseudo-inertial matrices I_{xx}, I_{yy}, I_{zz} etc and inertial coefficents d_{1ij} from Appendix D.

S1.11:Define weightages of performance criteria γ_1 and γ_2 and compute the cost matrices for torque resolution from (3.7-8).

S1.12:Compute constants and coefficients of forces and torques applied at the centre of mass from (3.9-42) and (3.9-44) and also constants and coefficients of joint torques from (3.9-54).

4.2.2 *Successive Linear Programming*

The linearized version of the trajectory planning problem was derived in Sec.3.10. This linearized problem is restated here as

$$\text{Minimize: } Z_{te}(\mathbf{h}^{j+1}) - Z_{te}(\mathbf{h}^{j}) = \sum_{k=1}^{M} u^{j}(k)\delta H^{j}(k) \qquad (4.2\text{-}7)$$

where,

$\mathbf{h}^{j}$ is the reciprocal time interval vector at jth iteration and its kth component is $H^{j}(k)$,

$$\text{and } u^{j}(k) = \frac{\partial Z_{te}(\mathbf{h}^{j})}{\partial H^{j}(k)} \qquad (4.2\text{-}8)$$

The objective function Z_{te}, is defined by (3.8-1) for minimum time problem and by (3.8-3) for minimum time plus energy problem.

Subject to:

Equality constraints (velocities at the end of path are zero)

$$\dot{q}_l{}^{j}(M) + \sum_{i=1}^{M} \frac{\partial \dot{q}_l{}^{j}(M)}{\partial H^{j}(i)} \delta H^{j}(i) = 0 \quad ; \; l = 1,2 \qquad (4.2\text{-}9)$$

Inequality constraints (limits on joint velocities and joint torques)

$$\dot{q}_{lmin} \leq \dot{q}_l{}^j(k) + \sum_{i=1}^{M} \frac{\partial \dot{q}_l{}^j(k)}{\partial H^j(i)} \delta H^j(i) \leq \dot{q}_{lmax} \; ; \; l=1,2 \; ; \; K=1,..M-1 \qquad (4.2\text{-}10)$$

$$\tau_{lmin} \leq \tau_l{}^{*j}(k) + \sum_{i=1}^{M} \frac{\partial \tau_l{}^{*j}(k)}{\partial H^j(i)} \delta H^j(i) \leq \tau_{lmax} \; ; \; l = 1,2 \; ; \; k=1,..M \qquad (4.2\text{-}11)$$

The expressions and the associated terms in (4.2-7) to 4.2-11) are explained in Sec. 3.10.

The optimization procedure is to start with some initial values of **h** vector with the iteration index j = 0, evaluates the variation $\delta\mathbf{h}$ through the linearized problem mentioned above, update the **h** vector and repeat the procedure till optimum value of **h** is obtained. The associated steps are briefly described below.

S.2.1:At the beginning of iterative procedure, the initialization is done with the following values:

i) Every element of $\mathbf{h}^0$ is taken to be 5 sec^{-1}, i.e. $H^0(k) = 2$ sec^{-1}; k = 1,2..M. (M=27 as total 28 knot points are selected and the starting point is the zeroeth knot point).

ii) At each iterative stage, the upper and lower limits on the variation, $\delta\mathbf{h}$, are imposed, such that $\Delta H_{max} \leq \delta H(k) \leq \Delta H_{min}$ for k = 1,2...M. The values selected are $\Delta H_{max} = 2\ sec^{-1}$ and $\Delta H_{min} = -2\ sec^{-1}$. The starting guess for $\delta\mathbf{h}$ is taken as $\delta H^{0}(k) = 1.5\ sec^{-1}$ for k = 1,2...M.

iii) The maximum and minimum allowable values of reciprocal time interval for every iteration is taken as $H_{max} = 200\ sec^{-1}$ and $H_{min} = 1\ sec^{-1}$.

Now the following iterative procedure is adapted for the iteration index j = 0,1,..... till optimum $\mathbf{h}^{*}$ is achieved.

S.2.2: With the known values of $\mathbf{h}^{j}$ compute, along the path (i.e. k=1,2,...M),

i) joint velocities $\dot{q}_{lp}^{j}(k)$ from (3.9-6) with $\dot{q}_{lp}^{j}(0) = 0$,

ii) Joint torques $\tau_{lp}^{*j}(k)$ from (3.9-55),

iii) Cofficient $u^{j}(k)$ in (4.2-7) from (4.2-8),

iv) coefficients $\dfrac{\partial \dot{q}_{l}^{j}(k)}{\partial H^{j}(i)}$ in (4.2-10) from 3.10-7),

v) Coefficients $\dfrac{\partial \tau_{l}^{*j}}{\partial H^{j}(i)}$ in (4.2-11) from (3.10-4).

S2.3: Compute the coefficients $\frac{\partial \dot{q}_1^{\,j}(M)}{\partial H^j(i)}$ in (4.2-9) from (3.10-7). This is needed to satisfy the equality constraint at the last knot point.

S2.4: The upper and lower limits on $\delta H^j(k)$ (denoted by $\delta H^j_{low}(k)$ and $\delta H^j_{upp}(k)$, respectively) are changed at every iteration subject to condition that these variations satisfy the bounds given in step S2.1 (iv). This is implemented as

$$\delta H^j_{low}(k) \leq \delta H^j(k) \leq \delta H^j_{upp}(k) \; ; \quad k = 1,2,.....,M \qquad (4.2\text{-}12)$$

where

$$\delta H^j_{low}(k) = \begin{cases} \Delta H_{min} & \text{for } H_{min} - H^j(k) \leq \Delta H_{min} \\ H_{min} - H^j(k) & \text{otherwise} \end{cases} \qquad (4.2\text{-}13)$$

$$\delta H^j_{upp}(k) = \begin{cases} \Delta H_{max} & \text{for } H_{max} - H^j(k) \geq \Delta H_{max} \\ H_{max} - H^j(k) & \text{otherwise} \end{cases} \qquad (4.2\text{-}14)$$

S2.5: Solve the linear programming problem defined by (4.2-7) to (4.2-11). This was done using NAG subroutine E04MBF. Thus obtain the variations $\delta H^j(k)$, k = 1,2...M at the jth iteration.

S2.6: Evaluate $H^{j+1}(k)$,k = 1,2....M, i.e. the refined reciprocal time intervals, for next iteration with following conditions:

i) If in the linearized objective function, the difference between two iterations is $Z_{te}(\mathbf{h}^j+\delta\mathbf{h}^j) - Z_{te}(\mathbf{h}^j)$ (from (4.2-7)) ≥ 0 then in step S2.1, new guess values for $\mathbf{h}^0$, ΔH_{max}, ΔH_{min}, and $\delta\mathbf{h}^0$ are taken and the program is restarted.

ii) If $Z_{te}(\mathbf{h}^j+\delta\mathbf{h}^j) - Z_{te}(\mathbf{h}^j)$ (from (4.2-7))<0, then $H^{j+1}(k) = H^j(k) + \delta H^j(k)$.

S2.7: Compute the original nonlinear function Z_{te} from (3.9-56). If $Z_{te}(\mathbf{h}^{j+1}) - Z_{te}(\mathbf{h}^j) < 0$ then go to step S2.2, else, if $Z_{te}(\mathbf{h}^{j+1}) - Z_{te}(\mathbf{h}^j) \geq 0$ then assign $\Delta H_{max} = 0.8\ \Delta H_{max}$ and $\Delta H_{min} = 0.8\ \Delta H_{min}$. Now if $\Delta H_{max} < 0.1$ or $|\Delta H_{min}|<0.1$ then terminate the program. Else go to step S2.2.

4.2.3 *Results with Minimum Time Criterion*

In this case the objective function Z_{te} is defined by (3.8-3) with the weightages $\beta_1=1$ and $\beta_2=0$. The redundancy in joint torques is resolved by the method outlined in Sec. 3.7. In the minimum time case, the attempt will be to utilize the maximum torque capacity. To this end, the weightages in (3.7-8) are taken as $\gamma_1 = 1$ and $\gamma_2 = 0$. The cost matrices in (3.7-8), C_{tb1} and C_{tb2}, are as determined in step S1.11.

With the initial guess values of $H^{0}(k)$, ΔH_{max} etc. as taken in step S2.1, the optimum values of reciprocal time interval, $H^{*}(k)$, and optimum time intervals, $\Delta t^{*}(k)$ are listed in Table 4.2. These values correspond to the results obtained after 70 iterations.

Table 4.2 Optimum time intervals and reciprocal time intervals in minimum time case of problem 1 after 70 iterations

k (interval number between kth and (k-1)th knot points)	$H^{*}(k)$ sec^{-1}	$\Delta t^{*}(k-1) = 1/H^{*}(k)$ sec
1	140.54	0.0071
2	150.51	0.0066
3	125.58	0.0080
4	123.99	0.0081
5	122.41	0.0082
6	120.83	0.0083
7	119.21	0.0084
8	117.57	0.0085
9	115.91	0.0086
10	114.23	0.0088
11	112.52	0.0089
12	110.78	0.0090
13	109.02	0.0092
14	107.23	0.0093
15	105.41	0.0095
16	103.56	0.0097
17	101.67	0.0098

Table 4.2 (Continued)

18	99.74	0.0100
19	97.78	0.0102
20	95.77	0.0104
21	93.72	0.0107
22	91.62	0.0109
23	89.47	0.0112
24	87.26	0.0115
25	84.99	0.0118
26	102.37	0.0098
27	99.13	0.0101

Thus the total time of travel, t^* is 0.25 sec. $\left(t^* = \sum_{k=1}^{M} \Delta t^*(k) \sum_{k=1}^{M} \frac{1}{H^*(k)}\right)$. Figure 4.3 presents the total time of travel versus the iteration number. The initial guess values of H(k) equal to 5 sec^{-1} imply the total time of travel equal to 5.4 sec.

As evident from Table 4.2, the optimum time intervals between equispaced knot points are not equal. It is to be noted here from Sec. 4.2.1, S1.4 that the distances between the first three and the last three knot points are taken to be smaller than the distances between other knot points. In the trial runs it was observed that if all the knot points are kept equispaced and if this distance between knot points is not very small then before the third joint reaches its torque limit, the velocity limit is reached. Therefore, the torque capacity can be maximally utilized by reducing the spacing between the knot points. Instead of reducing the spacings between all the knot points (which will

unduely increase the number of knot points and hence the size of problem) only the first two and the last two spacings, which are the important ones, are reduced.

Starting with a guess value of equal reciprocal time intervals of 5 sec^{-1} between knot points, Fig.4.4 shows the obtained values of reciprocal time intervals, $H^j(k)$, at iteration number j = 10,20,30,40,50,60and 70, where the abscissa represents the interval number k (k=1,2,...,27). The dots in Fig.4.4 represent the H values and these dots have been joined only to show that these belong to the same iterative stage. Tables 4.3(a) and 4.3(b) list the same information in tabular form.

Table 4.3(a) Reciprocal time intervals at intermediate stages in minimum time case of problem 1

k	j=10 travel time = 1.0883 sec.	j=20 travel time = 0.6046 sec.	j=30 travel time= 0.4189 sec.	j=40 travel time = 0.3210 sec.	j=50 travel time = 0.2703 sec.	j=60 travel time = 0.2563 sec.	j=70 travel time = 0.2531 sec.
1	25.00	45.00	65.00	85.00	105.00	117.41	134.08
2	25.00	45.00	65.00	85.00	105.00	125.00	145.00
3	24.34	43.45	61.22	78.93	95.84	112.20	123.67
4	25.00	45.00	65.00	85.00	105.00	121.52	124.01
5	24.51	44.06	64.06	84.06	104.06	122.43	122.43
6	25.00	45.00	65.00	85.00	105.00	120.83	120.83
7	24.60	44.19	64.19	84.19	104.19	119.21	119.21
8	25.00	45.00	65.00	85.00	105.00	117.57	117.57
9	24.52	44.52	64.52	84.52	104.52	115.91	115.91
10	25.00	45.00	65.00	85.00	105.00	114.23	114.23
11	24.69	44.69	64.69	84.69	104.69	112.52	112.52
12	25.00	45.00	65.00	85.00	105.00	110.78	110.78

Table 4.3(a) (Continued)

13	24.87	44.50	64.50	84.50	104.50	109.02	109.02
14	25.00	45.00	64.52	84.13	103.98	107.23	107.23
15	24.71	44.71	64.71	84.71	104.71	105.41	105.41
16	25.00	45.00	65.00	85.00	102.87	103.56	103.56
17	24.67	44.67	64.67	84.67	101.67	101.67	101.67
18	25.00	45.00	65.00	85.00	99.74	99.74	99.74
19	24.78	44.52	64.52	84.52	97.78	97.78	97.78
20	25.00	45.00	65.00	85.00	95.77	95.77	95.77
21	24.57	44.31	64.31	84.31	93.72	93.72	93.72
22	25.00	45.00	65.00	85.00	91.62	91.62	91.62
23	24.47	43.81	63.81	83.81	89.47	89.47	89.47
24	25.00	45.00	65.00	82.93	87.26	87.26	87.26
25	24.15	43.33	61.09	76.93	84.99	84.99	84.99
26	25.00	45.00	65.00	85.00	102.33	102.32	102.36
27	25.00	45.00	65.00	85.00	98.94	98.90	99.11

Table 4.3(b) Time intervals at intermediate stages in minimum time case of problem 1

k	j=10 travel time = 1.0883 sec.	j=20 travel time = 0.6046 sec.	j=30 travel time= 0.4189 sec.	j=40 travel time = 0.3210 sec.	j=50 travel time = 0.2703 sec.	j=60 travel time = 0.2563 sec.	j=70 travel time = 0.2531 sec.
1	0.0400	0.0222	0.0154	0.0118	0.0095	0.0085	0.0075
2	0.0400	0.0222	0.0154	0.0118	0.0095	0.0080	0.0069
3	0.0411	0.0230	0.0163	0.0127	0.0104	0.0089	0.0081
4	0.0400	0.0222	0.0154	0.0118	0.0095	0.0082	0.0081
5	0.0408	0.0227	0.0156	0.0119	0.0096	0.0082	0.0082

Table 4.3(b) (Continued)

6	0.0400	0.0222	0.0154	0.0118	0.0095	0.0083	0.0083
7	0.0406	0.0226	0.0156	0.0119	0.0096	0.0084	0.0084
8	0.0400	0.0222	0.0154	0.0118	0.0095	0.0085	0.0085
9	0.0408	0.0225	0.0155	0.0118	0.0096	0.0086	0.0086
10	0.0400	0.0222	0.0154	0.0118	0.0095	0.0088	0.0088
11	0.0405	0.0224	0.0155	0.0118	0.0096	0.0089	0.0089
12	0.0400	0.0222	0.0154	0.0118	0.0095	0.0090	0.0090
13	0.0402	0.0225	0.0155	0.0118	0.0096	0.0092	0.0092
14	0.0400	0.0222	0.0155	0.0119	0.0096	0.0093	0.0093
15	0.0405	0.0224	0.0155	0.0118	0.0096	0.0095	0.0095
16	0.0400	0.0222	0.0154	0.0118	0.0097	0.0097	0.0097
17	0.0405	0.0224	0.0155	0.0118	0.0098	0.0098	0.0098
18	0.0400	0.0222	0.0154	0.0118	0.0100	0.0100	0.0100
19	0.0404	0.0225	0.0155	0.0118	0.0102	0.0102	0.0102
20	0.0400	0.0222	0.0154	0.0118	0.0104	0.0104	0.0104
21	0.0407	0.0226	0.0155	0.0119	0.0107	0.0107	0.0107
22	0.0400	0.0222	0.0154	0.0118	0.0109	0.0109	0.0109
23	0.0409	0.0228	0.0157	0.0119	0.0112	0.0112	0.0112
24	0.0400	0.0222	0.0154	0.0121	0.0115	0.0115	0.0115
25	0.0414	0.0231	0.0164	0.0130	0.0118	0.0118	0.0118
26	0.0400	0.0222	0.0154	0.0118	0.0098	0.0098	0.0098
27	0.0400	0.0222	0.0154	0.0118	0.0101	0.0101	0.0101

It is observed from Fig.4.4 and Table 4.3 that upto twentieth iteration, the H values have been simply increased while maintaining nearly equal time intervals. Then upto fortieth iteration except H(3) and H(25), all other H values still increase by nearly equal amount, and there is an appreciable change in H(3) and H(25). As will be noted later, these are the intervals which separate the nearly uniform velocity regions from acceleration and

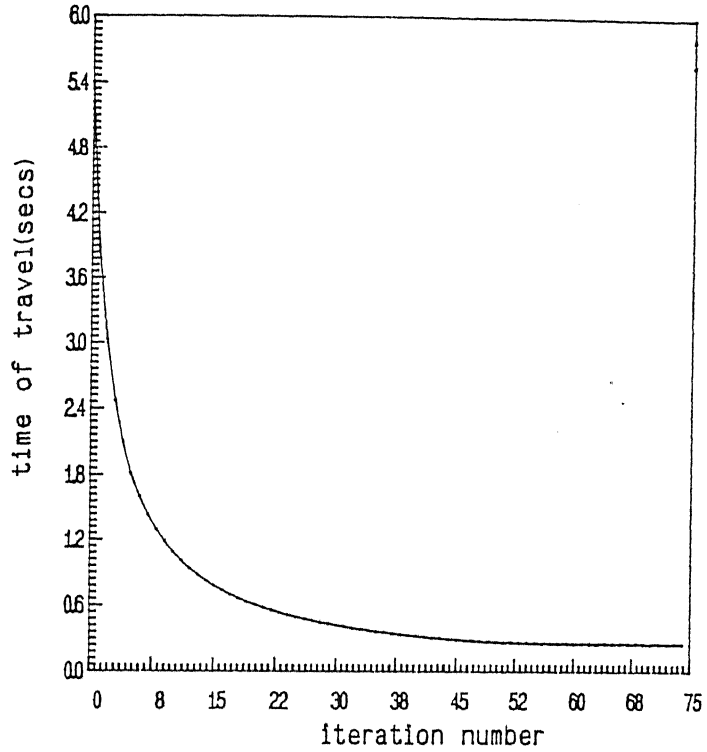

Fig. 4.3 Variation of travel time with iteration number in minimum time case for problem 1

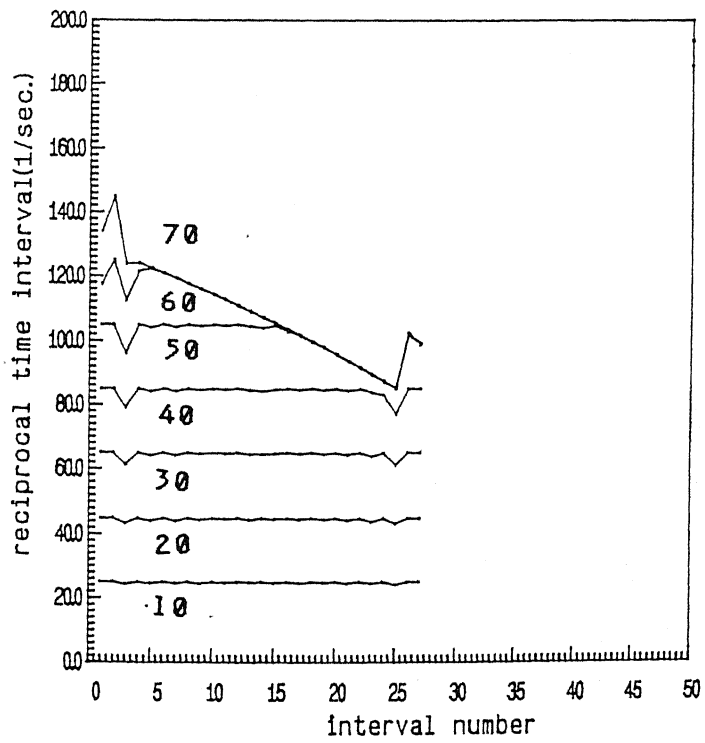

Fig. 4.4 Variation of reciprocal time intervals with iteration number in minimum time case for

deceleration regions. After fiftieth iteration, the H values get successively refined with marked changes in the values. Finally the optimum values of $H^*(k)$ are such that except at the beginning and the end, the $H^*(k)$ values monotonically decrease along the path, i.e., the time intervals between equispaced knot points become larger implying slower motion (as will be seen later in Fig.4.11).

With the optimum time of travel, t^* equal to 0.25 sec, and optimum time intervals as given in Table 4.2 (corresponding to 70th iteration), the joint velocities are plotted in Figs.4.5 and 4.6, and the joint torques are plotted in Figs.4.7 and 4.8. It may be noted from (4.2-1) to (4.2-4) that the arm configurations are such that the object path is symmetric with respect to both the arms. Therefore the velocity and torque distribution is identical in the two arms.

From Table F.3, the velocity limit on the third joint is 2.1 rad/sec and from Table F.4 the torque limits on the first and third joints are 97.6 N.m and 89.4 N.m. Thus it is observed from Figs.4.5 to 4.8 that the minimum time of travel is constrained by the limits on first and third joint. At the starting of trajectory, the third joint exerts maximum allowable torque over the first time interval but the velocity limit is not yet reached. The third joint then still applies torque in the second time interval with a reduced value of torque such that the third joint velocity limit constraint is not violated. By the end of second time interval, the third joint is moving at its maximum allowable velocity and thus it becomes the joint guiding the fastness of

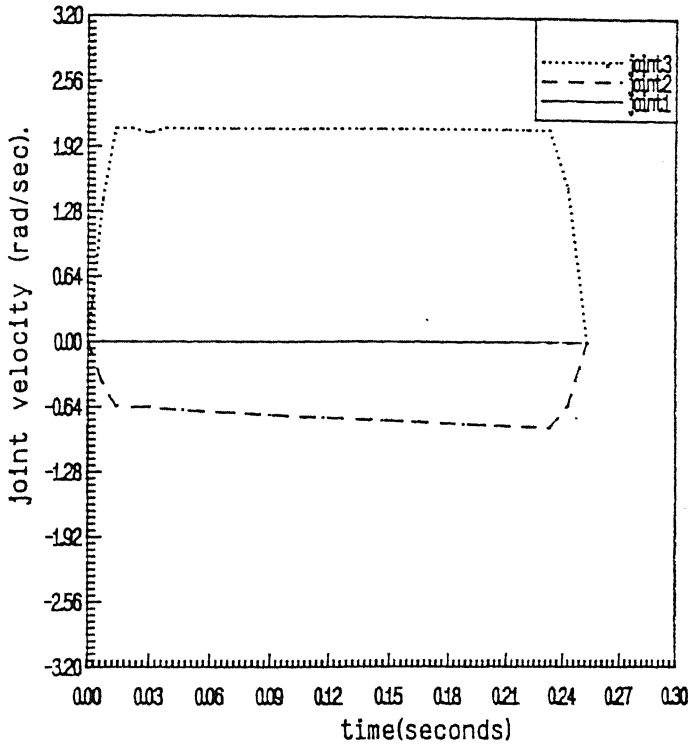

Fig. 4.5 Velocities of joints 1,2 and 3 for both arms with minimum time case for problem 1

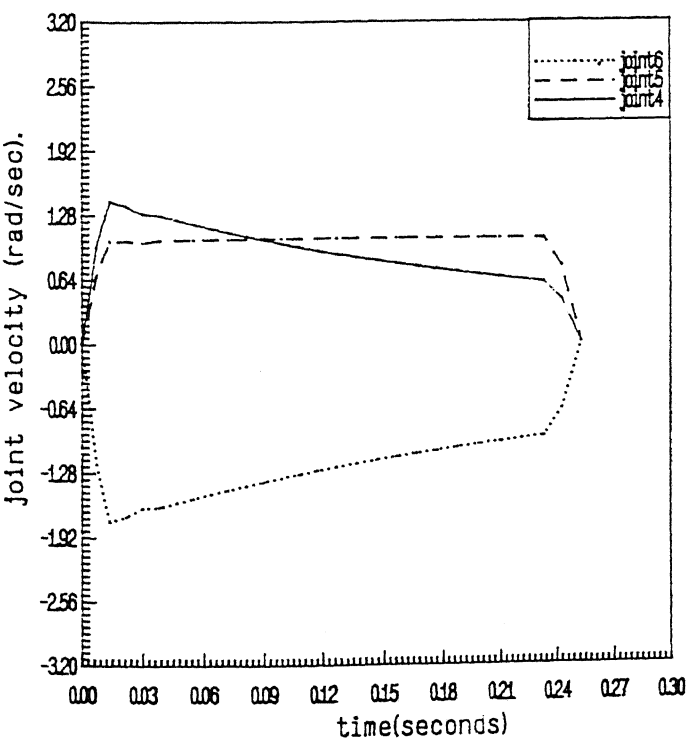

Fig. 4.6 Velocities of joints 4,5 and 6 for both arms with minimum time case for problem 1

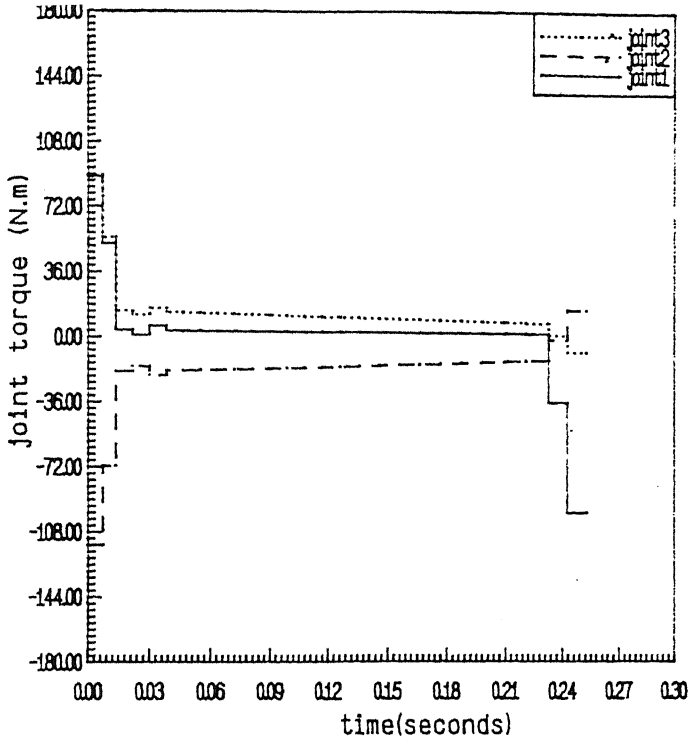

Fig. 4.7 Torques of joints 1,2 and 3 for both arms with minimum time case for problem 1

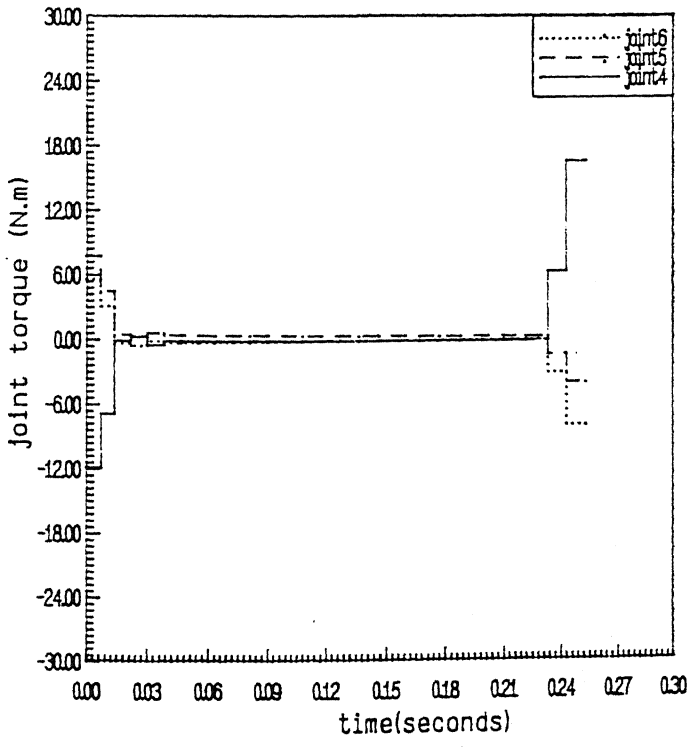

Fig. 4.8 Torques of joints 4,5 and 6 for both arms with minimum time case for problem 1

motion along the major portion of trajectory. At the end of the trajectory, when all the joints have to reach zero velocity, the torque limit of jointl is reached. Eventhough the joint 1 is not moving, there is a torque applied by jointl which is a reaction moment needed to keep jointl stationary.

It is noticed from Fig.4.3 and Table 4.3 that the time of travel does not reduce much after about 40th iteration. On the other hand, the individual time intervals between the knot points do change even after 40th iteration as shown in Fig.4.4. Therefore, the information from Fig.4.3 may not be sufficient to conclude a suboptimal solution. This is further elaborated in Figs.4.9 and 4.10 which show the time histories of velocity and torque of the third joint taken at 20th, 40th and 60th iteration. (Since all the equality and inequality constraints are satisfied at every stage of iteration, the time intervals taken from an intermediate interation yield valid time histories, though not an optimal one). At 20th iteration, the time of travel is still large (0.6 sec) and there are zagged fluctuations in the velocity time history. The time of travel is 0.321 sec at 40th iteration, 0.26 sec at 60th iteration and 0.25 sec at 70th iteration. Though the time does not reduce much after 40th iteration (by about 28%), the plots in Figs.4.9 and 4.5 show an appreciable improvment in the velocity time history. There are still marked fluctuations in the velocity profile at 40th iteration which become smooth at 60th iteration. Likewise the torque profile in Fig.4.10 shows fluctuations at 40th iteration which are eliminated at 60th iteration. The improvement from 60th iteration (Figs.4.9(c) and

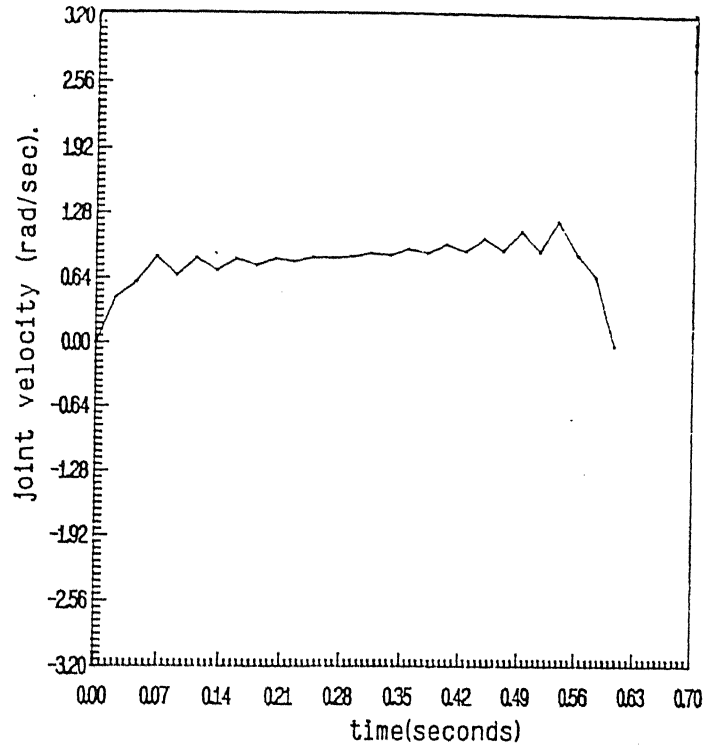

Fig. 4.9(a) Velocities of joint 3 for arm 1 with minimum time case for problem 1 after 20th iteration

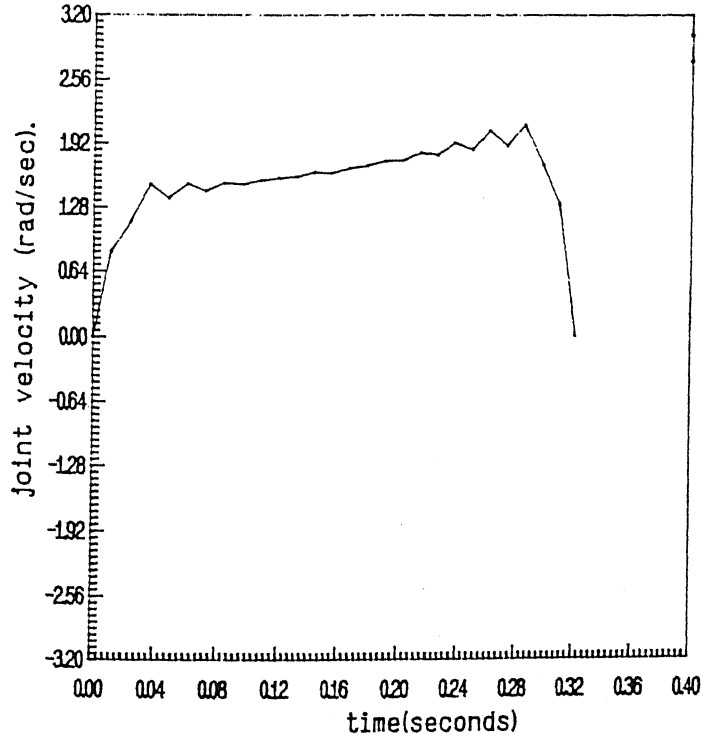

Fig. 4.9(b) Velocities of joint 3 for arm 1 with minimum time case for problem 1 after 40th

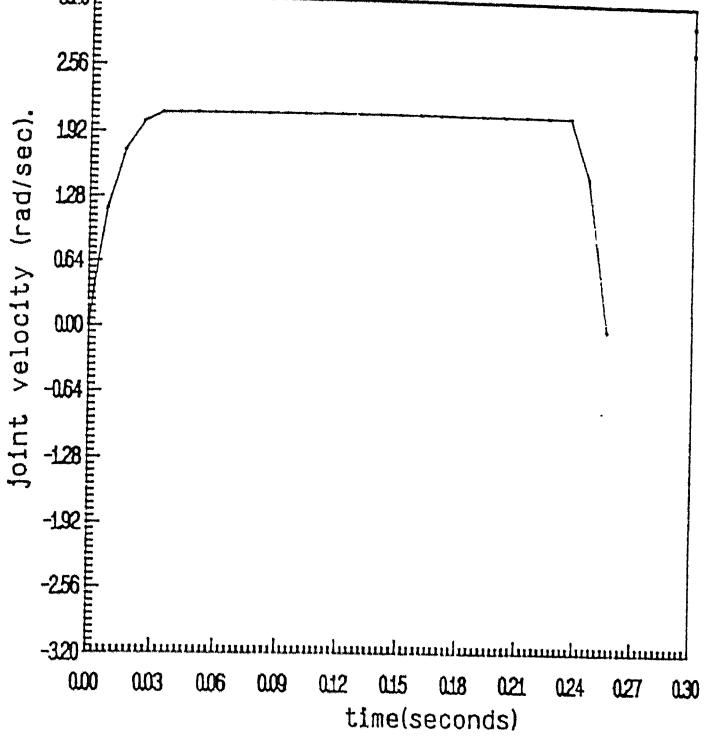

Fig. 4.9(c) Velocities of joint 3 for arm 1 with minimum time case for problem 1 after 60th iteration

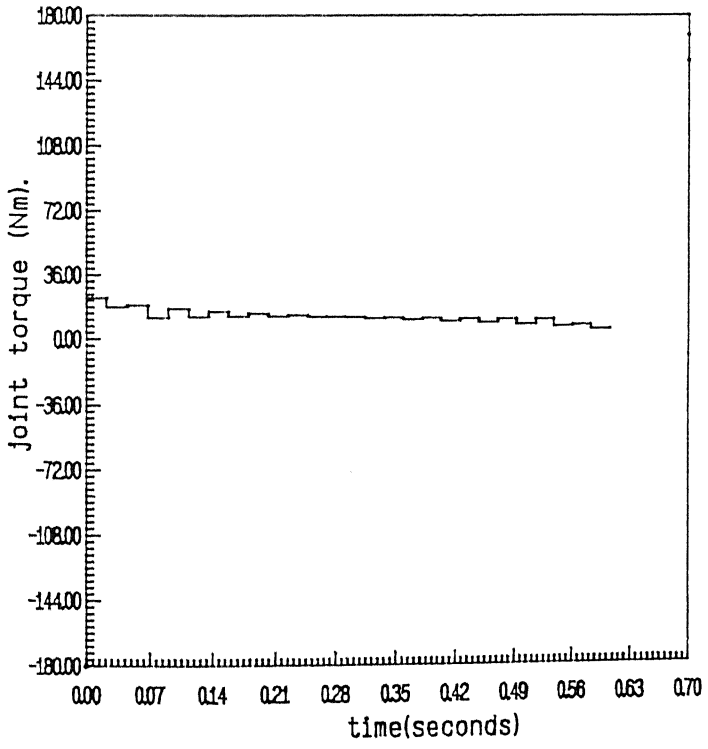

Fig. 4.10(a) Torques of joint 3 for arm 1 with minimum time case for problem 1 after 20th iteration

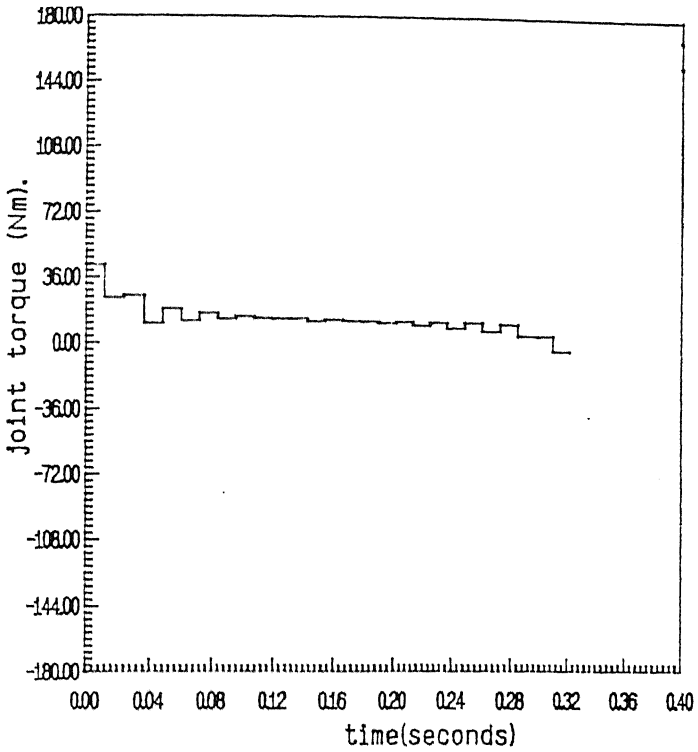

Fig. 4.10(b) Torques of joint 3 for arm 1 with minimum time case for problem 1 after 40th iteration

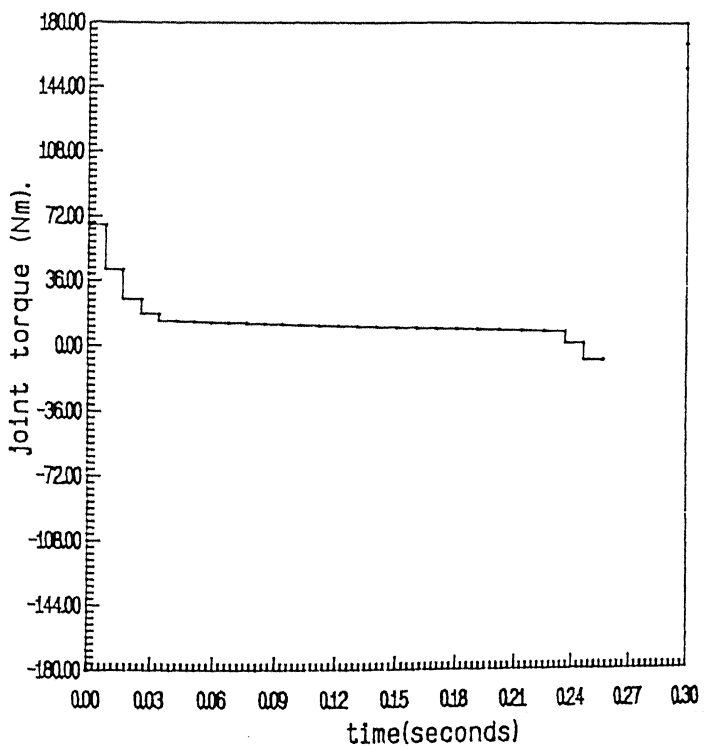

Fig. 4.10(c) Torques of joint 3 for arm 1 with minimum time case for problem 1 after 60th iteration

4.10(c)) to 70th iteration (Figs 4.5 and 4.7) is in taking the third joint torque to its maximum capacity in the first time interval, thereby reaching the velocity limit at an earlier time. The fluctuations observed at earlier stages of iteration are primarily due to the fact that the equality constraints on joint velocities (4.2-9) are to be satisfied.

The object velocity along the trajetory is plotted in Fig.4.11, where the dots represent the vertical component of the velocity of object centre. Since the path is straight and vertical; all the other velocity components are zero. As noted from Fig.4.4 also, the object moves at slower velocity as it progresses along the path. The object velocity rises from zero at the begininning to a maximum value of 0.63 m/sec at the end of second time interval. Then the velocity gradually decreases to 0.42 m/sec, whereafter it comes down to zero with a large decleration.

The arms exert forces and moments on the object through the end effectors, which were denoted by $^{w}f_1$ and $^{w}f_2$ in (3.6-11) and Fig.3.2. These interactive forces and moments are shown in Figs.4.12 and 4.13, where the components are taken along x,y,z directions of the world frame. Comparision of Figs.4.12(a) and 4.12(b) shows that, as expected, the forces by the two arms on the object balance along x and y dixections, and contribute equally in the z direction (which is the direction of motion). While the forces are large in the beginning, when the object is being accelerated upwards, the forces on the object are smaller at the end when the deceleration is assisted by gravity. The object does

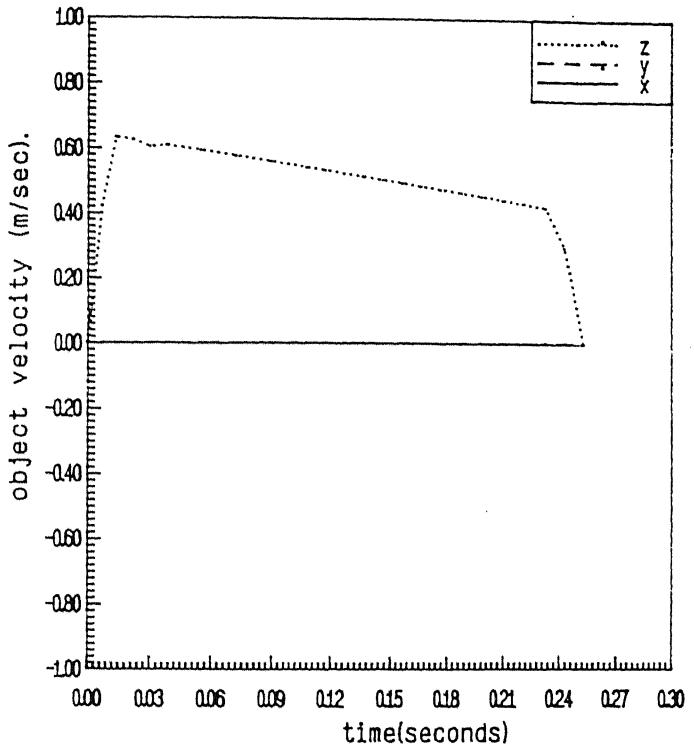

Fig. 4.11 Linear velocity of object in minimum time case for problem 1

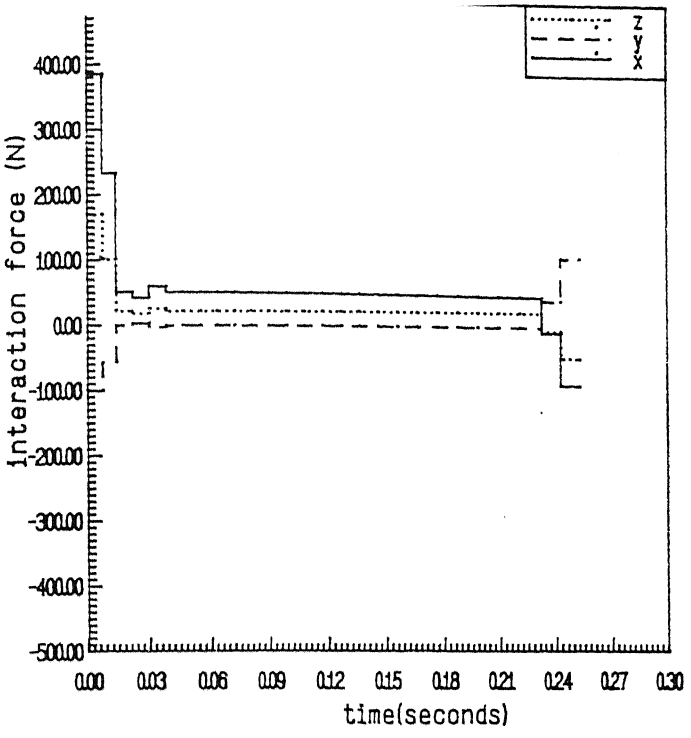

Fig. 4.12(a) Interaction forces by arm 1 on object in minimum time case for problem 1

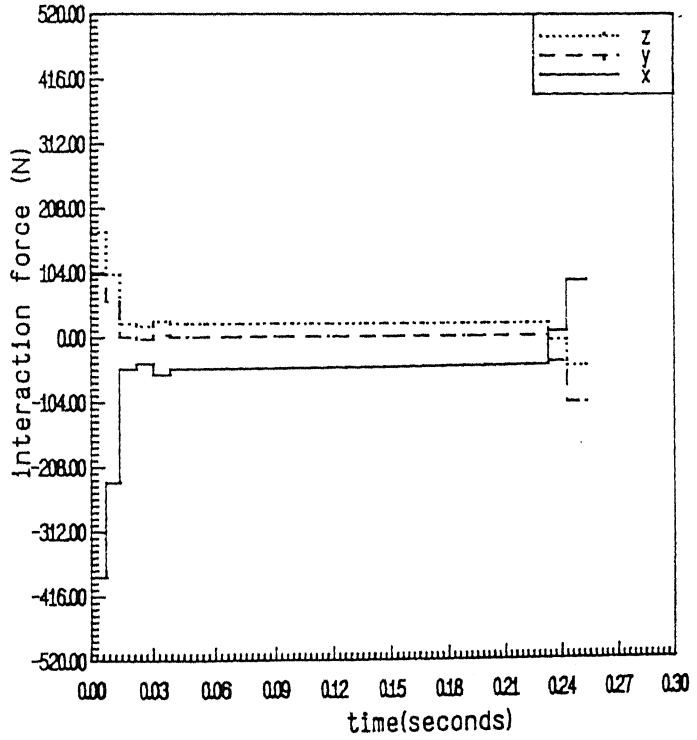

Fig. 4.12(b) Interaction forces by arm 2 on object in minimum time case for problem 1

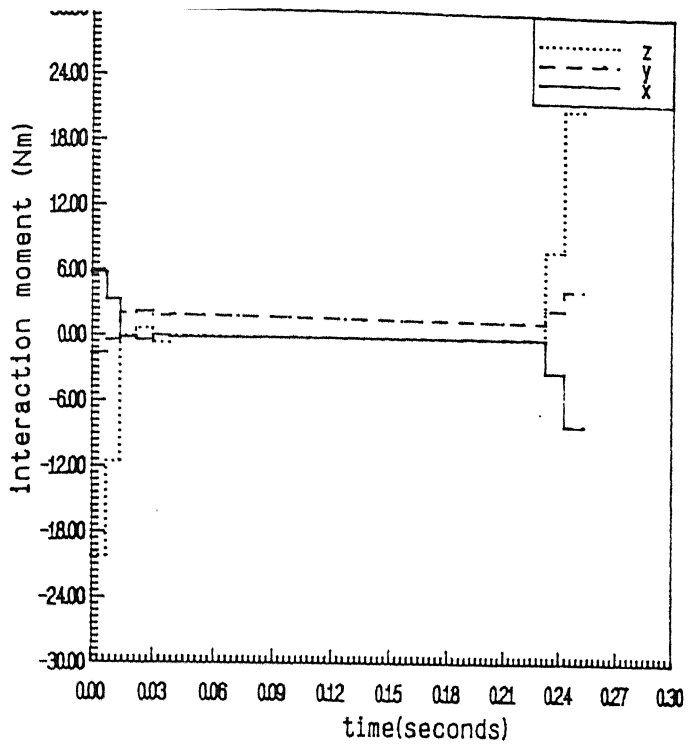

Fig. 4.13(a) Interaction moments by arm 1 on object in minimum time case for problem 1

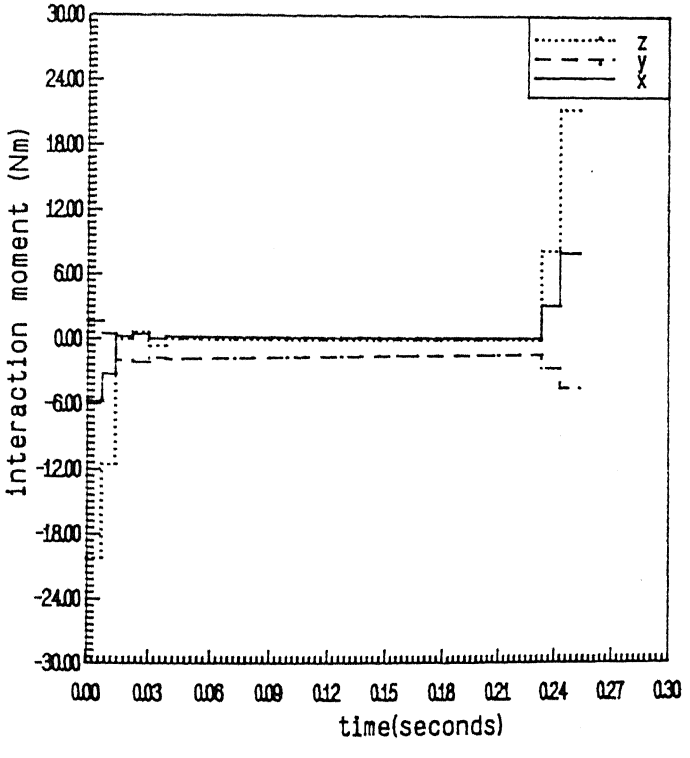

Fig. 4.13(b) Interaction moments by arm 2 on object in minimum time case for problem 1

not execute any angular motion along the trajectory. Figs.4.13(a) and 4.13(b) show that, for the major part of the path, the moments on the object about x and z disections are zero, while there is a small bending moment about the y direction. At the beginning and the end, all the three moment components are present such that (i) there is a twisting moment about x direction, (ii) there is a bending moment about y direction, and (iii) both the arms exert equal moments about z direction which balance the moments produced by equal and opposite nonzero interaction forces in the y direction.

The later Sec.4.2.4 discusses the minimum energy criterion,with the electrical consumption being defined (3.8-2). For minimum time case, being discussed here, the energy consumption versus the iteration numburis plotted in Fig.4.14. This figure shows that as the time of travel is reduced with increasing number of iterations, the energy first reduces with reduced time but later as time is further reduced towards minimum time, the energy starts increasing. This can be seen easily by noting that the energy is utilized in two main tasks. The first task is to support weights of the links and the object and this part of energy consumption will decrease with decreasing time of travel. The second task is to move the links and object and this part of energy consumption will be lower with lower velocities implying larger time of travel. Now it can be observed from Fig. 4.14 that the energy required to move the dual-arm system starts becoming dominant after 26th iteration and thus the total energy consumption thereafter increases as the time of travel is reduced.

4.2.3.1 Discussions on Reducing the Computation Time

As mentioned earlier, the results presented till now correspond to the initial guess value of $H^{0}(k)=5$ sec^{-1} $(k=1,2...27)$, $\Delta H_{max}=2$ sec^{-1} and $\Delta H_{min}=-2$ sec^{-1}. This choice of initial guess was made for two reasons. First, in the absence of any prior information ,the values were taken to be on the conservative side for the "cold start" of the program. Second, the intermediate stages in convergence to the minimum time was desired to be studied. On the other hand,one could get informations from some trial runs to have the "warm start" of the program. To this end, the computation time can be reduced by (i)selecting higher values of $H^{0}(k)$,and ΔH ,and (ii)reducing the number of knot points along the path.

While keeping the same number of knot points (equal to 28),various combinations of $H^{0}(k)$ and ΔH were tried. Large values of $H^{0}(k)$ and ΔH result in a much faster convergence but it requires a careful selection of the combination. To elaborate this, a higher value of $H^{0}(k)$ (same value for all intervals $k=1,2...27$) needs a higher value of ΔH also, otherwise the proper $\delta \mathbf{h}$ vector can not be obtained which will satisfy the end velocity constraints. This is evident from Table 4.2 also which shows that $H^{*}(k)$ varies significantly over the intervals and so large $\delta \mathbf{h}$ is needed for higher values of $H^{0}(k)$. It was observed that with $H^{0}(k)=85$ sec^{-1} $(k=1,2,....,27)$,$\Delta H_{max}=2$ sec^{-1} and $\Delta H_{min}=-2$ sec^{-1},the optimization program was terminated because within these bounds no feasible value $\delta \mathbf{h}$ satisfies the velocity constraints at the end of the path. On the other hand, the initial bounds on ΔH cannot be

increased arbitrarily because of the following reason. A large permissible bound on ΔH allows $\delta \mathbf{h}$ to be large while solving the linear programming problem. Though the linearized constraint equations are satisfied with this large value of $\delta \mathbf{h}$, the nonlinear constraint equations may be violated. For example, with $H^{0}(k)=85$ sec^{-1} $(k=1,2,\ldots,27)$, $\Delta H_{max}=40$ sec^{-1} and $\Delta H_{min}=-40$ sec^{-1}, the initial steps of $\delta \mathbf{h}$ taken were so large that after two iterations the H(k) values had almost converged to optimum values but the joint torque limits were violated. The starting torque at joint 3 was observed to be 92.25 N.m (the torque limit of this joint is 89.4 N.m) and the torque at joint 1 at the end of the path was found to be -99.5 N.m (the torque limit of joint 1 is 97.6 N.m). Table 4.4 lists the final H(K) values for this case. It was not possible to correlate the values of bounds on ΔH with the values of $H^{0}(k)$ because with $\Delta H_{max}=40$ sec^{-1} and $\Delta H_{min}=-40$ sec^{-1} while the torque constraints were violated with $H^{0}(k)=85$ sec^{-1} $(k=1,2,\ldots,27)$, the optimization procedure converged, without violating any constraints, in three iterations with $H^{0}(k)=65$ sec^{-1} $(k=1,2,\ldots,27)$ and in two iterations with $H^{0}(k)=95$ sec^{-1} $(k=1,2,\ldots,27)$. These optimum $H^{*}(k)$ values are also listed in Table 4.4 and are seen to tally with the values in Table 4.2.

Table 4.4 Optimum reciprocal time intervals for different starting H values in minimum time case of problem 1

$\Delta H_{max}=40\ sec^{-1}$, $\Delta H_{min}=-40\ sec^{-1}$ $H^*(k)$			
k	$H^0(k)=85\ sec^{-1}$ after two iterations	$H^0(k)=65\ sec^{-1}$ after three iterations	$H^0(k)=95\ sec^{-1}$ after two iterations
1	143.23	140.54	141.26
2	151.65	150.51	150.81
3	125.58	125.58	125.58
4	124.01	124.00	124.01
5	122.43	122.41	122.43
6	120.83	120.83	120.83
7	119.21	119.21	119.21
8	117.57	117.57	117.57
9	115.91	115.91	115.91
10	114.22	114.22	114.22
11	112.52	112.52	112.52
12	110.79	110.78	110.78
13	109.02	109.02	109.02
14	107.23	107.23	107.23
15	105.41	105.41	105.41
16	103.55	103.55	103.55

Table 4.4 (Continued)

17	101.67	101.67	101.67
18	99.74	99.74	99.74
19	97.78	97.78	97.78
20	95.77	95.77	95.77
21	93.72	93.72	93.72
22	91.62	91.62	91.62
23	89.46	89.46	89.46
24	87.26	87.26	87.26
25	84.99	84.99	84.99
26	102.78	102.36	102.39
27	100.08	99.13	99.19

The next attempt was to reduce the number of knot points. Since the minimization problem is subject to twelve equality constraints, given by (4.2.9), at least thirteen intervals (i.e., fourteen knot points) are required on the object path. A set of equispaced 14 knot points along the path length of 0.125 m (see also(4.2-5)) will imply large spacings between beginning and end knot points and hence the joint torque capacities will be underutilized as has been shown earlier in this section. Therefore, taking clues from the results discussed earlier, the following set of 14 knot points was selected.

$$ {}^{w}\mathbf{p}_{c}(0) = \begin{bmatrix} 0.6 \text{ meter} \\ 0.0 \text{ meter} \\ 0.6 \text{ meter} \end{bmatrix} $$

$$ {}^{w}\mathbf{p}_{c}(1) = \begin{bmatrix} 0.6 & \text{meter} \\ 0.0 & \text{meter} \\ 0.6015 & \text{meter} \end{bmatrix} $$

$$ {}^{w}\mathbf{p}_{c}(k) = \begin{bmatrix} 0.6 & \text{meter} \\ 0.0 & \text{meter} \\ 0.615+0.010(k-2) & \text{meter} \end{bmatrix} \qquad \text{for } k=2,\ldots,6. $$

$$ {}^{w}\mathbf{p}_{c}(k) = \begin{bmatrix} 0.6 & \text{meter} \\ 0.0 & \text{meter} \\ 0.670+0.010(k-7) & \text{meter} \end{bmatrix} \qquad \text{for } k=7,\ldots,11. $$

$$ {}^{w}\mathbf{p}_{c}(12) = \begin{bmatrix} 0.6 & \text{meter} \\ 0.0 & \text{meter} \\ 0.7235 & \text{meter} \end{bmatrix} $$

$$ {}^{w}\mathbf{p}_{c}(13) = \begin{bmatrix} 0.6 & \text{meter} \\ 0.0 & \text{meter} \\ 0.725 & \text{meter} \end{bmatrix} $$

(4.2-14)

The initial guess values of $H^{0}(k)$ $(k=1,2,\ldots,13)$ were also based upon the earlier results. Instead of taking equal values of $H^{0}(k)$ for each interval, as was done in all previous cases, now the program was "warm started" with the following values of $H^{0}(k)$ listed in Table 4.5.

Table 4.5 Starting H values for minimum time case of Problem 1 with 13 intervals

k	$H^{0}(k)$ sec^{-1}
1	60
2	15
3	20
4	20
5	20
6	20
7	10
8	20
9	20
10	20
11	20
12	15
13	60

The bounds on ΔH were taken as ΔH_{max}= 40 sec^{-1} and ΔH_{min}= -40 sec^{-1}. The optimization program converged in four iterations to yield the minimum travel time equal to 0.26 sec and the corresponding $H^{*}(k)$ values are listed in Table 4.6.

Table 4.6 Optimum H values for minimum time case of problem 1 with 13 intervals

k	$H^{*}(k)$ sec^{-1}
1	140.54

Table 4.6 (Continued)

2	38.54
3	60.81
4	56.10
5	54.52
6	55.82
7	35.73
8	51.30
9	49.38
10	47.37
11	45.26
12	27.24
13	98.87

It is to be noted that the minimum time of travel with 14 knot points is 0.26 sec while the same with 28 knot points was 0.25 sec. This slight increase in time is due to the fact that the second time interval is larger now and as noted in Table 4.5, the third joint velocity limit is reached at the end of this interval. Taking two more knot points so that the second and the last-but-one intervals are shorter (i.e., with total number of 16 knot points) reduces the minimum time to 0.25 sec.

The computations were performed on the Hp 9000/850S machine. The computation time for each iteration was on average 7 min. with 28 knot points and 1.25 min. with 14 knot points.

4.2.4 *Results with Minimum Energy Criterion*

The objective function Z_{te} is defined in this case by (3.8-3) with $\beta_1 = 0$ and $\beta_2 = 1$. The joint torques are also

resolved according to minimum power consumption so that in (3.7-8), the weightages are $\gamma_1=0$ and $\gamma_2=1$. The cost matrices in (3.7-8), C_{tp1} and C_{tp2}, are determined in step S1.11. The initial guess value of H(k) in step S2.1 was taken as 2 sec^{-1} implying the guess value of time of travel as 13.5 sec. The bounds on ΔH were taken as ΔH_{max}= 1 sec^{-1} and ΔH_{min}= -1 sec^{-1}.

The variation of energy consumption with iteration number is shown in Fig. 4.15. Compared with Fig. 4.14, the energy consumption in Fig 4.15 continuously decreases in successive iterations because the objective function is based upon energy criterion. Figure 4.15 also shows that convergence is fast in the beginning but very slow towards the end. The variation of time of travel with iteration number is shown in Fig. 4.16. Even with low starting H(k), energy reduces from 52.61 Joules to 4.23 Joules and time of travel reduces from 13.5 sec to 1 sec in merely 11 iterations. In the later stages of iterations, the convergence is so slow that after 70th iteration energy is 2.98 Joules (time of travel = 0.71 sec) and after 150th iteration energy is 2.68 Joules (time of travel = 0.62 sec).

As done in Sec. 4.2.3.1 for minimum time case , warm start was also tried for minimum energy case with various guess values of $H^0(k)$ and bounds on ΔH. The only saving thereby obtained was in the initial stages of iterations , the convergence in the later part being always very slow. The minimum energy problem inherently requires much larger number of iterations as compared to minimum time problem when the method of successive linear programming is used to solve the nonlinear optimization problem.

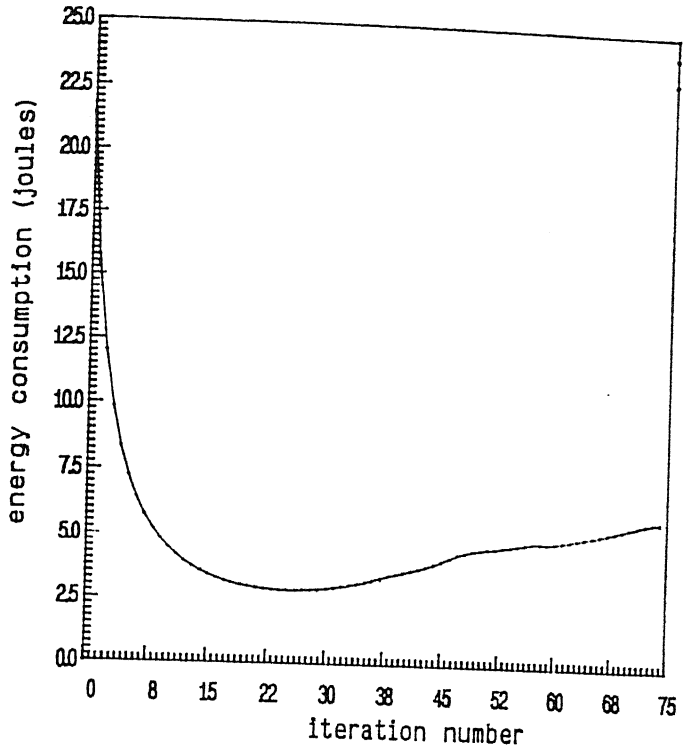

Fig. 4.14 Variation of energy with iteration number in minimum time case for problem 1

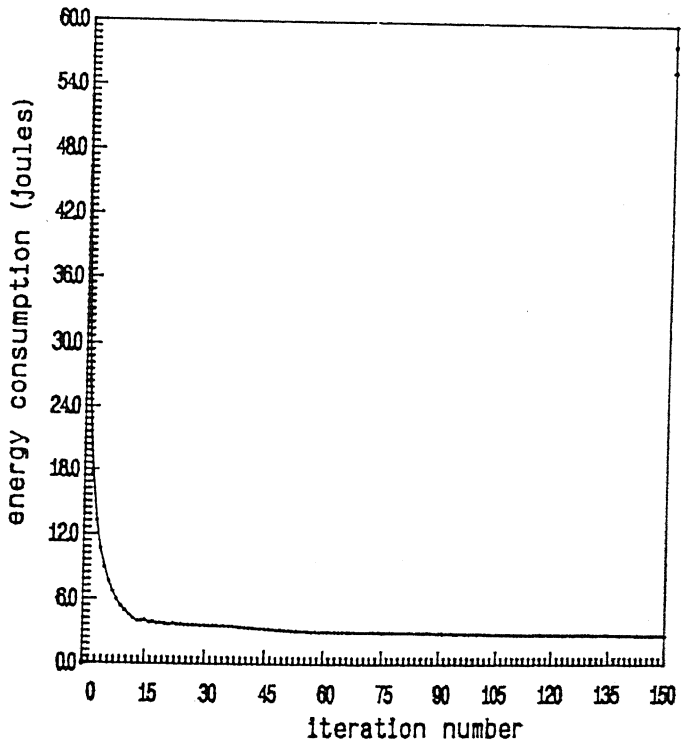

Fig. 4.15 Variation of energy with iteration number in minimum energy case for problem 1

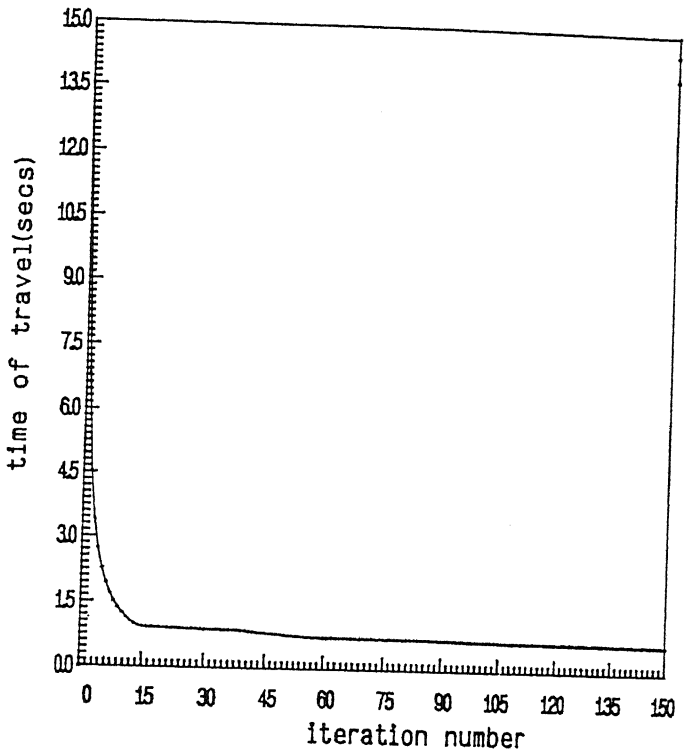

Fig. 4.16 Variation of travel time with iteration number in minimum energy case for problem 1

Table 4.7 (Continued)

19	45.56	0.0219
20	46.90	0.0213
21	46.01	0.0217
22	43.79	0.0228
23	40.76	0.0245
24	37.64	0.0266
25	32.11	0.0311
26	32.87	0.0304
27	29.20	0.0342

It is observed that compared to Table 4.2, the distribution of H(k) is more or less uniform.

The joint velocity profiles are shown in Fig.4.17 and 4.18. Comparing these with Figs. 4.5 and 4.6, it is seen that the joint velocities are now much lower but slightly irregular in nature. Minimization of energy alone is expected to lead to low velocities and low accelerations . In fact, if the gravity loading was not to be supported by the joint torques then an extremely slow movement over a large interval of time will lead to lower values of energy.

The joint torque profiles are shown in Fig. 4.19 and 4.20. The torques are much lower than in Figs.4.7 and 4.8 but somewhat fluctuating. Finally,the velocity profile of the object is shown in Fig.4.21. Here again the velocity is low compared to Fig. 4.11, but small fluctuations in the velocity are present.

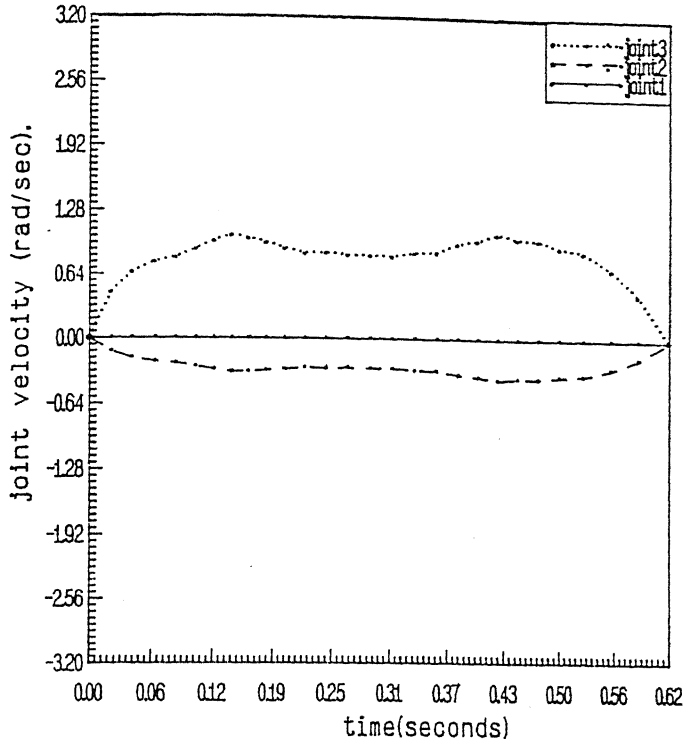

Fig. 4.17 Velocities of joints 1,2 and 3 for both arms with minimum energy case for problem 1

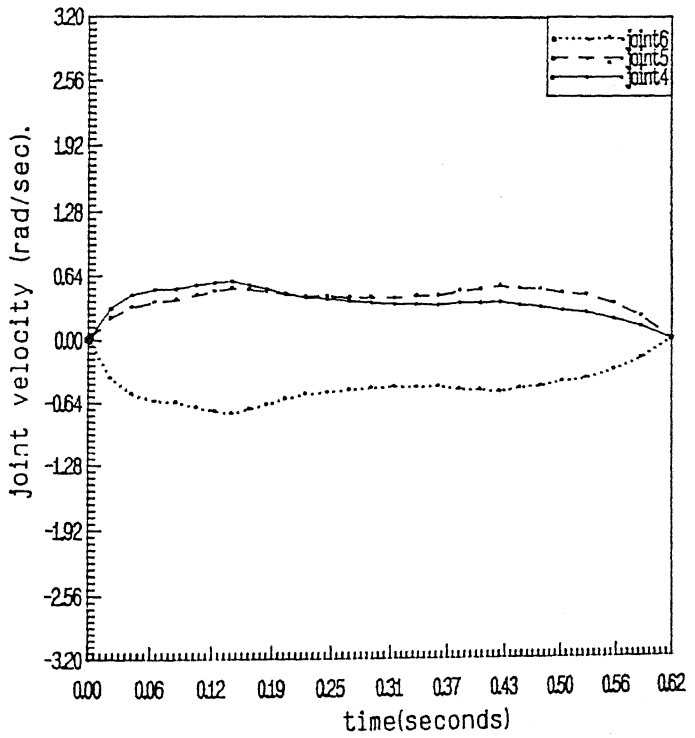

Fig. 4.18 Velocities of joints 4,5 and 6 of both arms with minimum energy case for problem 1

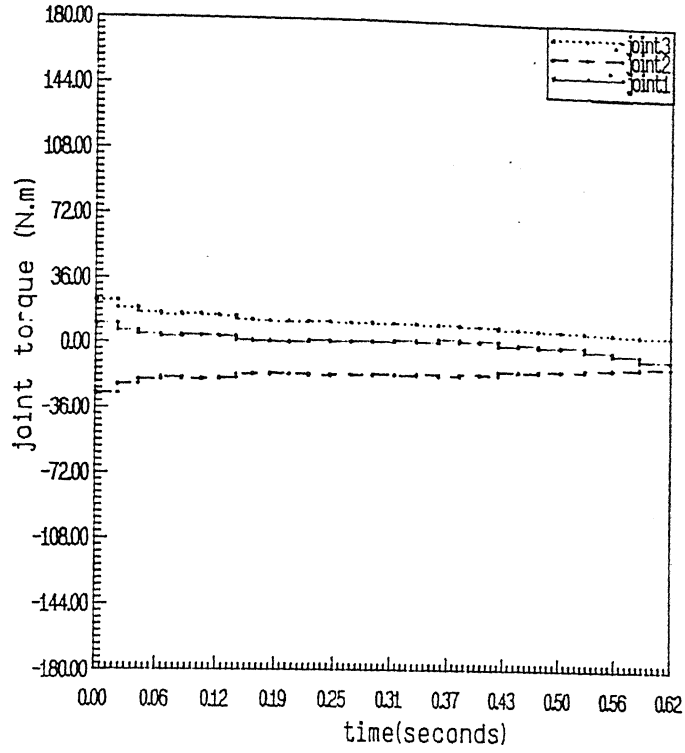

Fig. 4.19 Torques of joints 1,2 and 3 for both arms with minimum energy case for problem 1

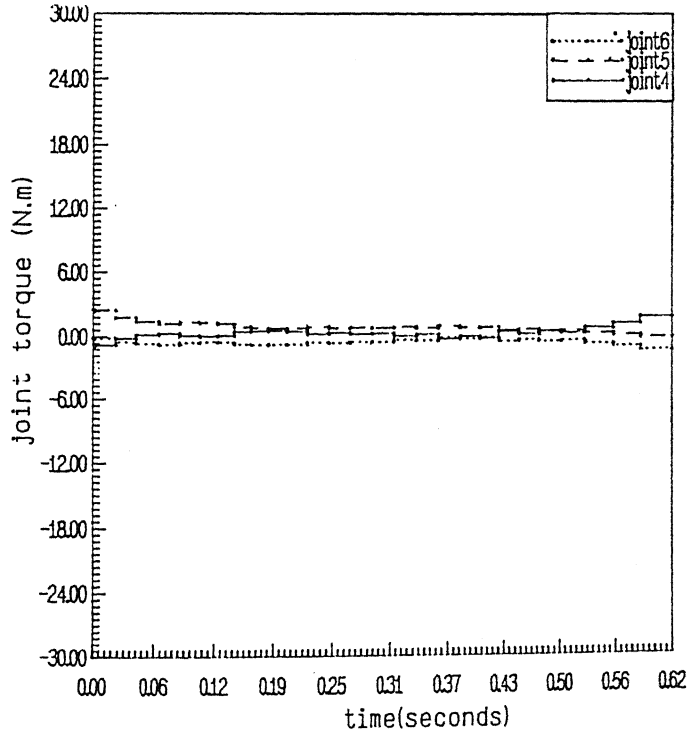

Fig. 4.20 Torques of joints 4,5 and 6 of both arms with minimum energy case for problem 1

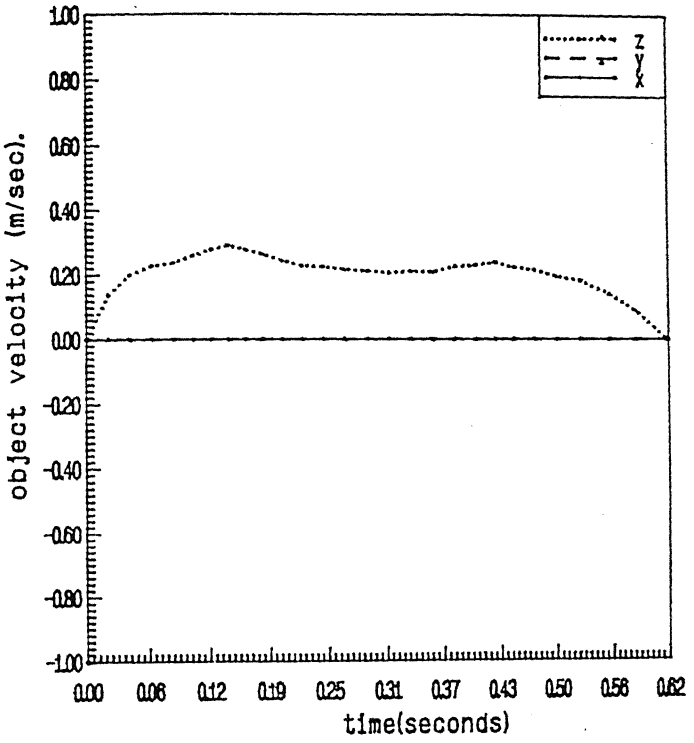

Fig. 4.21 Linear velocity of object in minimum energy case for problem 1

4.2.5 *Results with Minimum Time and Energy Criterion*

A combined objective function with weightages on both minimum time and minimum energy was used to find the time histories for the same problem. It was found that with this criterion the convergence was always slow in the later parts of iterations and warm start also did not help in reducing the number of iterations by any significant amount.

The results for two cases in this category are presented here. The first case corresponds to $\gamma_1 = \gamma_2 = 0.5$ and $\beta_1 = \beta_2 = 0.5$ in (3.7-8) and (3.8-3), respectively. These weights for the second case are taken as $\gamma_1 = \beta_1 = 0.9$ and $\gamma_2 = \beta_2 = 0.1$. With $H^0(k) = 2\ sec^{-1}$, $\Delta H_{max} = 2\ sec^{-1}$ and $\Delta H_{min} = -2\ sec^{-1}$, the number of iterations were nearly 200. Whereas, with $H^0(k) = 20\ sec^{-1}$, $\Delta H_{max} = 25\ sec^{-1}$, $\Delta H_{min} = -25\ sec^{-1}$, the initial convergence was very fast but the total number of iterations were still near 180. The optimum reciprocal time intervals and the objective functions for the above two cases are listed in Table 4.8, the joint

Table 4.8 Optimum reciprocal time intervals for minimum time-energy case of Problem 1

	Case 1 $\gamma_1 = \gamma_2 = 0.5$ $\beta_1 = \beta_2 = 0.5$ Optimum travel time = 0.57 sec. Optimum energy = 2.57 Joules Objective function = 1.57	Case 2 $\gamma_1 = 0.9$, $\gamma_2 = 0.1$ $\beta_1 = 0.9$, $\beta_2 = 0.1$ Optimum travel time = 0.44 sec optimum energy = 2.46 Joules Objective function = 0.64
k	$H^*(k)$ sec^{-1}	$H^*(k)$ sec^{-1}
1	51.40	61.41
2	55.56	67.74
3	50.10	63.93
4	53.27	73.36
5	54.93	78.54
6	58.18	81.31
7	60.25	80.71
8	60.22	77.36
9	58.00	73.80
10	54.28	70.33
11	50.40	67.48
12	48.02	63.01
13	46.48	54.87
14	45.26	48.66
15	44.34	50.27
16	44.03	56.20
17	44.60	62.30
18	46.58	66.75
19	49.54	69.31
20	51.22	68.56

Table 4.8 (Continued)

21	50.57	64.26
22	48.15	58.28
23	45.31	52.77
24	42.04	49.98
25	36.15	45.64
26	36.77	49.23
27	32.56	44.64

of problem 1 velocities are plotted in Figs.4.22 and 4.23, the joint torques are shown in Figs. 4.24 and 4.25, and the object velocity is shown in Figs. 4.26 and 4.27. For case 1, with β_1 = β_2 = 0.5, the objective function is more dominantly guided by the energy term and therefore except for a marginal reduction in travel time, the velocity and torque profiles resemble those in Figs. 4.17 to 4.21. The case 2 with β_1 = 0.9 and β_2 = 0.1 has equal numerical contributions from minimum time and minimum energy terms but the velocity and torque profiles still have trends like those in minimum energy case.

It is to be noted that contrary to the expectations, the energy has decreased with decreased weightage on the minimum energy term so that β_1 = 1, 0.5, 0.1 result in values of energy as 2.65 Joules, 2.57 Joules and 2.46 Joules, respectively. No fixed pattern or trend, however, could be seen while taking results with many other combinations.

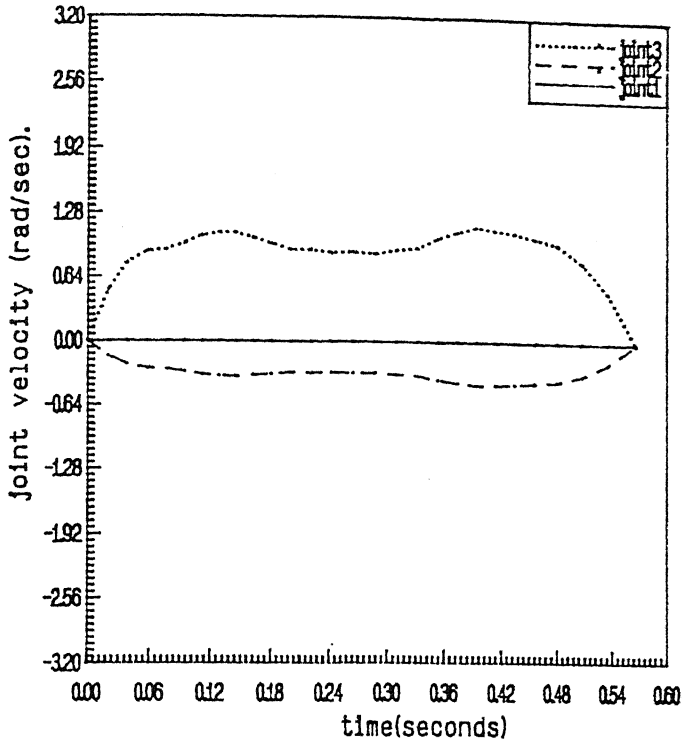

Fig. 4.22(a) Velocities of joints 1,2 and 3 for both arms with minimum time-energy case for problem 1 (case 1)

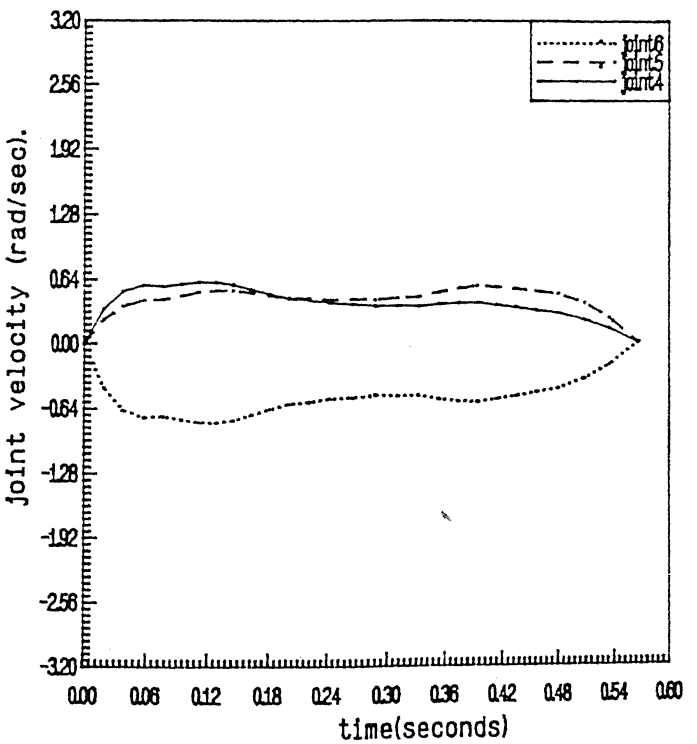

Fig. 4.22(b) Velocities of joints 4,5 and 6 of both arms with minimum time-energy case for problem 1 (case 1)

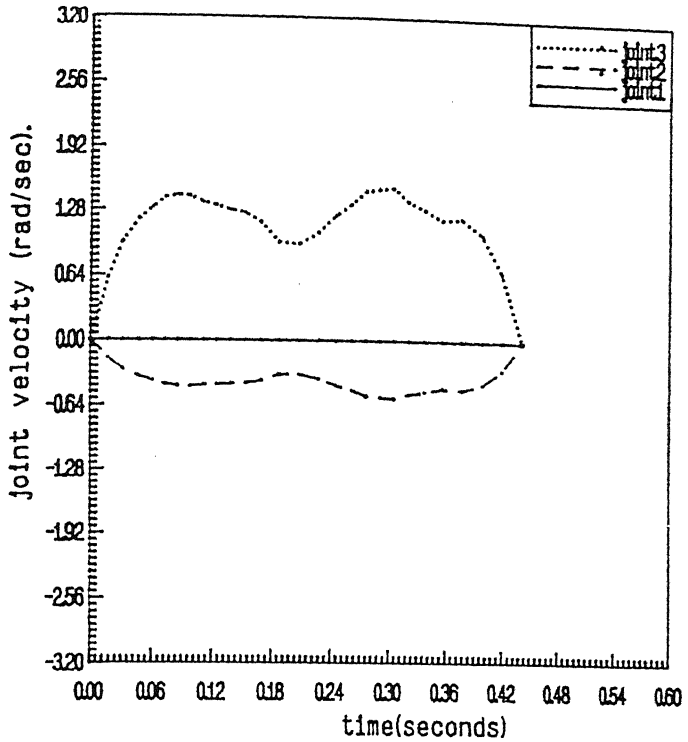

Fig. 4.23(a) Velocities of joints 1,2 and 3 for both arms with minimum time-energy case for problem 1 (case 2)

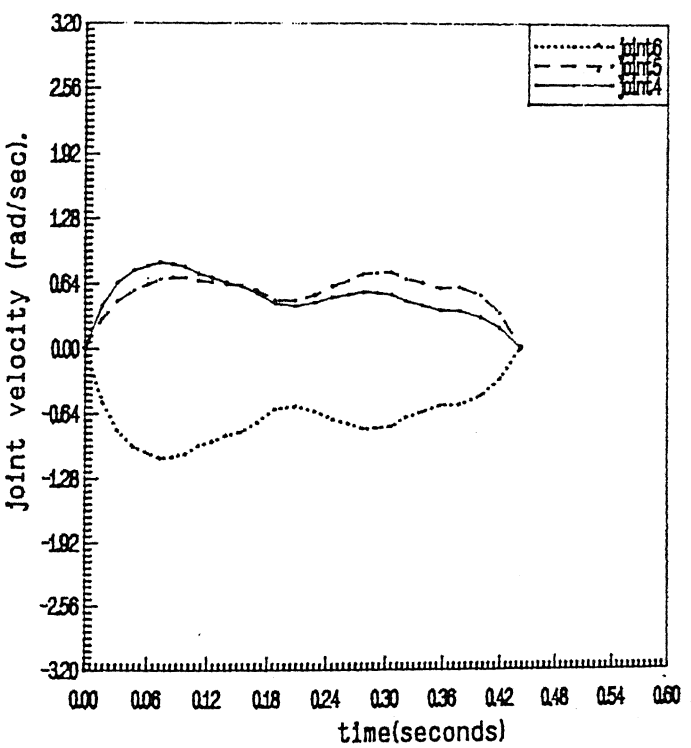

Fig. 4.23(b) Velocities of joints 4,5 and 6 of both arms with minimum time-energy case for problem 1 (case 2)

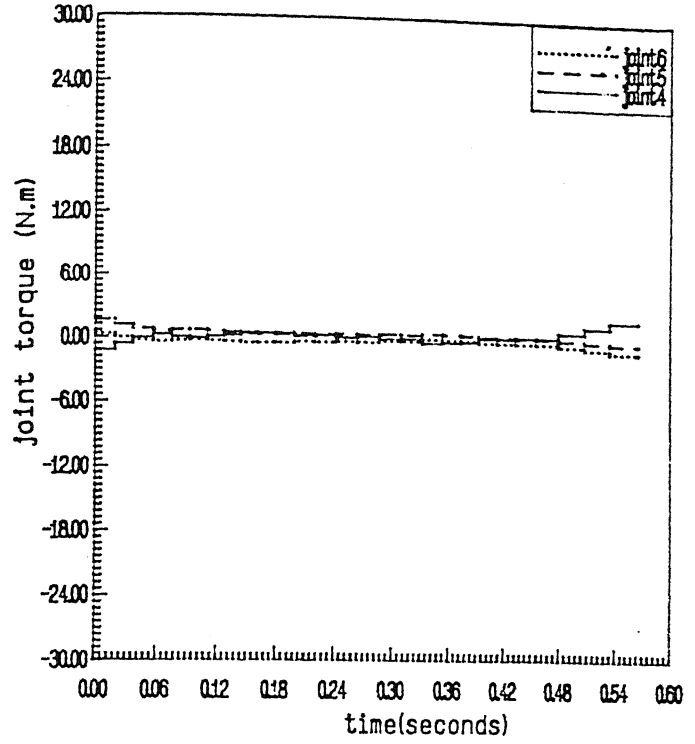

Fig. 4.24(a) Torques of joints 1,2 and 3 for both arms with minimum time-energy case for problem 1 (case 1)

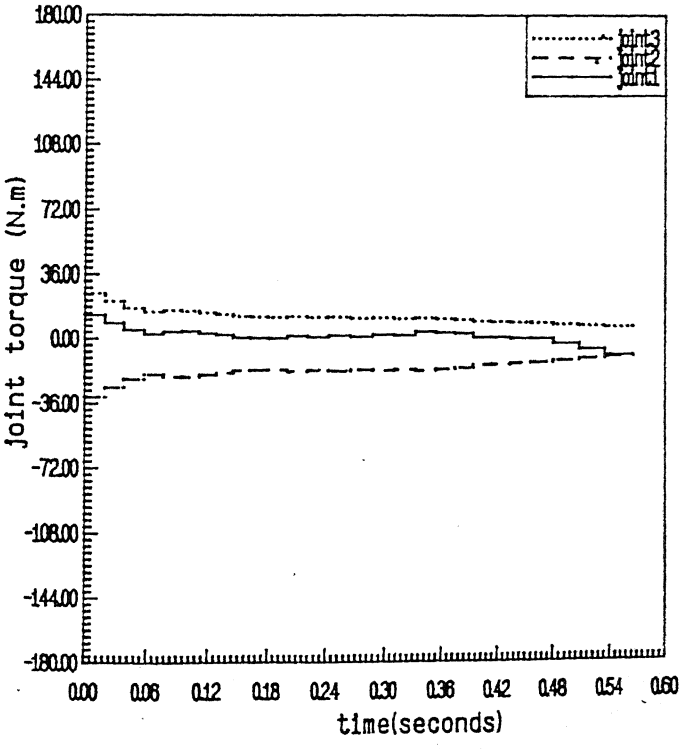

Fig. 4.24(b) Torques of joints 4,5 and 6 of both arms with minimum time-energy case for problem 1 (case 1)

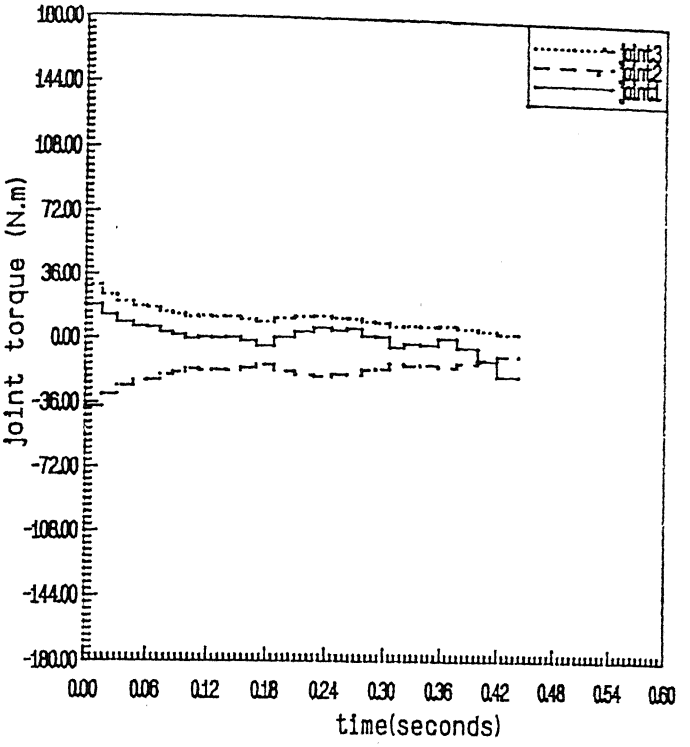

Fig. 4.25(a) Torques of joints 1,2 and 3 for both arms with minimum time-energy case for problem 1 (case 2)

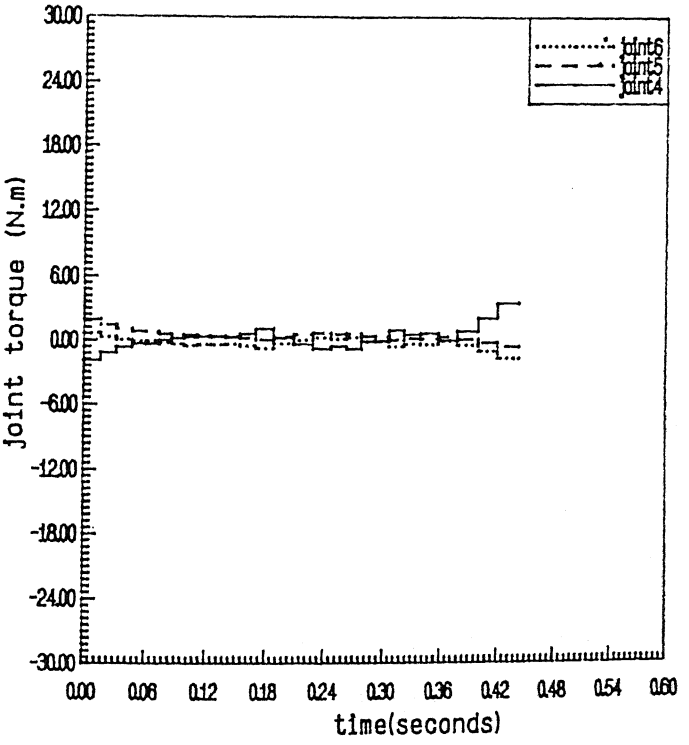

Fig. 4.25(b) Torques of joints 4,5 and 6 of both arms with minimum time-energy case for problem

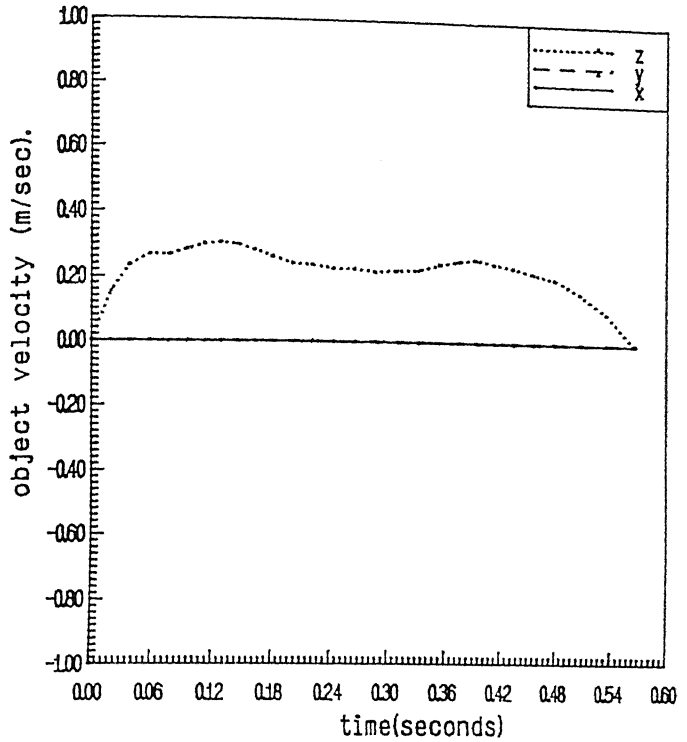

Fig. 4.26 Linear velocity of object with minimum time-energy case for problem 1 (case 1)

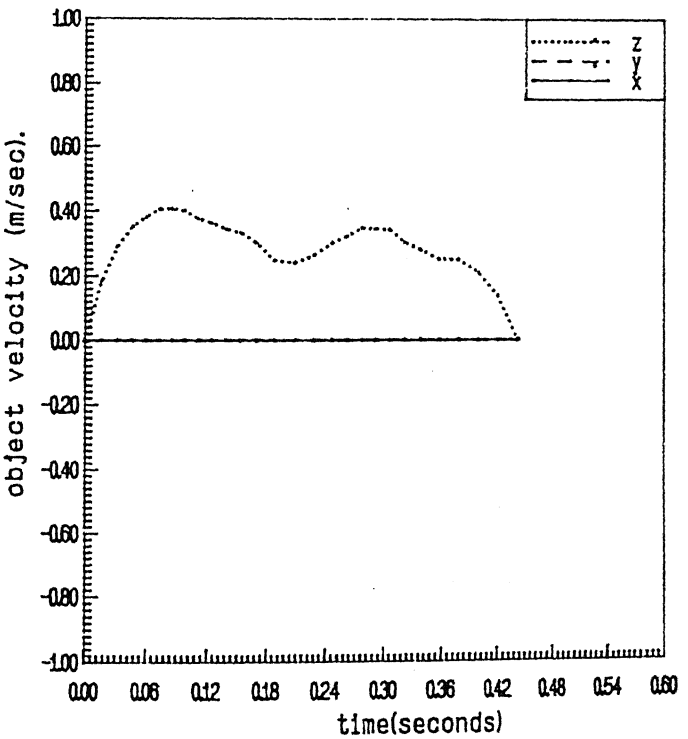

Fig. 4.27 Linear velocity of object with minimum time-energy case for problem 1 (case 2)

4.3 Problem 2: Results and Discussions

The problem 2 is an extension of the problem 1 where alongwith the vertical translation the object undergoes rotations also. The object is initially at rest and is again brought to rest at the end of the trajectory. The steps of two solution stages are as detailed for problem 1, and differ only in terms of the input parameters. The important input parameters for this problem 2 are listed below, where the step numbers refer to those in Secs. 4.2.1 and 4.2.2. Other input parameters are same as in problem 1. Input the object path and compute ${}^{w}T_{c}$. For the problem 2, the object path is specified by

$$ {}^{w}p_{c}(0) = \begin{bmatrix} 0.6 \text{ meter} \\ 0.0 \text{ meter} \\ 0.38 \text{ meter} \end{bmatrix} $$

$$ {}^{w}p_{c}(1) = \begin{bmatrix} 0.6 & \text{meter} \\ 0.0 & \text{meter} \\ 0.3825 & \text{meter} \end{bmatrix} $$

$$ {}^{w}p_{c}(K) = \begin{bmatrix} 0.6 & \text{meter} \\ 0.6 & \text{meter} \\ 0.385 + 0.005\ (k-2) & \text{meter} \end{bmatrix} \quad \text{for } K = 2,\ldots 25. $$

$$^{w}p_{c}(26) = \begin{bmatrix} 0.6 & \text{meter} \\ 0.0 & \text{meter} \\ 0.5025 & \text{meter} \end{bmatrix}$$

$$^{w}p_{c}(27) = \begin{bmatrix} 0.6 & \text{meter} \\ 0.0 & \text{meter} \\ 0.5050 & \text{meter} \end{bmatrix}$$

$$\Phi(0) = \begin{bmatrix} 90 \text{ degrees} \\ 90 \text{ degrees} \\ 0 \text{ degrees} \end{bmatrix}$$

$$\Phi(1) = \begin{bmatrix} 89.10 \text{ degrees} \\ 89.40 \text{ degrees} \\ 0.60 \text{ degrees} \end{bmatrix}$$

$$\Phi(K) = \begin{bmatrix} 88.20 - 1.8\,(k-2) \text{ degrees} \\ 88.80 - 1.2\,(k-2) \text{ degrees} \\ 1.2 + 1.2\,(k-2) \text{ degrees} \end{bmatrix} \text{ for } K = 2,....25.$$

$$\Phi(26) = \begin{bmatrix} 45.90 \text{ degrees} \\ 60.60 \text{ degrees} \\ 29.40 \text{ degrees} \end{bmatrix}$$

$$\Phi(27) = \begin{bmatrix} 45.00 \text{ degrees} \\ 60.00 \text{ degrees} \\ 30.00 \text{ degrees} \end{bmatrix}$$

$$q_1(0) = \begin{bmatrix} -154.30 \text{ degrees} \\ -73.52 \text{ degrees} \\ -18.30 \text{ degrees} \\ 86.30 \text{ degrees} \\ -25.76 \text{ degrees} \\ -175.81 \text{ degrees} \end{bmatrix}$$

$$q_2(0) = \begin{bmatrix} -154.30 \text{ degrees} \\ -73.52 \text{ degrees} \\ -18.30 \text{ degrees} \\ -93.78 \text{ degrees} \\ -25.76 \text{ degrees} \\ 4.19 \text{ degrees} \end{bmatrix}$$

(4.3-1)

4.3.1 *Results with Minimum Time Criterion*

In this case the objective function Z_{te} is defined by (3.8-3) with weightages $\beta_1 = 1$ and $\beta_2 = 0$. The redundancy in joint torque is resolved by the method outlined in Sec. 3.7. The weightages in torque resolution are taken as $\gamma_1 = 1$ and $\gamma_2 = 0$. The cost matrices are same as in problem 1. The initial guess

values of H(k) etc. are taken quite conservative. These values are taken as $H^{0}(k)$, = 2 sec^{-1} , ΔH_{max} = 2 sec^{-1}, ΔH_{min} = -2 see^{-1}. The joint velocity profiles are shown in Figs. 4.28 to 4.31. From velocity profiles it is observed that joint 5 of arm 1 reaches its velocity limit 2.1 rad./sec in the initial part of the path and joint 5 of arm 2 maintains this velocity upto the middle of the path. The joint 2 of arm 2 reaches its velocity limit 0.9 rad/sec in later half of the path. Thus the fastness of motion of the object is decided by these two joints. The joint torque profiles are shown in Figs. 4.32 to 4.35. From joint torque profiles it is observed that joints 2 and 3 have larger torque variation because these joints mainly carry the load against gravity. The torque exerted by joint 5 of each arm is quite low as this joint primarily causes rotation of the object. One interesting thing is that at the end of first time interval no joint reaches its velocity limit or torque limit. Therefore the trajectory is completed without any joint reaching its torque limit. The object velocity profiles are shown in Figs. 4.36 and 4.37. The total electrical energy consumption was 10.83 Joules. The optimum values of H(k) are given in Table 4.9. The number of iterations required

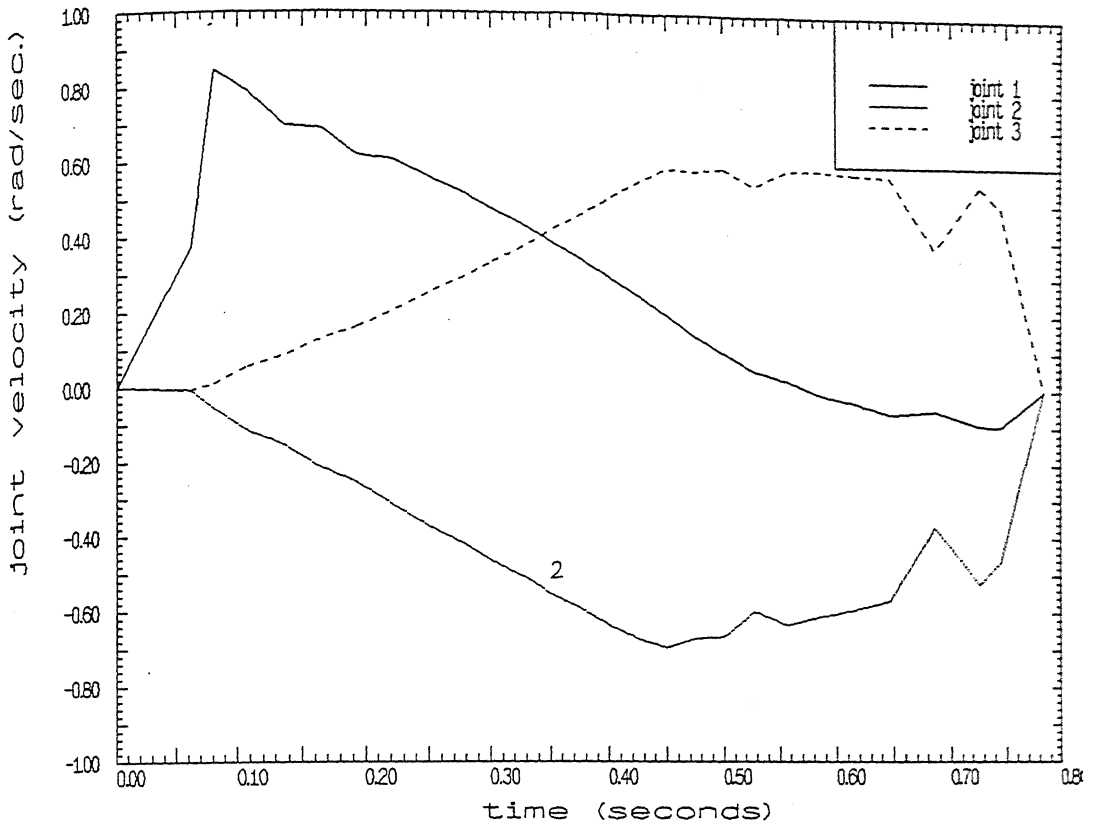

Fig. 4.28 Velocities of joints 1,2 and 3 for arm 1 with minimum time case for problem 2

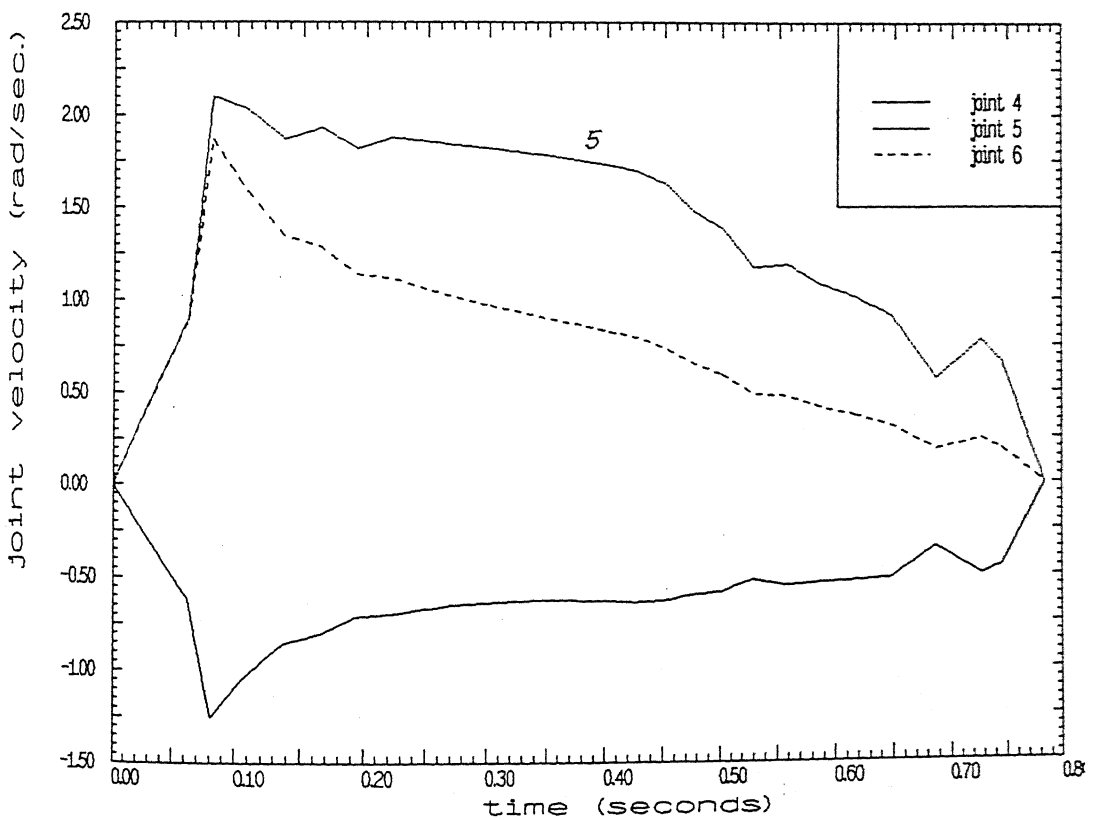

Fig. 4.29 Velocities of joints 4,5 and 6 for arm 1 with minim...

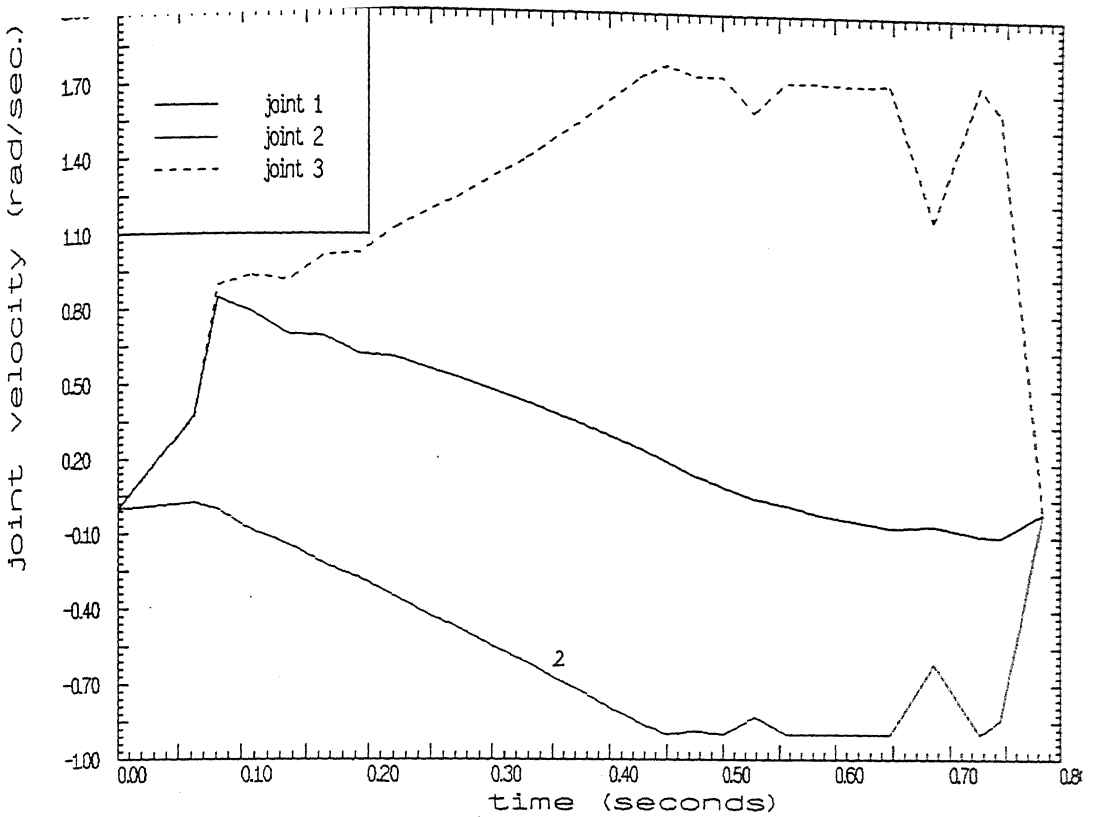

Fig. 4.30 Velocities of joints 1,2 and 3 for arm 2 with minimum time case for problem 2

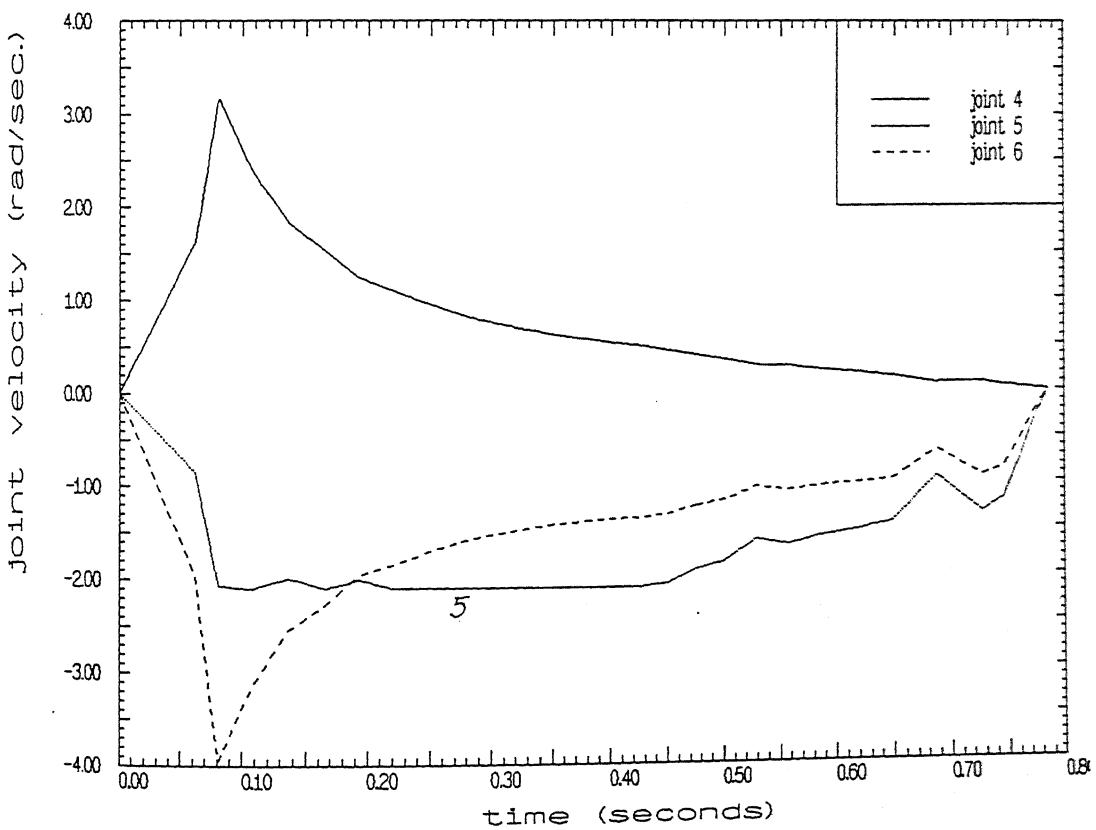

Fig. 4.31 Velocities of joints 4,5 and 6 for arm 2 with minimum time case for problem 2

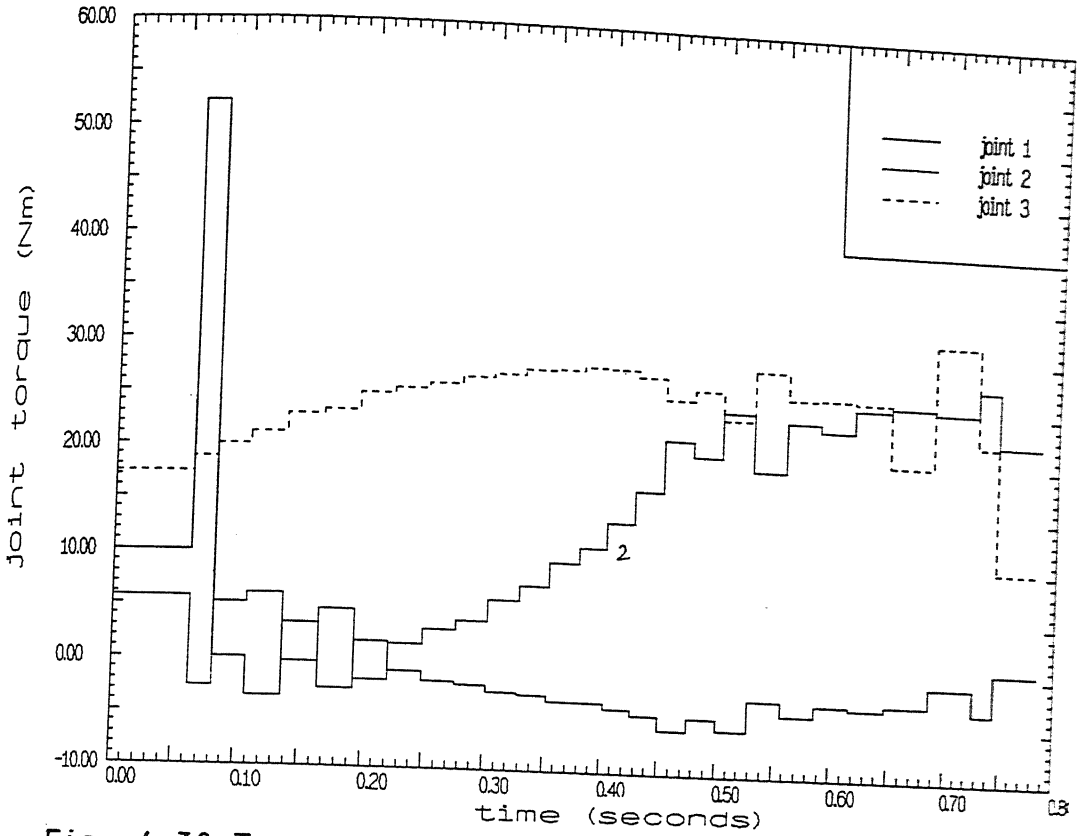

Fig. 4.32 Torques of joints 1,2 and 3 for arm 1 with minimum time case for problem 2

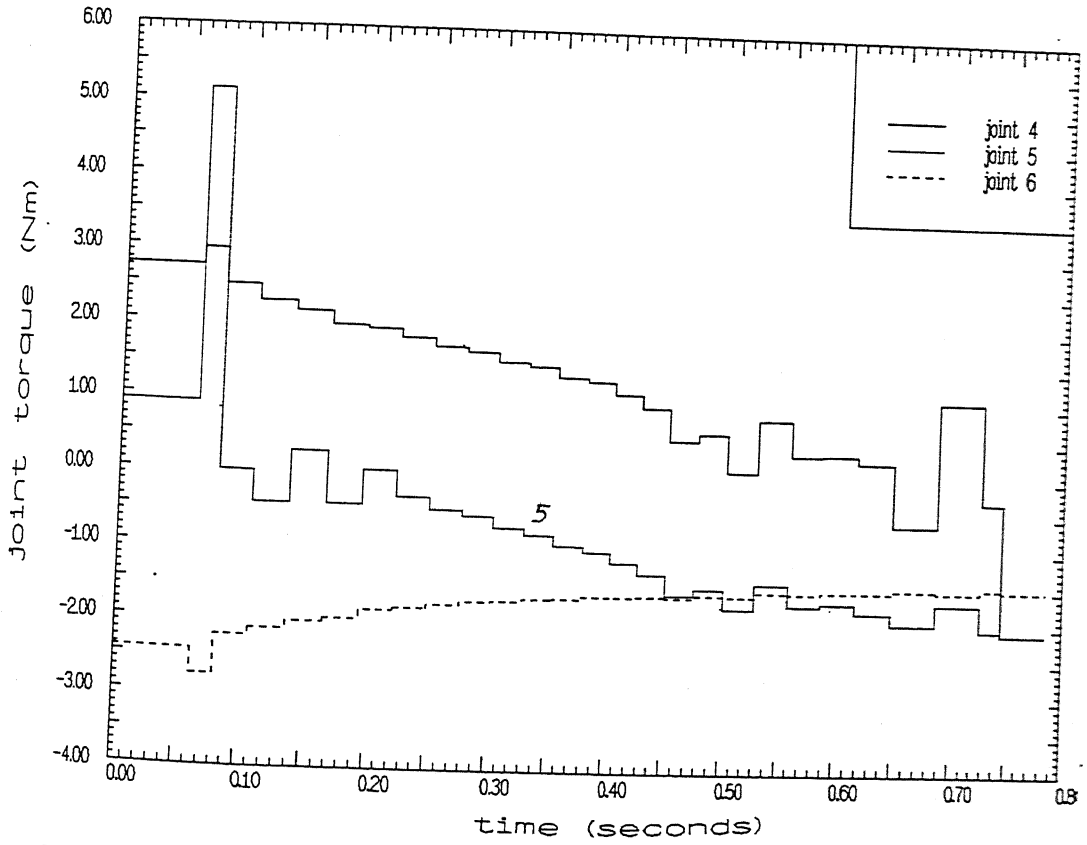

Fig. 4.33 Torques of joints 4,5 and 6 for arm 1 with minimum time case for problem 2

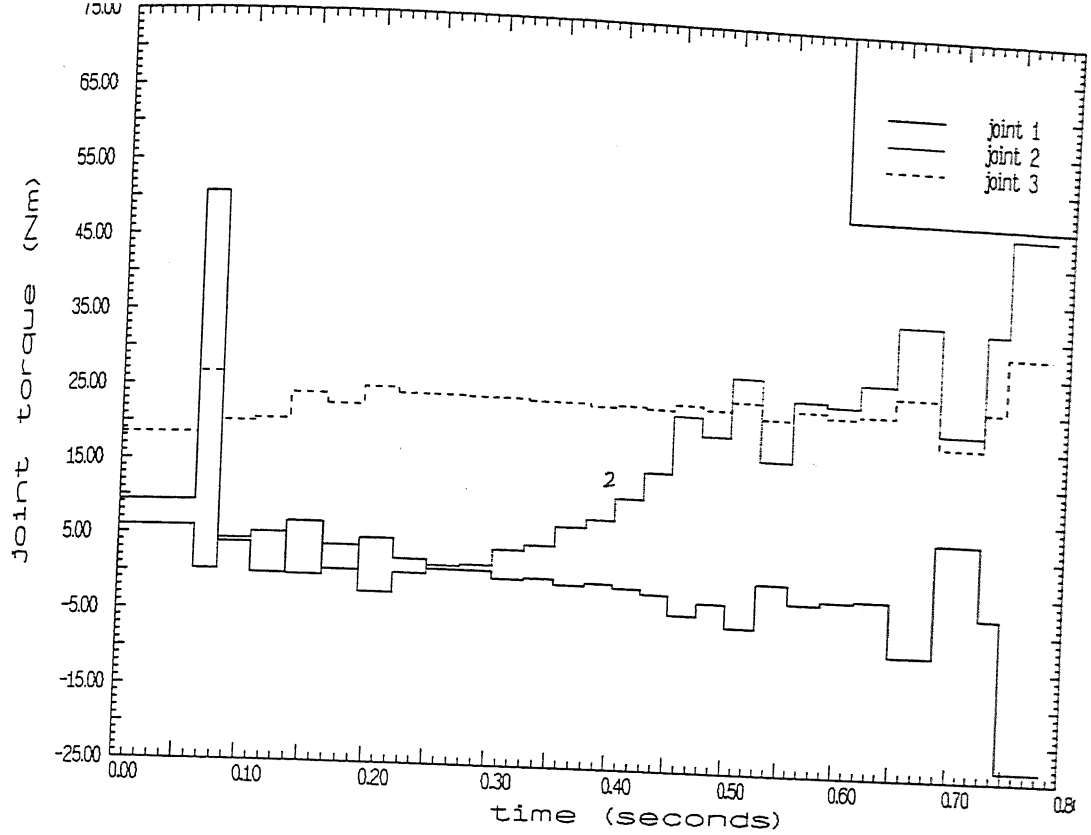

Fig. 4.34 Torques of joints 1,2 and 3 for arm 2 with minimum time case for problem 2

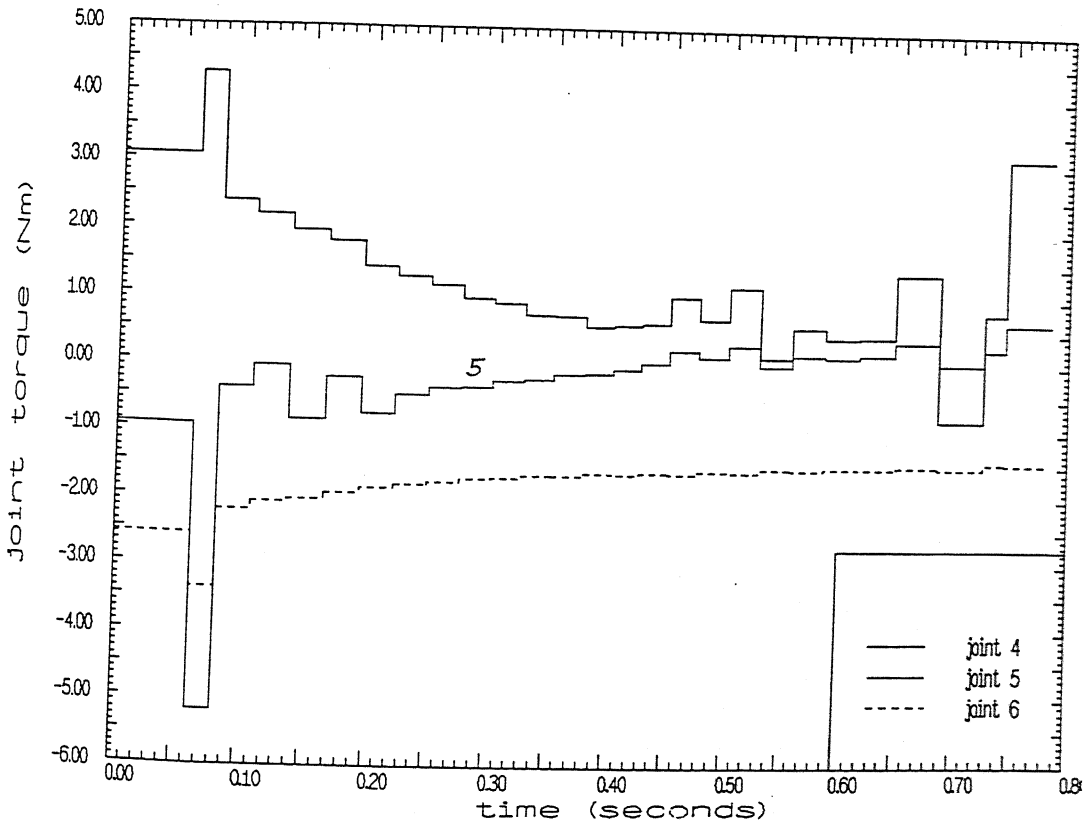

Fig. 4.35 Torques of joints 4,5 and 6 for arm 2 with minimum time case for problem 2

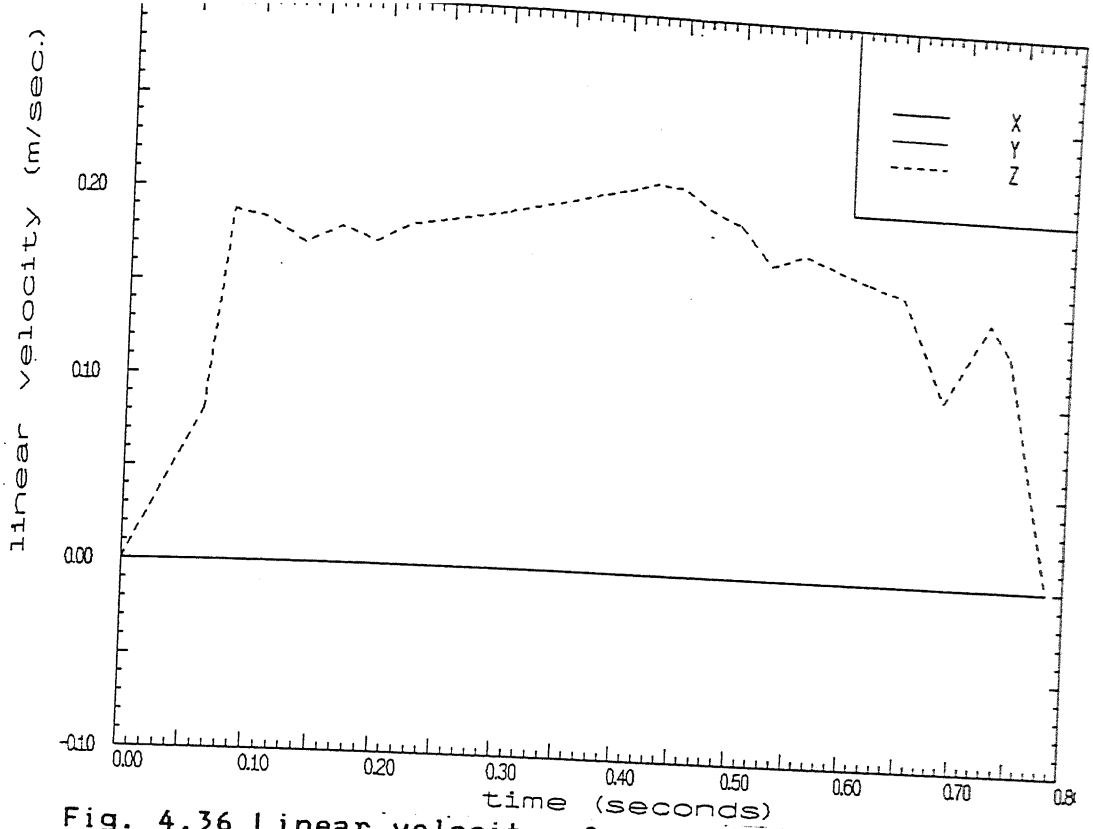

Fig. 4.36 Linear velocity of object with minimum time case for problem 2

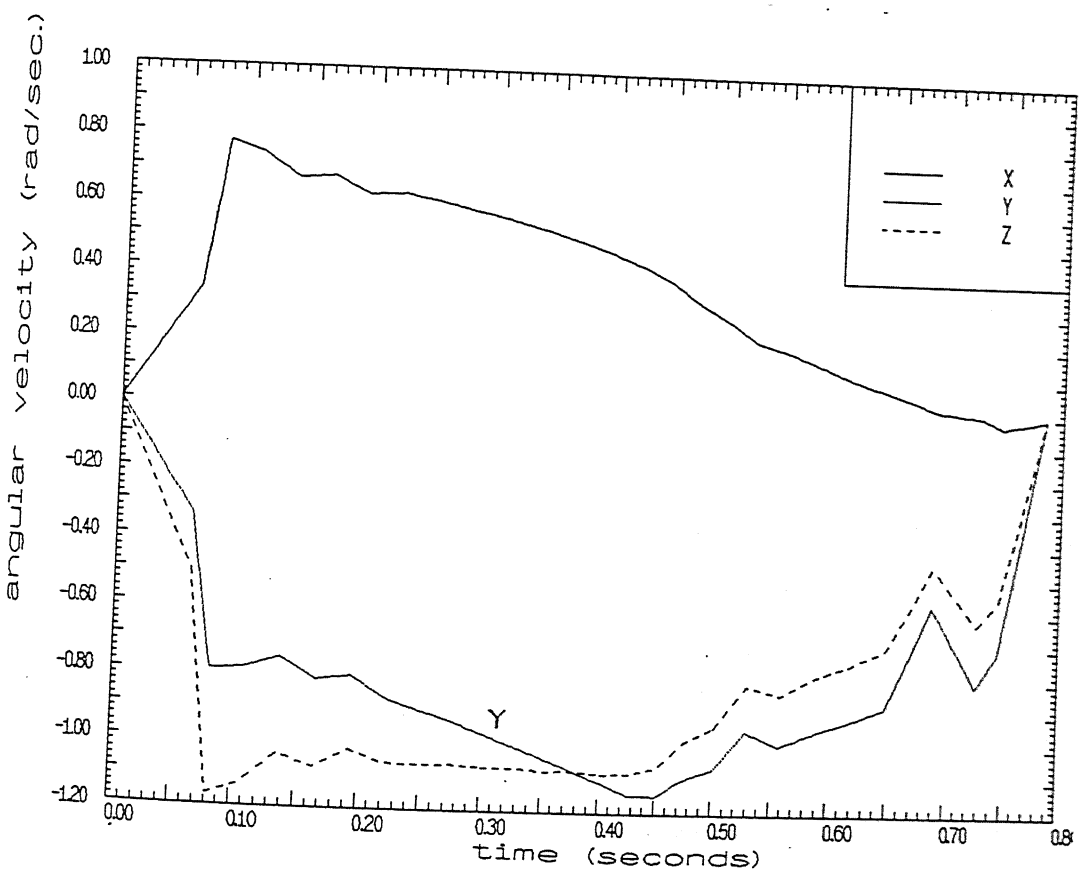

Fig. 4.37 Angular velocity components of object with minimum time case for problem 2

Table 4.9 Optimum time intervals and reciprocal time intervals for minimum time case of problem 2

k (interval number between kth and (k-1)th knot points)	$H^*(k)$ sec^{-1}	$\Delta t^*(k-1) = 1/H^*(k)$ sec.
1	16.11	0.0620
2	53.59	0.0187
3	37.06	0.0270
4	35.38	0.0282
5	35.04	0.0285
6	35.23	0.0284
7	35.49	0.0282
8	36.73	0.0272
9	37.30	0.0268
10	37.93	0.0264
11	38.65	0.0259
12	39.40	0.0254
13	40.16	0.0249
14	40.92	0.0244
15	41.69	0.0240
16	41.93	0.0238
17	40.70	0.0246
18	38.92	0.0257
19	36.06	0.0277
20	34.62	0.0289
21	34.64	0.0289
22	33.28	0.0300
23	31.94	0.0313
24	25.71	0.0389
25	24.55	0.0407
26	54.53	0.0183
27	25.67	0.0390

to get the solution was 26. The "warm start" with $H^{0}(k) = 25$ see^{-1}, $\Delta H_{max} = 20$ see^{-1} and $\Delta H_{min} = -20$ see^{-1} yielded the convergence in 4 iterations.

4.3.2 *Results with Minimum Energy Criterion*

In this case objective function Z_{te} is defined by (3.8-3) with weightages $\beta_1 = 0$ and $\beta_2 = 1$. For joint torque redundancy resolution the weightages taken are $\gamma_1 = 0$ and $\gamma_2 = 1$. The initial guess values of H(k), ΔH_{max} and ΔH_{min} are taken same as minimum time case. The joint velocity profiles are shown in Fig. 4.38 of 4.42. Here joint 5 of arm 1 does not reach the velocity limit but joint 5 of arm 2 reaches the velocity limit 2.1 rad/sec. and after few intervals maintains this velocity upto the middle of the path. But the joint 2 of arm 1 reaches its velocity limit 0.9 rad/sec near the middle of the path and maintains it in the later half of the path. In this case the velocity patterns are same as minimum time case but profiles are much smoother. The joint torque profiles are shown in Figs. 4.42 to 4.45. The torque patterns are also same as minimum time case but the torque values are in general lower. The object velocity profiles are shown in Figs. 4.46 and 4.47. Here also the velocity profiles are similar to minimum time case but the motions are smoothened. The optimum values of $H^{*}(k)$ are given in Table 4.10. The number of iterations

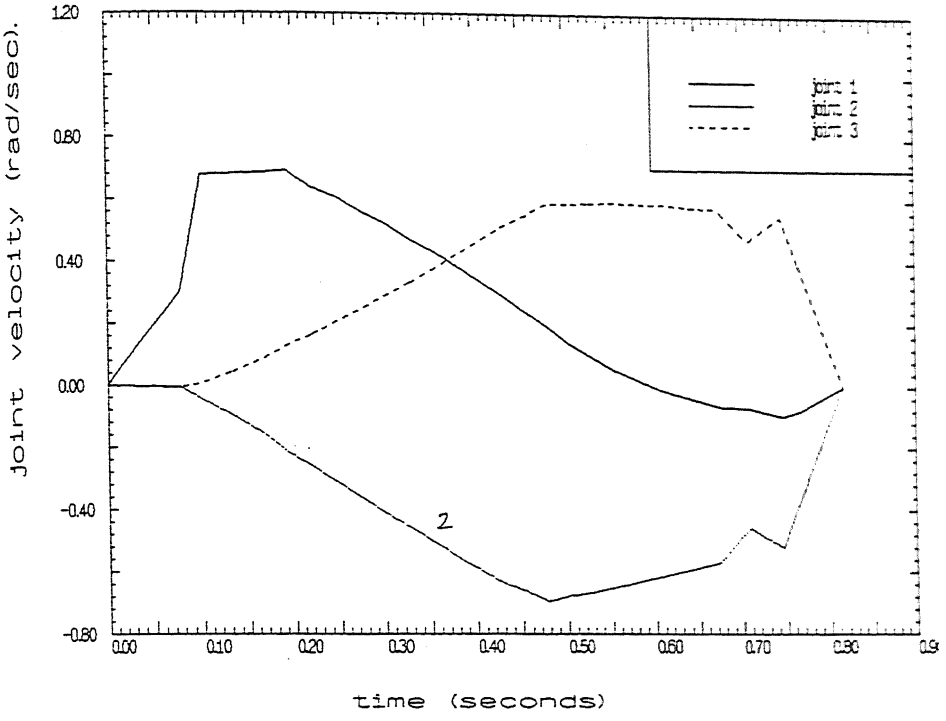

Fig. 4.38 Velocities of joints 1,2 and 3 for arm 1 with minimum energy case for problem 2

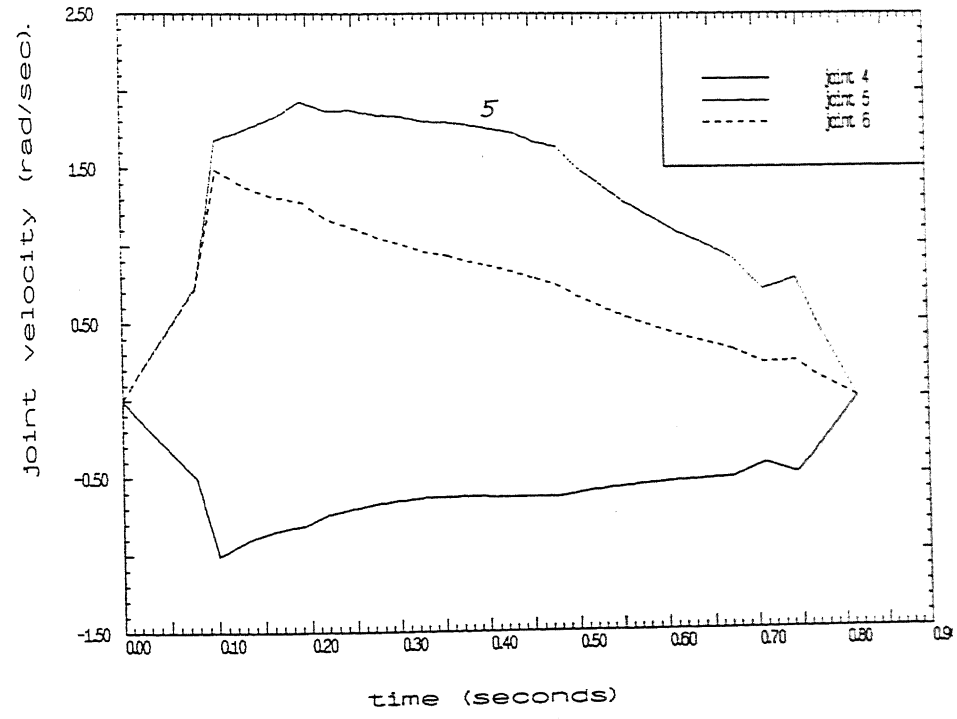

Fig. 4.39 Velocities of joints 4,5 and 6 for arm 1

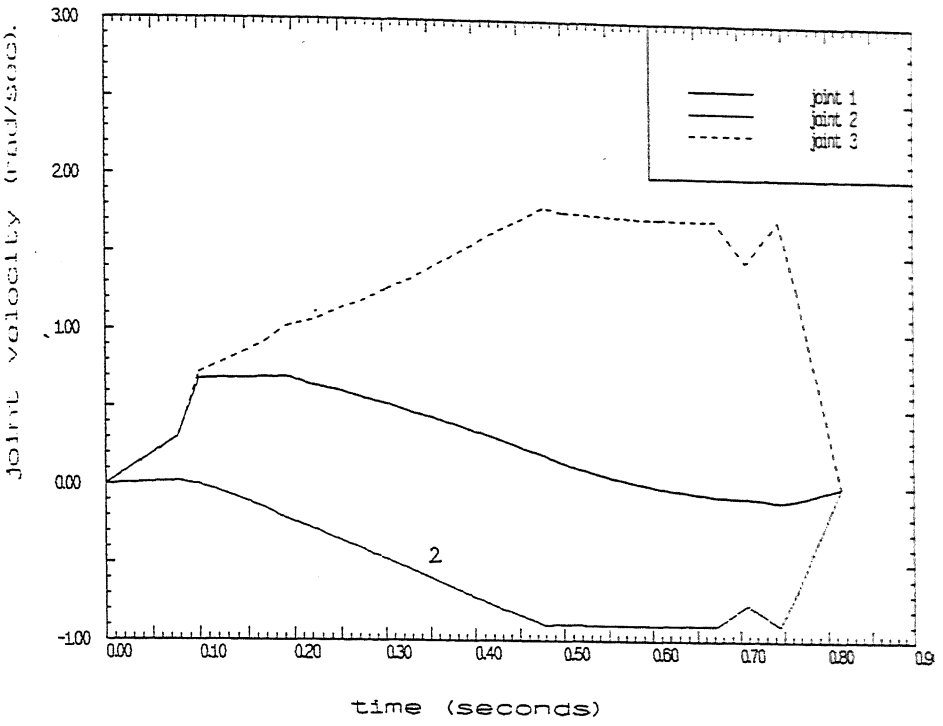

Fig. 4.40 Velocities of joints 1,2 and 3 for arm 2 with minimum energy case for problem 2

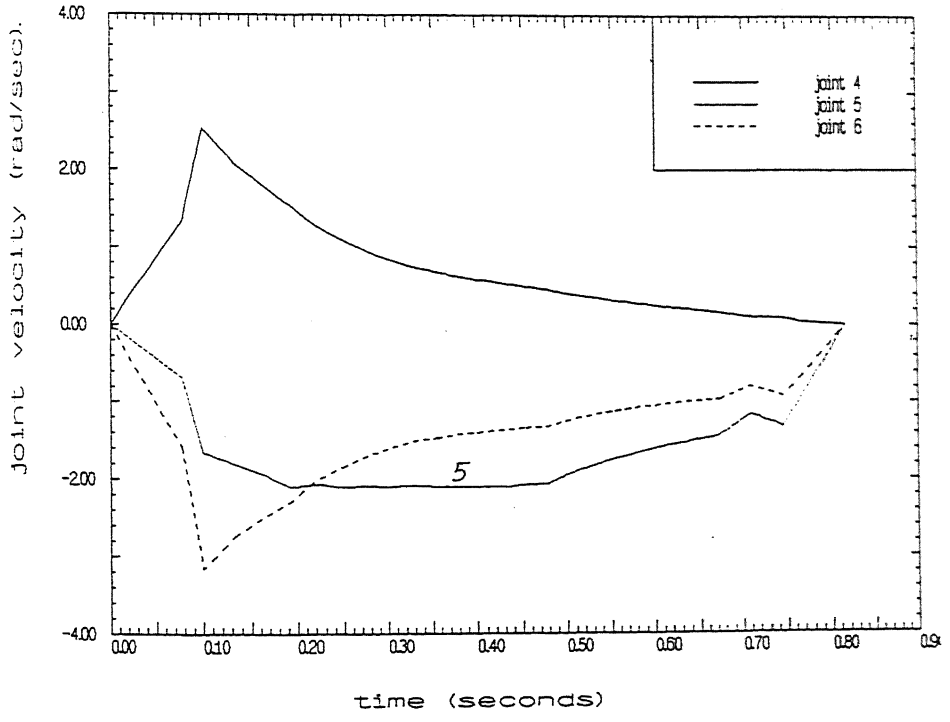

Fig. 4.41 Velocities of joints 4,5 and 6 for arm 2 with minimum energy case for problem 2

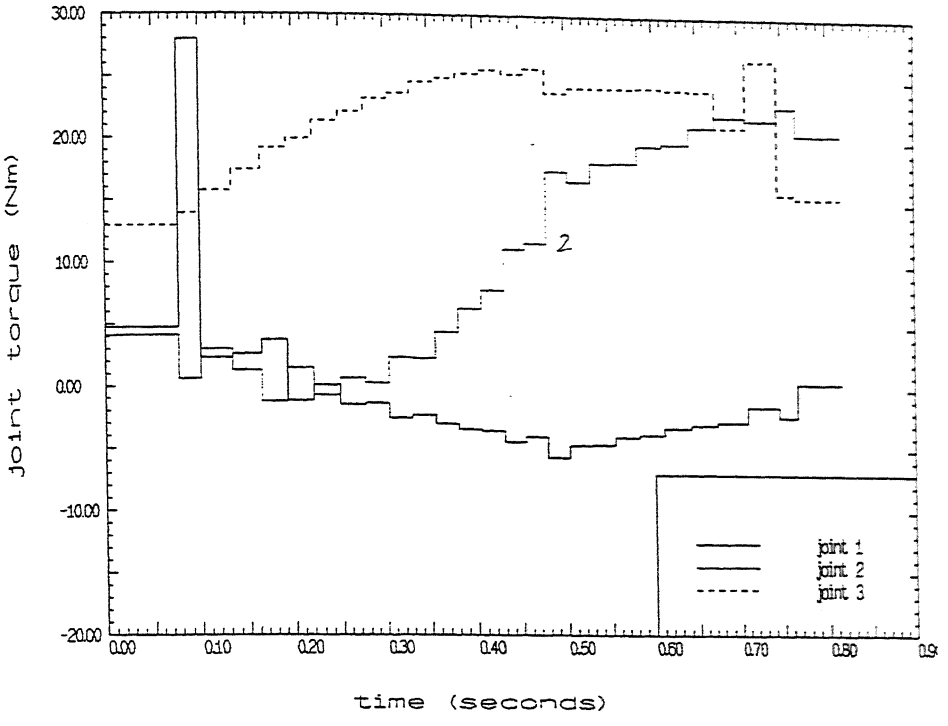

Fig. 4.42 Torques of joints 1,2 and 3 for arm 1 with minimum energy case for problem 2

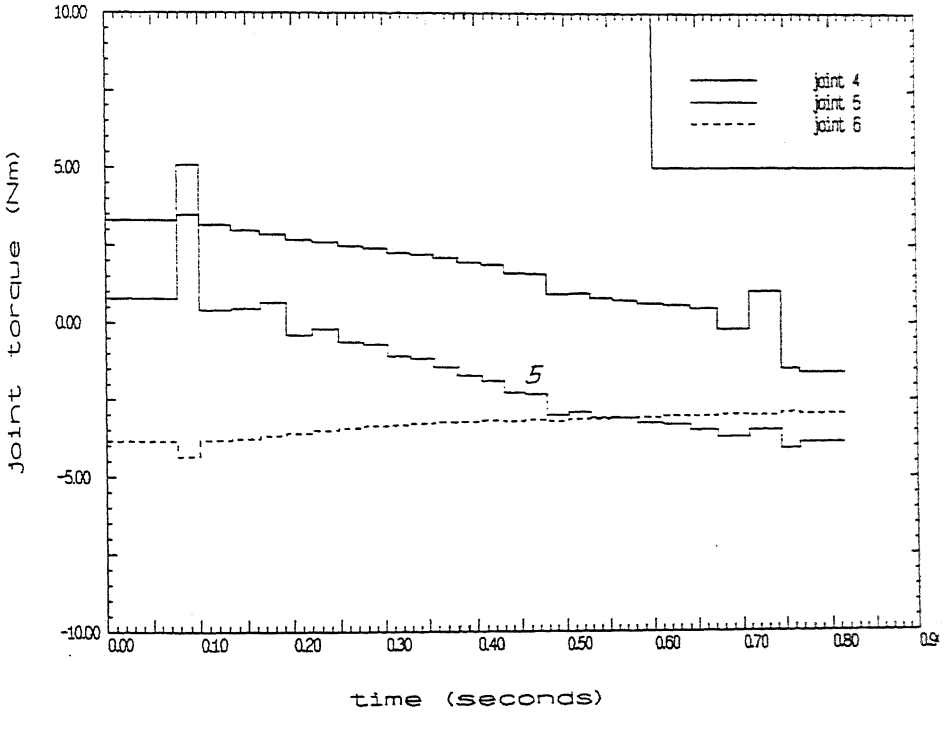

Fig. 4.43 Torques of joints 4,5 and 6 for arm 1

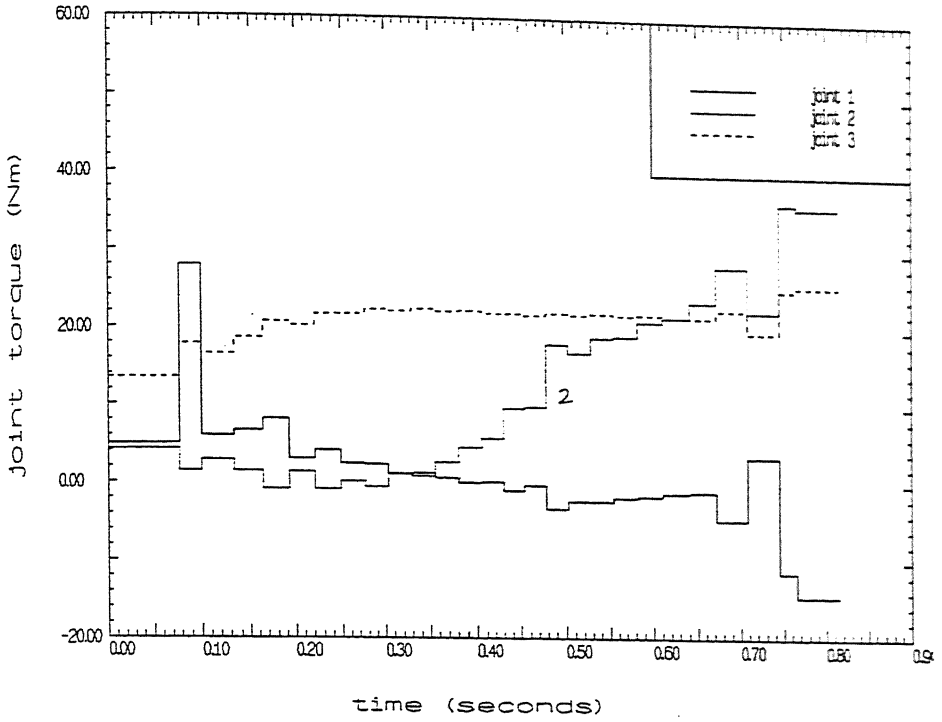

Fig. 4.44 Torques of joints 1,2 and 3 for arm 2 with minimum energy case for problem 2

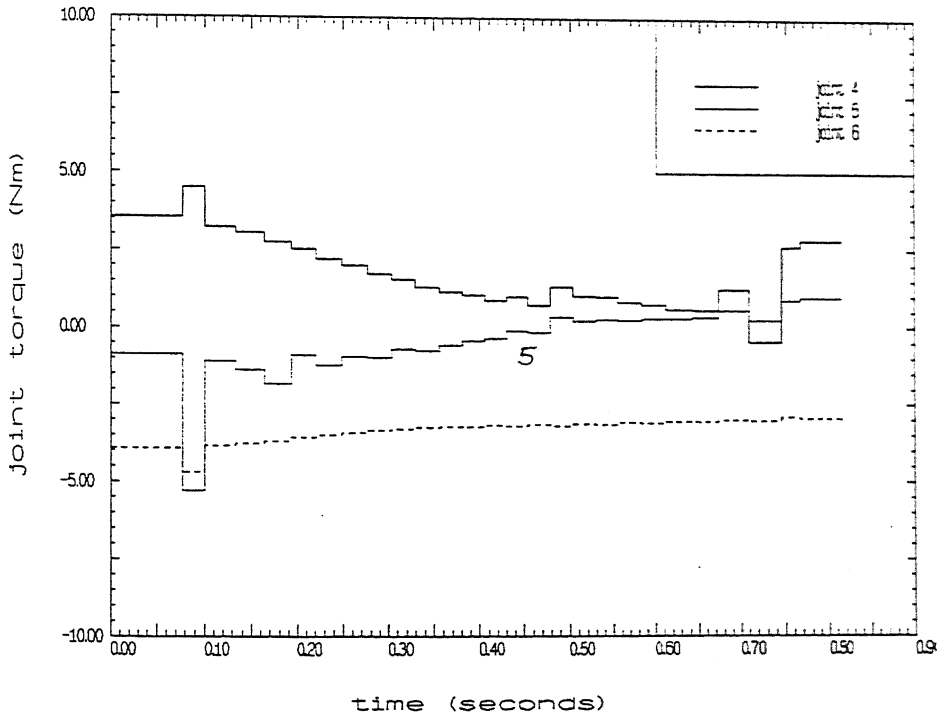

Fig. 4.45 Torques of joints 4,5 and 6 for arm 2 with minimum energy case for problem 2

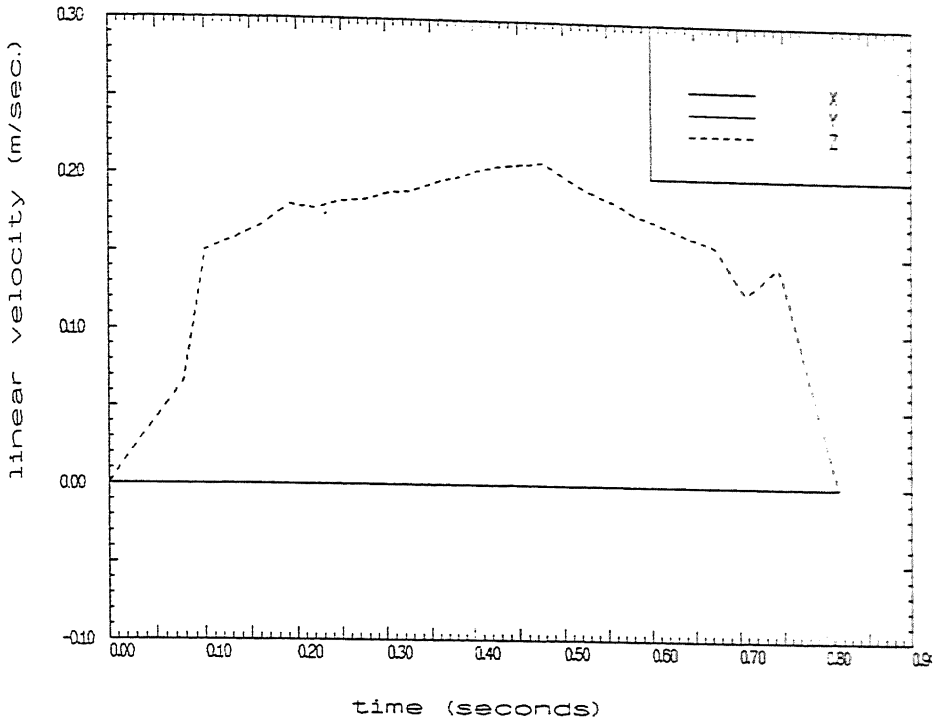

Fig. 4.46 Linear velocity of object with minimum energy case for problem 2

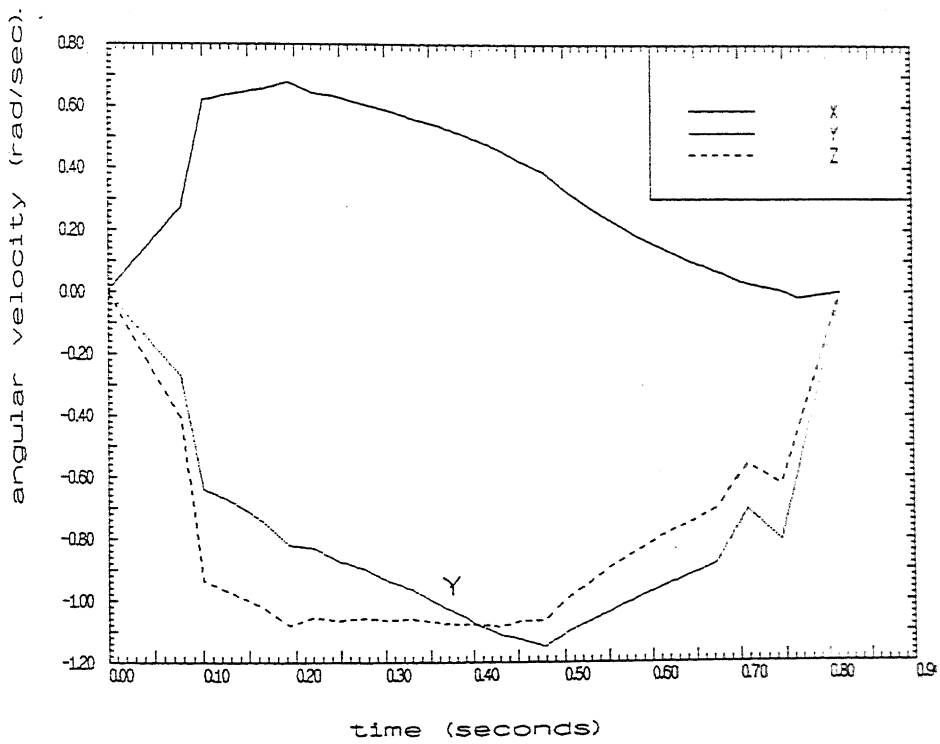

Fig. 4.47 Angular velocity components of object

Table 4.10 Optimum time intervals and reciprocal time intervals for minimum energy case of problem 2.

k (interval number between kth and (k-1)th knot points)	$H^*(k)$ sec^{-1}	$\Delta t^*(k-1) = 1/H^*(k)$ sec
1	12.95	0.0772
2	42.86	0.0233
3	30.76	0.0325
4	32.61	0.0307
5	34.79	0.0287
6	35.64	0.0280
7	35.89	0.0279
8	36.48	0.0274
9	37.05	0.0270
10	37.87	0.0264
11	38.59	0.0259
12	39.40	0.0254
13	40.17	0.0249
14	40.92	0.0244
15	41.26	0.0242
16	41.55	0.0240
17	40.99	0.0244
18	39.19	0.0255
19	37.56	0.0266
20	36.07	0.0277
21	34.64	0.0289
22	33.28	0.0300
23	31.94	0.0313
24	28.26	0.0354
25	26.98	0.0371
26	48.98	0.0204
27	20.28	0.0493

required is 124 and is much higher than the minimum time case. The energy required is 9.95 Joules. The total time of travel is 0.81 sec.

4.4 Problem 3: Results and Discussions

The problem 3 considers a parabolic path for the object. This path has ben selected to study a case where the velocities undergo reversal of sign. The object is initially at rest and is again brought to rest at the end of the trajectory. The steps of two solution stages are as detailed for problem 1, and differ only in terms of the input parameters. The important input parameters for this problem 3 are listed below, where the step numbers refer to those in section 4.2.1 and 4.2.2. Other input parameters are same as in problem 1. The base frames with respect to world coordinate frames are given by

$$
{}^{w}T_{10} = \begin{bmatrix} 1.0 & 0.0 & 0.0 & 0.0 \\ 0.0 & 1.0 & 0.0 & 0.0 \\ 0.0 & 0.0 & 1.0 & 0.0 \\ 0.0 & 0.0 & 0.0 & 1.0 \end{bmatrix}
$$

$$
{}^{w}T_{20} = \begin{bmatrix} -1.0 & 0.0 & 0.0 & 1.2 \\ 0.0 & -1.0 & 0.0 & 0.03 \\ 0.0 & 0.0 & 1.0 & 0.0 \\ 0.0 & 0.0 & 0.0 & 1.0 \end{bmatrix} \qquad (4.4\text{-}1)
$$

Input the object path and compute ${}^{w}T_{c}$. For problem 3, the object path is specified by

$$ {}^{w}p_{c}(k) \quad \begin{bmatrix} 0.6703 - 0.0031\,(7.0 - 0.5k)^{2} & \text{meter} \\ 0.14909 & \text{meter} \\ 0.4836 + .0031k & \text{meter} \end{bmatrix} $$

for $k = 0, 1, \ldots, 27$

$$ \Phi(K) \quad \begin{bmatrix} 90 \text{ degrees} \\ 90 \text{ degrees} \\ 0 \end{bmatrix} \qquad \text{for } K = 0.1, \ldots, 27 $$

$$ q_{1}(0) = \begin{bmatrix} -120.74 & \text{degrees} \\ -67.79 & \text{degrees} \\ -8.37 & \text{degrees} \\ -83.73 & \text{degrees} \\ -81.90 & \text{degrees} \\ -105.99 & \text{degrees} \end{bmatrix} $$

$$ q_{2}(0) = \begin{bmatrix} -141.37 & \text{degrees} \\ -89.32 & \text{degrees} \\ -8.88 & \text{degrees} \\ -78.27 & \text{degrees} \\ -39.62 & \text{degrees} \\ -105.08 & \text{degrees} \end{bmatrix} $$

(4.4-2)

4.4.1 Results with Minimum Time Energy Criterion

The results are presented for minimum time-energy case to show the nature of joint motions. The minimum time and minimum energy cases do not exhibit any additional features. In this case the objective function Z_{te} is defined by (3.8-3) with weightages $\beta_1 = 0.8$ and $\beta_2 = 0.2$. The redundancy in joint torque is resolved by the method outlined in Sec.3.7. The weightages in torque resolution are taken as $\gamma_1 = 0.5$ and $\gamma_2 = 0.5$. The cost matrices are same as in problem 1. The initial guess values of H(k), ΔH_{max} etc. are taken quite conservative. These values are taken as $H^0(k) = 2\ sec^{-1}$, $\Delta H_{max} = 2\ sec^{-1}$, $\Delta H_{min} = -2\ sec^{-1}$. The parabolic path in x-z plane is shown in Fig. 4.48. The joint velocity profiles are shown in Figs. 4.49 to 4.52. The joint 1,2,3 and 5 of each arm change the joint velocity direction in the middle of the path. This is due to the motion of the object in parabolic path where motion along x direction is much more than z direction. At the middle of the path the x-compenent of object velocity changes the direction due to which the velocities of joints 1,2 and 3 change the signs. Joint 2 of arm 1 reaches the velocity limit 0.9 rad/sec at initial part of the path and joint 2 of arm 2 reaches its limit at the end of the path. The joint torque profiles are shown in Figs. 4.53 to 4.56. No joint reaches its torque limit. The object velocity profile is shown in Fig. 4.57. The optimum values of H(k) are given in Table 4.11. The number of interations

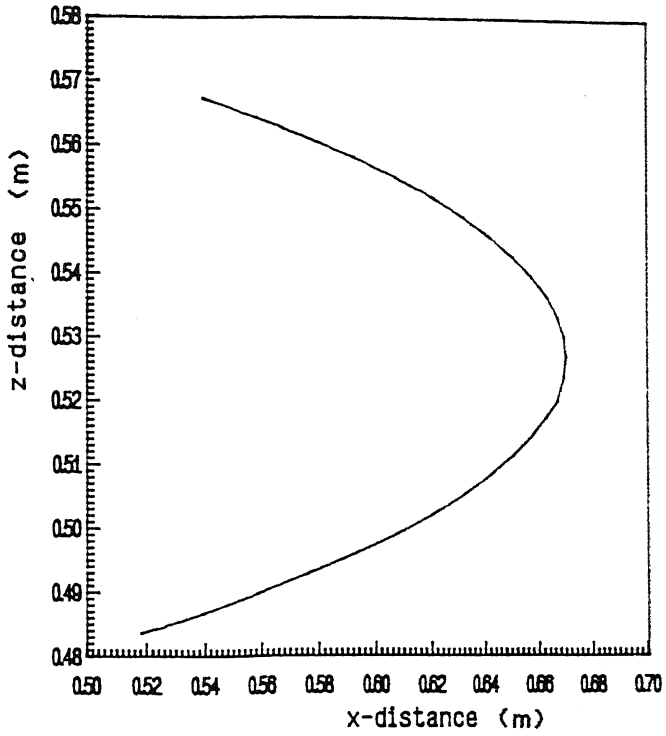

Fig. 4.48 Parabolic path of object for problem 3

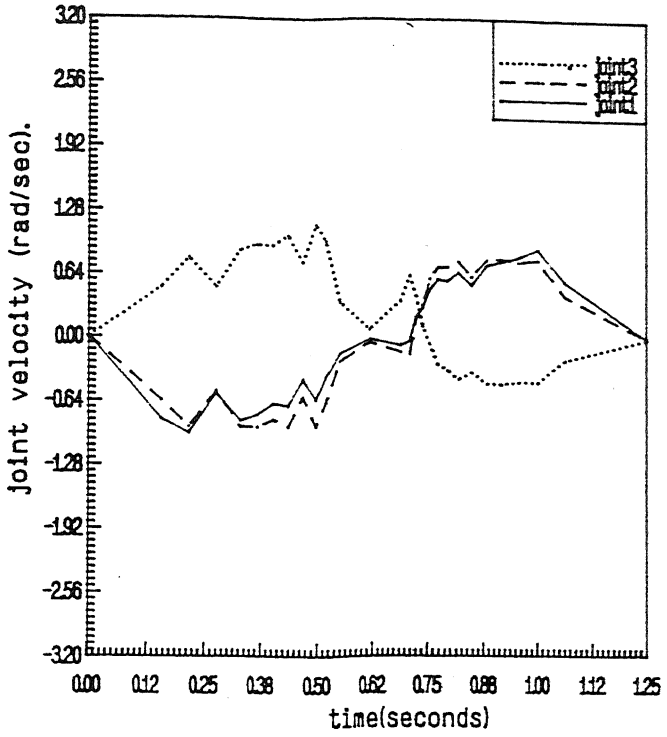

Fig. 4.49 Velocities of joints 1,2 and 3 for arm 1 with minimum time-energy case for problem 3

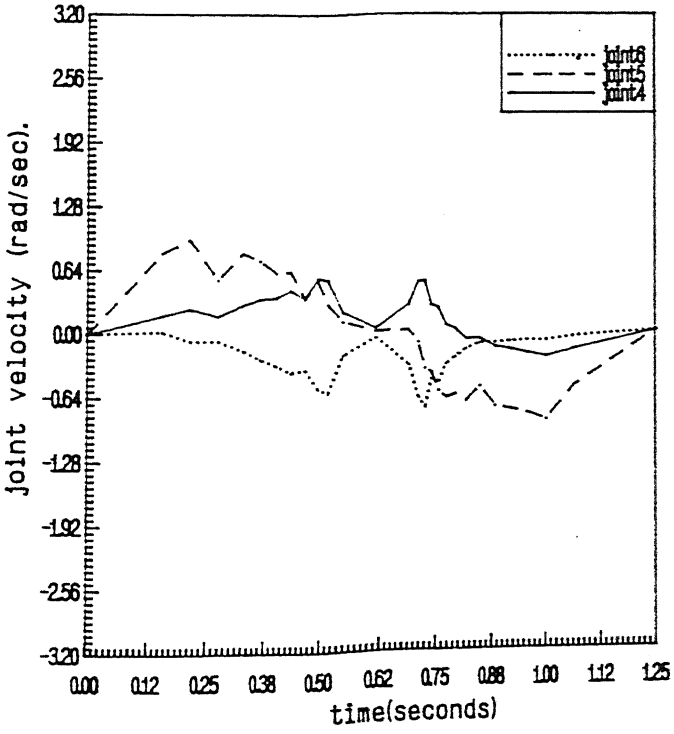

Fig. 4.50 Velocities of joints 4,5 and 6 for arm 1 with minimum time-energy case for problem 3

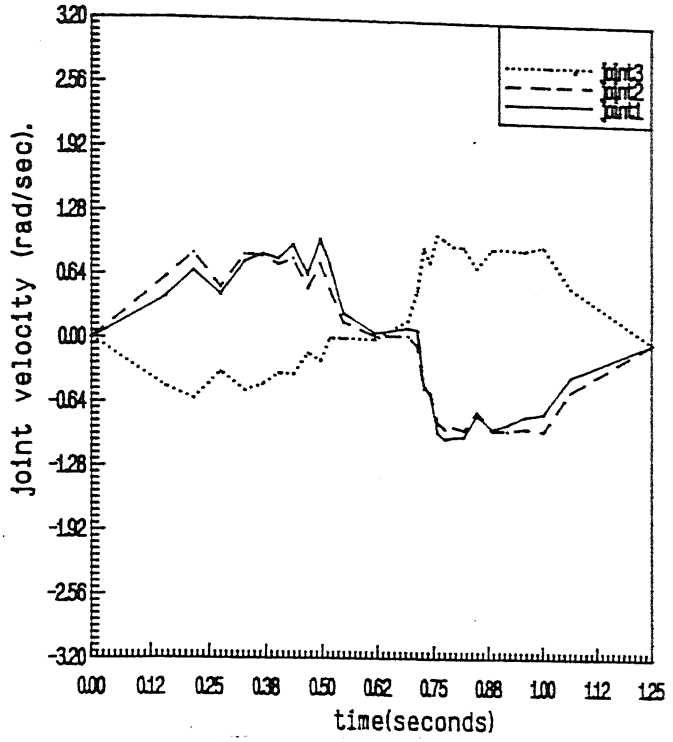

Fig. 4.51 Velocities of joints 1,2 and 3 for arm 2 with minimum time-energy case for problem 3

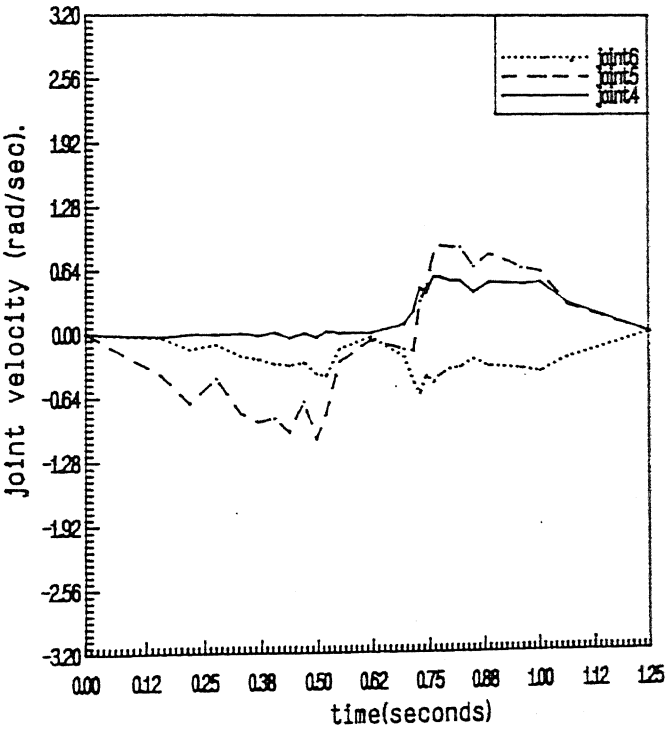

Fig. 4.52 Velocities of joints 4,5 and 6 for arm 2 with minimum time-energy case for problem 3

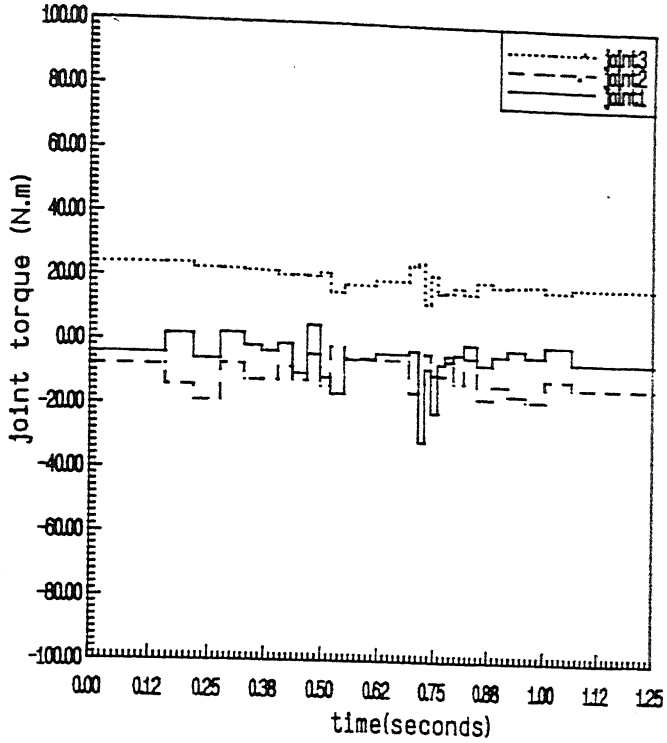

Fig. 4.53 Torques of joints 1,2 and 3 for arm 1 with minimum time-energy case for problem 3

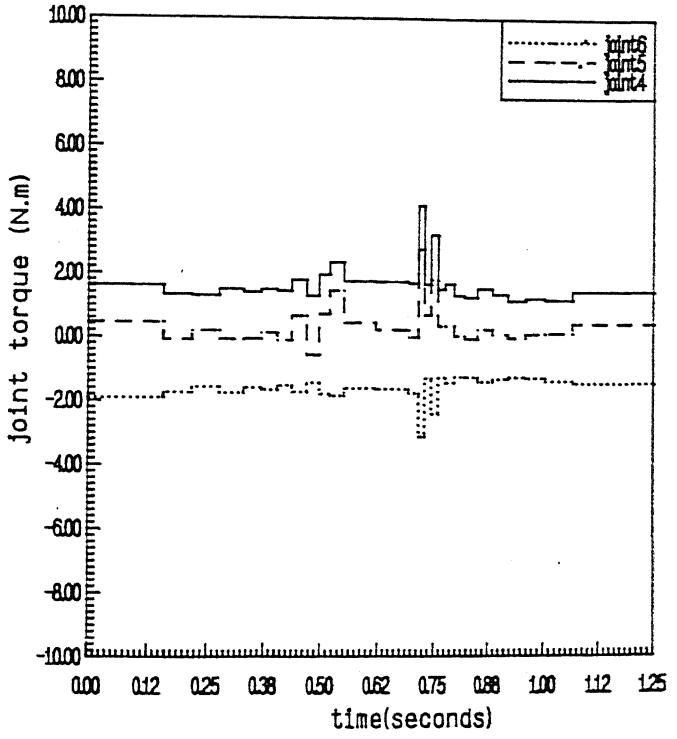

Fig. 4.54 Torques of joints 4,5 and 6 for arm 1 with minimum time-energy case for problem 3

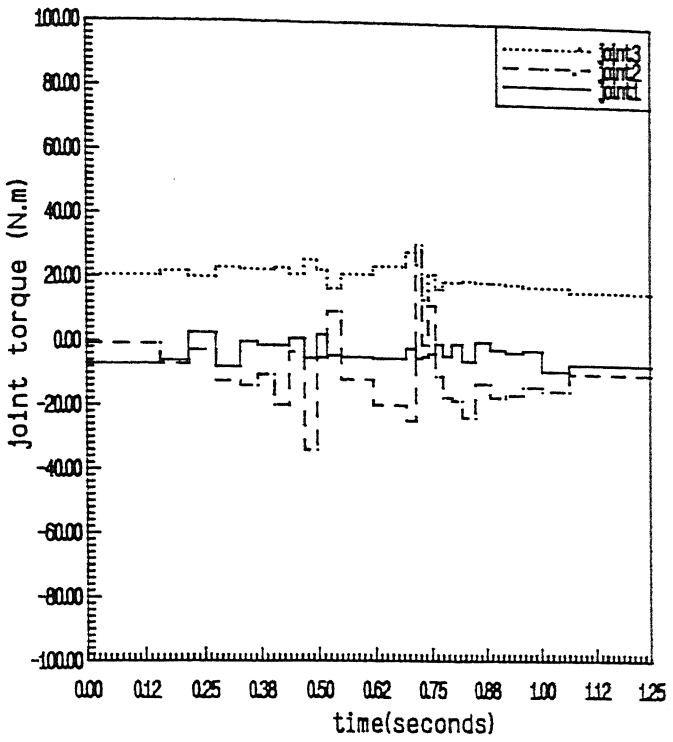

Fig. 4.55 Torques of joints 1,2 and 3 for arm 2 with minimum time-energy case for problem 3

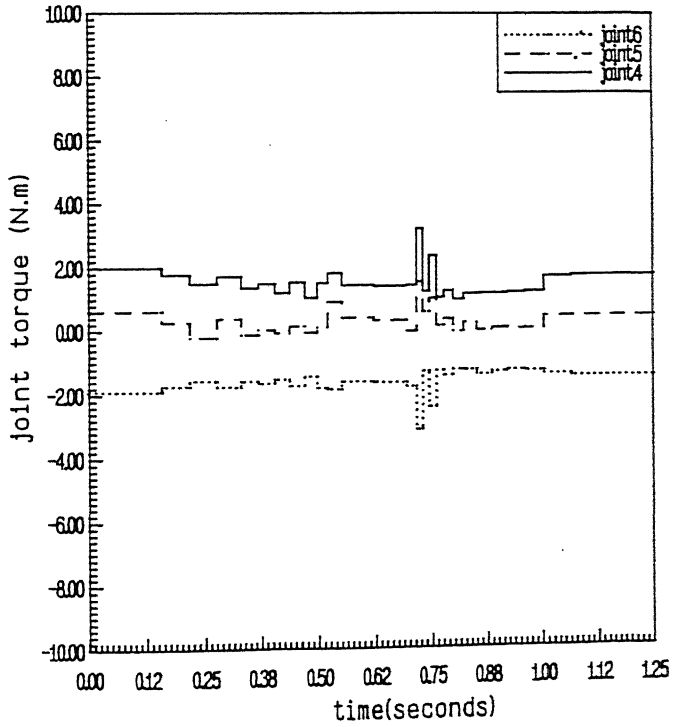

Fig. 4.56 Torques of joints 4,5 and 6 for arm 2 with minimum time-energy case for problem 3

Table 4.11 Optimum values of reciprocal time intervals and time intervals in minimum time energy case for problem 3

k (interval number between kth and (k-1)th knot points)	$H^*(k)$ sec^{-1}	$\Delta t^*(k-1) = 1/H^*(k)$ sec.
1	6.40	0.1562
2	16.76	0.0596
3	17.04	0.0586
4	18.61	0.0537
5	25.91	0.0386
6	27.47	0.0364
7	31.10	0.0321
8	30.71	0.0326
9	36.01	0.0278
10	44.68	0.0224
11	32.30	0.0309
12	14.24	0.0702
13	13.74	0.0728
14	46.79	0.0214
15	72.60	0.0138
16	70.07	0.0138
17	62.98	0.0159
18	60.86	0.0164
19	49.76	0.0201
20	42.18	0.0237
21	32.91	0.0304
22	28.93	0.0346

Table 4.11 (Continued)

23	28.57	0.0350
24	25.46	0.0393
25	22.96	0.0435
26	16.34	0.0612
27	5.26	0.1901

required is 52. The energy required is 11.3 Joules. The total time of travel is 1.25 sec.

CHAPTER 5

CONCLUSIONS AND SCOPE FOR FUTURE WORK

5.1 Conclusions

This thesis has presented two problems related to the coordinated motions of a dual-arm manipulator. The first problem dealt with the inverse kinematic solution when the two arms were involved in a peg-in-hole insertion type assembly operation and there was kinematic redundancy in the system. A specific example with two planar arms, each with three revolute joints, had been discussed. The kinematic redundancy had been utilized to perform the assembly operation with differently varying configurations depending upon the three local optimization schemes used. It was shown that as compared to the minimum velocity norm solution, the minimum acceleration norm solution is a better scheme since the joint velocities were then nearly constant with a marginal increase in the norm of joint velocities. On the other hand, the increased manipulability criterion was shown to offer a good solution when the dual-arm system has to be taken away from the near singular configurations. It was also shown that a gradual increase in manipulability, as the assembly progresses, is a better scheme as it avoided the undue large movements of the joints.

The second problem considered the dynamics of a dual-arm manipulator when the two arms formed a closed chain through a rigidly grasped object. This dual-arm system did not have

kinematic redundancy but had torque redundancy. The trajectory planning problem was considered for this system and a solution scheme as presented which combined the torque redundancy resolution alongwith minimization of time of travel and/or electrical energy over the trajectory. The resulting nonlinear optimization problem was solved by using trapezoidal discretization scheme and then employing successive linear programming technique. Some numerical examples were presented with two PUMA 560 manipulators acting as the dual-arm system. The main points observed from the simulated results are listed below.

The proposed scheme was particularly suitable in solving the minimum time problems. A proper warm start drastically reduced the number of iterations. But a careful selection of initial guess to reciprocal time intervals and the bounds on it was needed to warm start the program. Too small bounds on reciprocal time intervals did not satisfy the linear velocity constraints at the end of trajectory, and too large bounds resulted in violating the nonlinear torque constraints (though the linearized torque constraints in the linear programming part were satisfied). The minimum time objective was achieved by one or more joints reaching their respective torque and/or velocity limit(s). It was noted that spacing between the knot points in the beginning should not be too large otherwise the joint torques are not maximally utilized. Problem 2 of Chapter 4 showed that it is possible for the dual-arm system to execute minimum time motion without any joint reaching its torque limit (some joints obviously did reach their velocity limits).

Minimization of electrical energy over the trajectory was computationally not efficient. In this case the warm start also did not help and the convergence was very slow in the later stages of iterations, probably because this problem is highly nonlinear. The time of travel was not unduly large (as would have been the case if only velocity and acceleration terms were considered) due to presence of gravity induced torques. As the notions were much slower, no joint limits were reached.

Minimum time and energy criterion yielded intermediate results. Inclusion of energy term with a low weightage helped in smoothening the motions, though increasing the computation time.

5.2 Scope for Future Work

This thesis had dealt with two isolated problems: first one with only kinematic redundancy and the second one with only torque redundancy. The next step would be to have a dual-arm system which has both kinematic and torque redundancies. The trajectory planning problem can be further investigated with inclusion of jerk constraints as this would be expected to produce much smoother motion. Another important aspect would be to include the internal forces (i.e. the forces on the object by the end effectors which do not contribute to the motion of the object but only create internal stresses in the object) in the optimization scheme. This could be, attempted by putting the minimization of internal forces in the objective function, or by having the limits on internal forces as inequality constraints.

It was pointed out that successive linear programming technique yielded a very slow convergence for minimum energy problem, which was highly nonlinear. It is suggested that successive quadratic programming technique may be tried to achieve a faster convergence.

REFERENCES

Ahmad, Shaheen .and S. Luo, Shengwu. [1989]. "Coordinated motion control of multiple robotic devices for welding and redundancy coordination through constrained optimization in cartesian space," IEEE Trans. Robotics Automat., vol.5, no.4, pp.409-417.

Armstrong,Bien.,Khatib,Oussama. and Burdick,Joel.[1986]." The explicit dynamic model and inertial parameters od PUMA 560 arm," in Proc. IEEE Int. Conf. Robotics Automat.,(San Francisco, CA),pp.510-518.

Baillieul, J.[1985]. "Kinematic programming alternative for redundant manipulators," in Proc. IEEE Conf. on Robotics Automat.,(St. Louis, MO.) , pp.722-728.

Barraquand, Jerome., Langlois, Bruno. and Latombe, Jeen-Claude. [1992]. "Numerical potential field techniques for robot path planning" IEEE Trans. Syst., Man Cybern., vol.22, no.2, pp.224-241.

Benhabib, B.and Tabarah, E. [1989]. "Optimal joint trajectory planning for coordinated point-to-point motion of two-arm manipulators, "Mech. Mach. Theory, vol. 24, no.1, pp.9-17.

Bien, Zeungnam. and Lee, Jihong. [1992]. "A minimum-time trajectory planning method for two robots," IEEE Trans. Robotics Automat., vol.8, no.3, pp.414-418.

Bobrow, J.E., Dubowsky, S. and Gibson, J.S. [1985]. "Time-optimal control of robotic manipulators along specified paths," Int. J. Robot. Res., vol.4,no.3,pp.3-17.

Brooks, R.A. [1983]. "Solving the find-path problem by good representation of free space," IEEE Trans. Syst., Man. Cybern., vol.SMC-13, no.3, pp.190-197.

Brooks, R.A. [1985]. "Visual map making for mobile robots," in Proc. IEEE Int. Conf. on Robotics Automat.,(St. Louis, MO), pp.824-829.

Carignan, Craig R. and Akin, David L. [1988]. "Cooperative control of two arms in the transport of inertial load in zero gravity," IEEE J. Robotics Automat., vol.4, no.4, pp.414-419.

Carignan C.R. and Akin, D.L. [1989]. "Optimal force distribution for payload positioning using a planar dual-arm robot," Trans. ASME, J. of Dyn. Syst. Measurement Contr, vol.111, no.2, pp.205-210.

Chang, P.H. [1986], "A closed-form solution for the control of manipulators with kinematic redundancy," in Proc. IEEE Int. Conf. Robotics Automat.,(San Francisco,CA), pp.9-14.

Chen, Yaobin., Chien, Stanley Y.P. and Desrochers, Alan A. [1992]. "General structure of time-optimal control of robotic manipulators moving along prescribed paths," Int. J. Control, vol.56, no.4, pp.767-782.

Cheng, F.T.and Orin, D.E.[1989]. "Efficant algorithm for optimal force distribution in multiple-chain robotic systems - the compact-dual LP method," in Proc. IEEE Conf. on Robotics and Automat.,(Scotsdale ,AZ),pp.943-950.

Cheung, E. and Lumelsky, V. [1990]."Motion planning for a whole-sensitive robot arm manipulator," in Proc. IEEE Int. Conf. Robotics Automat.,(Cincinnati,OH), pp.344-349.

Chevallerean, C. and Khalil, W. [1988]. "A new method for the solution of the inverse kinematics of redundant robots," in Proc. IEEE Int. Conf. Robotics Automat., (Philadelphia, PA), pp.37-42.

Chiacchio , Pasquale., Chiaverini ,Stefano., Sciavicco Lorenzo , and Siciliano, Bruno.[1991a]. "Global task space manipulability ellispsoids for multiple-arm system," IEEE Trans. Robotics Automat., vol. 7, no.5, pp. 678-685 .

Chiacchio, P., Chiaverini, S., Sciavicco, L. and Siciliano, B. [1991b]. "Task space dynamic analysis of multiarm system configurations, "Int. J. Robotics Res., vol.10, no.6, pp.708-715.

Chien, Yung-Ping. and Xue, Qing. [1992]. "Path planning for twc planar robots moving in unknown environment," IEEE Trans. Syst. Man, Cybern., vol.SMC-22, no.2, pp.307-317.

Cole, Arlene A., Hsu, Ping. and Sastry, S. Shankar. [1992]. "Dynamic control of sliding by robot hands for regrasping," IEEE Trans. Robotics Automat., vol.8, no.1, pp.42-52.

Djurovic, Milan D. and Vukobratovic Miomir K. [1990]."A contribution to dynamic modeling of cooperative manipulation," Mech. Mach. Theory, vol 25, no.4, pp. 407-415.

Erdmann, M. and Lozano-Perez, T. [1987]. "On multiple moving objects," Algorithmica 2, no.4, pp.477-521.

Faverjon, B. [1984]. "Obstacle avoidance using an octree in the configuration space of a manipulator," in Proc. IEEE Int. Conf. Robotics and Automat, pp.504-512.

Fortune, S., Wilfong, G. and Yap, C. [1986]. "Coordinated motion of two robot arms," in Proc. IEEE Int. Conf. Robotics Automat.,(San Francisco, CA), pp. 1216-1223.

Franklin,G.F. and powell,J.D. [1980].Digital Control of Dynamic Systems. Reading,MA: Addison-Wesley.

Freeman, R.A. [1987], "Dynamic modeling of robotic linkage systems in terms of arbitrary generalized coordinates," in Proc. IEEE Int. Conf.Syst.Man,Cybern.,(Wastington,D.C.), pp.787-797.

Freund, E. and Hoyer, H. [1985]. "On the on-line solution of the findpath problem in multi-robot systems," in Proc. 3rd Int. Symp. Robotics Research, Gouvieux, France (MIT Press, Cambridge, MA), pp.253-262.

Freund, E. and Hoyer, H.[1986]."Pathfinding in multi-robot systems: solution and applications," in Proc.IEEE. Int. Conf. Robotics and Automat.,(San Francisco,CA), pp.103-111.

Freund, E. and Hoyer, H.[1988]."Real-time pathfinding in multirobot systems including obstacle avoidance," Int. J. Robotics. Res.,vol.7,no.1,pp.42-70.

Fu,K.S.,Gonzalez, R.C., Lee, C.S.G. [1987]. Robotics : control sensing, vision and intelligence. NewYork; McGraw-Hill.

Gilbert, E.G. and Johnson, D.W. [1985]. "Distance functions and their applications to robot path planning in the presence of obstacles," IEEE J. Robotics Automat., vol. RA-1, pp.21-30.

Gupta, Sunil. and Luh, J.Y.S. [1991]. "Closed loop control of manipulators with redundant joints using the Hamilton-Jacobi-Bellman equation," in Proc. IEEE Int. Conf. Robotics Automat., (Sacramento, CA), pp. 472-477.

Hayati, S.[1986]. "Hybrid position/force control of multi-arm cooperating robots," in Proc. IEEE Int. Conf. Robotics Automat, (San Francisco,CA),pp.82-89.

Hollerbach, J.M. [1984]."Dynamic scaling of manipulator trajectories," Trans. ASME J. Dynamic Syst. Measurement Contr.,vol.106,pp.102-106.

Hu, Yan-Ru. and Goldenberg, A.A. [1989]. "An adaptive approach to motion and force control of multiple coordinated robot arms," in Proc. IEEE Int. Conf. Robotics Automat., (Scottsdale, AZ), pp.1091-1096.

Huang, Han-Pang.[1992]. "Mathematical formulation of constrained robot systems: A unified approach," Mech. Mach. Theory, vol. 27, no.6, pp.687-700.

Hwang, Yong K. and Ahuja, Narendra.[1992]. "A potential field approach to path planning," IEEE Trans. Robotics Automat., vol.8, no.1, pp.23-32.

Jain, M. K.[1979]."Spline function approximation in discrete mechanics ,"Int. J. Nonlinear Mechanics , vol.14, no.5/6, pp.341-345.

Ishida, Tatsuzo.[1977]. "Force control in coordination of two arms," in Proc. 5th Int. Joint Conf. Artificial Intell., pp. 717-722.

Johansson, Rolf.[1990]."Quadratic optimization of motion coordination and control," IEEE Trans. Automat. Control, vol.35, no.11, pp.1197-1208.

Jouaneh, Musa K., Wang, Zhixiao. and Dornfeld,David A.[1990a], "Trajectory planning for coordinated motion of a robot and a positioning table: Part 1 - Path specification," IEEE Trans. Robotics Automat., vol.6, no.6, pp. 735-745.

Jouaneh, Musa K., Dornfeld, David A. and Tomizuka, Masayoshi. [1990b], "Trajectory planning for coordinated motion of a robot and a positioning table: Part 2-optimal trajectory specification," IEEE Trans. Robotics Automat., vol.6, no.6, pp. 746-759.

Kafrissen,Edward. and Stephans,Mark.[1984].Industrial Robots and Robotics.Reston,Virginia;Reston Publishing Company,Inc.

Kahn, M. and Roth, B.[1971]."The near-minimum time control of open loop articulated kinematic chains," Trans.ASME J. Dynamic Syst. Measurement Contr., vol.93, no.3,pp. 164-172.

Kajita, Shuuji., Yamayura, Tomio.and Kobayashi, Akira.[1992]. "Dynamic walking control of a biped robot along a potential energy conserving orbit," IEEE Trans. Robotics Automat., Vol.8, no.4.

Kazerounian, Kazem. and Wang, Zhaoyu. [1988]." Global versus local optimization in redundancy resolution of robotic manipulators," Int. J. Robotics Res.,vol.7, no.5,pp.3-12.

Kazerooni, H. [1988]." Compliance control and stability of cooperating robot manipulators," Robotica, vol.7, pp.191-198.

Khatib, O. [1986]. "Real-time obstacle avoidance for manipulators and mobile robots," The Int. J. Robotics Res., vol.5, no.1, pp.90-98.

Kim, Jin-Oh. and Khosla, Pradeep K. [1992]. "Real-time obstacle avoidance using harmonic potential functions," IEEE Trans. Robotics Automat., vol. 8, no.3, pp. 338-349.

Kim, Byung Kook. and Shin, Kang G. [1985]."Minimum-time path planning for robot arms and their dynamics," IEEE Trans. Syst. Man Cybern., vol.SMC-15, no.2, pp.213-223.

Koga,Masanobu., Kosuge, Kazuhiro., Furuta, Katsuhisa. and Nosaki, Kageharu.[1992]." Coordinated motion control of robot arms based on the virtual internal model," IEEE Trans. Robotics Automat., vol.8, no.1, pp.77-85.

Koivo,A.J. and Arnautovic, S.H. [1991]."Dynamic optimum control of redundant manipulators," in Proc. IEEE Conf. Robotics Automat., (Sacramento, CA), pp.466-471.

Koivo, A.J. and Unseren, M.A. [1990]. "Modeling closed chain motion of two manipulators holding a rigid object," Mech. Mach. Theory, vol.25, no.4, pp.427-438.

Laroussi, Kader., Hemami, Hooshang. and Goddard, Ralph E. [1988]. "Coordination of two planar robots in lifting," IEEE J. Robotics Automat., vol.4, no.1, pp.77-85.

Lee, B.H. [1986]. "Wrist collision avoidance of two robots: A collision map and time scheduling approach," in Proc. 25th Conf. Decision Contr., (Athens, Greece), pp.429-434.

Lee B.H. and Lee C.S.G. [1987], "Collision-free motion planning of two robots," IEEE Trans.Syst.,Man Cybern., SMC 17 ,no. 1, pp. 307-317.

Lee, Sukhan. [1989]. "Dual redundant arm configuration optimization with task-oriented dual arm manipulability," IEEE Trans. Robotics Automat., vol. 5, no.1, pp.78-97.

Li, Zuofeng., Tarn, Tzyh-Jong. and Bejczy, Antal K. [1991]. "Dynamic workspace analysis of multiple cooperating robot arms," IEEE Trans. Robotics Automat., vol. 7, no.5, pp.589-596.

Lim, Joonhong. and Chyung, Dong H. [1988]. "Admissible trajectory determination for two cooperating robot arms," Robotica, vol.6, pp.107-113.

Lozano-Perez, T. and Wesley, M.A.[1979]."An algorithm for planning collision-free paths among polyhedral obstacles," Communications of the ACM, vol. 22, no.10, pp.560-570.

Lozano-Perez, T. [1981]."Automatic planning of manipulator transfer movements," IEEE Trans. System., Man. Cybern., vol. SMC-11, no.10, pp.681-698.

Lozano-Perez, T. [1983]."Spatial planning: A configuration space approach" IEEE Trans. Computers, vol. C-32, no.2, pp. 108-120.

Luh J.Y.S. and Lin, C.S. [1981]. "Optimum path planning for mechanical manipulators, "Trans. ASME J. Dynamic Syst. Meas., Contr., vol. 102, no.2, pp.142-151.

Luh, J.Y.S. and Walker, M.W. [1977]. "Minimum-time along the path for a mechanical arm," in Proc. 16th Conf. Decision Contr., pp.755-759.

Luh, J.Y.S. and Zheng, Y.F. [1987]."Constrained relations between two coordinated industrial robots for motion control," Int. J. Robotics Res., vol.6, no.3, pp.60-70.

Montana, David J. [1992]."Contact stability for two-fingered grasps," IEEE Trans. Robotics Automat., Vol.8, no.4, pp. 421-430.

Moon, Seungbin B.and Ahmad, Shaheen.[1991], "Time scaling of cooperative multirobot trajectories," IEEE Trans. Syst.Man, Cybern., vol. 21, no.4,pp.900-908.

Nagy, Peter Victor .[1988]. "The PUMA 560 Industrial Robot: Inside-Out," Robot 12 and Vision' 88 Conference, vol.1, Detroit, Michigan, June 5-9,pp.4.67-4.79.

Nahon, M. and Angeles, J. [1992a]. "Minimization of power losses in cooperating manipulators," Trans. ASME, J. Dynamic Syst. Measurement Contr., vol. 114, pp.213-219.

Nahon, Meyer A. and Angeles, Jorge.[1992b]."Real-time optimization in parallel kinematic chains under inequality constraints," IEEE Trans. Robotics Automat., vol.8, no.4, pp.439-450.

Nakamura, Y.[1988]."Minimizing object strain energy for coordination of multiple robotic manipulators," in Proc. American Control Conf.,(Atlanta), pp. 499-504.

Nakamura, Y., Nagai, K. and Yoshikawa, T. [1987], "Mechanics of coordinative manupulation by multiple robotic mechanisms," in Proc. IEEE Int. conf. Robotics Automat. (Raleigh, NC),pp.991-998.

Neuman, C.P. [1985]."Discrete dynamic robot models," IEEE Trans. Syst.Man ,Cybern.,vol. SMC-15, no.2,pp.193-204.

O'Donnell, Patrick A. and Lozano-Perez, Tomas.[1989]. "Deadlock-free and collision-free coordination of two robot manipulations," in Proc. IEEE Int. Conf. Robotics Automat., (Scottsdale, AZ), pp.484-489.

Orin, D.E. and Oh, S.Y.[1981]."Control of force distribution in robotic mechanisms containing closed kinematic chains," Trans. ASME, J. Dynamic Sys.,Meas. Contr.,vol.102, pp. 134-141.

Palm,W.J.[1983].Modeling,Analysis and Control of Dynamic Systems. New York: Wiley.

Paul,R.P. [1981].Robot manipulators-Mathematics, Programming and Control, Cambridge, MA :MIT press.

Pennock, G.R. and Ryuh, B.S. [1987]. Advances in Design Automation, Boston, Mass., vol. DE-2, p.63.

Pfeiffer,F. and Johanni, R.[1987]. "A concept for manipulator trajectory planning, "IEEE J. Robotics Automat., vol. RA-3, no.2, pp. 115-123.

Rice, J.R. [1983].Numerical methods, Software and Analysis. New York: Mcgraw-Hill.

Schneider, Stanley A. and Cannon, Jr. Robert H. [1992]." Object impedance control for cooperative manipulation: Theory and experimental results," IEEE Trans. Robotics Automat., vol.8, no.3, pp.383-394.

Schwartz, J.T. and Sharir, M. [1983a]."On the paiano mover's problem-1: The special case of a rigid polygonal body moving amidst polygonal barriers," J. Commun. Pure Appl. Mathematics, vol.36, pp.345-398.

Schwartz, J.T. and Sharir, M.[1983b]."On the piano movers' problem-II: General techniques for computing topological properties of real algebraic manifolds," Advances in Applied Mathematics, vol.4, pp.298-351.

Schwartz, J.T. and Sharir, M. [1983c] "On the piano movers' problem-III: Coordinating the motion of several independent bodies- The special case of circular bodies moving amidst polygonal barriers," The Int. J. Robotics Res., vol.2, no.3, pp.46-75.

Seraji, H. [1988]."Coordinated adaptive position/force control of dual-arm robots," Int. J. Robotics Automat., vol.3, no.3, pp.140-149.

Shih, Ching-Long. and Gruver, Willian A. [1992]. "Control of a biped robot in the double-support phase," IEEE Trnas Syst., Man, Cybern.,vol.22, no.4, pp.729-735.

Shin, K.G. and Mckay, N.D. [1986]."A dynamic programming approach to trajectory planning of robotic manipulators,"IEEE Trans. Automat Contr., vol. AC-31, no.6, pp. 491-500.

Shin, Y. and Bein, Z. [1989]." Collision-free trajectory planning for two robot arms," Robotica , vol. 7,pp.205-212.

Shin, Kang G. and Zheng,Qin.[1992]."Minimum-time collision- free trajectory planning for dual-robot systems," IEEE Trans. Robotics Automat., vol.8, no.5, pp.641-644.

Singh, S. and Leu, M.C. [1987]."Optimal trajectory generation for robotic manipulators using dynamic programming," Trans. ASME J. Dynamic Syst.Measurement Contr., vol.109, no.2, pp. 88-96.

Suh, I.H. and Shin, K.G. [1989]."Coordination of dual robot arms using kinematic redundancy," IEEE Trans. Robotics Automat.,vol.5,no.2,pp.236-242.

Tan, H. H. and Potts, R.B.[1988]."Minimum time trajectory planer for the discrete dynamic robot model with dynamic constraints, "IEEE J. Robotics Automat., vol. 4, no.2, pp. 174-185.

Tan, H. H. and Potts, R.B. [1989]."A discrete trajectory planner for robotic arms with six degrees of freedom," IEEE Trans. Robotics Automat., vol.5, no.5, pp.681-690.

Tao, Jian M., Luh,J.Y.S. and Zheng, Yuan F. [1990]."Compliant coordination control of two moving industrial robots," IEEE Trans. Robotics Automat., vol.6, no.3, pp.322-330.

Tao, Jian M. and Luh, J.Y.S.[1991]."Position and force controls for two coordinating robots," in Proc. IEEE Int. Conf. Robotics and Automat.,(Sacramento, CA), pp.176-181.

Tarn,T.J.,Bejczy,A.K. and Yun, X.[1987]."Design of dynamic control of two cooperating robot arms:Closed chain formulation, "in Proc. IEEE Int. Conf. Robotics and Automat., (Raleigh, NC),pp.7-13.

Tarn,T.J. and Bejczy,A.K.[1988]."Software Elements," in International Encyclopedia of Robotics : Applications and Automation Eds. Richard C. Dorf and Shimon Y.Nof, John Wiley and Sons ,vol.3 ,pp.1608-1626.

Tourassis, V.D. and Neuman, C.P. [1985]. "The inertial characteristics of dynamic robot models,"Mech. Mach. Theory , vol. 20,no.1,pp.41-52.

Tournassoud, P. [1986]."A strategy for obstacle avoidance and its application to multi-robot systems," in Proc. IEEE Int. Conf. Robotics Automat., (San Francisco, CA), pp.1224-1229.

Udapa, S. [1977]. "Collision detection and avoidance in computer controlled manipulators," In Fifth International Joint Conference on Artificial Intelligence, Cambridge.

Uchiyama, Masaru and Dauchez, Pierre. [1988]."A symmetric hybrid position/force control scheme for the coordination of two robots," in Proc. IEEE Int. Conf. Robotics Automat., (Philadelphia, PA), pp.350-356.

Uchiyama, Masaru. and Yamashita, Toshiaki. [1991]. "Adaptive load sharing for hybrid controlled two cooperative manipulators," in Proc. IEEE Int. Conf. Robotics Automat.,(Sacramento, CA), pp. 986-991.

Unseren, M.A. and Koivo, A.J. [1989]."Reduced order model and decoupled control architecture for two manipulators holding an object," in Proc. IEEE Int. Conf. Robotics Automat., (Scottsdale, AZ), pp.1240-1245.

Unseren, M.A. [1991]."Rigid body dynamics and decoupled control architecture for two interacting manipulators," Robotica, vol.9, pp.421-430.

Volpe, Richard. and Khosla, Pradeep. [1990]. "Manipulator control with superquadric artificial potential functions: Theory and experiments," IEEE Trans. Syst. Man Cybern, vol.20, no.6, pp.1423-1436.

Vukobratovic, M. and and Kircanski, M. [1982]."A method for the optimal synthesis of manipulation robot trajectories," Trans ASME J. Dyn.Syst.Measurement Contr.,vol.104, pp.188-193.

Wenger, Philippe. and Chedmail, Patrick. [1991]."Ability of a robot to travel through its free work space in an environment with obstacles," The Int. J. Robotics Res., vol.10, no.3, pp.214- 227.

Walker,Ian D.,Freeman,Robert A. and Marcus, Steven I. [1991]."Analysis of motion and internal loading of objects grasped by multiple cooperating manipulators," Int. J. Robotics Res., vol. 10, no.4, pp.396-409.

Walker, Michael W., Kim, Dongmin. and Dionise, Joseph. [1989]. "Adaptive coordinated motion control of two manipulator arms," inProc. IEEE Int. Conf. Robotics Automat. (Scottsdale, AZ) pp. 1084-1090.

Whitney, D.E. [1972]. "The mathematics of coordinated control of prosthetic arms and manipulators ," Trans. ASME J. Dyn. Syst. Measurement. Contr., pp.303-309.

Yoshikawa, T., [1984]."Analysis and control of robot manipulators with redundancy," in Proc. 1st Int. Symp. of Robotics Research. Cambridge, MA: MIT press, pp.735-748.

Yun, Xiaoping. [1989]."Nonlinear feedback control of two manipulators in presence of enviromental constraints," in Proc. IEEE Int. Conf. Robotics Automat. (Scottsdale, AZ), pp.1252-1257.

Yun, Xiaoping.and Kumar, Vijay R. [1991]."An approach to simulataneous control of trajectory and interaction forces in dual-arm configurations," IEEE Trans. Robotics Automat., vol.7, no.3, pp.618-625.

Zheng Y.F. and Luh, J.Y.S. [1988]. "Optimal load distribution for two industrial robots handling a single object," in Proc. IEEE,Int. Conf. Robotics Automat.,(Philadelphia, PA), pp.344-349.

Zheng Y.F. and Luh, J.Y.S. [1989]. "Optimal load distribution for two industrial robots handling a single object," Trans. ASME J. Dynamic Syst. Measurement Contr.,vol.111,pp.232-237.

APPENDIX A

EULER ANGLES AND THE TRANSFORMATIONS

A set of three generalized coordinates can completely describe the orientation of a rotating rigid body with respect to a cartesian reference frame. One common choice is that of Euler angles denoted by ϕ_1, ϕ_2 and ϕ_3 (shown in Fig. A.1). The representation used here corresponds to the following sequence of rotations.

Initially let the object frame and the reference frames coincide [Fu et al., 1987].

1. A rotation of ϕ_1 angle about the Z axis of the reference frame.
2. A rotation of ϕ_2 angle about the current X axis of the object frame.
3. A rotation of ϕ_3 angle about the current Z axis of the object frame.

The resultant eulerian rotation matrix is given by

$$\mathbf{R} = \begin{bmatrix} \cos\phi_1 & -\sin\phi_1 & 0 \\ \sin\phi_1 & \cos\phi_1 & 0 \\ 0 & 0 & 1 \end{bmatrix} \begin{bmatrix} 1 & 0 & 0 \\ 0 & \cos\phi_2 & -\sin\phi_2 \\ 0 & \sin\phi_2 & \cos\phi_2 \end{bmatrix}$$

$$\begin{bmatrix} \cos\phi_3 & -\sin\phi_3 & 0 \\ \sin\phi_3 & \cos\phi_3 & 0 \\ 0 & 0 & 1 \end{bmatrix}$$

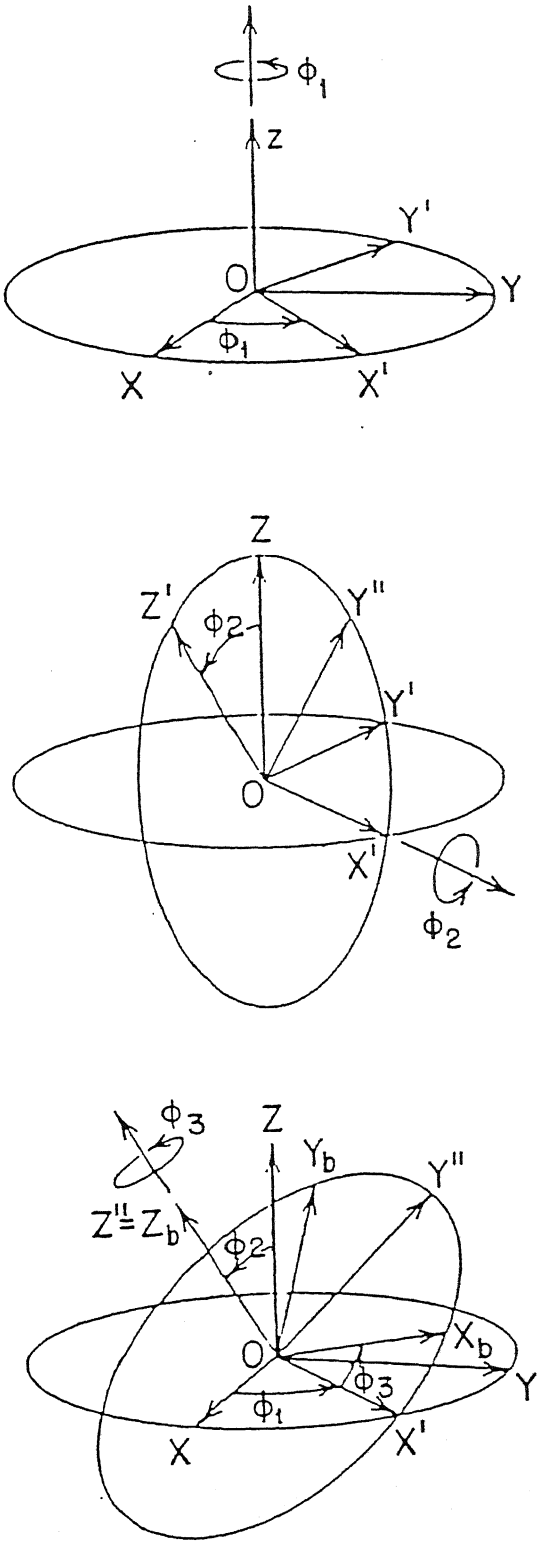

Fig. A.1 Three consecutive rotations used to define Euler angles

$$= \begin{bmatrix} \cos\phi_1\cos\phi_3 & -\cos\phi_1\sin\phi_3 & \sin\phi_1\sin\phi_2 \\ -\sin\phi_1\cos\phi_2\sin\phi_3 & -\sin\phi_1\cos\phi_2\cos\phi_3 & \\ \sin\phi_1\cos\phi_3 & -\sin\phi_1\sin\phi_3 & -\cos\phi_1\sin\phi_2 \\ +\cos\phi_1\cos\phi_2\sin\phi_3 & +\cos\phi_1\cos\phi_2\cos\phi_3 & \\ \sin\phi_2\sin\phi_3 & \sin\phi_2\cos\phi_3 & \cos\phi_2 \end{bmatrix} . \tag{A.1}$$

The inverse solution implies that a rotation matrix is given and the corresponding Euler angles are to be determined. If the rotation matrix is given in terms of direction cosines as

$$\mathbf{R} = \begin{bmatrix} n_x & s_x & a_x \\ n_y & s_y & a_y \\ n_z & s_z & a_z \end{bmatrix} \tag{A.2}$$

then the Euler angles are determined by the following relations.

$$\phi_1 = \tan^{-1}\left[\frac{a_x}{-a_y}\right]$$

$$\phi_3 = \tan^{-1}\left[\frac{-\cos\phi_1\, s_x - \sin\phi_1\, s_y}{\cos\phi_1\, n_x + \sin\phi_1\, n_y}\right]$$

$$\phi_2 = \tan^{-1}\left[\frac{\sin\phi_1 a_x - \cos\phi_1 a_y}{a_z}\right] \tag{A.3}$$

The angular velocity of an object can be expressed in terms of its components along the axes of cartesian reference frame, i.e. as $\Omega = \omega_x \mathbf{i} + \omega_y \mathbf{j} + \omega_z \mathbf{k}$. Alternately, the angular velocity could be written in terms of time rate of change of Euler angles, i.e. in terms of $\dot{\phi}_1$, $\dot{\phi}_2$ and $\dot{\phi}_3$. The relation between ω_x, ω_y, ω_z and $\dot{\phi}_1$, $\dot{\phi}_2$, $\dot{\phi}_3$ is established in the following way. The rotation matrix $\mathbf{R}$ is an orthogonal matrix i.e.

$$\mathbf{R}\,\mathbf{R}^T = \mathbf{I} \qquad (A.4)$$

where $\mathbf{I}$ is a 3x3 identity matrix.

Differentiation of (A.4) yields

$$\frac{d}{dt}(\mathbf{R})\,\mathbf{R}^T + \mathbf{R}\,\frac{d}{dt}(\mathbf{R}^T) = 0$$

or,
$$\mathbf{R}\,\frac{d}{dt}(\mathbf{R}^T) = -\left(\frac{d\mathbf{R}}{dt}\right)\mathbf{R}^T \qquad (A.5)$$

As $\mathbf{R}$ is rotation matrix its columns are orthogonal to each other and each is an unit vector. Hence as $\mathbf{R}$ changes with time its column vectors change orientation with rotation of the object. When the object frame rotates with angular velocity $\Omega = \left[\omega_x, \omega_y, \omega_z\right]^T$ each column vector of $\mathbf{R}$ also rotates with that velocity. The time rate of change of $\mathbf{R}$ can be expressed as

$$\frac{d\mathbf{R}}{dt} = \begin{bmatrix} \frac{d\mathbf{n}}{dt} & \frac{d\mathbf{s}}{dt} & \frac{d\mathbf{a}}{dt} \end{bmatrix}$$
$$= [\,\Omega \times \mathbf{n} \quad \Omega \times \mathbf{s} \quad \Omega \times \mathbf{a}\,] \qquad (A.6)$$

The cross product of Ω can be replaced by a skew symmetric matrix

as

$$S_\Omega = \begin{bmatrix} 0 & -\omega_z & \omega_y \\ \omega_z & 0 & -\omega_x \\ -\omega_y & \omega_x & 0 \end{bmatrix} \qquad (A.7)$$

Using (A.7) in (A.6)

$$\frac{dR}{dt} = S_\Omega [n\ s\ a] = S_\Omega R \qquad (A.8)$$

Now using (A.8) in (A.5)

$$R \frac{d}{dt}(R^T) = - S_\Omega R R^T \qquad (A.9)$$

Using (A.4) in (A.9)

$$R \frac{d}{dt}(R^T) = - S_\Omega \qquad (A.10)$$

Using (A.1) and (A.7) in (A.10) the time rate of change of Euler angles vector $\dot{\Phi} = \left[\dot{\phi}_1, \dot{\phi}_2, \dot{\phi}_3\right]^T$ and the angular velocity vector $\Omega = \left[\dot{\omega}_x, \dot{\omega}_y, \dot{\omega}_z\right]^T$ is determined as follows

$$\Omega = \begin{bmatrix} 0 & \cos\phi_1 & \sin\phi_1 \sin\phi_2 \\ 0 & \sin\phi_1 & -\cos\phi_1 \sin\phi_2 \\ 1 & 0 & \cos\phi_2 \end{bmatrix} \dot{\Phi} \quad . \qquad (A.11)$$

APPENDIX B

MANIPULATOR JACOBIAN

The end effector motion of an n degrees-of-freedom manipulator is described by two vectors, a translational velocity vector $\mathbf{v}$ and an angular velocity vector Ω, where $\mathbf{v}$ is the translational velocity of the origin of the hand coordinate frame, while Ω is the angular velocity of the hand frame. A six element vector $\dot{\mathbf{s}}$ representing these task space velocity vectors can be written as [Whitney, 1972]

$$\dot{\mathbf{s}} = \begin{bmatrix} \mathbf{v} \\ \Omega \end{bmatrix}. \qquad (B.1)$$

The joint angle vector is denoted by $\mathbf{q}$ and joint velocity vector by $\dot{\mathbf{q}}$, where each of these vectors is n dimensional vector. The transformation matrix of jth coordinate frame (attached to jth link) with respect to world coordinate is obtained from (2.3-2) and (2.3-3) and can be written in the following from :

$$^{w}\mathbf{T}_{j} = \begin{bmatrix} ^{w}\mathbf{R}_{j} & ^{w}\mathbf{p}_{j} \\ 0 & 1 \end{bmatrix} = \begin{bmatrix} ^{w}\mathbf{n}_{j} & ^{w}\mathbf{s}_{j} & ^{w}\mathbf{a}_{j} & ^{w}\mathbf{p}_{j} \\ 0 & 0 & 0 & 1 \end{bmatrix}. \qquad (B.2)$$

Let $\mathbf{v}_j$ and Ω_j respectively denote the end effector translational and rotational velocity vectors due to the jth rotational joint velocity $\dot{q}_j$ alone (i.e., all other joints, except the jth joint , are locked). The direction of $\dot{q}_j$ is along the Z-axis of (j-1) th

coordinate frame, i.e. along the unit vector a_{j-1}. Therefore the angular velocity of the end effector frame due to jth rotational joint alone is written as

$$\Omega_j = \dot{q}_j \, {}^{w}a_{j-1} \qquad (B.3)$$

The position vector of the end effector from the origin of (j-1) th frame is $\left({}^{w}p_n - {}^{w}p_{j-1}\right)$ and so the translational velocity of the end effector due to jth rotational joint alone is

$$v_j = q_j \, {}^{w}a_{j-1} \times \left({}^{w}p_n - {}^{w}p_{j-1}\right) \qquad (B.4)$$

The net end effector velocity vector is obtained by summing (B.3) and (B.4) over all the joints to get

$$v = \sum_{j=1}^{n} v_j$$

$$\Omega = \sum_{j=1}^{n} \Omega_j \, . \qquad (B.5)$$

(B.3) to (B.5) are now combined and written in matrix notations as

$$\dot{s} = J \, \dot{q} \qquad (B.6)$$

where J is a 6xn matrix, called Jacobian matrix, whose jth element is given by

$$J_j = \begin{bmatrix} {}^{w}a_{j-1} \times \left({}^{w}p_n - {}^{w}p_{j-1} \right) \\ {}^{w}a_{j-1} \end{bmatrix} \quad \text{for } j = 1, \ldots, n.$$

(B.7)

APPENDIX C

KINEMATIC RELATIONS FOR PLANAR DUAL-ARM MANIPULATOR

This appendix lists the kinematic matrices used for the planar dual-arm manipulator (each arm with three links and three rotary joints) which was used as an example in Chapter 2. For the sake of continuity, Fig. 2.3 is reproduced here as Fig. C.1 which shows all the link frames X_{li}, Y_{li} (l denotes the arm number, i.e. l= 1,2 and i denotes the link number, i.e. i = 0,1,2,3). The world frame X_w, Y_w is taken to be coincident with the base frame of first arm X_{10}, Y_{10}. The separation between the bases of two arms is denoted by b_s. Therefore the transformation matrices of the two base frames ($^{w}T_{10}$ in (2.3-23)) are

$$ {}^{w}T_{10} = \begin{bmatrix} 1 & 0 & 0 & 0 \\ 0 & 1 & 0 & 0 \\ 0 & 0 & 1 & 0 \\ 0 & 0 & 0 & 1 \end{bmatrix} \quad \text{and} \quad {}^{w}T_{20} = \begin{bmatrix} 1 & 0 & 0 & b_s \\ 0 & 1 & 0 & 0 \\ 0 & 0 & 1 & 0 \\ 0 & 0 & 0 & 1 \end{bmatrix} \qquad (C.1) $$

In Fig. C.1, the link lengths are denoted by a_{li} and the joint angles by q_{li} (l=1,2; i = 1,2,3). For jth link of lth arm, the A matrix of (2.3-1) becomes

$$ {}^{j-1}A_{lj} = \begin{bmatrix} \cos\psi & -\sin\psi & 0 & e \\ \sin\psi & \cos\psi & 0 & f \\ 0 & 0 & 1 & 0 \\ 0 & 0 & 0 & 1 \end{bmatrix} \qquad (C.2) $$

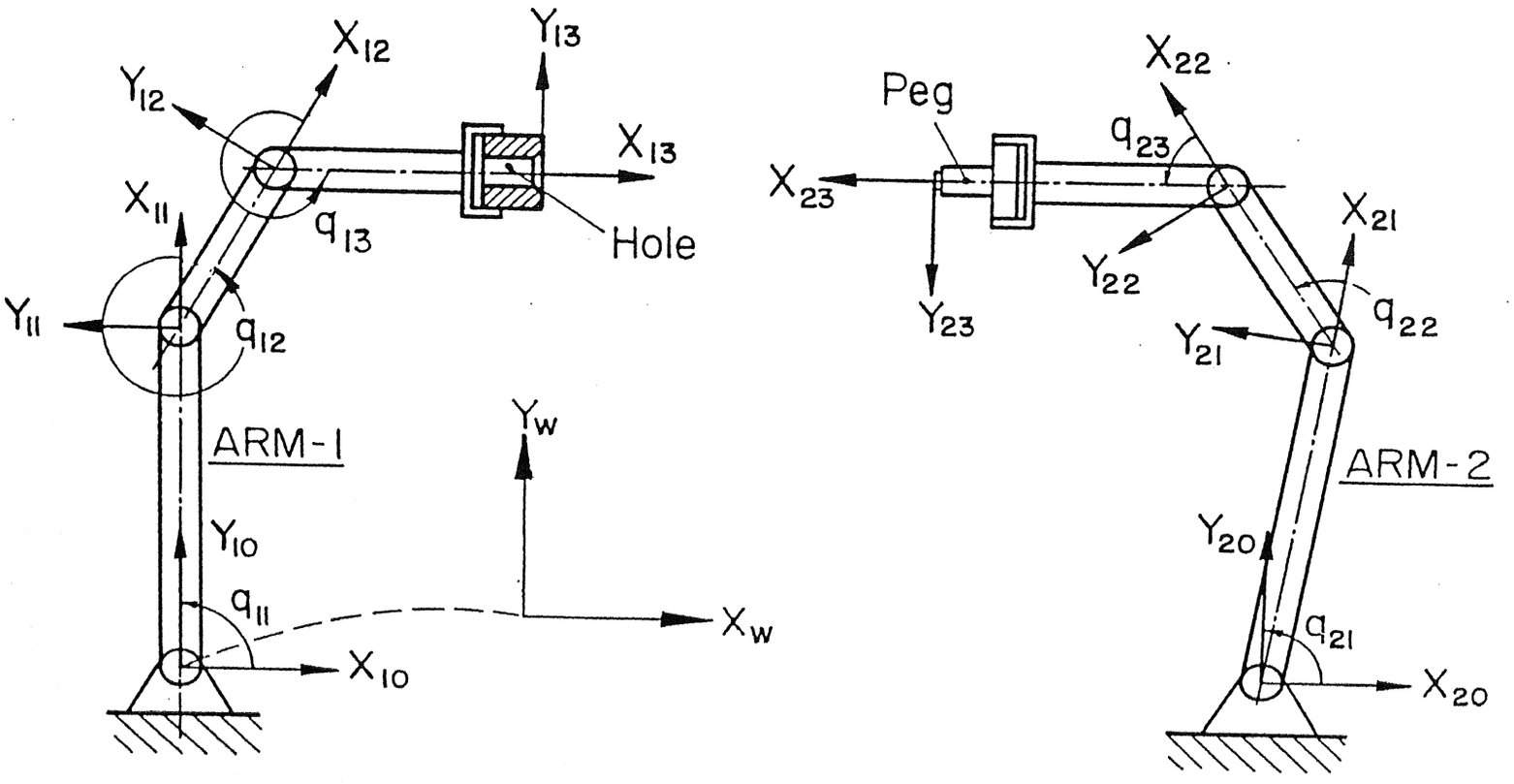

Fig. C.1 Planar dual-arm manipulator for assembly

where,

$$\psi = \sum_{i=1}^{j} q_{1i}$$

$$e = \sum_{i=1}^{j} a_{1i} \cos\left[\sum_{k=1}^{i} q_{1k}\right]$$

$$f = \sum_{i=1}^{j} a_{1i} \sin\left[\sum_{k=1}^{i} q_{1k}\right]$$

The end effector frame of arm 1, i.e. X_{13}, Y_{13}, is described in the world frame by the transformation ${}^{w}T_{13}$ which is partitioned in (2.3-7) into rotation matrix ${}^{w}R_{13}$ and the position vector ${}^{w}P_{13}$. With the help of (C.2), (2.3-2), (C.1) and (2.3-3) the description of X_{13}, Y_{13} in the world frame is

$${}^{w}R_{13} = \begin{bmatrix} \cos(q_{11}+q_{12}+q_{13}) & -\sin(q_{11}+q_{12}+q_{13}) & 0 \\ \sin(q_{11}+q_{12}+q_{13}) & \cos(q_{11}+q_{12}+q_{13}) & 0 \\ 0 & 0 & 1 \end{bmatrix} \qquad (C.3)$$

$${}^{w}P_{13} = \begin{bmatrix} a_{11}\cos q_{11} + a_{12}\cos(q_{11}+q_{12}) + a_{13}\cos(q_{11}+q_{12}+q_{13}) \\ a_{11}\sin q_{11} + a_{12}\sin(q_{11}+q_{12}) + a_{13}\sin(q_{11}+q_{12}+q_{13}) \\ 0 \end{bmatrix} \qquad (C.4)$$

Likewise, for arm 2 the end effector frame X_{23}, Y_{23} is represented in the world frame by

$$
{}^{w}R_{23} = \begin{bmatrix} \cos(q_{21}+q_{22}+q_{23}) & -\sin(q_{21}+q_{22}+q_{23}) & 0 \\ \sin(q_{21}+q_{22}+q_{23}) & \cos(q_{21}+q_{22}+q_{23}) & 0 \\ 0 & 0 & 1 \end{bmatrix} \qquad (C.5)
$$

$$
{}^{w}P_{23} = \begin{bmatrix} a_{21}\cos q_{21} + a_{22}\cos(q_{21}+q_{22}) + a_{23}\cos(q_{21}+q_{22}+q_{23}) + b_s \\ a_{21}\sin q_{21} + a_{22}\sin(q_{21}+q_{22}) + a_{23}\sin(q_{21}+q_{22}+q_{23}) \\ 0 \end{bmatrix}
$$

(C.6)

The solution (2.5-25) requires the evaluation of J_r matrix, which in turn requires J_{er} and J_{rel} as mentioned by (2.4-26). The expression for J_{er} is given in (2.4-27). Evaluation of J_{rel} from (2.4-22) to (2.4-24) also requires J_1 and J_2 besides (C.3) to (C.6). These Jacobian matrices for the two arms of Fig. C.1 can be obtained as

$$
J_l = \begin{bmatrix} -\sum_{i=1}^{3} a_{li}\sin\left(\sum_{k=1}^{i} q_{lk}\right) & -\sum_{i=2}^{3} a_{li}\sin\left(\sum_{k=1}^{i} q_{lk}\right) & -a_{l3}\sin\left(\sum_{k=1}^{3} q_{lk}\right) \\ \sum_{i=1}^{3} a_{li}\cos\left(\sum_{k=1}^{i} q_{lk}\right) & \sum_{i=2}^{3} a_{li}\cos\left(\sum_{k=1}^{i} q_{lk}\right) & a_{23}\cos\left(\sum_{k=1}^{3} q_{lk}\right) \\ 1 & 1 & 1 \end{bmatrix}
$$

$$
; \; l = 1,2 \qquad (C.7)
$$

APPENDIX D

INERTIAL COEFFICIENTS

The objective of this appendix is to derive the inertial coefficients needed in Sec. 3.9.3. These derivations follow the work of Tourassis and Neuman [1985]. A manipulator with N articulated joints is considered. The generalized coordinates of N degrees of freedom mechanism are q_1, q_2 ...q_N. The generalized coordinate q_i is defined as the rotational angle around Z_{i-1} axis of link i-1.

The kinetic energy of the manipulator, denoted by KE, equals the sum of the kinetic energies of the point masses which constitute the elements of the manipulator and is given by

$$KE = \frac{1}{2} \sum_{a} m_a \, (\dot{r}_a . \dot{r}_a) \qquad (D.1)$$

where, $r_a = r_a(q_1, \ldots . q_N)$ is the position vector of point mass m_a in the base frame of the manipulator. Thus,

$$\dot{r}_a = \sum_{i=1}^{N} \frac{\partial r_a}{\partial q_i} \dot{q}_i \quad . \qquad (D.2)$$

Substitution of (D.2) in (D.1) yields

$$KE = \frac{1}{2} \sum_{i=1}^{N} \sum_{j=1}^{N} \dot{q}_i \, d_{ij} \, \dot{q}_j \quad , \qquad (D.3)$$

where, the coefficients d_{ij} are given by

$$d_{ij} = \sum_{a} m_a \left\{ \left(\frac{\partial r_a}{\partial q_i} \right) \cdot \left(\frac{\partial r_a}{\partial q_j} \right) \right\} \quad .$$

If the point mass m_a belongs to link μ, then $r_a = r_a \ (q_1, \ldots q_\mu)$, and

$$d_{ij} = \sum_{\mu=\max(i,j)}^{N} \left[\sum_{a \in \mu} m_a \left(\frac{\partial r_a}{\partial q_i} \right) \cdot \left(\frac{\partial r_a}{\partial q_j} \right) \right] . \qquad (D.4)$$

Since r_a is the position vector from the origin of the base frame to the point mass m_a ,one can write (see Fig. D.1)

$$r_a = r_i + r_{ij} + p_{ja} = r_i + p_{ia} \quad . \qquad (D.5)$$

It is implied in (D.5) that $j \geq i$ is being considered

where,

r_i is the position vector from the origin of the base frame to the origin of frame (i-1),

r_{ij} is the position vector from the origin of frame (i-1) to the origin of frame (j-1),

p_{ia} is the position vector from the origin of frame (i-1) to the point mass m_a in link $\mu \geq i$, and

p_{ja} is the position vector from the origin of frame (j-1) to the point mass m_a in link $\mu \geq j$.

The partial derivatives of r_a in (D.5) with respect to the generalized coordinates q_i and q_j are now written as ($j \geq i$)

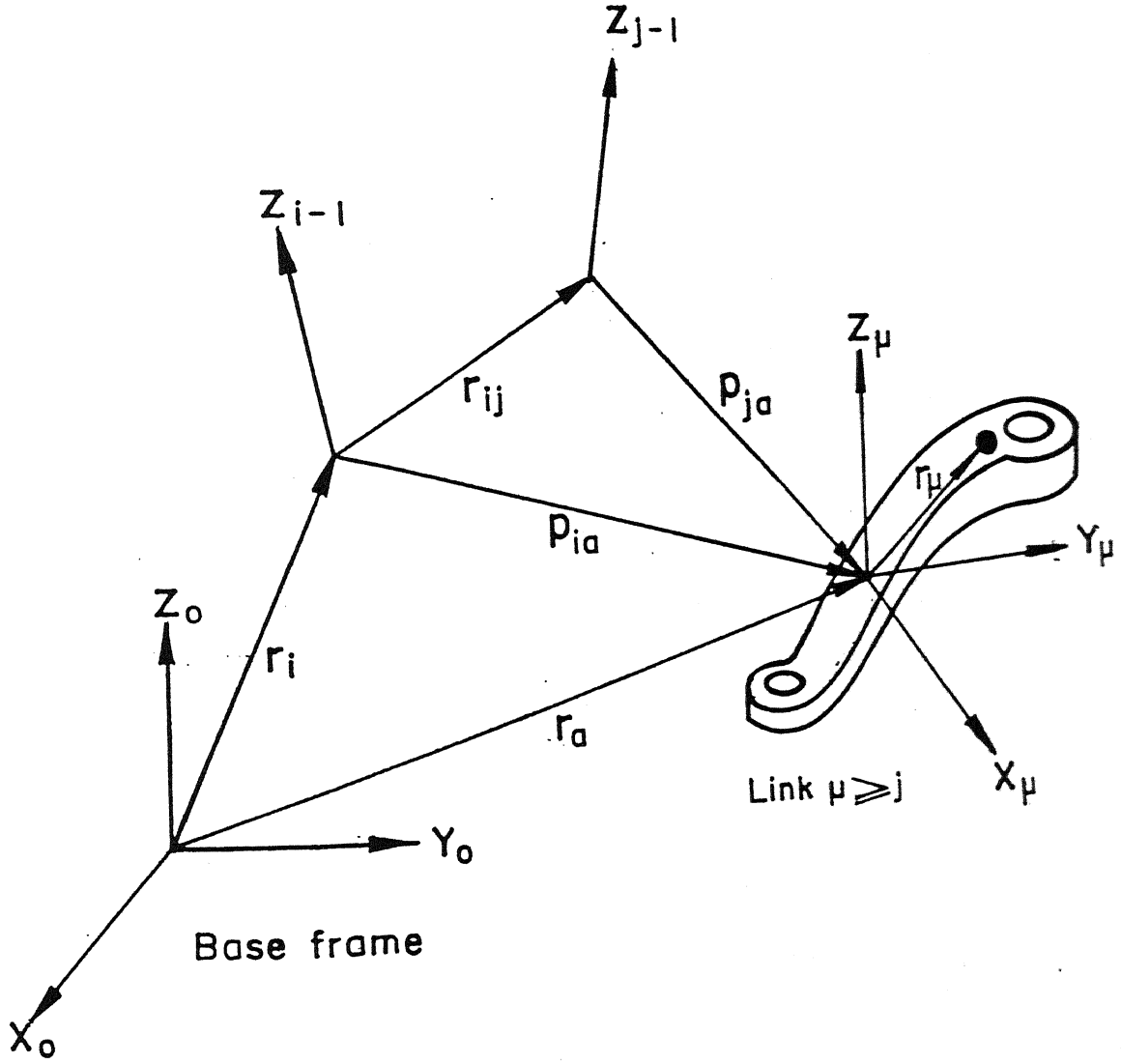

Fig. D.1 Position vectors in a kinematic chain with rotary joints

$$\frac{\partial r_a}{\partial q_i} = \frac{\partial p_{ia}}{\partial q_i} = z_{i-1} \times p_{ia} \qquad (D.6)$$

$$\frac{\partial r_a}{\partial q_j} = \frac{\partial p_{ja}}{\partial q_j} = z_{j-1} \times p_{ja} \qquad (D.7)$$

Substituting (D.6) and (D.7) into (D.4), the following explicit formula for the inertial coefficients is obtained

$$d_{ij} = \sum_{\mu=j}^{N} \sum_{a \in \mu} m_a (z_{i-1} \times p_{ia}) \cdot (z_{j-1} \times p_{ja}) \; ; \; j \geq i \qquad (D.8)$$

The normal, sliding, approach and translation vectors of the transformation matrix of (j-1) th frame with respect to (i-1) th frame all denoted by ${}^{i-1}n_{j-1}$, ${}^{i-1}s_{j-1}$, ${}^{i-1}a_{j-1}$ and ${}^{i-1}p_{j-1}$ respectively.

$$z_{i-1} \times p_{ja} = \left[\left({}^{i-1}s_{j-1,z}\, p_{jaz} - {}^{i-1}a_{j-1,z}\, p_{jay} \right), \right.$$

$$\left. - \left({}^{i-1}n_{j-1}\, p_{jaz} - {}^{i-1}a_{j-1,z}\, p_{jax} \right), \left({}^{i-1}n_{j-1,z}\, p_{jay} - {}^{i-1}s_{j-1,z}\, p_{jax} \right) \right]^T \qquad (D.9)$$

$$\text{and} \quad z_{j-1} \times p_{ja} = \begin{bmatrix} -p_{jay} & p_{jax} & 0 \end{bmatrix}^T \qquad (D.10)$$

Using (D.5) the following simplification of the expression under summation in (D.8) is obtained.

$$\left(z_{i-1} \times p_{ia} \right) \cdot \left(z_{j-1} \times p_{ja} \right) = \left(z_{i-1} \times r_{ij} \right) \cdot \left(z_{j-1} \times p_{ja} \right)$$

$$+ \left[z_{i-1} \times p_{ja}\right] \cdot \left[z_{j-1} \times p_{ja}\right] \qquad (D.11)$$

The first term on the right hand side of (D.11) defined in base frame can be expressed with respect to (i-1) th frame to get

$$\left[{}^{i-1}z_{i-1} \times {}^{i-1} r_{ij}\right] \cdot \left[{}^{i-1}z_{j-1} \times {}^{j-1}p_{ja}\right]$$

$$= \left[{}^{i-1}n_{j-1,x} \; {}^{i-1}p_{j-1,y} - {}^{i-1}n_{j-1,y} \; {}^{i-1}p_{j-1,x}\right] p_{jay}$$

$$- \left[{}^{i-1}s_{j-1,x} \; {}^{i-1}p_{j-1,y} - {}^{i-1}s_{j-1,x} \; {}^{i-1}p_{j-1,x}\right] p_{jax}. \qquad (D.12)$$

Similarly the second term on the right hand side of (D.11) defined in base frame can be expressed with respect to (j-1)th frame to get

$$\left[{}^{j-1}z_{i-1} \times {}^{j-1} p_{ja}\right] \cdot \left[{}^{j-1}z_{j-1} \times {}^{j-1}p_{ja}\right] =$$

$$- {}^{i-1}s_{j-1,z} \; p_{jay} \, p_{jaz} - {}^{i-1}n_{j-1,z} \; p_{jax} \, p_{jaz}$$

$$+ {}^{i-1}a_{j-1,z} \left[p_{jax}^2 + p_{jay}^2\right] \qquad (D.13)$$

From (D.9), (D.10), (D.11), (D.12) and (D.13) yields

$$\left[z_{i-1} \times p_{ia}\right] \cdot \left[z_{j-1} \times p_{ja}\right] = \left[{}^{i-1}n_{j-1,x} \; {}^{i-1}p_{j-1,y}\right.$$

$$- {}^{i-1}n_{j-1,y}\ {}^{i-1}p_{j-1,x}\Big)\ p_{jay} - \Big({}^{i-1}s_{j-1,x}\ {}^{i-1}p_{j-1,y}$$

$$- {}^{i-1}s_{j-1,x}\ {}^{i-1}p_{j-1,x}\Big)\ p_{jax} - {}^{i-1}s_{j-1,z}\ p_{jay}\ p_{jaz}$$

$$- {}^{i-1}n_{j-1,z}\ p_{jax}\ p_{jaz} + {}^{i-1}a_{j-1,z}\left(p_{jax}^2 + p_{jaz}^2\right) \qquad (D.14)$$

Before further simplification of d_{ij} the expressions for pseudo-inertia matrices are to be defined. For any link of an arm the mass, moments of inertia, products of inertia and position vector of the centre of mass of kth link from the axis of rotation expressed through pseudo inertia matrix as follows:

$$ {}^{\mu}I_{\mu} = \begin{bmatrix} \dfrac{-{}^{\mu}I_{\mu xx} + {}^{\mu}I_{\mu yy} + {}^{\mu}I_{\mu zz}}{2} & {}^{\mu}I_{\mu xy} & {}^{\mu}I_{\mu xz} & m_{\mu}\bar{x}_{\mu} \\ {}^{\mu}I_{\mu xy} & \dfrac{{}^{\mu}I_{\mu xx} - {}^{\mu}I_{\mu yy} + {}^{\mu}I_{\mu zz}}{2} & {}^{\mu}I_{\mu yz} & m_{\mu}\bar{y}_{\mu} \\ {}^{\mu}I_{\mu xz} & {}^{\mu}I_{\mu yz} & \dfrac{{}^{\mu}I_{\mu xx} + {}^{\mu}I_{\mu yy} - {}^{\mu}I_{\mu zz}}{2} & m_{\mu}\bar{z}_{\mu} \\ m_{\mu}\bar{x}_{\mu} & m_{\mu}\bar{y}_{\mu} & m_{\mu}\bar{z}_{\mu} & m_{\mu} \end{bmatrix} $$

(D.15)

where,

${}^{\mu}I_{\mu xx}$, ${}^{\mu}I_{\mu yy}$, ${}^{\mu}I_{\mu zz}$ are the moments of inertia of μ th link in μ th frame,

$^{\mu}I_{\mu xy}$, $^{\mu}I_{\mu yz}$, $^{\mu}I_{\mu xz}$ are the products of inertia,

m_{μ} is the mass of μ th link,

and

$\left[\bar{x}_{\mu}, \bar{y}_{\mu}, \bar{z}_{\mu}\right]^{T}$ is the position vector of the centre of mass.

The pseudo-inertia matrix $^{\mu}I_{\mu}$ is transformed from μ th coordinate frame to j-1 th frame by the following relation.

$$^{j-1}I_{\mu} = {}^{j-1}T_{\mu}\ {}^{\mu}I_{\mu}\left({}^{j-1}T_{\mu}\right)^{T} \qquad (D.16)$$

To determine d_{ij} it is required to transform the moments of inertia of all the links beyond j-1 and add to get the effective inertia of those links at the joint j which is given by

$$I^{j} = \sum_{\mu=j}^{N} {}^{j-1}I_{\mu}. \qquad (D.17)$$

Now the moments of inertia, products of inertia and mass corresponding to I^{j} are determined in terms of its matrix elements by the following relations

$$m^{j} = I^{j}(4,4) = \sum_{k=j}^{N} m_{k}\ , \qquad I^{j}_{xx} = I^{j}(2,2) + I^{j}(3,3)\ ,$$

$$\bar{x}^{j} = I^{j}(1,4)/m^{j}\ , \qquad I^{j}_{yy} = I^{j}(1,1) + I^{j}(3,3)\ ,$$

$$\bar{y}^{j} = I^{j}(2,4)/m^{j}\ , \qquad I^{j}_{zz} = I^{j}(1,1) + I^{j}(2,2)\ ,$$

$$\bar{z}^{j} = I^{j}(3,4)/m^{j}\ , \qquad I^{j}_{xy} = I^{j}(1,2)\ ,$$

$$I^{j}_{xz} = I^{j}(1,3)\ , \qquad I^{j}_{yz} = I^{j}(3,2)\ . \qquad (D.18)$$

The quantity $I^{j}(i1,j1)$ in (D.18) is the element of I^{j} in i1 th row and j1 th column.

Now using (D.14) and (D.18) in (D.8) theexpression for d_{ij} becomes

$$d_{ij} = {}^{i-1}a_{j-1,z}\, I^{j}_{zz} - {}^{i-1}s_{j-1,z}\, I^{j}_{yz} - {}^{i-1}n_{j-1,z}\, I^{j}_{xz} + (m_j + \ldots + m_N)$$

$$\cdot\Big[\big({}^{i-1}n_{j-1,x}\ {}^{i-1}p_{j-1,y} - {}^{i-1}n_{j-1,y}\ {}^{i-1}p_{j-1,x}\big)\ \bar{y}^{j} -$$

$$\big({}^{i-1}s_{j-1,x}\ {}^{i-1}p_{j-1,y} - {}^{i-1}s_{j-1,y}\ {}^{i-1}p_{j-1,x}\big)\ \bar{x}^{j}\Big]. \qquad \text{(D.19)}$$

APPENDIX E

INVERSE POSITION KINEMATICS OF PUMA 560

This appendix gives the inverse kinematics solution of PUMA 560 when the transformation matrix of end effector frame with respect to base frame (3.3-3) is given. The details of the method [Fu et al., 1987] are not discussed here, and only the expressions for joint angles are given. For a particular end effector position and orientation the arm, elbow and wrist may have different onfigurations which are described by three indicators ARM, ELBOW and WRIST. The values of these indicators for different configurations are listed below.

$$\text{ARM} = \begin{cases} +1 & \text{RIGHT arm} \\ -1 & \text{LEFT arm} \end{cases} \qquad \text{(E.1)}$$

$$\text{ELBOW} = \begin{cases} +1 & \text{ABOVE arm} \\ -1 & \text{BELOW arm} \end{cases} \qquad \text{(E.2)}$$

$$\text{WRIST} = \begin{cases} +1 & \text{WRIST DOWN} \\ -1 & \text{WRIST UP} \end{cases} \qquad \text{(E.3)}$$

Using the conventions used in (2.3-2) the given transformation matrix ${}^{0}T_{6}$ (for which the joint angles are to be calculated) is written in terms of its elements as follows:

$$ {}^{0}T_{6} = \begin{bmatrix} {}^{0}n_{6x} & {}^{0}s_{6x} & {}^{0}a_{6x} & {}^{0}p_{6x} \\ {}^{0}n_{6y} & {}^{0}s_{6y} & {}^{0}a_{6y} & {}^{0}p_{6y} \\ {}^{0}n_{6z} & {}^{0}s_{6z} & {}^{0}a_{6z} & {}^{0}p_{6z} \\ 0 & 0 & 0 & 1 \end{bmatrix} . \qquad (E.4) $$

The expression for first joint angle is given by

$$ q_1 = \tan^{-1} \left[\frac{-ARM\ {}^{0}p_{6y} \sqrt{{}^{0}p_{6x}^2 + {}^{0}p_{6y}^2 - d_2^2} - {}^{0}p_{6x}\, d_2}{ARM\ {}^{0}p_{6x} \sqrt{{}^{0}p_{6x}^2 + {}^{0}p_{6y}^2 - d_2^2} + {}^{0}p_{6y}\, d_2} \right] \qquad (E.5) $$

The second joint angle is calculated from

$$ q_2 = \tan^{-1} \left[\frac{\sin(q_2)}{\cos(q_2)} \right] \quad -\pi \le q_2 \le \pi \qquad (E.6) $$

where,

$$ \sin q_2 = \sin(alp1)\cos(bet1) + (ARM.ELBOW)\cos(alp1)\sin(bet1), \qquad (E.7) $$

$$ \cos q_2 = \cos(alp1)\cos(bet1) - (ARM.ELBOW)\sin(alp1)\sin(bet1), \qquad (E.8) $$

$$ \sin(alp1) = \left[- {}^{0}p_{6z} \Big/ \sqrt{{}^{0}p_{6x}^2 + {}^{0}p_{6y}^2 + {}^{0}p_{6z}^2 - d_2^2} \right] \qquad (E.9) $$

$$ \cos(alp1) = \left[- ARM \sqrt{{}^{0}p_{6x}^2 + {}^{0}p_{6y}^2 - d_2^2} \right] / $$

$$\sqrt{{}^{0}p_{6x}^{2} + {}^{0}p_{6y}^{2} + {}^{0}p_{6z}^{2} - d_2^2}\Big]$$

(E.10)

$$\cos(\text{bet1}) = \left[{}^{0}p_{6x}^{2} + {}^{0}p_{6y}^{2} + {}^{0}p_{6z}^{2} + a_2^2 - d_2^2 - (d_4^2 + a_3^2)\right] \Big/ \left[2a_2\sqrt{{}^{0}p_{6x}^{2} + {}^{0}p_{6y}^{2} + {}^{0}p_{6z}^{2} - d_2^2}\right]$$

(E.11)

$$\sin(\text{bet1}) = \sqrt{1-\cos^2(\text{bet1})} \qquad \text{(E.12)}$$

The third joint angle is given by

$$q_3 = \tan^{-1}\left[\frac{\sin q_3}{\cos q_3}\right] \qquad -\pi \le q_3 \le \pi \qquad \text{(E.13)}$$

where,

$$\sin q_3 = \sin(\text{phi2})\cos(\text{bet2}) - \cos(\text{phi2})\sin(\text{bet2}) \qquad \text{(E.14)}$$

$$\cos q_4 = \cos(\text{phi2})\cos(\text{bet2}) - \sin(\text{phi2})\sin(\text{bet2}) \qquad \text{(E.15)}$$

$$\cos(\text{phi2}) = a_2^2 + (d_4^2 + a_3^2) - \left[{}^{0}p_{6x}^{2} + {}^{0}p_{6y}^{2} + {}^{0}p_{6z}^{2} - d_2^2\right] \qquad \text{(E.16)}$$

$$\sin(\text{phi2}) = \text{ARM. ELBOW}\sqrt{1-\cos^2(\text{phi2})} \qquad \text{(E.17)}$$

$$\sin(\text{bet2}) = d_4 / \sqrt{d_4^2 + a_3^2} \qquad \text{(E.18)}$$

$$\cos(\text{bet2}) = \| a_3 \| / \sqrt{d_4^2 + a_3^2} \qquad \text{(E.19)}$$

The fourth joint angle is given by

$$q_4 = \tan^{-1}\left[\frac{\sin q_4}{\cos q_4}\right] \qquad \text{(E.20)}$$

where,

$$+ \sin q_4 \sin (q_2 + q_3)\ {}^{0}n_{6z} \qquad \text{(E.30)}$$

$$\cos q_6 = \left[-\sin q_1 \cos q_4 - \cos q_1 \cos (q_2 + q_3) + \sin q_4\right] {}^{0}s_{6x}$$

$$+ \left[\cos q_2 \cos q_4 - \sin q_1 \cos(q_2 + q_3) \sin q_4\right] {}^{0}s_{6y}$$

$$+ \sin q_4 \sin (q_2 + q_3)\ {}^{0}s_{6z} \qquad \text{(E.31)}$$

APPENDIX F

KINEMATIC AND DYNAMIC PARAMETERS OF PUMA 560 MANIPULATOR

In Chapter 4 the trajectory planning problem is solved for a dual-arm manipulator consisting of two PUMA 560 arms. For the computation of different quantities needed in trajectory planning, various geometric, kinematic and dyanamic parameters of PUMA 560 are required. These parameters are presented sequentially in this appendix.

The geometric parameters of PUMA 560 are given in Table F.1 [Fu et al., 1987]. The geometric parameters are link lengths a_i, offset dimensions α_i and d_i (see (2.3-1)),range of joint angles etc.

Table F.1 Geometric parameters of PUMA 560

Joint i	α_i (degrees)	a_i (mm)	d_i (mm)	Range of joint angle q_i (degrees)
1	-90	0	0	-160 to + 160
2	0	431.8	149.09	-225 to 45
3	90	-20.32	0	-45 to 225
4	-90	0	433.07	-110 to 170
5	90	0	0	-100 to 100
6	0	0	56.25	-266 to 266

Table F.2 lists the link masses, radii of gyration, location of

centres of mass in the respective link frame (see Fig. D.1).

Table F.2 Inertia parameters of PUMA 560 [Tarn and Bejczy, 1988]

Link	Mass	Distance of centre of mass			Square of radius of gyration		
i	m_i (kg)	$\bar{x}_i$ (m)	$\bar{y}_i$ (m)	$\bar{z}_i$ (m)	k^2_{ixz} (m^2)	k^2_{iyy} (m^2)	k^2_{izz} (m^2)
1	12.96	0.0	0.3088	0.0389	0.1816	0.0152	0.1811
2	22.37	-0.3289	0.0050	0.2038	0.0596	0.1930	0.1514
3	6.97	0.0136	0.0092	0.1522	0.0783	0.0786	0.0021
4	1.18	0.0	0.0863	-0.0029	0.0119	0.0029	0.0118
5	0.62	0.0	-0.0102	0.0013	0.0009	0.0009	0.0009
6	0.16	0.0	0.0	0.0029	0.0008	0.0008	0.0004

The principal moments of inertia are then calculated as

$$\begin{aligned} I_{ixx} &= m_i\ k^2_{ixx} \\ I_{iyy} &= m_i\ k^2_{iyy} \\ I_{izz} &= m_i\ k^2_{izz} \end{aligned} \qquad \text{(F.1)}$$

The products of inertia terms are assumed to be zero. These inertias from (F.1) are used to calculate pseudo-inertia matrices by (D.15) of Appendix D. Each joint of PUMA 560 has a velocity limit depending on the servometer at the joint. The joint velocity limits come as constraints are required in the constraints (3.10-6) of trajectory planning problem. The joint velocity limits are given in Table F.3.

Table F.3 Joint velocity limits of PUMA 560 [Kafrissen and Stephans, 1984]

Joint	1	2	3	4	5	6
Max velocity (rad/sec)	1.4	0.9	2.1	4.0	2.1	7.9

The joint torque limits are required in the joint torque constraint relations in (3.10-5). These limits for a PUMA 560 arm are given in Table F.4.

Table F.4 Joint torque limits of PUMA 560 [Armstrong et al., 1986]

Joint	1	2	3	4	5	6
Max Torque (N.m)	97.6	186.4	89.4	24.2	20.1	21.3

The gear ratios used in (3.7-5) are given in Table F.5.

Table F.5 Gear ratios (c_i^g) of PUMA 560 [Nagy,1988]

Joint	Range of ratio	ratio used
1	62.6115-62.6127	62.6111
2	107.8167-107.8188	107.8175
3	53.704-53.70	53.705
4	76.035-76.038	76.037
5	71.920-71.924	71.922
6	76.685-76.692	76.689

In the minimum electrical energy considerations, the motor constant c_i^m and the power supply resistance c_i^r are required in (3.7-5). These constants are listed in Table F.6.

Table F.6 Motor constants and power supply resistances of Servomotors [Nagy, 1988]

Joint	1	2	3	4	5	6
c_i^r (Ohm)	1.6	1.6	1.6	3.8	3.8	3.8
c_i^m (Kg.cm/A)	2.58	2.58	2.58	0.973	0.973	0.973